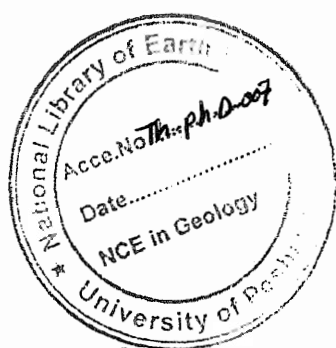


Tectonic Evolution of Southeast Kohistan, Northwest Himalaya, Pakistan

A thesis submitted to the National Centre of Excellence in Geology,
University of Peshawar, in partial fulfillment of the requirement for
the Degree of Doctor of Philosophy



Mohammad Ahmed Khan

National Centre of Excellence in Geology,
University of Peshawar
1997

for Love.
which is amaranthine



Approved by

PROF. DR. M. ASIF KHAN
(Supervisor)
National Centre of Excellence in Geology
University of Peshawar

PROF. DR. M. QASIM JAN
(Co-Supervisor)
National Centre of Excellence in Geology
University of Peshawar

DR. KHURSHID ALAM BUTT
(External Examiner)
Head G.S.D.
Atomic Energy Mineral Centre
Lahore, Pakistan

DIRECTOR
National Centre of Excellence in Geology
University of Peshawar
Peshawar, Pakistan

*Seminar Library
Centre of Excellence
in Geology
University of Peshawar*

TECTONIC EVOLUTION OF SOUTHEAST KOHISTAN, NORTHWEST HIMALAYA, PAKISTAN

Mohammad Ahmed Khan

PhD thesis, University of Peshawar, Pakistan, 1997

This is an excellent, first-class piece of work. The candidate has studied a little-known, but key, region of the Kohistan terrane. In so doing he provides valuable information on the geological and tectonic evolution of this particular island arc, which is an important part of the Himalaya, but he also contributes new ideas and data to an improved understanding of the ways in which the lower levels of island arcs are constructed, and this is one of the fundamental problems of Earth Sciences today.

The candidate has mapped the main sections of a large region, the mountains and relief of which make it difficult of access. Yet he has produced a new basic geological map, and has collected a lot of stratigraphic data which provide an essential tool for working out the structural and tectonic history. In the laboratory he has produced a lot of major and trace element analyses of his key rocks, and this geochemical data-set has enabled him to discriminate between alternative models of petrogenesis of the lower levels of the Kohistan arc.

In the thesis a lengthy, useful introduction is followed by chapters on the Sapat mafic-ultramafic complex, the complex amphibolite belt and the Thak granitoid sheets, each of which contains details of the field features and relations, modal compositions and petrography, whole rock geochemistry, petrogenesis, and tectonic evolution. In the final chapter of conclusions the candidate shows how his discoveries relate to the overall evolution of the Kohistan arc. The thesis is illustrated with many stratigraphic tables, field photos, micro-photographs, and plots of geochemical data. Throughout he demonstrates an acute mastery of his subject, whether it be geochemical petrogenesis, the geology of the Himalayas or island arcs. There is much original and publishable material in this thesis; the candidate should produce several papers in international journals.

Being very impressed with the high quality of this thesis, I readily recommend that for it the candidate be awarded the degree of Doctor of Philosophy.

Brian F. Windley

6th December 1997.

B. Windley

COMMENTS FOR THE EVALUATION OF THE THESIS SUBMITTED
BY MR. MUHAMMAD AHMAD KHAN FOR THE AWARD OF PH.D.
DEGREE.

It is quite honorable for me to have an opportunity to evaluate
the thesis by Mr. Muhammad Ahmad Khan.

I evaluate this thesis quite excellent by the following points;

1) Amphibolitic layered gabbro together with mafic-ultramafic rocks were distinguished as Sapat mafic-ultramafic complex from amphibolite belt. By the whole rock geochemistry the complex was characterized first time as arc-related being correlative to the Jijal Complex. It is also important to find the direct geological relation that the complex is overlain by metavolcanics of amphibolite belt.

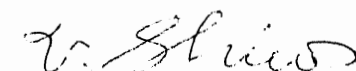
2) Within amphibolite belt, rocks were classified geochemically as well as petrographically into three different amphibolites, MORB-type, tholeiitic and calc-alkaline subduction related affinities. Although MORB-type metavolcanics were already recognized by M.A.Khan et al. (1993), detailed study revealed their occurrence and distribution which give much implication to the initial stage of the Kohistan arc.

3) Granitoids in the amphibolite belt were first described in detail and classified into three affinities with enormous numbers of chemical analyses. The occurrence of high Ti-gabbro-tonalite-trondhjemite gneisses and trondhjemite dykes/veins are quite interesting. Age determinations of these granitoids may contribute much to the timing of generation of the Kohistan arc.

4) Dealing with whole rock geochemistry of metamorphosed and altered volcanic rocks, even though detection limits of some trace elements are high, immobile elements were carefully selected and adequately used for discriminating arguments. As the writer mentions, analysis of REE may provide more evidences to the constraints.

I do not hesitate to say that this thesis deserves the award of Ph.D. Degree.

October 28, 1997



Dr. Teruo Shirahase
Senior Researcher
Geological Survey of Japan

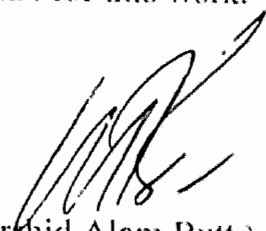
Report on Ph.D. thesis of Mr. Ahmad Khan Peshawar University

This thesis is a significant contribution towards understanding the genesis of Kohistan island arc crust. Based on geology, structural interpretation, geochemistry and a comprehensive synthesis of previous studies, the author has suggested a three stage model for the development of the crust of Kohistan island arc. Since Kohistan island arc provides one of the few complete sections of an island arc crust, it is probably one of the best areas to investigate the problem of crustal thickening beneath an island arc. Kohistan island arc developed as an intra oceanic island arc. Oceanic crust that initially underlay the arc has been demonstrated to thicken initially by mafic-ultramafic magmatic activity. This was followed by structural emplacement of Kamila Amphibolites and intrusion of Chilas complex. The final stage envisages an Andean margin stage of intermediate to acid volcanism and plutonism.

This is a well-documented study of SE part of Kohistan Island arc. Geochemical discrimination presented therein provide ample constraints on the tectonic environments. These include a variety of plutonic and volcanic rocks ranging from mafic and ultramafic intrusions of Sapat complex of island arc affinity, amphibolites of arc tholeiitic chemistry, amphibolites of MORB-type character and mafic, intermediate, acid and trondjemitic intrusions with geochemical signature of subduction related plutonics. A synthesis of this volcano-plutonic activity through time amply substantiated the development of an intra oceanic island arc and its collision with Asia.

The data presentation of this thesis is excellent. The model presented is well formulated and logically very convincing. As with any geological problem, there is room for debate but that, in no way, reduces the merit of this study. In fact, it is likely to invoke further interest in the study of Kohistan island arc.

I must congratulate the author and his supervisor for this excellent piece of work. I have absolutely no hesitation in strongly recommending the award of a Ph.D. for this work.



(Dr. Khurshid Alam Butt)

CONTENTS

	Page
List of Figures -----	i
List of Tables -----	v
List of Plates -----	vii
Acknowledgements -----	xii
Abstract -----	xiii
Chapter 1 Introduction	
Previous Work -----	3
Aims and Objectives -----	7
Thesis Format -----	8
Methodology -----	9
Laboratory Techniques -----	9
Chapter 2 Regional Setting	
Initial Statement -----	12
Introduction -----	12
Plate Tectonic History of North Pakistan -----	13
Afghanistan -----	15
Tibetan Plateau -----	18
Karakoram Plate -----	20
The Northern Suture -----	22
The Indus Suture -----	24
Kohistan Arc -----	25
Intraoceanic Stage of Crustal Growth	
Volcanic-Sedimentary Succession -----	27
Fluvial Sediments (Purit and Asambar Sedimentary Units)---	30
Yasin Group -----	31
Chalt Group -----	33
Gilgit Formation -----	35
Kamila Amphibolite Unit -----	38
Intrusive Rock Units -----	42
Mafic-Ultramafic Complexes -----	42
Jijal Complex -----	42
Sapat Mafic-Ultramafic Complex -----	44
Chilas Complex -----	45
Intermediate-Felsic Intrusions -----	46
Thak Granitoid Sheets -----	46
Matum Das Trondhjemites -----	46
Continental-Margin Stage of Crustal Growth -----	47

Kohistan Batholith -----	48
Dir Group -----	51
Correlation between Kohistan and Ladakh -----	52
Indian Plate -----	53
Tethyan Shelf Sediments -----	55
The High Himalaya -----	57
Lesser Himalaya -----	58
Sub-Himalayan Molasse (Siwalik Group) -----	58
Existing Models for the Tectonic History of the Kohistan -----	59
Local Geology -----	69
Structure -----	73
Jal Shear Zone -----	74

Chapter 3 The Sapat Mafic-Ultramafic Complex

Introduction -----	75
General Characteristics -----	76
Modal Composition and Petrography -----	83
Ultramafic Rocks -----	83
Gabbroic Rocks -----	87
Geochemistry -----	90
Geochemical Variations -----	92
Compatible Major and Trace Elements -----	92
Incompatible Trace Elements -----	96
Petrogenesis -----	100

Chapter 4 The Amphibolite Belt

Introduction -----	104
Babusar Amphibolites -----	106
Field Features and Relations -----	106
Modal Composition and Petrography -----	109
Niat Amphibolites -----	115
Field Features and Relations -----	115
Modal Composition and Petrography -----	119
Sumal Amphibolites -----	125
Field Features and Relations -----	125
Modal Composition and Petrography -----	126
Jal Amphibolites -----	129
Field Features and Relations -----	129
Modal Composition and Petrography -----	136
Whole-Rock Geochemistry -----	140
Alteration during Solidification -----	140
Grouping -----	142
Inter-relationship between Jal and Niat Amphibolites -----	145

Jal and Niat Amphibolites	150
Scrutiny of the Data	150
Classification	154
Tholeiitic Nature	154
Fractionation Assemblage	157
Trace Element Variations	157
Ferromagnesian Elements	159
Inter-Element Ratios	160
Trace-Element Patterns as Spidergrams	160
Estimation of Parent Magma	164
Tectonic Environment	166
Petrogenesis	168
Babusar Amphibolites	171
Classification	173
Fractionation Assemblage	173
Trace Element Variations	176
Ferromagnesian Elements	176
Trace-Element Patterns as Spidergrams	176
Tectonic Environment	178
Sumal Amphibolites	181
Classification	181
Major Element Variation Diagrams	185
Trace Element Variations	186
Spiderdiagrams	186
Trace Element Characteristics of Subduction-related Magmas ..	188
Tectonic Environments	190
Petrogenesis	192

Chapter 5 The Thak Granitoid Sheets

Introduction	195
Previous Studies	196
Field Relations	197
Niat Gah	198
Thak Gah	200
Buto Gah	203
Thor Gah	203
Summary	204
Modal Composition and Petrography	205
Shai Granitoid Group	206
Khun Granitoid Group	210
Minor Intrusions	217
Dioritic Pegmatoids	217
Granitic and Trondhjemitic Pegmatites	223
Geochemistry	

Classification -----	228
Geochemical Characteristics -----	232
Niat Gah -----	235
Thak Gah -----	241
Buto Gah -----	248
Thor Gah -----	250
Petrogenesis -----	254
HFSE Enriched Group-----	254
HFSE Depleted Group-----	256
Trondhjemites-----	259

Chapter 6 Summary and Conclusion

Introduction-----	262
Geology of SE Kohistan: A Synthesis-----	262
The Sapat Mafic-Ultramafic Complex-----	263
The Amphibolite Belt-----	265
The Thak Granitoid Sheets -----	267
Discussion-----	270
Constitution of the Lower Arc Crust-----	271
Thickening of the Lower Arc Crust-----	273
Conclusion-----	279

References -----	281
-------------------------	------------

Appendices

Appendix 1 -----	310
Appendix 2 -----	320

LIST OF FIGURES

	page
Chapter 1 Introduction	
Figure 1.1 Simplified geographic map of northern Pakistan.	2
Figure 1.2 Map showing the investigated area lying between the Chilas Complex and the Main Mantle Thrust.	4
Chapter 2 Regional Setting	
Figure 2.1 Regional map of north Pakistan showing the main thrust zones.	14
Figure 2.2 Sketch map of the Indian plate and its margins, showing the tectonic position of the Kohistan and Ladakh terrane.	16
Figure 2.3 The principal mountain ranges, microcontinental fragments and faults.	19
Figure 2.4 Simplified geological map of the western Himalayas--Karakoram.	28
Figure 2.5 Map of Himalayan orogen showing main lithological and structural units.	56
Figure 2.6 Tectonic model of the thermal structures in the Kohistan obducted island arc (Bard, 1983).	60
Figure 2.7 Magmatic and tectonic evolution of the Kohistan Terrane (after Petterson and Windley, 1991).	62
Figure 2.8 Schematic section through the Kohistan arc (after Coward et al., 1987).	62
Figure 2.9 A speculative model for the tectonic evolution of northern Pakistan (after Khan and Jan, 1993).	64
Figure 2.10 Model for the N.W.Himalayas (after Debon et al., 1987).	65
Figure 2.11 A model for the tectonic and petrological evolution of the Kohistan terrané (T. Khan, 1994).	67
Figure 2.12 Geological map of SE Kohistan.	70

Chapter 3 The Sapat Mafic-Ultramafic Complex

Figure 3.1	Plots of major oxides of the studied rocks.	93
Figure 3.2	Binary plots showing the fractionation of Ni, Zn, Cr and Sc.	95
Figure 3.3	Binary plots showing the relationship of the incompatible trace elements.	95
Figure 3.4	Binary plots showing the mutual ratios between incompatible trace elements.	98
Figure 3.5	Primordial mantle normalized multi element patterns of the gabbros and ultramafics.	99
Figure 3.6	Spidergram showing the difference of studied rocks from the MORB type volcanics of Niat unit.	102

Chapter 4 The Amphibolite Belt

Figure 4.1	AFM ternary plot differentiating the studied amphibolites into tholeiites and calc-alkaline suites.	144
Figure 4.2	Binary plots of major oxides versus Zr.	151
Figure 4.3	The chemical classification of the studied rocks using the total alkalies versus SiO ₂ plot.	155
Figure 4.4	Classification of studied rocks using the parameters R1 and R2 (after de la Roche et al., 1980).	156
Figure 4.5	AFM diagram showing the tholeiitic trend of studied rocks.	158
Figure 4.6	Bivariate plot of %AN versus Al ₂ O ₃ of the studied rocks (after Irvine and Barager, 1971).	158
Figure 4.7	Bivariate plot of SiO ₂ versus FeO/MgO (after Miyashiro, 1974).	158
Figure 4.8	Spidergrams of selected incompatible trace elements (Nb, P, Zr, Ti and Y) of four samples.	163
Figure 4.9	Conventional spidergram for four selected samples of Jal-Niat amphibolites.	163
Figure 4.10	Binary plot of the Mg/(Mg+FeO) versus the An/(An+Ab+Or) for the Jal-Niat amphibolites.	167
Figure 4.11	Various established discrimination diagrams .	169

Figure 4.12	Primordial mantle normalized diagram comparing the patterns.	169
Figure 4.13	Chemical classification of Babusar amphibolites using the total alkalis versus SiO ₂ plot.	174
Figure 4.14	Ternary plot of classification (after Jensen, 1976).	174
Figure 4.15	AFM diagram (after Irvine and Barager, 1971).	174
Figure 4.16	Binary plots of major oxides versus SiO ₂ .	175
Figure 4.17	Binary plots of trace elements versus SiO ₂ .	177
Figure 4.18	Spidergrams of the Babusar amphibolites showing the spiked patterns.	179
Figure 4.19	Diagram showing enrichment of low ionic potential elements and depletion of high ionic potential elements.	180
Figure 4.20	Chemical classification of the Sumal amphibolites.	183
Figure 4.21	Jensen ternary plot of classification.	183
Figure 4.22	Subdivision of subalkalic rocks using the K ₂ O versus silica diagram of Le Maitre et al. (1989).	184
Figure 4.23	AFM diagram showing the calc-alkaline trend of the studied rocks (after Irvine and Barager, 1971).	184
Figure 4.24	Binary plots of trace elements versus Zr.	187
Figure 4.25	Spidergrams showing the spiked patterns.	189
Figure 4.26	Diagram showing depletion of high field strength elements in Sumal amphibolites relative to N-type MORB.	191
Figure 4.27	Various discrimination diagrams showing the island arc setting environments for the Sumal Amphibolites.	191
 Chapter 5 The Thak Granitoid Sheets		
Figure 5.1	Chemical classification of the granitoid rocks using total alkalis versus silica diagram (after Le Bas et al., 1986).	230
Figure 5.2	Classification of rocks using the parameters R1 and R2 (after De la Roche et al., 1980).	230
Figure 5.3	Q-B-F classification plot (after Debon and Le Fort, 1983).	233

Figure 5.4	Ab-An-Or ternary plot classifying the more silicic rocks of Thak granitoid sheets.	233
Figure 5.5	Binary plots showing the behaviour of granitoid rocks from Niat Gah.	236
Figure 5.6	Primordial mantle normalized multi element patterns for the granitoid rocks of Niat Gah.	239
Figure 5.7	Binary plots showing the behaviour of granitoid rocks from Thak Gah.	243
Figure 5.8	Binary plots of transitional elements against SiO ₂ .	246
Figure 5.9	Spidergram showing the similar patterns of rocks exposed near Babusar Rest House.	247
Figure 5.10	Spidergrams of granitoid rocks from Thak Gah.	249
Figure 5.11	Spidergrams of intrusive rocks from Buto Gah.	251
Figure 5.12	Binary plots of granitoids from Buto and Thor valleys.	252
Figure 5.13	Spidergrams of intrusive rocks from Thor Gah.	255
Figure 5.14	Spidergram showing the similar pattern of three samples.	258
Chapter 6 Summary and Conclusion		
Figure 6.1	Summary of radiometric ages from southern Kohistan terrane.	275
Figure 6.2	Schematic representation of two-stage model of crustal thickening in Kohistan terrane.	277

LIST OF TABLES

	page
Chapter 2 Regional Setting	
Table 2.1 Summary of the sedimentary and volcanic lithological units in Kohistan terrane.	29
Table 2.2 Summary of emplacement of plutonic rocks in the Kohistan terrane.	43
Table 2.3 Lithological comparison of the Kohistan and Ladakh arc terranes.	54
Chapter 3 The Sapat Mafic-Ultramafic Complex	
Table 3.1 Modal composition of ultramafic rocks.	84
Table 3.2 Modal composition of Gabbros.	88
Table 3.3 XRF analyses of ultramafic and gabbroic rocks.	91
Chapter 4 The Amphibolite Belt	
Table 4.1 Modal composition of Babusar Amphibolites.	112
Table 4.2 Modal composition of Niat volcanic rocks.	124
Table 4.3 Modal composition of Sumal volcanic rocks.	127
Table 4.4 Modal composition of Jal rocks.	137
Table 4.5 Mean composition of the amphibolite rocks.	143
Table 4.6 Major and trace element composition of Jal Amphibolites.	146
Table 4.7 Major and trace element composition of Niat volcanic rocks.	148
Table 4.8 Comparison of mean composition of studied rocks with the various tectonic settings.	161
Table 4.9 Comparison of major and trace element composition of primitive samples with tectonic settings.	165
Table 4.10 Major and trace element composition of Babusar Amphibolites.	172

Table 4.11	Major and trace element composition of Sumal volcanic rocks.	182
Chapter 5	The Thak Granitoid Sheets	
Table 5.1	Modal composition of granitoid rocks of Shai group.	209
Table 5.2	Modal composition of intrusive rocks of Khun Group.	213
Table 5.3	Modal composition of intrusive rocks from Minor Bodies.	220
Table 5.4	Modal composition of Trondhjemites.	220
Table 5.5	Geochemical data of selected rock types.	229
Table 5.6	Studied rocks showing different names in various classification schemes and in this study.	234

LIST OF PLATES

	Page
Chapter 3 The Sapat Mafic-Ultramafic Complex	
Plate 3.1 Rhythmic layering near Shotti pass.	78
Plate 3.2 Amphibolitized foliated gabbro near Tuno in Jalkot Nala.	78
Plate 3.3 Layering in gabbros near Chochargah in Jalkot Nala.	80
Plate 3.4 Folding in the layered gabros at Buto gali.	80
Plate 3.5 Rhythmic layering and faulting in gabbros at Kot gali in Sapat Nala.	81
Plate 3.6 Syngenetic faulting visible in layered gabbros.	81
Plate 3.7 Foliated gabbro with medium and coarse grained bands.	82
Plate 3.8 Shear zone in gabbros near Kalawan.	82
Plate 3.9 Foliated gabbro with medium and coarse grained bands.	86
Plate 3.10 Relics of olivine in serpentine.	86
Plate 3.11 Relics of pyroxene in a matrix of serpentine.	89
Plate 3.12 Strongly sheared and mylonitized mafic and felsic bands in the gabbros.	89
Chapter 4 The Amphibolite Belt	
Plate 4.1 Babusar amphibolites at Batsi Sangar, south of Keo gali in Jalkot Nala.	107
Plate 4.2 Foliation and shearing in the Babusar amphibolites, south of Utla Babusar (Thak valley).	107
Plate 4.3 Quartzofeldspathic bands in Babusar amphibolite.	108
Plate 4.4 Shear zone in Babusar amphibolites, north of Buto Gali.	108
Plate 4.5 Ductile shearing in the Babusar amphibolites at Buto Pass.	110
Plate 4.6 Shear zone at Sherman Gali.	110

Plate 4.7	Mylonite zone near Shotti Pass in Babusar amphibolites.	111
Plate 4.8	Fine-grained, foliated and gneissic banding in the Babusar amphibolites.	111
Plate 4.9	Large crystal of amphibole enclosed with quartz, sphene and hornblende.	114
Plate 4.10	Same in crossed polars.	114
Plate 4.11	Folding in Niat volcanics, near Nigaran in Niat valley.	116
Plate 4.12	Open folding in the Niat volcanics near Nigaran.	116
Plate 4.13	Deformation and folding in Niat volcanics in Buto valley.	117
Plate 4.14	Folding and strong deformation in Niat volcanics in Buto valley.	117
Plate 4.15	Granitic intrusion in Niat volcanics, just north of Butogal village in Buto valley.	118
Plate 4.16	Contact between Niat volcanics and diorite/granodiorite, north of Tushkal in Keo valley.	118
Plate 4.17	Alternate bands of volcanics/amphibolites and diorites in Niat valley.	120
Plate 4.18	Mix zone of diorites and amphibolites in Keo valley.	120
Plate 4.19	Stretched pillows in Niat volcanics in the front of Dalupar gah in Buto valley.	121
Plate 4.20	Strongly sheared pillows in Niat volcanics (Buto valley).	121
Plate 4.21	Fine-grained, foliated and gneissic Niat volcanics.	123
Plate 4.22	Deformed rock containing plagioclase, quartz, chlorite, epidote, muscovite and sphene.	123
Plate 4.23	Perfect cleavage of hornblende with inclusions of sphene and show orientation along foliation.	128
Plate 4.24	Sumal volcanics containing feldspar, hornblende, chlorite, muscovite and sphene.	128
Plate 4.25	Bands of granite, andesitic and amphibolite in the Jal amphibolite in Thak valley.	130

Plate 4.26	Andesitic veins in Jal amphibolites.	130
Plate 4.27	Contact of diorite and Jal amphibolites in Thor valley, between Sarin and Gabbar.	131
Plate 4.28	Contact of Jal amphibolites with the gneisses of Indian plate in Bunar valley.	131
Plate 4.29	The contact between Jal amphibolites and the gneisses of Indian plate at Halala, in Bunar valley.	132
Plate 4.30	Strongly sheared and mylonitized amphibolites and granite of Jal unit in Thak valley.	132
Plate 4.31	Ptygmatic folding in Jal amphibolites, Thak valley.	134
Plate 4.32	Banding, shearing and folding in Jal amphibolites, Bunar valley	134
Plate 4.33	Banding and shearing in Jal amphibolites, Bunar valley.	135
Plate 4.34	Bands of amphibolite and granite in Jal amphibolites at Gabbar, Thor valley.	135
Plate 4.35	Bands of amphibolite and granite near the confluence of Chirat gah and Thak gah.	138
Plate 4.36	Mafic and felsic bands in parallel rows.	139
Plate 4.37	Same in crossed polars.	139
Chapter 5	The Thak Granitoid Sheets	
Plate 5.1	Alternating bands of diorites and Niat volcanics/ amphibolites at Gurmali in Niat valley.	199
Plate 5.2	Fine-grained xenoliths of different shapes and sizes in diorites.	199
Plate 5.3	Perfect alignment of elongated and flattened xenoliths along foliation in the diorites.	202
Plate 5.4	Sharp contact between the diorites (Khun) and Niat volcanics near Chakkar in Buto valley.	202
Plate 5.5	Medium- and coarse-grained, strongly foliated and sheared diorite.	207
Plate 5.6	Shearing with double deformation in a dioritic body exposed around Babusar Rest House, Thak valley.	207

Plate 5.7	Xenoliths of varying sizes in diorites.	208
Plate 5.8	Saussuritized plagioclase in Shai diorites.	208
Plate 5.9	Distribution of sphene in quartz diorite.	211
Plate 5.10	Quartz veins in fine-grained diorite, Keo valley.	211
Plate 5.11	Network of quartz veins in medium-grained diorite near Makheli in Thor valley.	214
Plate 5.12	Diorite from south of Gabbar showing chlorite, epidote, quartz, feldspar and sphene.	214
Plate 5.12a	Same in crossed polars.	215
Plate 5.13	Plagioclase with a lot of inclusions of epidote, apatite and sericite.	215
Plate 5.14	Foliated diorite consisting of plagioclase, quartz, muscovite and epidote.	216
Plate 5.15	Large grains of epidote with discrete zoning of different colours.	216
Plate 5.16	Diorite from Khun group consisting amphibole, chlorite, quartz, and muscovite.	218
Plate 5.17	Diorite consisting of a feldspar, quartz, amphibole, epidote, biotite and sphene.	218
Plate 5.18	Diorite from the south of Thak consisting of feldspar, quartz, hornblende and biotite.	221
Plate 5.19	Diorite consisting of plagioclase, quartz with amphibole and biotite.	221
Plate 5.20	Granite from minor body at Gabbar.	222
Plate 5.21	Trondhjemite from north of Utlā Babusar consisting of feldspar, quartz, amphibole and epidote.	222
Plate 5.22	Trondhjemite from south of Rehmal.	225
Plate 5.23	Plagioclase shows a strong normal zonation in trondhjemite.	225
Plate 5.24	Trondhjemite from north of Halala.	226

Plate 5.25	Trondhjemite from Utla Babusar showing the prismatic hornblende crystals.	226
Plate 5.26	Trondhjemite from north of Tushkal showing plagioclase, quartz, biotite and epidote.	227

ACKNOWLEDGEMENTS

I am extremely grateful to my supervisors for giving me the opportunity to work on the project. So, first of all, I would like to express thanks to Professor Dr. M. Qasim Jan and Dr. M. Asif Khan for continued guidance, enthusiasm and support and I am highly thankful to Dr. M. Asif Khan who analyzed samples for me in USA. I also received valuable assistance and great encouragement in scientific, social and domestic matters from my supervisors, friends, colleagues and family members during this project.

Three field seasons (1991, 1992 and 1993) in the area have been tied in mountaineering expeditions and I am extremely thankful to all my climbing and trekking companions for making each expedition so enjoyable and memorable. I was lucky enough in the company of a nice person Sufyan Qazi during the field trips. Little of this would have been possible without the friendly services of numerous local porters throughout the northern areas. Mohammad Akram of Besal provided first-class cooking and valuable local assistance. I would also like to thank Mohammad and Qamar Zaman for their hard and tough driving in the remote areas during the field work. I am pleased to acknowledge the cooperation of Rasool Mohammad and Mumtaz during the laboratory work. I extend my due regards to Sabz Ali and Mir Alam for their late time services during this work. Financial support was provided from NSRDB grant (ESC 24) to M. Qasim Jan for defraying part of the field expenses.

I would like to express my sincerest thanks to Professor A. A. K. Ghauri, Dr. Hamidullah, Dr. Tahir Shah, M. Irshad, Tazeem Khan, Ismat and ShahJahan who provided me full cooperation and hospitality during my time in Peshawar. Special thanks to the members of the tea club who gave me a very special and friendly environment and also added worthwhile information about the spectrum of life and society to my knowledge.

I am grateful to Ch. Abdul Hameed (former Principal and Director), M.H. Mussaddi (Principal, G.C. Sargodha), Malik Mureed Hussain (Principal, G.A.M.C. Sargodha), Munawar Ahmed and Zahid Naveed (lecturers), whose encouragement and cooperation helped me to pursue my Ph.D research. I am also thankful to my students and friends who spared me for a long time for this research work with open heart and smiling face.

Finally, I would like to thank my parents, brother and, particularly, my wife Rizwana, who have been a constant source of support and beads of moisture.

ABSTRACT

The Kohistan island arc terrane in the northwestern Himalayas of N. Pakistan is sandwiched between the Indian and Karakoram plates. Structures related to collision tectonics have exposed more or less a complete crust of the arc terrane from its very base at Moho to its subaerial volcano-sedimentary cover. Within southeastern Kohistan, recent geological mapping along a N-S transect across the lower to middle crustal part of arc terrane, provides new and important information relating to the magmatic emplacement of the principal units. The base of the arc here, is occupied by a major stratiform ultramafic-gabbroic complex (the Sapat-Babusar complex), which overrides the crust of the Indian plate along the Indus suture (i.e., the Main Mantle Thrust; MMT). The complex was intruded into the base of a thick pile of metavolcanics (the Kamila belt), which comprise a tectonic collage of MORB-type tholeiitic basalts (Jal-Niat amphibolites), island-arc tholeiites (Babusar amphibolites) and calc-alkaline andesites (Sumal amphibolites). The Chilas complex comprising ultramafic and gabbro-norite rocks, is also intrusive into the Kamila belt but unlike the Sapat-Babusar complex, it was emplaced onto the top, rather than the base, of the belt. The Kamila belt is intruded by a suite of granitoid rocks (gabbro, gabbro-diorite/tonalite-granodiorite-granite and trondhjemite). The first group is closely comparable with the host Jal-Niat amphibolites, second group rocks are similar to the subduction-related plutonic rocks from Kohistan (e.g., Kohistan batholith), and the trondhjemites were formed from the partial melting of Jal-Niat amphibolites. The field relations suggest a two-stage history of crustal thickening in lower and middle part of the arc crust. From its initiation at ca. 125-120 Ma until ca. 90 Ma, the arc grew by magmatic emplacement, into its base, of stratiform ultramafic-gabbroic plutonic complexes, one below the other. In stage two, the focus of crustal growth shifted upwards from the base of the arc with the emplacement of the Chilas complex on top of the Kamila belt. This stage of crustal thickening was accompanied by crustal shortening associated with 90-80 Ma aged Kohistan-Karakoram collision.

Chapter 1

INTRODUCTION

The Northern Areas of Pakistan lie between latitudes 35° and 37° N and longitudes $72^{\circ} 30'$ and 77° E, comprising Baltistan (Skardu and Gangche, Khapalu), Ghizar (including Gupis, Yasin and Ishkuman), Gilgit (including Hunza and Nagar) and Diamir (Chilas) districts (Figure 1.1). These cover a total area of 60,000 square kilometers and constitute the highest mountain region of the world. The region under discussion has a rugged topography and a very high relief. Some famous peaks (like K-2: 8611 meter, Nanga Parbat: 8125 meter and Rakaposhi: 7788 meter high) with all their glamour and mystery are present in the Northern areas. Numerous peaks are perpetually snow-covered and the area is the most extensively glaciated outside the polar regions. Three mountain ranges, the Karakoram, Hindukush and Himalayas, occupy the region. Indus, Gilgit, Hunza and Shigar rivers, along with their numerous tributaries, drain the area. Population is sparse and restricted to irrigated plains in rugged ranges. Skardu, Hunza, Gilgit and Chilas are the main towns.

The area investigated during the course of the present work is located to the south of Chilas. It lies between latitudes 35° to $35^{\circ} 20'$ N and longitudes $73^{\circ} 45'$ to 75° E, and covers about 600 square kilometers. Chilas is the headquarter of Diamir district and falls in the Survey of Pakistan toposheet No 43/I, 1: 250,000. Some 492 km from Islamabad, it is situated along the Karakoram Highway (KKH). The KKH is a metalled and all-weather road, but temporary road closures happen due to rock sliding and mud flow.

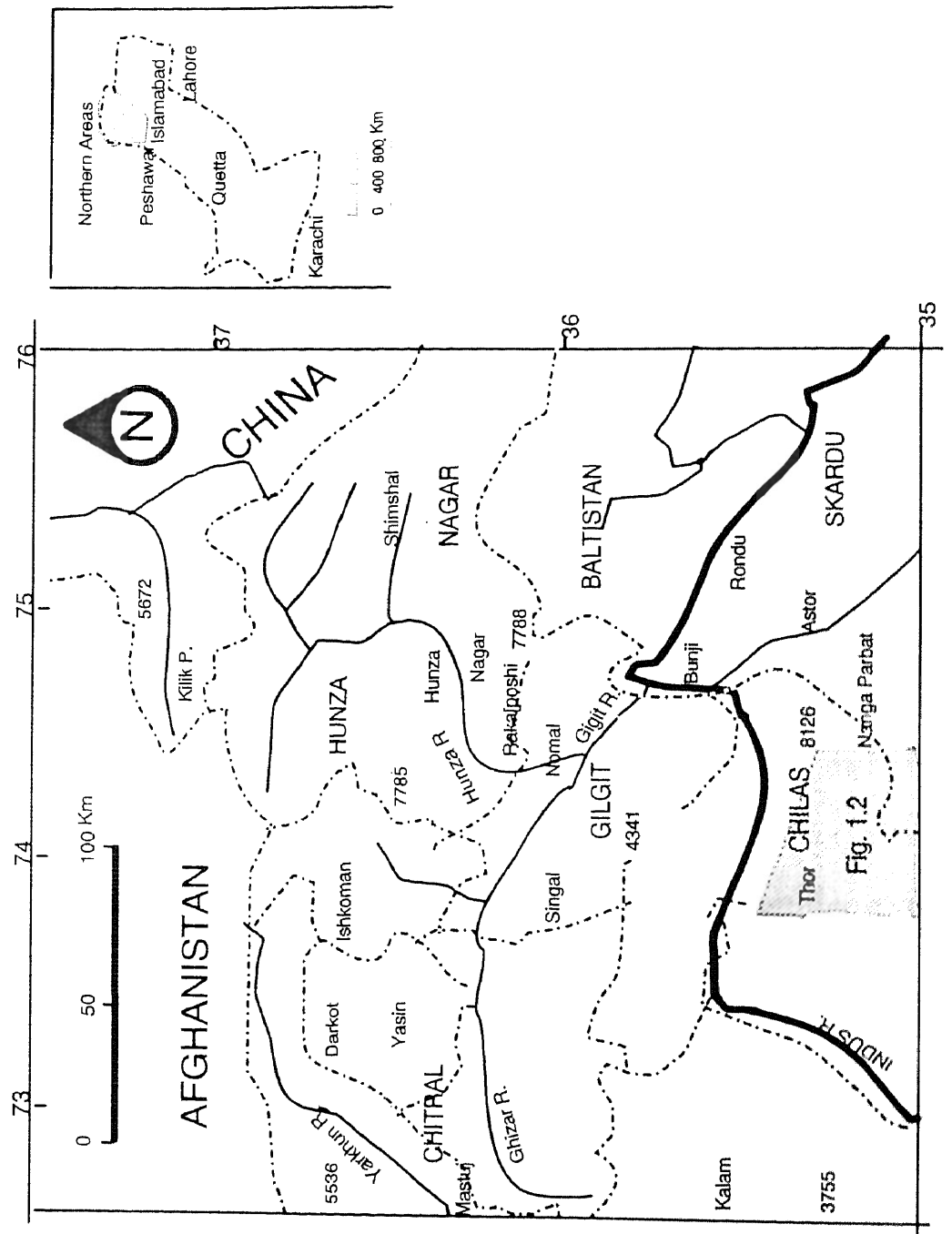


Figure 1.1. Simplified geographic map of northern Pakistan showing the studied area, major towns, rivers, peaks and district boundaries.

The project area is in the south-eastern part of Kohistan, between the Chilas Complex (gabbros/ gabbro-norites with subordinate ultramafic rocks: Khan et al., 1989) in the north and the rocks of the Indian plate in the south. The latter are separated from the Kohistan arc by a major fault known as the Main Mantle Thrust (Tahirkheli et al., 1979). In the east, the lithologies of the thesis area are juxtaposed against the Nanga Parbat-Haramosh massif. The area is accessed by southern tributaries of Indus river, from west to east: Thor, Buto, Thak, Niat and Bunar gah (Figure 1.2). The maximum height is 4646 m near Buto gah gali and 1538 m is the minimum at Bunar.

The present study involves a detailed characterization of the area, in terms of mapping, petrology, geochemistry and tectonics. The area is occupied by the ultramafic rocks, layered gabbros (now changed into banded amphibolites), metavolcanics, diorites and granites. All the rocks are deformed and display foliation and lineation. Shear zones, forming blastomylonites and mylonites are developed in all the lithologies. This area could not be surveyed for a long time due to difficulty of access. Previous studies are preliminary, but in the recent past Ghazanfer and Chaudhry (1991) have given a more detailed account.

Previous Work

Prior to the partition of India and Pakistan, a number of geologists (e.g., Lydekar, 1882, 1883, McMahon, 1900; Hayden, 1916; Wadia, 1932) provided a base for geological investigation of northern Pakistan. After 1950, many geologists worked on the Karakoram and Hindukush ranges and published their findings in different journals. There also are many regional papers on the geology of North Pakistan, with special reference to its tectonic framework. Most of these studies are confined to readily accessible valleys.

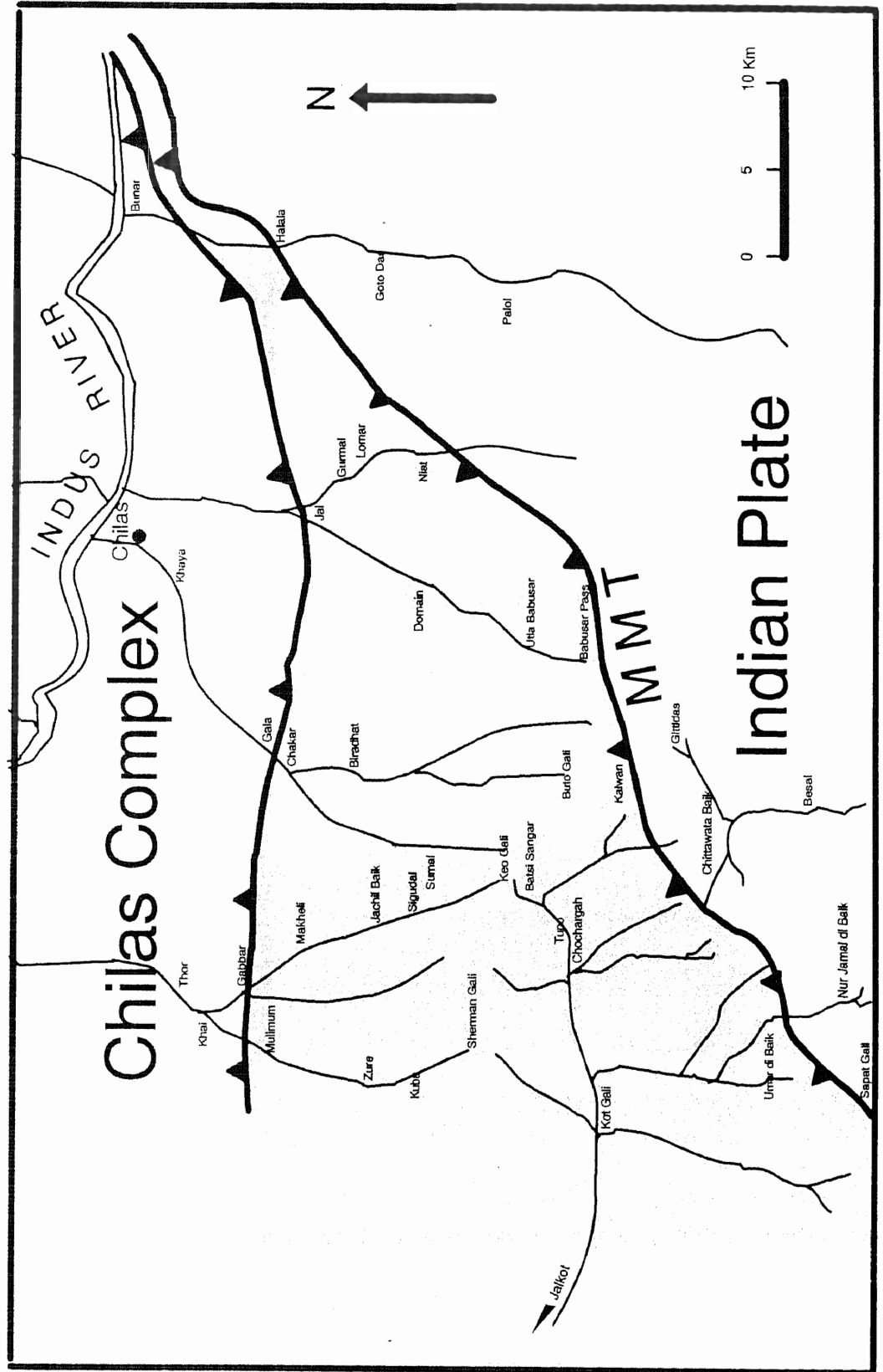


Figure 1.2. Map showing the investigated area, bounded by the Chilas Complex in the north and the Main Mantle Thrust in the south with the main valleys, from west to east - Thor, Buto, Thak and Bunoar, and upper Jalkot in the southwest.

Martin et al. (1962), Jan and Tahirkheli (1969) and Jan and Kempe (1973) separated the igneous rock series of Kohistan terrane from the Indian plate rocks. Tahirkheli et al. (1979) named the major thrust separating the two terranes as the Main Mantle Thrust and assigned it the status of a suture zone. Previously, Ivanac et al. (1956) and Bakr and Jackson (1964) presented comprehensive and systematic geological accounts of the Gilgit and Hunza areas. The stratigraphy and rock nomenclature used by them was accepted widely. Gansser (1964) proposed a three-fold subdivision of the area, viz. the northern sedimentary zone, a central metamorphic zone, and a southern volcanic schist zone. Subsequently, he (1978, 1979) provided a more comprehensive account of the stratigraphy, tectonics and magmatism of the Karakoram and Hindukush. Desio (1964) described sedimentary and metamorphic formations and different igneous bodies in the Gilgit, Khunjerab, and Skardu areas. Earlier (1974) he described the Kohistan region as a tectonic zone of the Karakoram.

Discovery of blueschists (Shams, 1972) provided a base for tectonic modelling of the area. By late seventies, in the light of plate tectonic theory, Tahirkheli and Jan (1979) and Tahirkheli et al. (1979) defined the "Kohistan island arc sequence". Sufficient geological data had been collected by then, resulting in a preliminary geological map. They proposed that the Kohistan terrane represents an ancient island arc trapped between the Indian and Eurasian Plates. Bard et al. (1980) and Bard (1983) presented an account of the metamorphism of the area and a tectono-metamorphic model for its evolution. Coward et al. (1982, 1986) described the structure of the Kohistan arc and adjacent areas as part of the tectonic framework of north Pakistan, followed by more details by Coward et al. (1987).

The eastern and western parts of the Kohistan batholith have been extensively surveyed in accessible valleys. Calkins et al. (1981) reported abundant occurrences of granitic rocks along the Indus, Gilgit, Ghizar, and Swat rivers. Jan and Asif (1983) presented geochemical data for calc-alkaline plutonic rocks from Swat Kohistan. Radiometric ages of the plutonic rock of the batholith vary between 102 Ma and 29 Ma (Casnedi et al., 1978; Windley et al., 1986; Debon et al., 1987; Treloar et al., 1989; Petterson and Windley, 1985, 1991; Petterson et al., 1993).

The first important work in the southern part of Kohistan terrane in Swat area was carried out by Martin et al. (1962). They described the main lithological units, and reported that a fault separated the "upper Swat Hornblendic group" (the southern Amphibolite Belt of the Kohistan Arc) from the "lower Swat Buner schistose group". Jan (1970), Jan and Mian (1971), and Jan and Kempe (1973) mapped much of the Swat valley. In a preliminary petrological study, Jan and Kempe (1973) pointed out the similarities of the amphibolites and gabbro-norites of the Swat area with those of the (calc-alkali) basalt-andesite series of orogenic belts. From geochemical data, Jan (1977) also concluded that the basic rocks from the southern parts of the Kohistan area have chemical affinities of calc-alkaline magmatic rocks of orogenic belts and island arcs. Chaudhry et al. (1974, 1977) performed extensive field and petrographic studies in Dir district and published several reports.

Geographically and geologically, Kohistan is a very large area and a very big mass respectively. So far it has been studied only in isolated patches. The previous studies conducted in various parts of the Kohistan terrane are mostly restricted to those valleys which are easily accessible. Shams (1975), Ahmed and Chaudhry (1976), and Khan and Thirlwall (1988) performed preliminary studies in

the Thak valley, followed by a more detailed account of the area north of MMT by Ghazanfer and Chaudhry (1991). The area lying between the Chilas Complex in the north and MMT in the south is the focus of the present research. This area was ignored because of high altitude and relief, remoteness and inaccessibility.

Aims and Objectives

The Kohistan sequence in north Pakistan is unique for its exposure of a more or less complete island arc crust. Several studies have been performed on detailed aspects of various lithologies along accessible routes and valleys in terms of field disposition, mineralogy, petrology, metamorphism, structure and radiometric dating. The main purpose of the present research is to understand the geological evolution of the southeast Kohistan which was not studied in detail prior to this work. The study deals with rocks exposed between the Chilas Complex and the Main Mantle Thrust in different valleys which, from west to east, are: Thor, Buto, Thak, Niat, and Bunar. The main objectives of this research are:

- 1– Preparation of a detailed geological map on 1: 50,000 scale, delineating the principal component lithologies.
- 2– Observation and collection of field data for structural, stratigraphic and petrological analyses.
- 3– Construction of cross-sections to improve the interpretation of structures, in terms of three dimensional geometry.
- 4– Investigation of the mineralogy, geochemistry and petrogenesis of the rocks.
- 5– Integration of field and laboratory studies into a model for the geotectonic history of the Kohistan arc.

Thesis Format

This study is a small contribution to understand the tectonic evolution of Kohistan terrane and presented in the following way. From the present Chapter 1 of introduction is followed by Chapter 2, which places the Kohistan arc terrane in a regional perspective. This involves a brief review of the geology of the Himalaya paying particular attention to the Cretaceous to Recent subduction-related magmatism. A review of the geology of the Kohistan arc terrane with a brief description of local geology is also presented in this chapter. A preliminary introduction of Sapat mafic-ultramafic complex of the Indus suture zone is presented in Chapter 3, along with field relations, petrology and geochemistry. Chapter 4 examines the detailed aspects of the amphibolite rocks of the area in terms of their distribution, field features, petrology, geochemistry and, finally, their possible tectonic origin. Chapter 5 describes the field relations, petrography and geochemical characteristics of the granitoid rock occurrences in the field area. The trondhjemites, found within the upper middle part of the studied area, are also examined briefly in this chapter. Finally, Chapter 6 presents a synthesis of the magmatic and tectonic history of the southeast Kohistan, along with a tectonic model.

An ample variety of data was collected and generated during this study just as in any multi-disciplinary regional study. This is listed in the Appendices at the end of the thesis. Appendix 1 tabulates all handspecimen descriptions and indicates which samples were selected for geochemical and petrographic investigation. Details of topographic base-maps are presented in Appendix 2.

Methodology

This research project involves a detailed field survey and intensive laboratory work. Survey of Pakistan toposheets Nos. 43 E/12, 43 E/15, 43 E/16, 43 I/3, 43 I/4, 43 I/7 and 43 I/8 were used as base maps. The field work includes:

1-- Mapping of about 600 square kilometers area south of Chilas on a scale of 1:50,000, with additional details in geologically important areas such as Chochar Gah, Umar Di Baik, Sapat Gali, Jalkot Nala and Saleh Di Baik.

2-- Collection of more than 350 representative rock samples for petrographic and geochemical studies. A total of 170 rock samples were selected for thin-section study to identify the rock units and their petrographic characteristics.

Based on these studies, samples were chosen for major and trace element whole-rock analysis. Shimadzu (VF-310 model) X-Ray Fluorescence Spectrometer was used for the analysis. Much of the laboratory work was conducted in the MCI in Geology University of Peshawar, Peshawar. Samples were also analysed at the University of Oklahoma, Norman, USA. The data obtained from the selected samples is used to formulate a base for the petrogenesis of the studied rocks of southeast Kohistan. The two sets of data demonstrate similar concentrations of major and trace elements.

Laboratory Techniques

For whole-rock analysis, samples were cleaned, crushed and powdered in the following way. Weathered surfaces were removed by hammer. Large samples were split to <1cm using a Jaw crusher. Approximately 50 g of sample was put in a tungsten carbide ring of Swing Mill for two minutes to powder it to 200 mesh. This powder was stored in a sealed plastic bag. To minimize the possibility of contamination, each time the tungsten carbide ring was cleaned carefully and dried

after every run. The 200 mesh powdered sample was further powdered for 5 minutes to gain the fine powder (300 mesh) by using the Heiko Vibrating Mill. This fine powder was used for making the pellets and fused glass discs (beads) to analyse the trace and major elements, respectively.

Trace elements were analysed from 46 mm diameter pressed powder pellets using 15 g of powdered whole rock. A powdered pellet was pressed at 18 tons per square inch by using Shimadzu press machine, and allowing the pellet to dry overnight. The pellet was labelled with a number, each storage bag was also labelled with the number. Samples were run on a Shimadzu X-Ray Fluorescence Spectrometer fitted with Rhodium tube. The analysed elements are Nb, Zr, Y, Sr, Rb, Th, Pb, Ga, Zn, Cu, Co and Ni. During each machine run a set of international and internal standards was run to monitor the machine accuracy and precision.

Major elements were determined from fused glass discs. Fused discs were prepared by the following method. Approximately 4-5 g of each powdered sample was dried overnight at 110 °C to remove H_2O^- . Loss of ignition (H_2O^+) was calculated after the dried sample was placed in a muffle furnace at 950 °C to 1000 °C for four hours. Porcelain crucibles were used to contain the samples inside the furnace. All major element analyses were performed on glass discs (fusion beads). To make the bead, 1.0 g of ignited sample was thoroughly mixed with 5.0 g of flux (lithium tetraborate). The sample and flux mixture was ignited in a 95% Pt/ 5% Au crucible at 950 °C to 1000 °C for 10 minutes. While preparing the beads, the crucible was swirled over a burner continuously to ensure the homogeneity of the melt. The melt was cast between aluminium discs, and left between the discs for 5 minutes to ensure annealing. After labelling, the finished bead was stored in a polythene bag before analysis. Twelve USGS standard reference samples were

used for the calibration of the instrument. One standard reference sample was used with every group of six samples to check the precision of the instrument.

Relative accuracies could be derived from the standardised sample calibration curves. Standard deviation and variance fell within acceptable limits for both the major and trace elements. Matrix corrections were calculated from the major element composition. The results were normalised on a volatile-free basis with total iron expressed as Fe_2O_3 . A total of 21 major and trace elements were analyzed. Accuracy for the major elements in weight percentage of the amount present is: $\text{SiO}_2=0.02$; $\text{TiO}_2=0.009$; $\text{Al}_2\text{O}_3=0.12$; $\text{Fe}_2\text{O}_3=0.09$; $\text{MgO}=0.05$; $\text{CaO}=0.07$; $\text{Na}_2\text{O}=0.04$; $\text{K}_2\text{O}=0.05$ and $\text{P}_2\text{O}_5=0.009$. Accuracy for the trace elements determination in parts per million is: $\text{Nb}=0.5$; $\text{Zr}=0.9$; $\text{Y}=0.8$; $\text{Sr}=1.1$; $\text{Rb}=0.7$; $\text{Th}=0.5$; $\text{Pb}=0.6$; $\text{Ga}=1$; $\text{Zn}=1.6$; $\text{Cu}=1.3$; $\text{Co}=2.2$ and $\text{Ni}=1.8$.

Chapter 2

REGIONAL SETTING

Initial Statement

The Kohistan terrane, which is the focus of this research, developed as a consequence of northwards subduction of Tethyan oceanic crust of the Indian Plate and as such is intimately linked to the overall evolution of the Himalayan orogeny. Thus the primary concern of this chapter is to place the Kohistan terrane in a regional perspective. This is achieved by examining the general geology of the Himalaya with a particular attention to those aspects which are most pertinent to subduction-related processes. A brief review of the tectonic history of Kohistan, both prior to and subsequent to accretion with Eurasia, is followed after the individual tectonic features have been described. The geology of different units of Kohistan terrane is described briefly in this chapter. In addition, the existing tectonic and magmatic models for Kohistan are commented briefly. Finally, a short description of the local geology and structure of the studied area is presented in this chapter.

Introduction

North Pakistan is located to the south of the Pamir knot which is a union of some of the world's greatest mountain ranges including Himalaya, Karakoram and Hindu Kush. The NW-SE strike of the western end of the Himalaya and Karakoram is almost perpendicular to the NE-SW strike of the Hindu Kush. Nanga Parbat Haramosh massif separates the Ladakh and Deosai plateau in the east from Kohistan in the west. The highlands of Ladakh and Deosai plateau recede south into the valley of Kashmir, the Pir Panjal ranges, and finally the plains of northern

India. The Kohistan highlands pass south into the foothill regions and major valleys, from west to east, of Dir, Swat, Indus, Hazara and Kaghan. Further south are located the hill ranges, from west to east, of Attock Cherat, Kala Chitta, Margala and the Galis. In the west, Peshawar and Attock basins lie between the foothills and hill ranges. The Kohat and Potwar Plateaus lie south of the hill ranges and are bound by the frontal mountains of the Salt Range. South of Salt Range, the plains of the Indus foreland basin extend up to the sea (Figure 2.1).

This thesis examines the southeastern part of the Kohistan terrane immediately to the west of the Nanga Parbat syntaxis. A major part of this research has been executed in parts located remotely from the major metalled roads. The study area is located to the south and southwest of Chilas town and covers the valleys of Thor (west), Buto, Thak, Niat and Bunar Gah (east) and upper reaches of Jalkot. The area examined is bounded by the MMT in the south and Chilas Complex in the north, and consists of rocks generally metamorphosed under amphibolite facies conditions. These are represented by massive or banded amphibolites with ultramafics, gabbros, diorites, tonalites, granites and trondhjemites.

Plate Tectonic History of North Pakistan

South-Central Asia is a tectonic amalgamation of microplates of both Eurasian and Gondwanic affinities. The original boundary of Eurasia is preserved in the Kun Lun-northern Pamir parts of the Central Asia. The Gondwana supercontinent was a coherent block till Triassic (Parker and Gealy 1983). When it suffered regional rifting and block faulting, a strip of the northern margin of Gondwana (now called Karakoram Plate or block) separated from the main mass, started rotating anticlockwise, and drifted northward to be accreted to the Asiatic

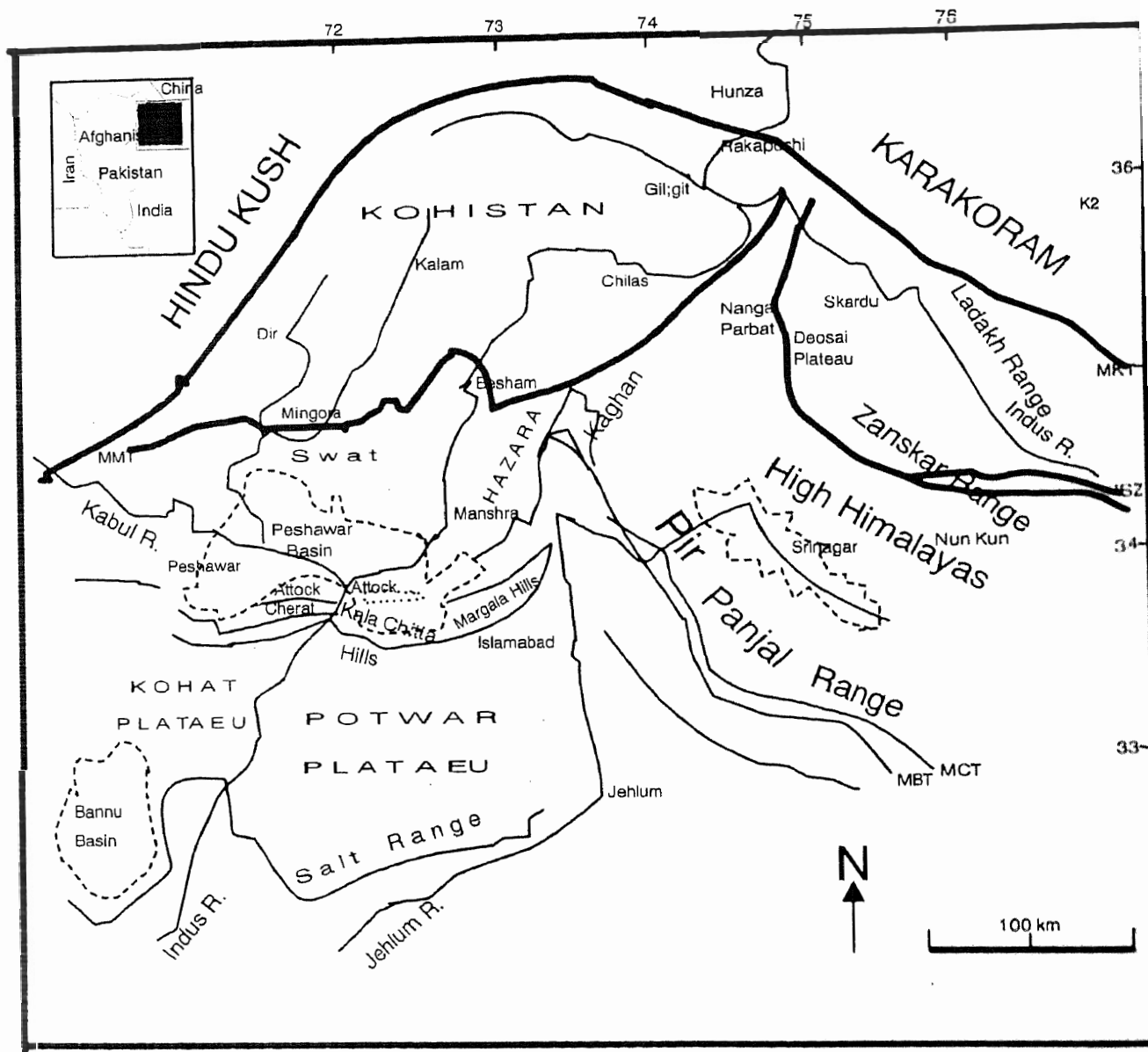


Figure 2.1. Regional map of north Pakistan showing the relationship between the main tectonic elements, plateaus, mountains and hill ranges.

continent by the end of Jurassic time (Gaetani, 1990). The Indian plate was separated from the eastern Gondwanic continent about 120 Ma ago in early Cretaceous (Powell, 1979). Upto 80 Ma ago, India moved northwest relative to Australia and Antarctica at a rate of 3 to 5 cm/yr. From 80 Ma to approximately 53 Ma, it moved rapidly towards north relative to Australia and Antarctica, at an average rate exceeding 15 cm/yr. From 53 Ma to the present, India seemed to have moved northward at much slower rates of 4 to 6 cm/yr (Powell, 1979). The abrupt slowing down is almost surely a consequence of the collision with Eurasia during the early Tertiary (LeFort, 1975; Molnar and Tapponier, 1977; Powell, 1979; Klootwijk et al., 1992). The collisional boundary in southern Tibet is traceable along the Indus-Tsangpo suture (ITS), which bifurcates further west into the Main Karakoram Thrust (MKT), also called as Northern suture (Coward et al., 1982, 1986; Pudsey, 1986) or Shyoke suture (Rex et al., 1988; Searle et al., 1989), and the Main Mantle Thrust (MMT, also referred to as the Indus suture). The two sutures have been regarded to enclose an ancient island arc terrane called the Kohistan-Ladakh Island arc (Figure 2.2). It is believed that closure between the Kohistan-Ladakh and the Karakoram plate occurred along the MKT in the north some 85-102 Ma ago (Pettersen and Windley, 1985; Treloar et al., 1989) and that between the Kohistan-Ladakh and the Indian plate along MMT in the south about 55 Ma ago (Powell, 1979; Klootwijk et al., 1992).

Afghanistan

In southern Afghanistan, there are indications that this region formed the continental margin of Eurasia prior to the Mesozoic (Tapponnier et al., 1981). During the Mesozoic, the southern Afghanistan experienced accretion of terranes which belonged to Gondwana during the Palaeozoic (Tapponnier et al., 1981).

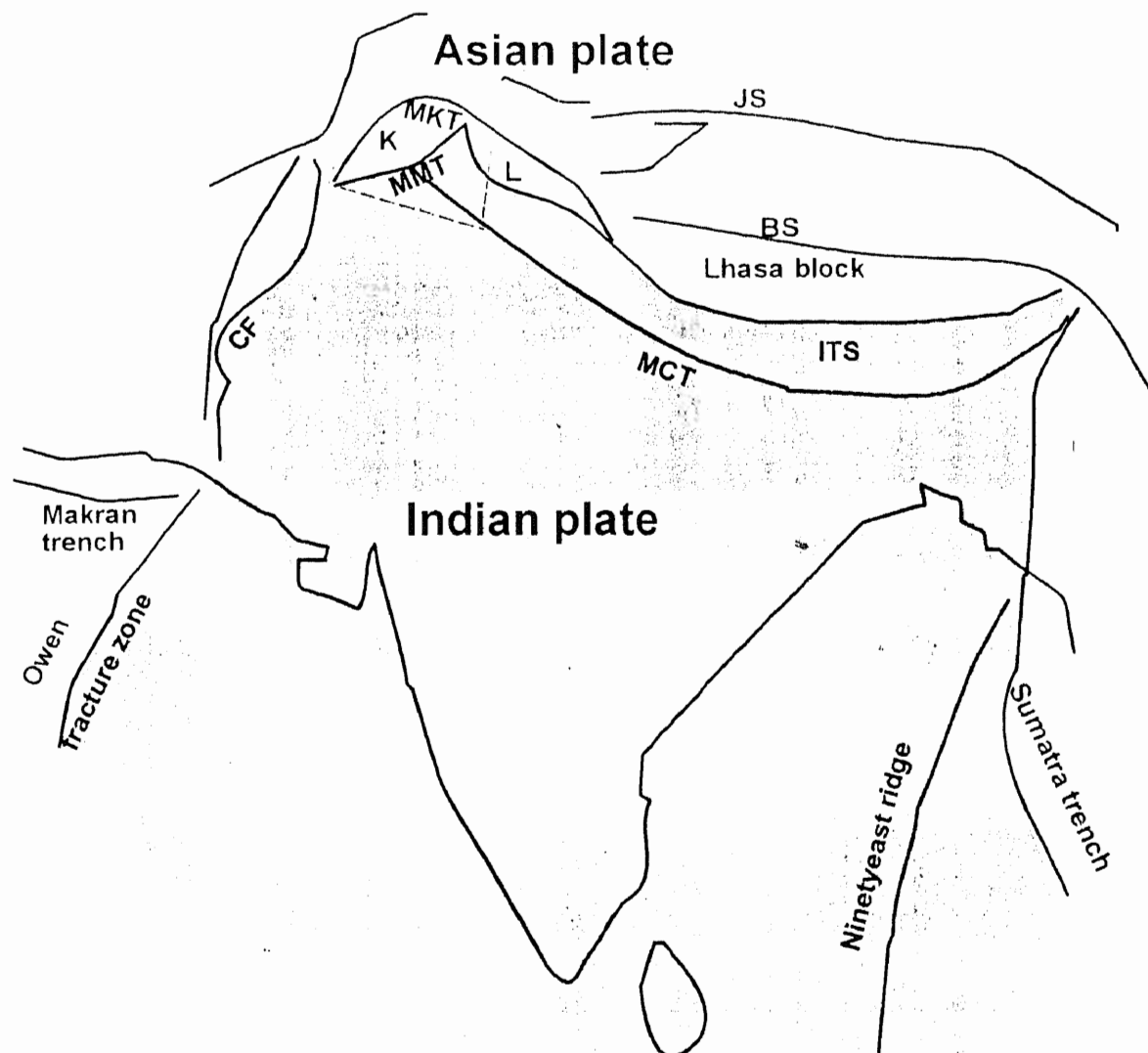


Figure 2.2. Sketch map of the Indian plate (shaded) and its margins, showing the tectonic position of the Kohistan and Ladakh terrane (modified after Pudsey, 1986).

ITS= Indus Tsangpo Suture, MKT= Main Karakoram Thrust, MMT= Main Mantle Thrust, MCT= Main Central Thrust, K= Kohistan, L= Ladakh, JS= Jinsha Suture, BS= Banggong Suture and CF= Chaman Fault.

These blocks have Precambrian basement, and were intruded by 500 Ma granitoids related to crustal anataxis subsequent to crustal thinning (Debon et al., 1987a).

A Triassic calc-alkaline batholith records subduction of Paleo-Tethys within western Badakhshan and the western Hindukush. This culminated in ocean closure and accretion of the Farah Terrane along the Herat Suture. It is not clear whether this subduction was to the north (Tapponnier et al., 1981) or to the south (Debon et al., 1987a). This collision was also responsible for Jurassic deformation within the Hindu Kush. This first suturing event was followed to the south by accretion of South Central Afghanistan (Helmand Terrane) along the Panjao Suture in the late Jurassic. This collision gave rise to further deformation and obduction of the Panjao ophiolite (Blaise et al., 1978).

After this collision, subduction migrated southwards with the development of an extensive Upper Jurassic-Lower Cretaceous calc-alkaline magmatic arc within South Central Afghanistan. During the mid-Cretaceous, plutonic activity was particularly intense resulting in the Helmand, Arghandab, Safed-Khers and Wakhan plutonic belts (Debon et al., 1987a). These plutons and associated volcanics, represent the western end of the Trans-Himalayan Batholith. The Upper Cretaceous Albian-Aptian Kandahar Volcanics represent volcanism and sedimentation within a marginal basin during the initial stages of Neo-Tethyan subduction (Montenat et al., 1979).

During the Palaeocene, the Zhob, Khost and Muslimbagh ophiolites were emplaced onto the western margin of the Indian plate (Asrurallah and Abbas, 1979; Searle, 1986). However, the Kabul block remained separate from India by oceanic crust to the east and southeast until the mid- to late Oligocene. Treloar et al. (1992b) suggests that an eastward extension of the Kabul block collided with

India prior to 51 Ma and was responsible for the anomalous thickening and metamorphic ages recorded within Indian plate metasediments (Treloar et al., 1992b).

Tibetan Plateau

This plateau extends from the northern side of the Trans-Himalayan magmatic belt to the southern side of the Kun Lun range. Regionally it can be divided into three microcontinental fragments: Lhasa, Changtang (Qiantang) and Kun Lun terranes, separated by the Banggong-Nujiang and Jinsha sutures respectively (Chang et al., 1986)(Figure 2.3). The Kun Lun represents the Hercynian margin of the Eurasia and as such correlates with the Northern Domain in Afghanistan (Tapponnier et al., 1981). Formation of the Jinsha suture during late Triassic-early Jurassic times signalled the demise of Palaeo-Tethys and the opening of Neo-Tethys (Sengor, 1986). However, more problematical is the origin of the Banggong suture. Remnants of dismembered ophiolites occur along the suture and cover the northern part of the Lhasa terrane (Girardeau et al., 1985). The suture formed in the late Jurassic-early Cretaceous (Lin and Watts, 1988) and is believed to represent closure of a marginal basin or small sea (Tanggula-Waser ocean) which separated a microcontinental archipelago which had crossed the Neo-Tethys.

The northern part of the Lhasa terrane consists of Precambrian gneissic rocks overlain by Carboniferous to Jurassic sediments. These in turn are covered by a thick lower Cretaceous shallow shelf succession which become more continental with time (i.e., red bed of the Takeda Formation). The southern part of the Lhasa terrane consists of amphibolites with an overlying Triassic-Jurassic sedimentary succession.

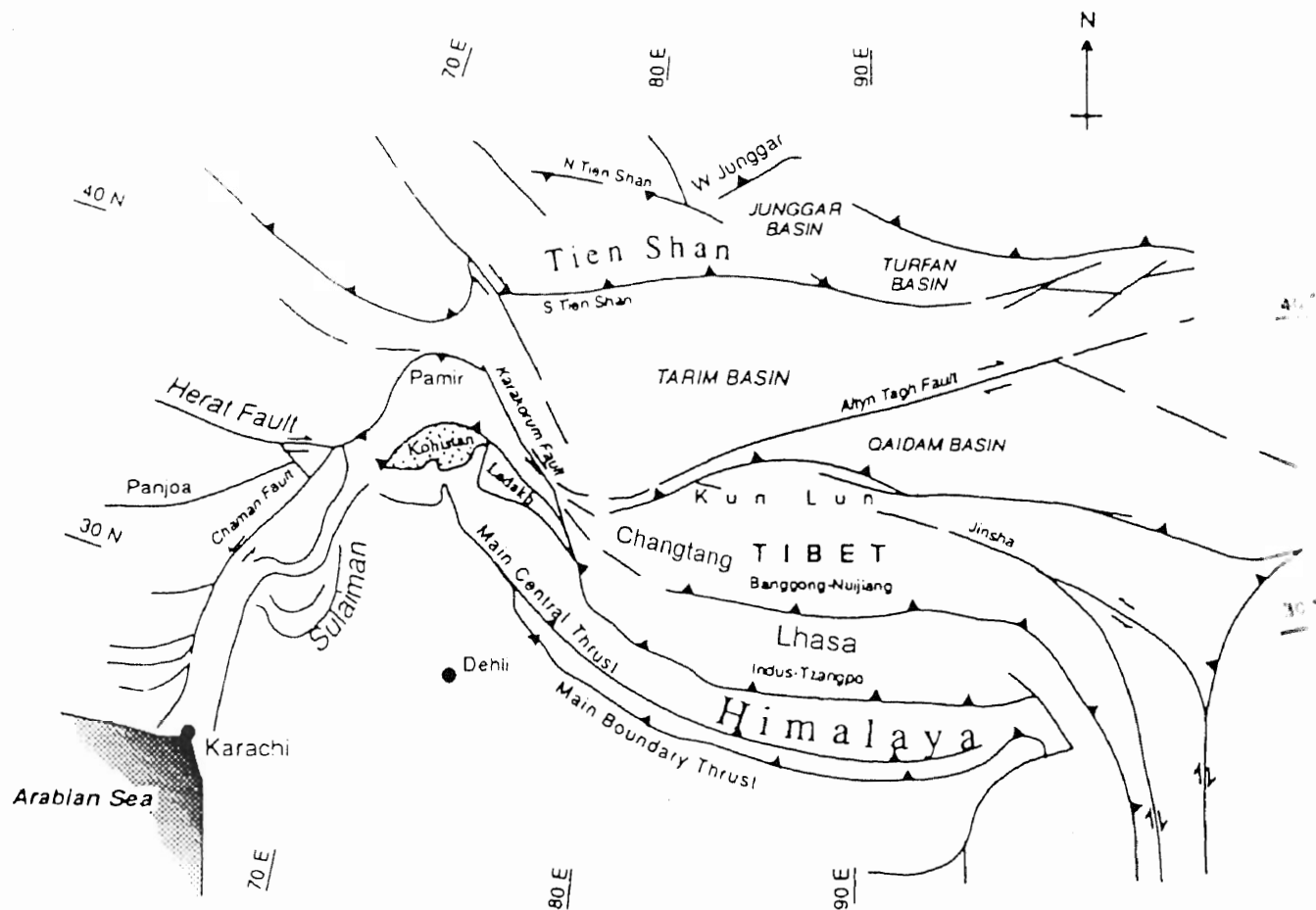


Figure 2.3. Sketch map of central Asia showing Himalayas, Karakoram, Hindukush, Pamirs, Tien Shan and Kun Lun mountain ranges, and the three microcontinental fragments, Lhasa, Changtang(Quantang) and Kun Lun terranes seperated by the Bonggong-Nujiang and Jinsha sutures(after Searle and Tirrul, 1991).

Within Tibet, igneous activity is recorded somewhat discontinuously from Cambrian to Recent times. Xu et al. (1985) reported a 513 ± 14 Ma age from granitic gneisses within the Changtang block and this confirms a Gondwana origin. However, as yet no igneous rocks have been identified which date the closure of Palaeo-Tethys. Gariepy et al. (1985) reported Pb isotope data for the Anduo and Bange intrusive belts (120-140 Ma) which indicate crustal anataxis that was a direct consequence of crustal thickening during and subsequent to formation of the Banggong-Nujiang Suture.

Direct correlation can be drawn between the events recorded in Tibet and those in the Karakoram and in Afghanistan. The Changtang terrane is identical to the North Central Domain with the Banggong-Nujiang suture equivalent to the Panjao suture. Furthermore the Lhasa terrane is probably equivalent to the South Central Domain and the Karakoram microplate.

Karakoram Plate

The Karakoram plate is a crustal block which belongs to the geopuzzle of Central Asia, lying between the Himalayan range and the Pamirs, and was formed by repeated collisions of continental blocks and plates, from Jurassic to Present (Gaetani et al., 1996). Tapponnier and others (1981b) considered it to be a part of the Gondwana plate and it may be equivalent to the Lhasa microplate.

The oldest rocks of the Karakoram microplate are Paleozoic sediments which are exposed between the Main Karakoram thrust (MKT) and the Afghanistan border to the northwest of Kohistan, in the Hindukush (Pudsey and others, 1985; Pudsey, 1986). One isolated Ordovician outcrop was reported at Baroghil, but a Devonian unit of dominantly carbonate rocks (limestones, dolomites, quartzites, and calcareous sandstones) extends from NNE of Chitral town eastwards through

Buni and possibly all the way to Baroghil, immediately NW of the Reshun fault (Talent et al., 1982). This lithology provides an evidence of very shallow marine conditions on a continental shelf. Gaetani et al. (1996) also suggested that the area remained for most of the time under subaerial to shallow water conditions.

To the northeast of Kohistan, along the Baltoro glacier toward K2, well-cleaved Carboniferous slates are overlain by a Permian-Triassic and Jurassic carbonate sequence (Desio, 1964, 1979; Desio and Zanettin, 1970). The Baltoro black slates are underlain by fissile shales and highly strained conglomerates interbedded by lithic tuffs and intruded by subvolcanic porphyries and quartz diorites. A carbonate platform of Mesozoic age was stable on this Tethyan plate margin until initial collision of the Karakoram microplate with the Kohistan-Dras island arc to the south during the mid-Cretaceous.

The western part of the Karakoram plate includes Upper Palaeozoic to Tertiary lithologies. Pudsey et al. (1985) identified two tectonic units separated by a northward dipping reverse fault (Reshun Fault). The northwestern Lutkho-Turikho terrane is structurally complex, comprising Devonian carbonates (Talent et al., 1982) and Devonian-Permian shales, quartzites and minor limestones (Lun Shales - Desio, 1959). Minor tuff horizons and andesitic debris is present within shales. Metamorphic grade varies from lower greenschist facies to garnet-staurolite to the northeast of the Tirich Mir pluton. This foliated granitoid is dated at 115 ± 4 Ma (Rb-Sr on biotite - Desio, 1964), and represents a continuation of the Karakoram batholith.

The central Kunar-Yarkhun terrane is bounded to the north by the Reshun fault and to the south by the Shyok Suture. The oldest rocks are the Permian-Carboniferous Darkot Group (Ivanac et al., 1956) that consists of slates and quartzite, and a few major carbonate beds (Yarkhun Limestone). To the west, the

Chitral Slates of possible Jurassic age replace the Darkot Group. Associated with these slates are greenschists believed to represent meta-tuffs (Pudsey et al., 1985). The early Cretaceous Krinj Limestone (Desio, 1959) overlies the Chitral Slates and interfingers tectonically with the Reshun Formation. It attains a maximum thickness of 2500 m and is probably equivalent to the southern Gahiret Limestone which has a similar thickness. The Tertiary molasse of the Reshun Formation varies considerably in thickness and represents material shed from the Kohistan arc. Most contacts of the Reshun Formation are tectonic, but in the vicinity of Reshun it conformably overlies Chitral Slate and Koghozi Greenstone.

The Northern Suture

This suture separates the Cretaceous-Tertiary Kohistan-Ladakh Arc from the late Paleozoic metasediments of the Karakoram Plate and is also called as Main Karakoram Thrust (MKT) and Shyok Suture in Ladakh. The Northern suture was closed in late Cretaceous times (Tahirikheli et al., 1983; Coward et al., 1985). This is based on (a) an Aptian-Albian age for limestones of the Yasin Formation (Pudsey et al., 1986); (b) structural evidence, i.e. the volcanics and sediments of the Kohistan Arc are folded into steeply inclined, northward-verging folds with associated thrusts along the suture (Coward et al., 1986); and (c) 100 Ma and 80-85 Ma ages respectively for deformed granitoids in the Kohistan batholith and undeformed basic dykes cross-cutting them (Pettersson and Windley, 1985; Treloar et al., 1989d).

In the Chitral area, the Northern suture melange of volcanic, sedimentary and serpentinite blocks in a slate matrix separates the Karakoram plate from the Kohistan arc (Pudsey et al., 1985). The melange occupies a zone up to 3 km wide in the lower Shishi valley and 2 km wide at Harchin. It is reduced to a fault zone

only 150m wide in Naz Bar. This comprises Cretaceous volcanic rocks with some sediments (Shaniran Volcanic Group, Drosh, Purit and Gawuch Formation) intruded by aphyric diorites, tonalites and granites. The volcanic rocks and sediments dip to the north and have a horizontal lineation suggesting that the suture zone in its western parts experienced an oblique collision.

The suture in Hunza valley is more complex; it forms a kilometer wide zone of sheared basic rocks and sediments with strong deformation. The Northern suture in Hunza (Coward et al., 1982) and Baltistan (Rex et al., 1988) initially constituted a north-dipping thrust zone. This was steepened to sub-vertical during collision at the southern suture, and has subsequently been cut by the south moving Main Karakoram Thrust in Baltistan (Rex et al., 1988), which may be equivalent to the Hunza Shear found in the hanging wall of the Northern suture in Hunza (Coward et al., 1986). Here, north and east of the suture zone, these northward-verging structures are refolded. The later fold has an intensely sheared overturned but gently dipping limb and a linear fabric which is dominantly sub-horizontal, trending ESE.

East of Nanga Parbat, in the Shigar and Shyok valleys, this late folding is more complex; there are several large S-facing folds which refold the earlier, often recumbent but northward-verging folds of the Kohistan arc. Near Khapalu, 50 km east of Skardu, there is a melange on the suture, consisting of disrupted units of serpentinite, pyroxenite, greenschist, amphibolite, gabbro, phyllite, gneiss, marble, chert and muscovite-chloritoid schist (Zanettin, 1964; Brookfield, 1981). Further east in the Shyok valley, Rai (1982) reported a molasse containing pebbles of granite and rhyolite attributed to the late Eocene Ladakh Batholith, interbedded with andesitic lava flows and interthrust with serpentinites in the suture.

The Indus Suture

This suture, locally called as the Main Mantle Thrust (MMT) in Pakistan (Tahirkheli et al., 1979; Bard, 1983), extends the entire length of the Himalayan chain and separates the Cretaceous Kohistan-Ladakh Arc from the Indian Plate and the Lhasa block. It contains a wide variety of rocks ranging from late Precambrian pelites and Cambrian granites (Le Fort et al., 1980) to Paleozoic-Mesozoic sediments mostly in a highly deformed and metamorphosed state. The suture is intensely deformed along the MMT. Several melange units occur locally in a complex thrust zone (Lawrence et al., 1983; Kazmi et al., 1984), some of which bear blueschist facies assemblages (Shams, 1972; Shams et al., 1980), together with piemontite schists and serpentinites (Jan and Symes, 1977). The 200 km² Jijal-Pattan Complex contains high pressure plagioclase-bearing and plagioclase-free garnet granulite (recrystallized in the range 700-850 °C and 11-15 kbar) and meta-ultramafic rocks. The ultramafic rocks are dominated by diopsidites and minor dunites, peridotites and hurzburgites metamorphosed at 800-850 °C and 8-12 kbar (Jan and Howie 1981; Yamamoto, 1994). These high pressure assemblages may represent sub-island arc metamorphism, prior to collision.

In Ladakh, ophiolite melanges are prominent in the Indus suture (Honegger et al., 1982). However, there may also have been pre-continental collisional oceanic thrusting associated with the obduction of the Ladakh-Kohistan arc, and the obduction of the Spontang ophiolite in late Cretaceous and early Paleocene times (Searle et al., 1988). To the west of Ladakh the Indus suture zone is embayed northwards by the Nanga Parbat syntaxis, almost as far to the north as the Northern suture,. Thus the Nanga Parbat antiformal structure separates the Ladakh portion of the arc in the east from the Kohistan part in the west. This

structure is developed from that part of the Indian plate which was initially subducted below the arc terrane; it was uplifted to dissect the arc only since the past 7 Ma (Zeitler et al., 1985; Smith et al., 1992). The eastward continuation of the Indus suture in the southern Tibet is called the Yarlung-Tsangpo suture (Yarlung and Tsangpo are the Tibetan and Chinese names respectively of the Indus and Brahma Putra rivers).

Palaeomagnetic studies in the Indian ocean indicate that the main continental collision of the Indian and Asian plates occurred from 55 Ma to 50 Ma (Klootwijk., 1979; Powell., 1979, Patriat and Acache, 1984). Closure of the Indus suture zone at 50 Ma is also constrained by the initiation of molasse sedimentation (of the Indus Group) on late Paleocene shallow marine limestones (Searle et al., 1987).

Kohistan Arc

The Kohistan -Ladakh terrane developed in response to northward-directed subduction of Neo-Tethys ocean lithosphere during late Jurassic and Cretaceous time (Searle et al., 1987). The arc covers 36,000 square kilometer area in the western Himalaya, southern Karakoram and eastern Hindukush. It consists of a variety of volcanic and plutonic rocks and subordinate sedimentary rocks that have undergone varying degrees of deformation and metamorphism. It is split into Ladakh and Kohistan as its eastern and western parts by the N-S trending Nanga-Parbat Haramosh massif. The terrane is juxtaposed against the Asian plate to the north along the Main Karakoram Thrust (MKT) and against the Indian Plate to the south along the Main Mantle Thrust (MMT) and is, thus, bounded by two major sutures (Tahirkheli and Jan, 1979; Coward et al., 1982, 1986; Bard., 1983a).

The terrane is known for its excellent exposures of a more or less complete island arc crust from the top sedimentary cover to those at the Moho (Tahirkheli et al., 1979; Jan, 1980; Bard et al., 1980; Coward et al., 1985; Miller and Cristenson, 1994). Broad aspects of the tectonic evolution of the terrane are now reasonably well- constrained as a result of reconnaissance mapping, structural analysis and radiometric dating in the last decade or so. The terrane was conceived within the Neo-Tethys as a result of north-dipping intraoceanic subduction. Maturing into a well-developed intraoceanic island arc for about 30-40 Ma (Khan et al., 1993), the terrane got accreted to the southern margin of the Karakoram plate at the site of the Shyok suture about 90 Ma ago (Pettersen and Windley, 1985; Coward et al., 1986; Treloar et al., 1989). It was then intruded by a major batholith in an Andean-type continental-margin setting until about 55 Ma ago when it was obducted onto the Indian plate at the site of the Indus suture.

Several factors, including a high relief, lack of roads, and a tribal political status of the area, restricted the past geological work in Kohistan to only major river valleys (e.g., Indus, Swat and Dir). This resulted in a generalized approach towards tectonostratigraphic reconstruction of the terrane. A preliminary classification of the Kohistan terrane, based on the work of Tahirkheli et al. (1979), Bard et al. (1980) and Coward et al. (1982, 1986) is still applicable to Kohistan, there are major advances on the understanding of mutual relationship between various lithotectonic units. Principal recent contributions in this regard come from Ghazanfar et al. (1991), Sullivan et al. (1993), M. A. Khan et al. (1993), Jan et al. (1993), T. Khan et al. (1994), and this work. A major part of this recent work has been executed in parts located remotely from the major metalled roads, adding several new dimensions to the geological understanding of the Kohistan terrane.

This chapter presents an updated map of the Kohistan terrane together with a new lithotectonic classification (Figure 2.4). Several aspects of the geology of Kohistan are being highlighted in this section including 1) presence of a major mafic-ultramafic layered plutonic complex in the basal parts of the arc, 2) recognition that much of the Kamila amphibolite belt represents the pre-arc oceanic basement, and 3) stratigraphic reconstruction of mid Cretaceous volcano-sedimentary sequence in the central and northern parts and their relationship with the Kamila Amphibolite at their base and the late Paleocene-early Eocene volcano-sedimentary succession on their top, exposed in the west central parts of Kohistan (e.g., Dir and Swat). Petterson and Windley (1985) and Coward et al. (1986) noted that the Kohistan terrane evolved through two stages of crustal growth, initially in an intraoceanic setting, i.e., between ~120 to 90 Ma and then as an Andean-type continental margin until the 50 Ma Kohistan-India collision. Likewise, the lithotectonic elements will be discussed in two groups in the coming pages.

Intraoceanic Stage of Crustal Growth

Volcanic-Sedimentary Succession

The volcanic-sedimentary sequence in Kohistan may be divided into five lithotectonic units. A brief information of these units is presented in Table 2.1. A description of the units of volcanic-sedimentary succession with is presented in the following stratigraphic order:

Purit (fluvial) Unit ?mid Cretaceous

Yasin Flysh Unit late early Cretaceous

Chalt Volcanic Unit early Cretaceous

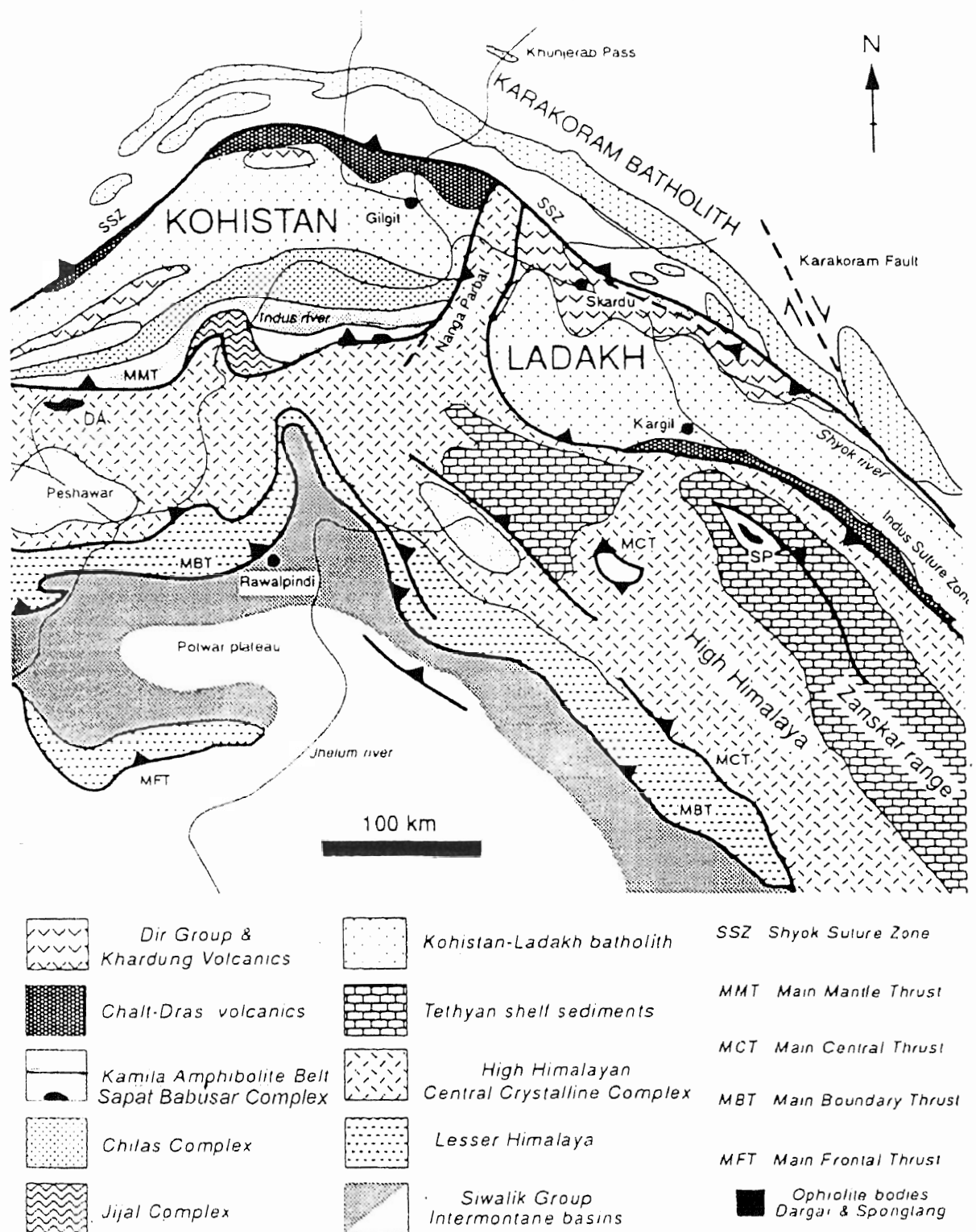


Figure 2.4. Simplified geological map of the western Himalayas-Karakoram showing the position of the Kohistan and Ladakh arc terranes with regard to the major Himalayan tectonic zones. For clarity, details of the Karakoram plate have been omitted (modified by author from Searle and Asif, 1996).

Table 2.1. Summary of the sedimentary and volcanic lithological units in Kohistan.

Units	Type Section	Base	Top	Lithology	Tectonic Setting	Age
Purit Formation:	Purit Gol, Drosh, Chitral	Unconformable on diorites and Gawuch Formation.	Base of Drosh Formation	Red shales, sandstone and conglomerate.	Fluvial.	?mid Cretaceous
Yasin Group	Yasin valley or the KKH road section near Thalichi.	Transitional with the underlying Rakaposhiv volcanics.	Unconformable with the overlying Purit Formation.	Turbidites (interbedded shales, siltstone, sandstone and conglomerate), limestones (marbles), volcaniclastic sediments.	Back-arc basin.?"	late-early Cretaceous
Chalt Volcanics	Hunza valley	Transitional over the Gilgit Formation.	Transitional below the Yasin Group of sediments.	Massive and pillowed metabasalts, volcanoclastic amphibolites and greenschists, minor intercalations of metasediments.	A complex mixture of island arc and back arc magmatism.	early Cretaceous.
Gilgit Formation	Sai Nala, NW of Jaglot	Conformable over the Kamila Amphibolite	Transitional with the overlying Chalt Volcanics	Paragenisses, migmatites, schists, quartzites, massive, banded and pillowed amphibolites.	Pelagic sediments from layer III of the Neo-Tethys oceanic crust.	?Jurassic-early Cretaceous
Kamila Amphibolite	Thak Valley	Intruded by the Sapat Complex	Conformable with the overlying Gilgit Formation	Fine-medium grained metavolcanic amphibolite, medium-coarse grained metagabbroic amphibolites, minor metasediments, diorite and trondhjemite intrusions.	E-MORB/OIB from layer II of the Neotethys oceanic crust.	Jurassic-early Cretaceous

Gligit Formation ?Jurassic– early Cretaceous

Kamila Amphibolite Unit Jurassic– early Cretaceous

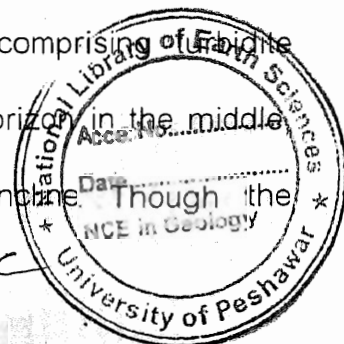
Fluvial Sediments (Purit and Asambar Sedimentary Units)

The Purit Formation is one of the sedimentary units described by Pudsey et al. (1985) from the Drosh area, Chitral. The unit is exposed along the southern side of the Kunar (Chitral) river and extends eastwards into the Sissi valley for a distance of about 40 km. According to Pudsey et al. (1985), the unit unconformably overlies the diorites of the Kohistan batholith and has a faulted lower contact with the Gawuch Formation, whereas its upper contact with the Drosh Formation is considered conformable. From about 1 km thickness in the SW, the unit becomes progressively thinned in the Sissi valley before complete obliteration. Red shales are the main rock type, whereas conglomerate and sandstone constitute about one-third of the formation. The unit is considered fluvial in origin. The equivalents of the Purit Formation are exposed near the Shyok suture in the area between Yasin and Ishkuman valleys. Pudsey (1986) described a sequence of red shales, thin sandstones and conglomerates underlying a thick sequence of conglomerates termed Asambar conglomerates. The Asambar conglomerates are massively bedded pebble- and cobble-conglomerates containing clasts of fine-grained volcanics (about one third), recrystallized limestones, grey and green slates and volcanic-lithic sandstones. The Asambar conglomerates overlie the Yasin Group and thus resemble the Purit Formation in their stratigraphic position. Additionally, they are fluvial in origin as is the case with the Purit Formation.

Yasin Group

Hayden (1914) reported a group of sediments comprising sandstone, fossiliferous shaly limestone and conglomerate unconformably overlying a succession of volcanics near the village of Yasin in north-central part of the Kohistan terrane. Ivanac et al. (1956) lumped these sediments with a suite of lavas, tuffs and agglomerates, and assigned them the name Yasin Group. Tahirkheli (1979, 1982) used the term Yasin Group only for the sedimentary part and included the volcanic component into his Chalt Volcanic Group. Additionally he recognised the presence of sediments all along the Shyok suture. Further detailed work on the Yasin Sediments has been done by Pudsey et al. (1985) and Pudsey (1986). She mapped a synclinal belt nearly 20 km long east of Mastuj, and continuous through Yasin and Hunza to the east. In the Yasin area she divided the group into a lower sedimentary unit (~ 1 km thick), comprising conglomerates, sandstones, tuffs, slates, rudist limestone and grey slates (distal turbidites) and an upper fine-grained unit (up to 2 km thick) comprising red, purple, green and grey shales with interbedded greenstone (tuff). This division, however, does not apply everywhere. In the Ishkuman valley, the sediments are almost devoid of limestone and consist of slates, silty quartzites and pebble-cobble conglomerates. In the Hunza valley, the Yasin Group comprises mainly terrigenous clastics and volcanoclastics in the form of distal turbidites and slates with massive greywackes predominant in the lower part.

The stratigraphy of the Hunza valley is tectonically repeated south of Gilgit in the Jaglot area. Here a thick sequence of slates (comprising of mudstones, siltstones and quartzites), with a thick marble horizon in the middle occupies the core of the regionally extensive Jaglot syncline. Though the



sediments have not yielded any fossils, their stratigraphic position above the Gashu-Confluence Volcanics (=Chalt Volcanic Group), which in turn overlie the Gilgit Formation, suggests a sound correlation with the Yasin Group. Westward in Chitral area, Pudsey et al. (1985) recognised a succession of volcanics and sediments south of the Shyok suture, which they divided into Gawuch Formation at the base, Purit Formation in the middle and Drosh Formation on the top.

The equivalents of the Yasin Group in the Baltistan area occur in two separate belts, on either side of the Katzarah Formation (=Gilgit Formation). Hanson (1989) described a succession of volcanoclastic sediments, interbedded with slates, phyllites, carbonates and conglomerates from north of Skardu, and called them the Bauma-Harel Formation. Lower Cretaceous fossils, Globoturcana from near Tissar at the western bank of the Shigar valley (Tahirkheli, 1982) and turritellid gastropod from a shale horizon in the upper part of the Bauma-Harel Formation, confirm the affiliation of this sequence with that of the Yasin Group. A discrete belt of volcanic and sedimentary rocks is exposed south of Skardu at the northern slopes of the Deosai plateau. Casheni and Ebblin (1977) termed this as the Shigarthang sedimentary group, but Desio (1978) considered this to be a continuation of his Burji Formation. The Burji Formation comprises slates, phyllites, chlorite-epidote greenschists derived from volcanogenic sediments, and limestone. Desio (1978) reported an assemblage of Upper Cretaceous fossils from this formation. The occurrence of Upper Cretaceous metavolcanics and sediments to the north and south of the Katzarah Formation in the Skardu area presents a situation very similar to that of the Gilgit area as described above. It is tentatively suggested that the Bauma-Harel Formation to the north of the Katzarah Formation and the Burji Formation to the south are tectonic repetitions of a sequence similar

to the combined Chalt Volcanic Group and the overlying Yasin Group. Lithological resemblance and similar age deduced from the reported fossils support this correlation.

Chalt Volcanic Group

The Chalt Volcanic Group (also called as the Greenstone Complex and Rakaposhi Volcanic Group) occurs as an arcuate belt to the south of the Shyok suture along more or less the entire length of the Kohistan terrane. The group is best exposed in the valley along the Gilgit River and its northern tributaries like Hunza, Ishkuman and Yasin. Brief descriptions of Chalt volcanics are given in Ivanac et al. (1956), Tahirkheli (1979, 1982), Coward et al. (1982), Petterson et al. (1990) and Petterson and Windley (1991). The group comprises amphibolites and greenschists derived from massive as well as pillowed lavas, agglomerates, tuff, volcanic breccia and minor intercalations of sediments. The grade of metamorphism decreases westwards from high greenschist-amphibolite in Hunza to low greenschist near Ishkuman. Petterson et al. (1990) and Petterson and Windley (1991) presented detailed geochemistry of the Chalt volcanics and identified island arc tholeiite and calc-alkaline rocks with compositions ranging between basaltic komatiite, boninite and high-Mg andesite to calc-alkaline basalt, andesite and dacite-rhyolite.

The Drosh Volcanics (Pudsey et al., 1985; Pudsey, 1986) in Chitral form the western extension of the Chalt volcanic Group. The lower half of the Gawuch Formation (Pudsey et al., 1985), to the south of Drosh Volcanics, comprises greenschist metavolcanics very similar to those of Drosh, suggesting tectonic repetition. In the Shandur Pass area in north-central part of the terrane, two types of volcanics are recognised (Pudsey, 1986; Khan and Coward, 1990; Sullivan et

al., 1993). The volcanic rocks in the lower part of the succession, exposed immediately to the south of the suture in the Harchin-Shandur Pass area, are migmatized amphibolitic gneisses. From the Shandur Pass eastward, there is a sequence of generally low-grade, flat-lying or gently north-dipping metavolcanic rocks, termed the Shamran Volcanic Group. These show compositional variations from basalts, through andesites, to rhyolites. Andesites are predominant, comprising massive, amygdaloidal porphyritic flows and massive crystal-lithic tuffs. Acidic lavas and tuffs are finely bedded and are intercalated with shaly sediments. Locally there are pillow lavas, chert bands and volcanic breccia and agglomerates. Pudsey et al. (1985) demonstrated on the basis of their field studies that the Shamran Volcanics occupy a stratigraphic position below the mid Cretaceous Yasin Group of sediments. Recently, Sullivan et al. (1993) have correlated Shamran Volcanics with those of Dir on the basis of close compositional resemblance and an Ar-Ar age spectra of 58 Ma (Treloar et al., 1989).

The extension of the Chalt Volcanic Group into Baltistan, east of the Nanga Parbat Syntaxis, has been called Bauma-Harel Formation (Desio, 1963; Hanson, 1989). The unit consists of volcanoclastic sediments interbedded with slates, phyllites, carbonates and conglomerates, and probably equates not only with the Chalt Volcanic Group but includes the overlying Yasin Sedimentary Group. Hanson (1989) reported turritellid gastropods of a possible Cretaceous age from this unit. Along the northeastern termination of the Nanga Parbat Spur, the Askore Amphibolite in the Indus Valley, between Tungas and the confluence with the Turmik Valley (Le Fort et al., 1995), may also be the continuation of the Chalt Volcanic Group.

In the interior of the Kohistan terrane, equivalents of the Chalt Volcanic Group occur to the south of Gilgit as a part of the Jaglot Group of Khan et al. (1994). In this area a thick sequence of pillowed basalts, massive basalts, agglomerates and tuffs (termed Gashu Confluence Volcanics by Khan et al., 1994), metamorphosed into amphibolite-greenschist facies, overlies the Gilgit Formation transitionally. Khan et al. (1993, 1994) believe that these volcanics are a tectonic repetition of the Chalt Volcanic Group at the limbs of the Gilgit anticline and Jaglot syncline of Coward et al. (1987). The probable equivalents of the Chalt Volcanic Group in the Dir and Swat areas are the Mankial metavolcanics of Sullivan et al. (1993). These metavolcanics occupy a stratigraphic position above the Peshmal Schists (= Gilgit Formation), which in turn overlie the Kamila Amphibolite. This stratigraphic position resembles closely with that of the Gashu-Confluence Volcanics in the area south of Gilgit, which are interpreted to be the equivalents of the Chalt Volcanic Group. It may be noted, however, that the Mankial metavolcanics, unlike the Chalt Volcanic Group, comprise essentially of volcanoclastic metasediments with little component of lava. The minimum age of the Chalt Volcanic Group is constrained by its stratigraphic position below the Yasin Group sediments which have yielded Albian-Aptian fossils (Desio, 1963; Pudsey et al., 1986).

Gilgit Formation

Occurrences of high-grade metasediments (paragneisses, migmatites and schists) in the Kohistan terrane are mentioned in several reports, but were always considered either localised or anomalous. Coward et al. (1987) recognized a group of metasediments from south of Gilgit in the core of a major antiformal fold, which they considered to represent "stratigraphically lowest metasediments" in the

Kohistan terrane. These metasediments were recently studied in detail in terms of their stratigraphic relations and were formally classified as the Jaglot Group (T. Khan et al., 1994). The stratigraphic unit forming the basal part of the Jaglot Group is termed Gilgit Formation which comprises a sequence of medium- to high-grade paragneisses, migmatites, schists and quartzites. Other lithologies include amphibolites and calc-silicates. The amphibolites are frequent and form laterally continuous horizons. Although some of the amphibolites may be transposed dykes and sills, others are definitely derived from basic tuffs and volcanic flows. One such horizon in the Sai Nala (northwest of Jaglot) comprises a four meter thick sequence of stretched pillows. The calc-silicate horizons are common in the upper part of the formation, above the pillowed-amphibolite horizon.

The rocks of the Gilgit Formation show evidence of regional metamorphism upto sillimanite grade. The metamorphic index minerals in the paragneisses and schists include biotite, garnet, kyanite and sillimanite. The topmost unit in the Gilgit Formation is biotite schist grading downward into garnetiferous schists, and kyanite and sillimanite gneisses. In the deeper levels the paragneisses have undergone anatexis, giving rise to migmatites. As said, the Gilgit Formation is overlain by the Gashu-Confluence Volcanics (Khan et al., 1994), which are regionally equitable to the Chalt Volcanic Group of Petterson et al. (1991). The basal contact of the Gilgit Formation is not exposed at least in the east-central Kohistan. There are indications, however, that the formation was underplated by the Chilas Complex. For instance, at the Gilgit River-Sai Nala Confluence, south of Jaglot, the paragneisses enclose a block of the layered basic rocks that resemble closely those of the Chilas complex. The northern contact of the Chilas complex is against a group of intercalated amphibolites and metapellites, as observed in the

upper reaches of Kiner and Hudur valleys (Khan, 1988). Screens and xenoliths of biotite schists and paragneisses belonging to the Gilgit Formation are abundantly enclosed in the Chilas complex near its upper contact as observed in the east-central Kohistan (Khan, 1988; Khan and Jan, 1992).

Rocks showing strong resemblance in lithological characteristics and stratigraphic position to the Gilgit Formation are reported from other parts of Kohistan. A succession of sediments, metamorphosed upto sillimanite grade, is termed Katzarah Formation (Desio, 1978; Tahirkheli, 1982; Hanson, 1989) in the north central parts of Deosai, which is considered the western extension of the Kohistan terrane. The high grade pelitic assemblage not only has a compositional similarity with the Gilgit Formation but occupies a similar stratigraphic position at the base of a volcano-sedimentary succession resembling Chalt Volcanic Group and Yasin Group of metasediments. In the west, equivalents of the Gilgit Formation are exposed in the Kandia, Swat and Dir valleys. In the Kandia valley, there are poorly described metasediments (Jan, 1970) and an isolated outcrop of high-grade rocks overlying epidote-amphibolites of the Kamila belt (Yamamoto, 1993). A succession of schists (termed Peshmal schists by Sullivan et al., 1993) occurs in the Swat valley (south of Kalam) and in Dir area overlying the Kamila amphibolite. A mineral assemblage comprising biotite-muscovite \pm garnet \pm clinopyroxene, a predominantly pelitic composition and a stratigraphic position above the Kamila amphibolite, suggest a sound correlation with the metasediments in the Gilgit Formation.

Kamila Amphibolite Unit

Amphibolites of Cretaceous to ?late Jurassic age occur in the form of a linear belt intervening between the Indus Suture and the Chilas Complex. These amphibolites have been given several names. Martin et al. (1962), on the basis of their pioneer reconnaissance work in the Swat valley, proposed the term "Upper Swat Hornblendic Group" for the basic igneous rocks of the Kohistan terrane. Jan and Kempe (1974) renamed the group, as the Kohistan Basic Complex, comprising an extensive suite of amphibolites and gabbro-norites (the latter belonging to the Chilas Complex). These amphibolites have also been referred to as the southern amphibolites (Jan, 1979; Bard et al., 1980) or, more commonly, the Kamila amphibolite belt (Tahirkheli and Jan, 1979; Coward et al., 1982; 1986, Jan, 1988). Along the Indus, the amphibolites are strongly deformed and the zone has been referred to as the Kamila shear zone. Despite several detailed studies in various parts of the belt (Jan, 1970; Chaudhry et al., 1974; Ahmed and Chaudhry, 1976; Khan, 1988, Khan and Thirlwall, 1988), the nature of the Kamila amphibolite unit has remained equivocal. Miller et al. (1991), on the basis of their work in the Indus valley, suggested that the Kamila amphibolite belt is nothing but a stack of basic plutons (also see Louks et al., 1990; Miller and Christensen, 1994). Likewise there are ^{discrepancies} ~~descripencies~~ in the proposed tectonic settings of origin for the belt. Whereas Tahirkheli et al. (1979) and Bard et al. (1980) considered the Kamila belt to represent the oceanic basement for the intrusion of the Kohistan island arc, Coward et al. (1986), Jan (1988), Khan and Coward (1990), Miller et al. (1991), Shah and Majid (1992), Miller and Christensen (1994) suggested a subduction-related origin.

The Kamila amphibolite belt has a vast distribution in southern Kohistan. Previously, it was considered to occupy the entire southern part of the Kohistan terrane between the MMT in the south and the southern contact of the Chilas Complex in the north. The only exception was the Indus valley, where the belt was considered to overlie the Jijal Complex which occupies the hangingwall of the MMT. Recent mapping has revealed that the Kamila amphibolite belt is in direct contact with the MMT only in the extreme eastern and western parts of the Kohistan terrane. In the area between the Babusar and the Indus valley, the belt occupies a position between a basal mafic-ultramafic layered complex in the hangingwall of the MMT (the Sapat complex of Jan et al., 1993) and the Chilas complex.

The Kamila amphibolites comprise a complex assemblage of lithologies. Two rock types are predominant. Fine- to medium-grained amphibolites are the most predominant rock-type in the eastern part of the belt exposed in the southern tributaries of the Indus river (i.e., Bunar, Niat, Thak, Buto and Thor). In the central and western part of the belt (i.e., Indus, Swat and Panjkora valleys) the proportions of the fine-medium grained amphibolites become relatively subordinate in favour of medium-coarse grained amphibolites. The fine-medium grained amphibolites are commonly foliated and include both banded and homogeneous varieties. Both the varieties are derived from volcanic precursors (Jan, 1979, 1988; Khan et al., 1993). Some of the banded varieties are derived from tectonic stretching of pillowed lavas, while the others are derived from tuff-lava intercalations. Mafic flows with pillow structures, often stretched due to tectonism, have been observed locally from the entire extension of the belt (e.g., Dir, Swat, Buto and Thak valleys). This supports the notion that the fine-medium grained amphibolites in the Kamila belt are derived

from basic volcanics. There are rare occurrences of sedimentary rocks in association with the banded amphibolites (e.g., amphibole-bearing quartzites, marbles, calc-silicates, biotite \pm garnet paragneisses).

Locally the Kamila amphibolite belt is intruded by a network of veins and sheets of tonalite/trondhjemite composition. These range in thickness from a centimeter to several tens or hundreds of meter. A majority of them intrude the amphibolites along the foliation planes but some cross-cut the foliation. The "veined amphibolites" are particularly common in parts of the belt in the vicinity of tectonic contact with the Chilas complex. These trondhjemite/tonalite veins and dykes probably owed their origin to partial melting of the Kamila amphibolites.

The origin of the medium-coarse grained amphibolites is relatively more straightforward. The homogeneous, foliated and banded varieties of this category are derived from basic plutonic rocks (e.g., gabbros, gabbronorites, troctolites and anorthosites). The banding is largely after the primary igneous layering, but shearing has also contributed to banding in some cases. The intrusive contacts of the amphibolitized basic plutons are rarely preserved because of common shearing. The shear zones in the Kamila belt are typically anastomosing. Within the shear zones the rocks are blastomylonitic medium-fine grained, sometime difficult to be distinguish^{ed} from the fine-grained variety of the amphibolites. However, gabbroic rocks with their intact igneous texture occur as lensoid blocks between the anastomosing branches of the shear zones. The scale of the shear zones and the relict blocks of unaffected gabbroic rocks is highly variable, ranging from cm to kilometeric scale (see Treloar et al., 1990 for details).

The tectonic setting of origin for the Kamila amphibolites has remained controversial. Using whole-rock geochemistry of the amphibolites mainly from Swat and Indus valleys, Jan (1988) suggested a calc-alkaline nature of the Kamila amphibolites implying subduction-related origin. Khan (1987, 1988), based on the geochemistry of Kamila amphibolite samples from the Thak valley (south of Chilas), recognized the presence of E-MORB component in the Kamila amphibolite. Khan et al. (1993), based on a reconnaissance survey of the entire belt, suggested the presence of both E-MORB and subduction-related calc-alkaline mafic rocks in the Kamila belt.

The relationship of the Kamila amphibolite belt with the rest of the volcanic, volcanoclastic or metasedimentary units, exposed mainly in the middle or northern parts of the Kohistan terrane, has remained unclear due to the presence of an extensive belt of plutonic rocks of the Chilas Complex intervenned between the two. In the eastern and central parts of Kohistan, rocks equivalent to the Kamila amphibolite are absent from north of the Chilas Complex. In contrast, in the west (e.g., Panjkora valley) a sequence of amphibolites does occurs to the north of the Chilas Complex. This has led some workers to suggest the presence of an additional group of amphibolites in the Kohistan terrane, which they termed the "Northern amphibolites" (Chaudry et al., 1974) or the "Northern Amphibolite Belt" (Bard et al., 1980). The presence of the Kamila Amphibolites on either side of the Chilas Complex may be due to tectonic repetition. Despite a lack of evidence, it is assumed that at least the volcanics of the Kamila amphibolite unit pre-date the Gilgit Formation and Chalt Volcanic Group.

Intrusive Rock Units

Several phases of intrusion mark the intra-oceanic stage of development in the Kohistan terrane (Table 2.2). On the basis of their composition, two types of plutonic phases are distinguished, 1) mafic and ultramafic complexes, and b) intermediate to felsic intrusions. The mafic-ultramafic complexes, like the Jijal, Sapat and Chilas Complexes, were emplaced into the Kamila Amphibolite, while felsic intrusions were intruded and emplaced both within the Kamila Amphibolite as well as in the presumably overlying younger tectonostratigraphic units like the Gilgit Formation and Chalt Volcanics.

Mafic-Ultramafic Complexes

Jijal Complex

The Jijal Complex is an ultramafic-mafic plutonic body exposed in the hangingwall of the MMT in the Indus valley. The body is ~150 square km in area and is a fault-bounded tectonic wedge (Jan, 1977; Jan and Howei, 1981). It is divisible into a lower ~ four km thick succession of layered ultramafic rocks and an upper seven km thick succession of garnet granulites. The ultramafic part comprises, from base to top, 1) a sequence of multiple cyclic units consisting chiefly of olivine clinopyroxenite, wehrlite, dunite and chromitite, 2) websterite, 3) hornblende clinopyroxenite, and 4) garnet- hornblende clinopyroxenite (Miller et al., 1991). According to Jan and Howei (1981) and Yamamoto (1993), the garnetiferous basic rocks in the Jijal Complex crystallized as layered gabbros, gabbro-norites and anorthosites, which were transformed into garnet granulites during a phase of high pressure metamorphism (pressure 10-17 kbars, temperature 700-950 °C, Yamamoto, 1993). Miller et al. (1991), in contrast,

Table 2.2. Summary of plutonic intrusions in the Kohistan.

Lithological Unit	Composition and Internal Features	Emplacement Mode/Country Rocks	Age	Tectonic Significance of origin
Kohistan Batholith	Mainly comprising quartz diorites, tonalites, gabbros and hornblendites. Latest phases are leucogranitic aplites or pegmatites.	Multiple intrusions. Individual plutons commonly oval to circular in shape. Southern plutons intrude the Chilas Complex or the KAB. Bulk of the batholith intrudes volcanic-sedimentary lithologies in northern Kohistan.	Four whole-rock Rb-SR isochron ages available; 102, 60, 40 and 33-28 Ma. Combined with Ar-Ar ages, the batholith is divided into Phase I (102 Ma); Phase II (80-40 Ma) and Phase III (33-28 Ma.)	Phase I (102 Ma) intraoceanic island-arc or back arc setting. Phase II in continental margin setting. Phase III related with partial melting due to post-collisional crustal thickening.
Chilas Complex	Predominantly non-cumulate gabbro-norites and pyroxene diorites, with minor cumulate ultramafics and anorthosites.	Large lopolith emplaced at the contact between the KAB and the Gilgit Formation. (KAB is Kamila Amphibolite Belt)	Ar-Ar age data suggest 74-85 Ma age of pyroxene-granulite facies metamorphism. Mid Cretaceous age of emplacement speculated on geological basis.	Crystallization from a basaltic andesite magma, in mature arc or back-arc rift environments.
Sapat Complex	Stratiform pluton: ultramafic cumulates at the base, layered gabbros in the middle and isotropic gabbros at the top. Epidote-amphibolite or greenschist facies of regional metamorphism.	Large lopolith. Basal contact tectonic with MMT (or with the Jijal Complex). Intrusive upper contact with KAB.	Age data entirely lacking.	Crystallisation from a basaltic magmatism in intraoceanic-island arc setting.
Jijal Complex	Stratiform pluton: ultramafic cumulates at the base, overlain by gabbros/gabbro-norites. Metamorphosed to garnet granulite facies of regional metamorphism.	?Originally a lopolith intruded into an oceanic basement comprising KAB. Currently a fault-bounded wedge in the hangingwall of the MMT.	No data on emplacement age; assumed to be Mid Cretaceous on geological grounds. Sm/Nd ages of 91-104 Ma. date metamorphism.	Crystallisation from a high-Mg basalt in an intraoceanic island arc setting.

advocated an igneous nature of the garnetiferous basic rocks relating the garnet crystallisation to the depth (~ 15 kbars) of magma emplacement and crystallization. In either case, the Jijal Complex represents one of the principal cumulate ultramafic-mafic bodies from the root zone of the Kohistan island arc terrane. Jan and Windley (1990) suggested crystallisation from a primitive island-arc tholeiite magma. This was substantiated independently by Loucks (1990) who suggested a subduction-generated, hydrous, low-k, picritic high-Mg tholeiitic magma for the precipitation of the Jijal Complex.

Sapat Mafic-Ultramafic Complex

Between Babusar and Indus valley, the MMT is overlain by the Sapat Complex (Jan et al., 1993), which comprises ultramafic and gabbroic rocks metamorphosed from epidote-amphibolite to greenschist facies and lacking garnet. The complex, in the Sapatgali area of upper Kaghan, contains about a kilometer thick body of serpentinized dunites and peridotites at its base. Upsection, the ultramafic body is overlain by a zone of layered peridotites, gabbronorites, anorthosites and pyroxenites, which gives way to weakly layered to isotropic gabbros. A large lensoid body of pyroxenites occurs upsection within the isotropic gabbros (Ghazanfar et al., 1991). Minor bodies of ultramafics and amphibolites at Babusar (Ahmed and Chaudhry, 1976; Khan and Thirlwall, 1988; Ghazanfar et al., 1991) are the eastern continuation of the Sapat Complex. The complex has an exposed width of about ten km in the southern Kohistan owing to repetition through folding. The Sapat Complex contains spinel with high Cr No. which is comparable to the Jijal Complex, suggesting closer affinity with the latter than with the Chilas Complex (Jan et al., 1993). There is a possibility that the Pattan and Kayal Complex of Miller et al. (1991) and Loucks et al. (1992) are the westward

continuation of the Sapat Complex in the Indus valley. The Kawaza Khela body of troctolites and gabbros in lower Swat valley (Jan and Karim, 1995) and Tora Tigga ultramafic-mafic complex in Dir (Jan et al., 1983) may be the continuation of the Sapat Complex further westward.

Chilas Complex

This is a large mafic-ultramafic body occupying the medial part of the Kohistan terrane for a distance of about 300 km between Dir in the west and Nanga Parbat in the east (Jan et al., 1984; Khan et al., 1989). The body is internally coherent and attains a maximum width of about 40 km in the central part. Isotropic gabbro-norite and pyroxene diorite are the two principal rock types having gradational relationship with each other. Locally the gabbro-norites are layered and contain websterite-anorthosite layers. An association of dunites, peridotites, minor chromitites, anorthosites, troctolites, olivine gabbros and gabbro-norites (characterized by highly calcic plagioclase $An > 85$ mole%) occurs as lensoid bodies, mainly in the east-central part of the complex near Chilas. The southern margin of the complex is commonly hydrated and amphibolitized (Jan, 1979; Treloar et al., 1990). Until recently, the relationship of the Chilas Complex with the other lithologies of the Kohistan terrane has remained unclear. Khan and Jan (1992) noticed occurrence of xenoliths of fine-grained metavolcanics in the southern marginal parts of the complex exposed in the interiors of the Thor valley, suggesting intrusive relationship between the Chilas Complex and the Kamila Amphibolite. In contrast, the northern marginal parts the Chilas Complex contains xenoliths and screens of garnet-biotite schists and paragneisses (Khan, 1988; Khan and Jan, 1992). The lithologies in the xenoliths are similar to those which occur in the roof zone of the Chilas complex, which in turn are similar to those of

the Gilgit Formation of T. Khan et al. (1994). Westward in the Swat and Dir Valleys, the complex appears to be emplaced at a stratigraphic horizon well below the upper contact of the Kamila amphibolite with the Peshmal schists. The Kargil Complex in Ladakh, to the east of Nanga Parbat, displays similar lithologies as the Chilas Complex (Rai and Pande., 1983). However, Honegger et al. (1982) suggested that the Kargil Complex represents cumulates of the magma chamber of the Dras Volcanics. A calc-alkaline composition and island arc/ back arc setting of magma generation have been ascertained for the Chilas Complex on the basis of mineral and whole-rock chemistry (Khan et al., 1989, 1993).

Intermediate-Felsic Intrusions

Thak Granitoid Sheets

South of Chilas in the valleys of Niat, Thak, Buto and Thor (area of this research), the Kamila Amphibolites are intruded by sheets of intermediate to felsic plutonic rocks. These range in thickness from a meter dyke to several hundreds of meter. Likewise the composition is highly variable. In the Thak valley, near the village of Loshi, at least five varieties of intermediate plutonic rocks are observed. The sheets are almost always foliated, suggesting their intrusion prior to the deformation in the Kamila Amphibolite.

Matum Das Trondhjemites

A bimodal suite, predominantly comprising trondhjemites but also including gabbros and diorites, displaying a penetrative fabric, was distinguished by Petterson and Windley (1985) from northern parts of Kohistan around Gilgit. The type pluton of this kind occurs some 20 km upstream in the Hunza valley in the Matum Das, Jutal, Nomal area (Petterson et al., 1990), and in the ridge just to the

north of Gilgit. These deformed plutons are metamorphosed and intrude both the Chalt volcanics as well as the Gilgit Formation. Whole-rock Rb-Sr isochron of the Matum Das trondhjemite has yielded an age of 102 Ma (Petterson and Windley, 1985). The age of deformation event responsible for the penetrative fabric in these rocks was determined to be earlier than 75 Ma on the basis of Ar-Ar dating of a cross-cutting suite of undeformed basic dykes. The continuity of structures, from within the Matum Das trondhjemite to those marking the Shyok suture, led Coward et al. (1986) to suggest that it was the accretion of the Kohistan terrane with the Karakoram plate which caused the penetrative deformation of Matum Das and related plutons. Petterson et al. (1990), on the basis of their observations around Gilgit, suggested that some 30% of the batholith contains penetrative deformation related with the Shyok suture. Sullivan et al. (1993) have reported a complete absence of plutons equivalent to those of Matum Das in Dir and Swat area. Thus it may be concluded that only a minor component of the Kohistan batholith (e.g., Matum Das trondhjemite) was intruded during the intraoceanic phase development of the Kohistan terrane. Some of the highly deformed tonalites in Upper Swat (Jan and Asif, 1983) may also be of this age.

Continental-Margin Stage of Crustal Growth

The accretion of the intraoceanic Kohistan terrane with the southern margin of the Karakoram-Eurasian plate took place sometime between 100 and 75 Ma (Petterson and Windley, 1985; Coward et al., 1986). The subduction at the site of the Shyok suture ceased as suggested by the absence of subduction-related magmatism in the Karakoram batholith later than 95 Ma (U-Pb date on zircon). However, at the southern margin of the accreted Kohistan-Karakoram-Eurasia the southern segment of the Neo-Tethys continued subduction. Three lithologies in the

Kohistan terrane are related with this stage of crustal growth; 1) Kohistan batholith, 2) Baraul Banda Slate Formation, and 3) Utror Volcanic Formation.

Kohistan Batholith

The Transhimalayan intrusive belt is spread over 2700 km length between Afghanistan and Burma. The Kohistan batholith, about 280 km long with maximum thickness of 60 km, is a part of this belt. Gilgit is located almost in the center of the granitic belt. Ivanac et al. (1956), Tahirkheli and Jan (1979) and Jan et al. (1981) identified the presence of a major belt of granitic rocks in the northern parts of the Kohistan terrane, which was later termed as the Kohistan Batholith by Peterson and Windley (1985) and Coward et al. (1986). As mentioned above, except for a minor component, e.g., Matum Das, Jutal, Nomal, North Gilgit Ridge, and Upper Swat, the Kohistan batholith comprises undeformed or only mildly deformed intermediate to felsic plutonic rocks. Furthermore, a large component of the batholith demonstrably intrudes the large-scale fold structures in the Gilgit Formation, Chalt Volcanics and the Yasin sediments, suggesting intrusion subsequent to accretion of the Kohistan terrane with the southern margin of the Karakoram plate.

The Kohistan batholith has been studied in detail in the Chilas-Gilgit-Hunza transect (Peterson and Windley, 1985, 1986; Khan et al., 1994) and in the Dir and Swat valleys (Jan and Mian, 1971; Chaudhry et al., 1974; Jan and Asif, 1983; Sullivan, 1992). In the Chilas-Gilgit-Hunza transect, the principal body of the Kohistan batholith is termed Gor pluton (Khan et al., 1994). Oriented NW-SE, the body is up to 30 km wide and 60 to 70 km long, occupying the drainage divide between the Indus and Gilgit rivers. The Gor pluton is a coherent mass of mainly

quartz diorite composition. Some 15% of the pluton consists of other phases including granodiorite, granite and adamellite. The Gor pluton has a linear intrusive contact with the Chilas Complex in the south and Jaglot Syncline in the north. A two km wide and some 25 km long plutonic body occurs SW of Gilgit, stretched across the Sai Nala, Shinghai Gah and Kar Gah. This pluton comprises gabbros and diorites and is commonly sheared and amphibolitized. Several plutons with circular to oblong outlines, intrusive into the Gilgilt Formation or Chalt Volcanics, have been mapped by Petterson and Windley (1985) in the Gilgit and Hunza valleys. Of these the basic to intermediate phases are considered to be between 85 and 60 Ma (K/Ar and Ar-Ar age data of Coward et al., 1986; Treloar et al., 1989). Granites have ages between 60 and 40 Ma, on the basis of Rb-Sr whole-rock isochron of three plutons (Gilgit 54 ± 4 Ma, Shirot 40 ± 6 and Gindai 59 ± 2). A phase of aplite-pegmatite leucogranite sheets intrude the earlier phases of the Kohistan batholith in the vicinity of Indus-Gilgit confluence. This swarm of acid sheets has yielded 34 ± 14 and 29 ± 8 Ma Rb-Sr whole-rock ages (Petterson and Windley, 1985).

The Kohistan batholith in the upper Swat valley comprises several discrete plutons in the age bracket of 80-30 Ma (Sullivan, 1992). Two groups are distinguished, a southern and a northern. The southern group of plutons is exposed to the south of Kalam and forms the basement for a succession of late Paleocene-early Eocene sediments and volcanics. The principal pluton, in this group, occurs in the form of an east-west trending belt between Asrit in the south and Peshmal in the north, occupying a discrete stratigraphic level just above the Chilas Complex. A basic migmatite zone at Asrit, comprising hornblende-plagioclase pegmatite veins and dykes in the (Kamila) amphibolite protolith, mark

the roof zone of the Chilas Complex. The pluton comprises quartz diorites, tonalites and granodiorites. An ^{40}Ar - ^{39}Ar date from a granodiorite within the pluton, indicates 78 ± 1 Ma age for the cooling of the hornblende (Treloar et al., 1989). A small pluton of granodiorite composition at Kalam is 76 ± 2 Ma in age. North of Kalam, the Matiltan granitic pluton, is intruded into the Mankial Metavolcanics (=Chalt Volcanics) and is considered to be equivalent to the other two plutons in this group. The northern group of plutons occurs in the hangingwall of the thrust which marks the northern boundary of the Utror Volcanics. These plutons range in composition from quartz diorite to adamellite. Gabral and Ankar Gol plutons are the type examples. Treloar et al. (1989) report a ^{40}Ar - ^{39}Ar age of 48 ± 1 Ma for the Gabral pluton.

A complex set of plutonic lithologies is exposed in the Upper Ushu valley in the Mahodand and Falkser areas. Quartz diorite make the principal plutonic lithology with minor occurrences of orbicular diorites and hornblende diorite (Jan and Mian, 1971; Khalil and Afridi, 1979). At Falkser, a pluton of adamelite-granodiorite composition intrudes the quartz diorites. Sullivan (1992) suggest an early Eocene or later age for the northern group of plutons in upper Swat, but the Deshai quartz diorite pluton is strongly deformed and may be pre-collision.

The part of the Kohistan batholith in the Dir valley is also divisible into southern and northern groups of plutons. An age of 45.2 ± 0.4 Ma (on hornblende) from a granodiorite from the Lowari pluton (Zeitler, 1985) suggests contemporaneity with the northern group of plutons in upper Swat (e.g., Gabral pluton). No age data is available from the plutons south of Dir (e.g., Warrai pluton) and their correlation with the 75-80 Ma old southern plutons in Swat is not possible at this stage.

Dir Group

A 15-20 km wide and more than 120 km long belt of slates and volcanic rocks (Dir Group, Tahirkheli, 1979) stretches in a NE-SW trend across the Dir and Swat valleys in western Kohistan (Tahirkheli and Jan, 1979). On the basis of paleontological and radiometric evidence the rocks have been assigned a Late Palaeocene-Early Eocene age (Kakar et al., 1971; Khan, 1979; Treloar et al., 1989; Sullivan et al., 1993). The rocks of the Dir Group unconformably overlie a deep erosion surface cut into the Kohistan batholith and its host rocks (Kamila Amphibolite, Gilgit Formation and Chalt Volcanic Group). Following, Tahirkheli (1979), Sullivan et al. (1993) have divided the group into two units, Baraul Banda Slate Formation (BBSF) and Utror Volcanic Formation (UVF). The BBSF was studied in detail by Sullivan (1992) for systematic sedimentology and stratigraphy. The formation is about three kilometer in thickness and comprises 30-70 m thick basal succession of conglomerates, breccia and pebbly sandstone, overlain by a ~2500 m thick succession of thinly bedded-laminated sandstone, siltstone and mudstone. Rare limestones in the Dir area have yielded an abundant fauna of *Actinosiphon tibeticus* and *Miscellanea miscellansu* (Sullivan et al., 1993).

A distal turbidite nature for the Baraul Banda Slate Formation has been deduced by Sullivan et al (1993). According to these workers, the BBSF was deposited in an elongated arc-parallel extensional fore-arc basin at the southern margin of the Kohistan-Karakoram continental margin. The overlying Utror Volcanic Formation (UVF) has a tectonic basal contact with the BBSF along the Dir Thrust (Tahirkheli, 1982; Sullivan et al., 1993). The formation comprises a complex and diverse succession of volcanoclastic rocks and lava flows, including heterolithic polymict volcanic breccia, sandstones and siltstones, andesite and

rhyolite lava flows, pyroclastic flows and ignimbrites. Sullivan et al. (1993) have inferred deposition and eruption in a subarerial environment with an explosive eruptive style for the UVF. Two ^{40}Ar - ^{39}Ar ages are available for the UVF. Treloar et al. (1989) presented a ^{40}Ar - ^{39}Ar age of 55 ± 2 Ma for a hornblende separate from an andesite. In contrast, an age of 70 ± 9 Ma (48% of plateau) was obtained for a hornblende from an andesite by Hamidullah and Onstat (1993). The Dir Group has a tectonic northern contact with the northern group of plutons of the Kohistan batholith.

Correlations between Kohistan and Ladakh

The Nanga Parbat-Haramosh syntaxis, consisting of Indian plate gneisses, separates the Kohistan and Ladakh arc terranes. The Dras-Nindam volcanics, within the Indus-Tsangpo Suture Zone (ITSZ), have the characteristics of island-arc volcanics. These are equivalent to the Chalt Volcanic Group and Yasin Group within the Kohistan terrane. Radiometric ages from 105-65 Ma have been estimated for these rocks (Sharma et al., 1978; Honegger et al., 1982; Scharer et al., 1984; Reuber et al., 1987; 1989). However, uncommon interbedded radiolarian cherts yield Upper Jurassic ages (Honegger et al., 1982). In the central part of the suture zone Orbitolina bearing limestones of Albian-Aptian age (mid Cretaceous) stratigraphically overlie the Dras volcanics. There is no equivalent of the Kamila Shear Zone within the Ladakh terrane. Later shears with mylonitised amphibolite cut the intrusive rocks (Searle et al., 1988). Rai and Pande, (1978) and Dietrich et al. (1983) described the gabbro-norites in the vicinity of Kargil, which may be equivalent to the Chilas Complex. No high pressure equivalents to the Jijal Complex garnet granulites or ultramafics are observed within Ladakh.

The batholith shows comparable ages of emplacement (Honegger et al., 1982; Reynolds et al., 1983; Scharer et al., 1984), ranging from ~ 103 to 60 Ma in Ladakh and 102 to 29 Ma in Kohistan. Along the Shyok Suture in Ladakh, the Khardung Volcanics (originally known as the Shyok Volcanics - Sharma and Gupta, 1978; Srimal et al., 1982; Sharma, 1983) have ages of 38 ± 2 Ma (Sharma et al., 1978). However, using oxygen isotopes, Srimal et al. (1987) demonstrated that the volcanic pile has been subject to intense hydrothermal alteration. On the basis of palaeontological and stratigraphical evidence they suggested a late-Cretaceous - Eocene age. This being the case, these volcanics may be correlated with the Dras II volcanoclastics further to the south within the ITSZ (Reuber, 1989) and the Dir group of Kohistan. A more comprehensive review of the geology of Ladakh is given by Searle et al. (1988) and Sharma (1991). A simplified lithological comparison between the Kohistan and Ladakh arc terranes is given in Table 2.3.

Indian Plate

In India and Nepal, the Himalayan margin of the Indian Plate comprises a pile of variably metamorphosed sedimentary rocks ranging in age from Precambrian to Mesozoic. They outcrop in laterally consistent terranes often extending the whole length of the Himalayan range (i.e. at least 1500 km) (e.g. Gansser, 1980; Shackleton, 1981; Windley, 1983; Searle et al., 1986). In Pakistan, however, the adjacent terranes along the Himalayan margin of the Indian plate represent a different lithostratigraphy (Lawrence et al., 1988; Treloar et al., 1989a,b,c).

Further south in the hill ranges, Mesozoic and Tertiary sediments were not metamorphosed by the Himalayan tectonism, and they outcrop in more laterally consistent belts. The WSW - ENE striking hill ranges of north Pakistan curve north

Table 2.3. Lithological comparison of the Kohistan and Ladakh arcs.

Kohistan		Ladakh	
Dir Group	58 – 55 Ma ¹	Khardung volcanics	Upper Cretaceous - Lower Tertiary ^b
		Dras II Volcanic Group	
Kohistan Batholith	102 ± 12 – 29 ± 8 Ma ²	Deosai-Ladakh Batholith	103 ± 3 – 60 ± 0.4 Ma ^c
Chalt Volcanic Group	pre 110 Ma ^{3, 11}	Dras I Volcanic group	Upper Jurassic ^d
Kamila Amphibolites	circa 110 Ma		
Yasin Group	(Albian-Aptian) ⁴	Nindam Formation	circa 97 Ma ^e
Purit Formation	85 Ma ¹⁰ (U-Pb zir)		
Chilas Complex		Kargil Complex	
Jijal Complex	103 ± 0.9 Ma ⁵		

1. Treloar et al., 1989; 2. Petterson & Windley 1985, Debon et al., 1987, Treloar et al., 1989; 3. Pudsey et al., 1985, Treloar et al., 1989; 4. Pudsey et al., 1985; 5. Coward et al., 1986; 6. Srimal et al., 1987, Reuber, 1989; 7. Honegger et al., 1982, Schare & Allegre 1982, Scharer et al., 1984; 8. Honegger et al., 1982; 9. Searle et al., 1988; 10. Zeitler et al., 1985; 11. Ivanac et al., 1956.

into the Hazara–Kashmir syntaxis, and then turn into the NW - SE striking Pir Panjal range of Kashmir. Tertiary molasse deposits occupy the core of the Hazara Kashmir syntaxis and are extended towards north about 30 km south of the MMT. Some details of the main lithological and structural units of the Indian Plate rocks belonging to Himalayan margin are given in the next pages to understand the continued subduction process (Figure 2.5).

Tethyan Shelf Sediments

Fossiliferous marine sediments extend from Zaskar along the southern edge of Tibet into the northern corner of India (Windley, 1988). These sediments represent a relatively continuous Paleozoic to Mesozoic passive continental margin succession developed along the northern margin of India (Gupta and Kumar, 1975; Fuchs, 1979; Thakur, 1981; Tapponnier et al., 1981; Baud et al., 1984; Gaetani et al., 1985; Nicora et al., 1987). The succession is stratigraphically divided into the Paleozoic (Lahoul Supergroup) and the Mesozoic (Zaskar Supergroup), and is separated by the Permian Panjal Traps. The Panjal rocks are continental flood basalts formed in Carboniferous-Permian rifts which evolved into the passive margin of Neo-Tethys during the Mesozoic (Searle et al., 1987). In Zaskar, during the early Mesozoic, the deposition of shelf carbonate facies was characteristic with only minor transgressive phases (i.e., Spitti Shales). Shallow marine conditions continued until late Cretaceous. Sea-level fluctuations continued until the Eocene when the first volcanic arenites from the Eurasian magmatic arc were deposited (Gaetani et al., 1985; Garzanti et al., 1987; Nicora et al., 1987). The shelf carbonate sequence is drastically reduced in Pakistan, reflecting the probable western extent of the Indian continental margin (Searle et al., 1987). Evidence for early Paleozoic basement comes from the 514 Ma (Rb-Sr) age for the Mansehra granite (Le Fort et al., 1980), which intrudes the Hazara slates and

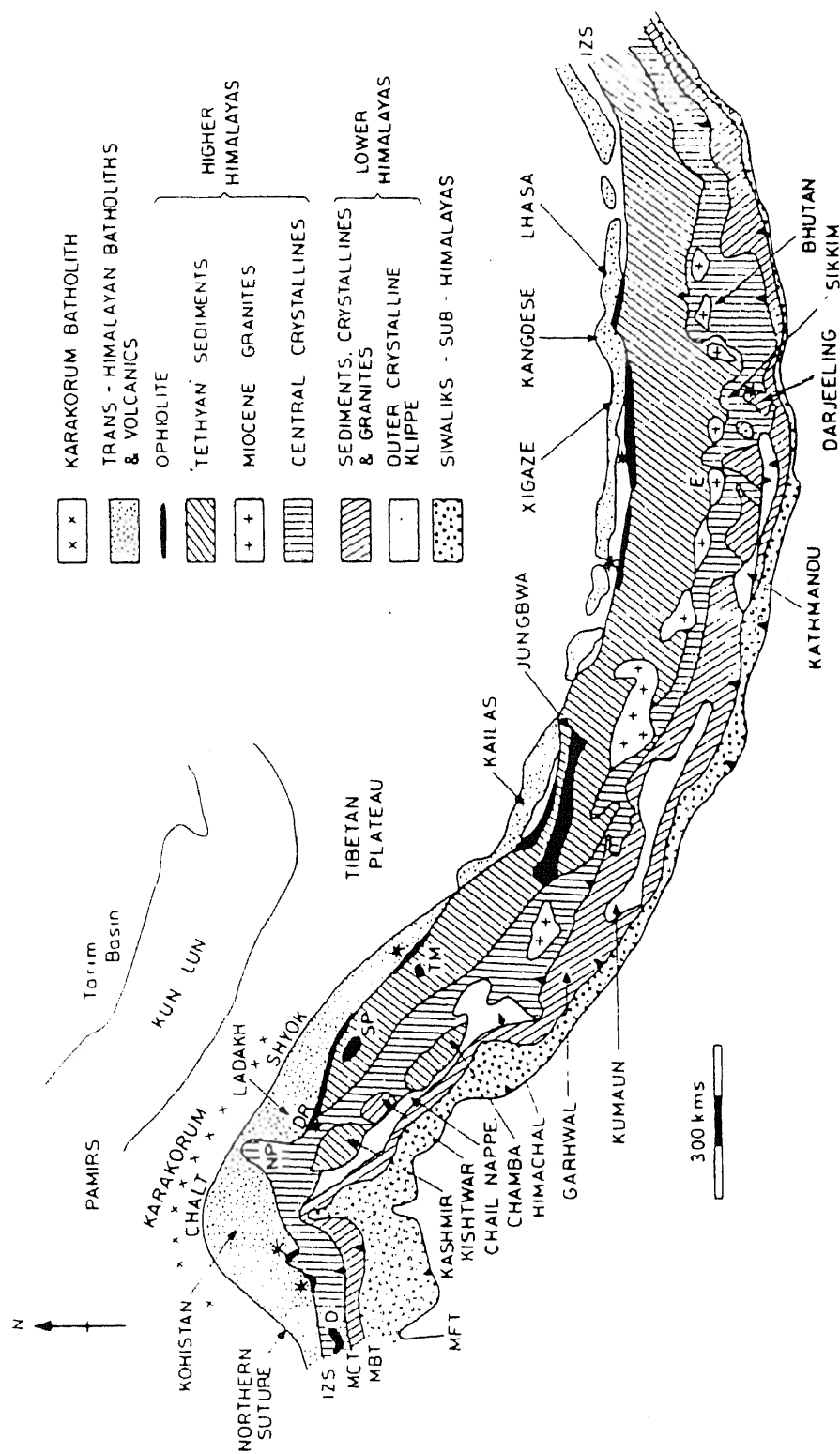


Figure 2.5. Map of Himalayan orogen showing main lithological and structural units (after Jan, 1991).

SSZ = Shyok Suture Zone, MMT = Main Mantle Thrust, ITSZ = Indus Tsangpo Suture Zone, MCT = Main Central Thrust, MBT = Main Boundary Thrust, and MFT = Main Frontal Thrust.

correlates with intrusions of similar age reported in Tibet, Afghanistan and High Himalaya of northwest India.

The High Himalaya

The Central Crystalline Complex of the Higher Himalaya (Gansser, 1964) represents the metamorphic basement to the Tethyan Shelf Sequences. It is bound to the south by the Main Central Thrust (MCT) and to the north by a northward-dipping normal fault. Within the Tibetan region this normal fault formed due to gravity collapse of thrust-thickened Himalayan crust (Burg et al., 1984). In Zaskar the fault (Zaskar Shear Zone) is listric (Searle, 1986), and has a vertical displacement of ~20 km (Herren, 1987). This was caused by culmination collapse during and subsequent to uplift of the High Himalaya. The lithologies include ortho- and para-gneisses, amphibolite, marble, schist and migmatite (Burg et al., 1987).

The MCT zone is a major southward-verging intra-continental shear zone, developed during Oligocene thrust propagation across the northern edge of the Indian Plate. The exact timing of this is uncertain, but associated leucogranites are dated as Oligocene-Miocene. Thrusting and associated syn-deformational metamorphism (Le Fort, 1975; 1981) folded the metamorphic isograds into a 'S', juxtaposing sillimanite grade rocks over staurolite-kyanite grade rocks. In detail, Hodges et al. (1988) identified a number of episodes directly responsible for the formation of leucogranites in the early Miocene. Later collapse due to normal faulting resulted in further exhumation and prevented re-equilibration of the rocks. Two-micas leucogranites, ranging from 25 to 18 Ma age, intrude the Central Crystalline Complex (Scharer et al., 1984; Deniel, 1987). These granites are S-type (Chappell and White, 1974) minimum melts and often contain garnet, sillimanite and tourmaline. Initial Sr ratios vary between 0.78 and 0.75 (Daniel et al., 1985; Le Fort et al., 1987) and reflect the isotopic heterogeneity of the source

region. A currently favoured model for the leucogranite generation involves the release of fluids from overthrust sediments fluxing hot gneisses which correspondingly undergo wet melting (Le Fort, 1981; Vidal et al., 1982). Hodges et al. (1988) relate the restricted distribution of leucogranites in the High Himalaya to localised high concentrations of heat-producing elements.

Lesser Himalaya

This zone is a 20 km thick thrust-slice, bounded to the north by High Himalayan crystallines and to the south by the Main Boundary Thrust (MBT). It consists of a pile of late Proterozoic gneisses and Paleozoic-Mesozoic sediments (slates, phyllites, sandstones and flysch). The Mesozoic succession suggests a shelf origin, thickening towards the north. These rocks have been overthrust by high-grade gneisses originating from the High Himalaya (Thakur, 1981). Ages from the overthrust nappes are consistent with ages from granites in the High Himalaya.

Sub-Himalayan Molasse (Siwalik Group)

The unmetamorphosed molasse basin deposits record the unroofing of the Himalayas to the south of the MBT. The Siwalik Group consists of fluvial conglomerates, arkoses, siltstones and shales that were deposited in a fore-deep along the southern margin of the mountain chain. Sedimentation started 20-15 Ma ago (Johnson et al., 1985) with detritus dominated by High Himalayan lithologies, where uplift (and therefore erosion) was greatest (Cerveny et al., 1989). Locally however, there is evidence of early Eocene molasse as in the Hazara syntaxial area (Bossart and Ottiger, 1983).

The Kashmir and Peshawar intermontane basins are situated a little to the north of the MBT and are embedded within an active thrust belt (Burbank and Johnson, 1983). In the Peshawar basin sedimentation began three Ma ago as a

consequence of uplift within the Attock hills (Burbank and Johnson, 1983; Burbank and Tahirkheli, 1985). The Skardu intermontane basin lies within an aseismic part of the Himalayan thrust belt and developed due to rapid uplift of Nanga Parbat. Uplift resulted in a temporary ponding of the Indus river, with sediment deposition between 3.2 to 0.75 Ma (Cronin, 1989).

Existing Models for the Tectonic History of the Kohistan

The western Himalayas is one of the best places in the world to study collision tectonics because it contains sutures, plates, batholithic belts and an island arc. The first model for the tectonic history of Kohistan arc was postulated by Tahirkheli et al., 1979; and Bard et al., 1980. They considered that the entire sequence from Jijal to Yasin and Utror and Drosh represents a single island arc, which they named the Kohistan island arc. The model envisaged northward intraoceanic subduction of the oceanic part of the Indian plate in the Tethys, leading to the formation of an island arc and eventual suturing of India with the island arc forming the MMT. This was followed by the northward subduction in the marginal sea leading to the suturing of Kohistan Island arc with Asia forming the MKT (Figure 2.6).

Petterson and Windley (1985, 1991) and Petterson et al. (1990, 1993) have recognized three stages of magmatism in the Kohistan batholith. The earlier phase granitic plutons yield a Rb/Sr whole-rock isochron age and Nd isotope data of 102 ± 12 Ma emplacement, whereas the Kohistan island arc was still in the intra-oceanic tectonic setting. The second stage of magmatism is suggested to have taken place after the accretion of the Kohistan island arc with the Karakoram microplate, forming an Andean-type continental margin. This magmatism was mostly basic from 85 to 60 Ma and acidic from 60 to 40 Ma. The stage three

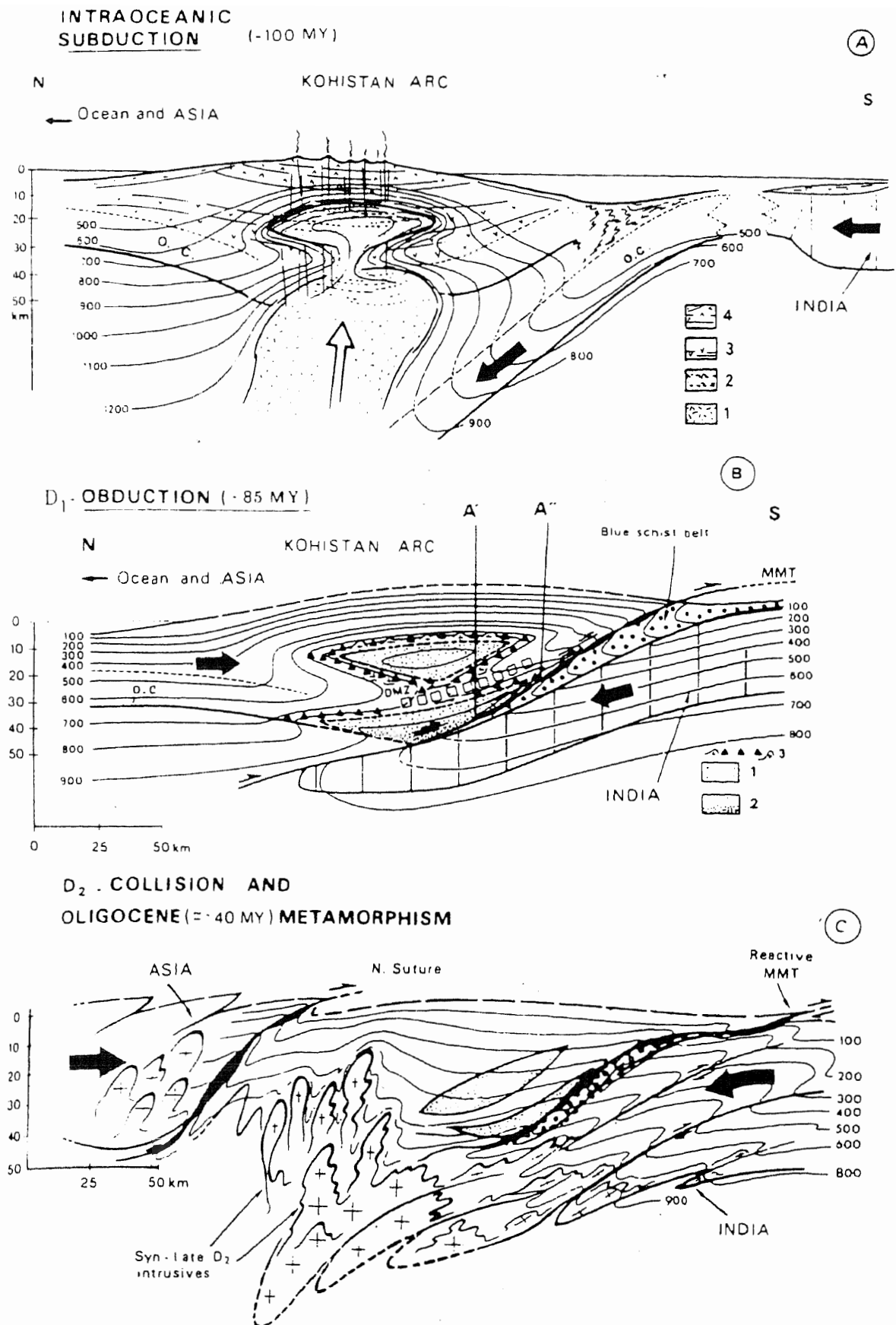


Figure 2.6. Tectonic model of the thermal structures in the Kohistan obducted island arc during its tectonometamorphic evolution by Bard, 1983a.

A: Intraoceanic subduction stage with arc building ~ 100 My ago i.e., just after the last emplacement of calc-alkaline plutonic and volcanic rocks. B: Obduction stage ~ 85My ago and D₂ event. C: Oligocene collision of India (north-western edge) against Asia during the D₂ tectonometamorphic event.

magmatic activity comprises dense swarms of leucogranitic sheets at ca. 30 Ma, which are the possible melts of the Kohistan crust (Figure 2.7).

Coward et al. (1982) considered the Jijal and Chilas complexes as the basal units of the Kohistan arc, overlain by the Kamila amphibolites and Chalt volcanics. This configuration was thought to result from folding of the arc crust. Coward et al. (1987) realized that when the isoclinally folded and imbricated Kohistan arc sequence is restored back to its original dimensions, it is abnormally large (>200 km in the N-S direction: not comparable to any present day intra-oceanic arc) (Figure 2.8).

More recently, Coward et al. (1987), Khan and Thirlwall, (1988) and Treloar et al. (1990) proposed that the Kohistan is a composite island arc system. One arc is represented by the Jijal, Allai, Sapat gali and Babusar ultramafic complexes and overlying metamorphosed gabbros / basalts, the Babusar amphibolites; and the second arc comprises Chilas complex at the base and the Chalt volcanic rocks in the upper crustal levels. The southern arc formed in the Tethys probably earlier than the northern calc-alkaline main Kohistan arc. The two arcs were considered to have accreted along the Kamila-Jal shear zone (Khan and Coward, 1990; Treloar et al., 1990) probably at the same time when the marginal basin between Kohistan and the Karakoram plate closed to form the Northern suture (Pudsey et al., 1985; Coward et al., 1986). This shear zone represents the most intense deformation in the southern Kohistan, comparable to that observed at MMT. However, the rocks bounding the Kamila shear zone are calc-alkaline in geochemistry, and there is a complete absence of such rocks which can be considered to represent remnants of a closed ocean.

A third model presented by Khan(1988) suggests that the original Kohistan arc crust consisted of the Jijal complex, tholeiitic Babusar amphibolites and

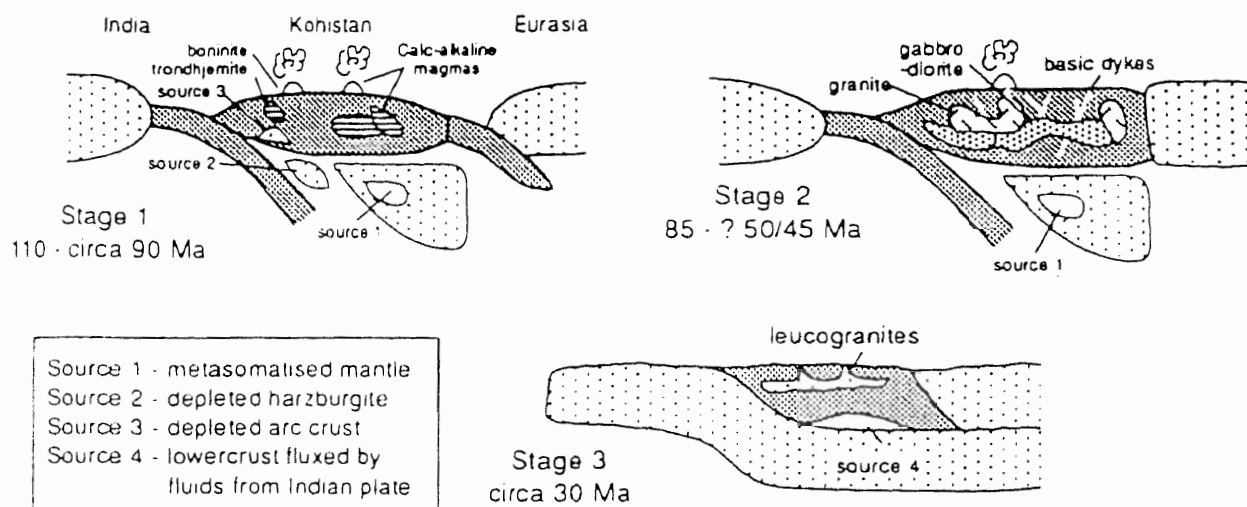
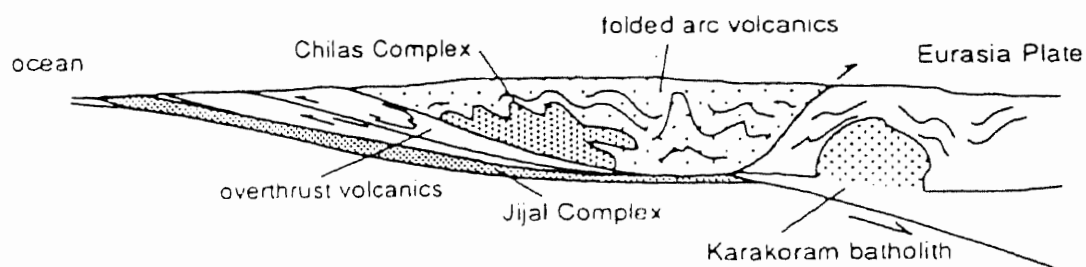
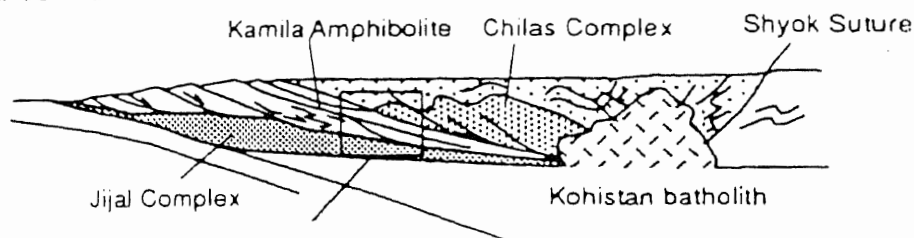


Figure 2.7. Magmatic and tectonic evolution of the Kohistan Terrane showing different proposed source regions (after Petterson and Windley, 1991).

(a) circa 90 - 100 Ma



(b) circa 80 Ma



(c) circa 20 Ma

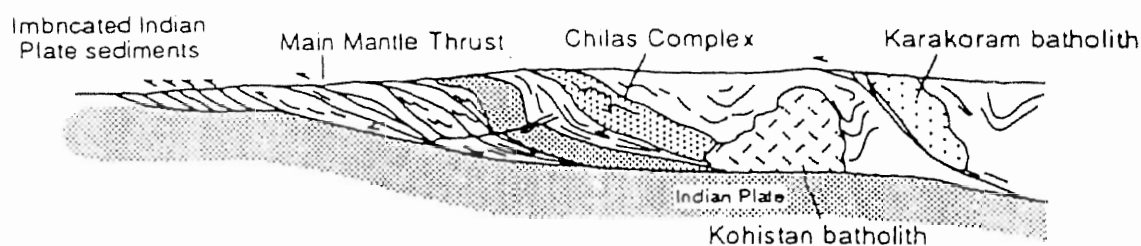


Figure 2.8. Schematic section through the Kohistan arc to show structures developed during (a) accretion of arc to Eurasia, (b) post-collisional continental margin deformation and (c) India-Eurasia collision (after Coward et al., 1987).

tholeiitic to calc-alkaline arc volcanics now represented by those of Chalt. According to this model the Chilas complex with most of the Kamila amphibolites was generated from a mantle diapiric rise and emplaced in an intra-arc setup or a back-arc basin. Khan et al. (1989,1993) suggestion that the Chilas complex represents a separate magmatic entity within the Kohistan arc and is supported by several attributes of the complex, such as a high liquid cumulate ratio, and a calc-alkaline geochemical characteristics of mature arcs (rather than early arc tholeiites). In fact, the Chilas complex shows a reversal to tholeiitic composition in the younger dyke phase, the amphibolite dykes of Jan et al. (1984) and Khan (1988) which is opposite to the evolutionary way in progressively maturing arcs. According to Khan et al. (1993) model, the earlier basement of the Kohistan island arc is represented by the metavolcanics of Kamila amphibolite belt (Figure 2.9).

Debon et al. (1987) discussed the geodynamic evolution of the NW part of the Indian-Asian suture zone. They suggest partly synchronous closures, by northward dipping subduction, of the two Tethys. The northern branch very likely closed before the southern one, and both are assumed to have encircled the Kohistan arc in upper Mesozoic times and generated the Karakoram and Kohistan intrusives of Cretaceous and Paleogene ages (Figure 2.10). Following the proposed model, mid-Cretaceous Karakoram granitoids of Koz Sar alkaline complex (88 Ma) are related to the N-dipping subduction of a northern Neo-Tethys during the ongoing Kohistan-Karakoram collision. On the other hand, Lower Cenozoic (63-43 Ma) Karakoram granitoids have been related to the northward subduction of the southern Neo-Tethys and incipient India-Eurasia collision (Debon, 1996).

Ghazanfar et al. (1991) considered the Chilas complex, with spreading center affinities, to have been emplaced tectonically between two belts of island

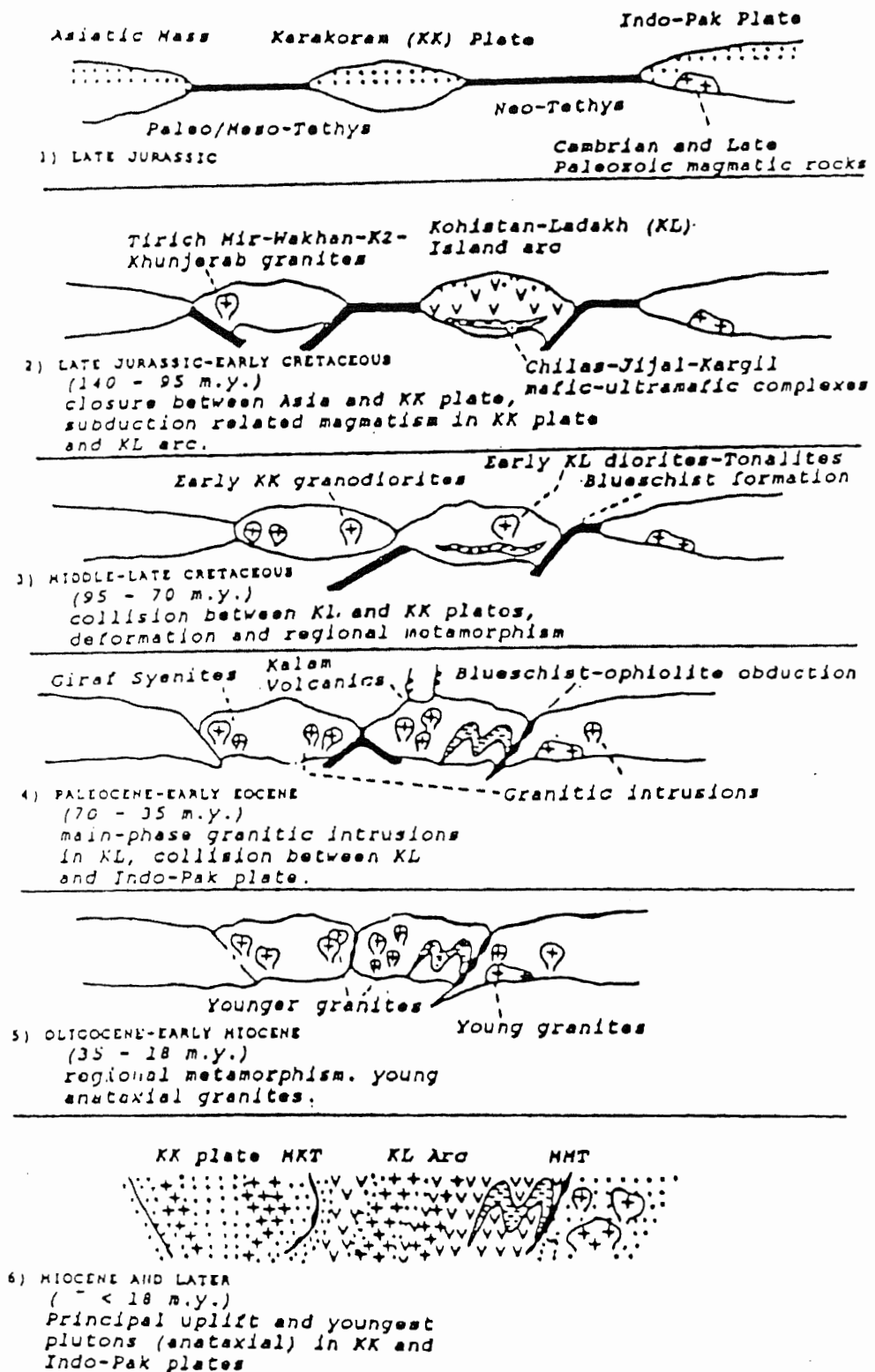


Figure 2.9. A speculative model for the tectonic evolution of northern Pakistan (after Khan and Jan, 1983).

MMT = Main Mantle Thrust and MKT = Main Karakoram Thrust.

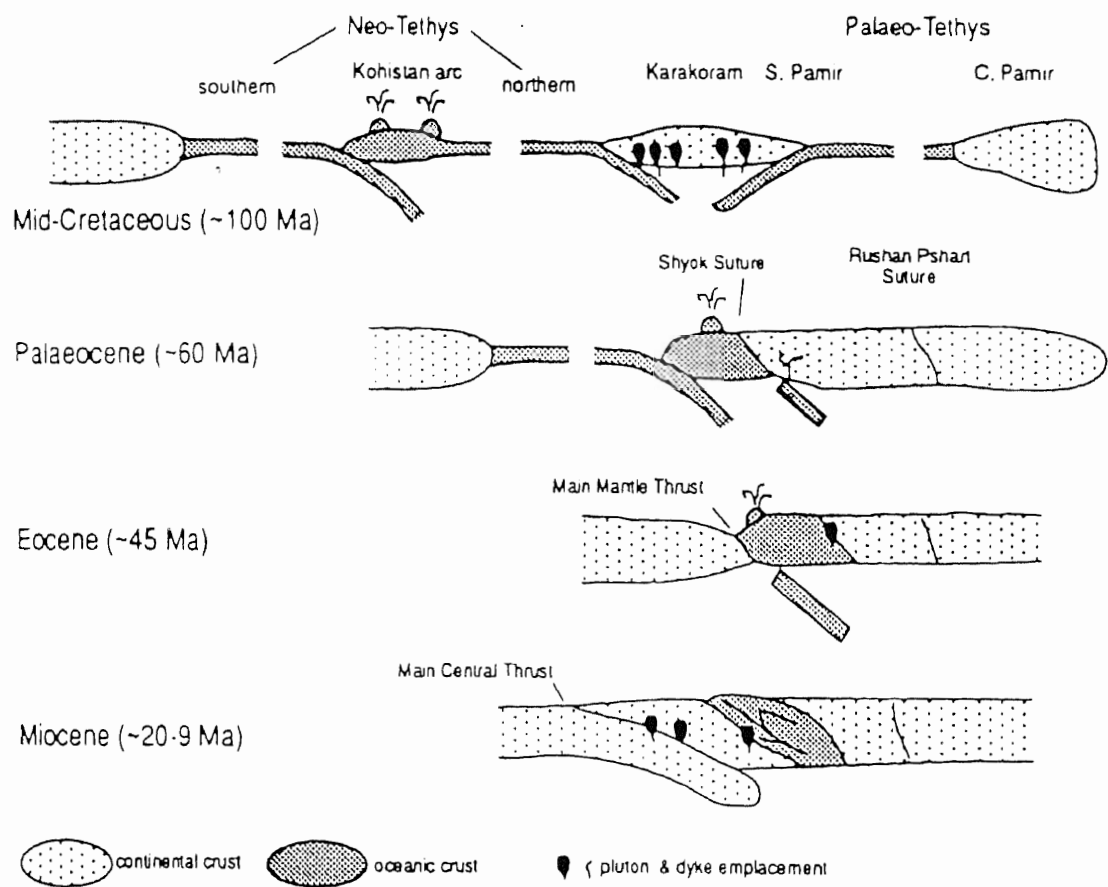


Figure 2.10. Model for the mid-Cretaceous - Miocene evolution of the India - Eurasia suture zones in the N.W. Himalayas (after Debon et al., 1987).

arcs. That to the north of the complex was considered younger than the one to its south. The stark difference in the grade of metamorphism of ophiolitic greenstone and amphibolites is probably not related to age and may only indicate different levels of subduction. The number of intrusions are not arc related, nor indeed a melting product of amphibolites. They are S-type and indicate a mainly continental derivation. These may be related to underthrusting along MMT and thrust piling of Indian mass.

Virdi (1992) considered the Kohistan and Ladakh regions as western Pacific-type subduction zone with back-arc and fore-arc basins on the northern and southern sides, respectively, of a magmatic arc. The development and evolution of the back-arc is due to the northward movement and consumption of the oceanic crust of the Tethys along the Benioff zone at the southern margin of Tibet during the building of an island arc. According to Yamamoto (1993), the Kohistan arc forming at least a 55 km thick crust before and/or during closure of a back-arc basin, consisting of amphibolites, granulite and ultramafic rocks.

Khan, T (1994) proposed a modified tectonic model for the Kohistan terrane. According to his model, the Kamila amphibolite belt is considered to represent an arc magmatism related to the northward subduction of the Neo-Tethyan lithospheric plate. A marginal or back-arc basin developed between the Kamila arc and the Karakoram plate. The Chilas Complex formed from a magma that was probably derived from a metasomatised mantle diapir, and intruded the back-arc basin assemblages. All these lithologies were folded and imbricated due to closure of the back-arc basin. Subsequently, collision of the Kohistan terrane with the Indian plate (Figure 2.11) occurred.

The nature of the Main Mantle Thrust(MMT) too has been disputed. Tahirkheli et al. (1979) and Bard et al. (1980) suggested that the MMT was one of

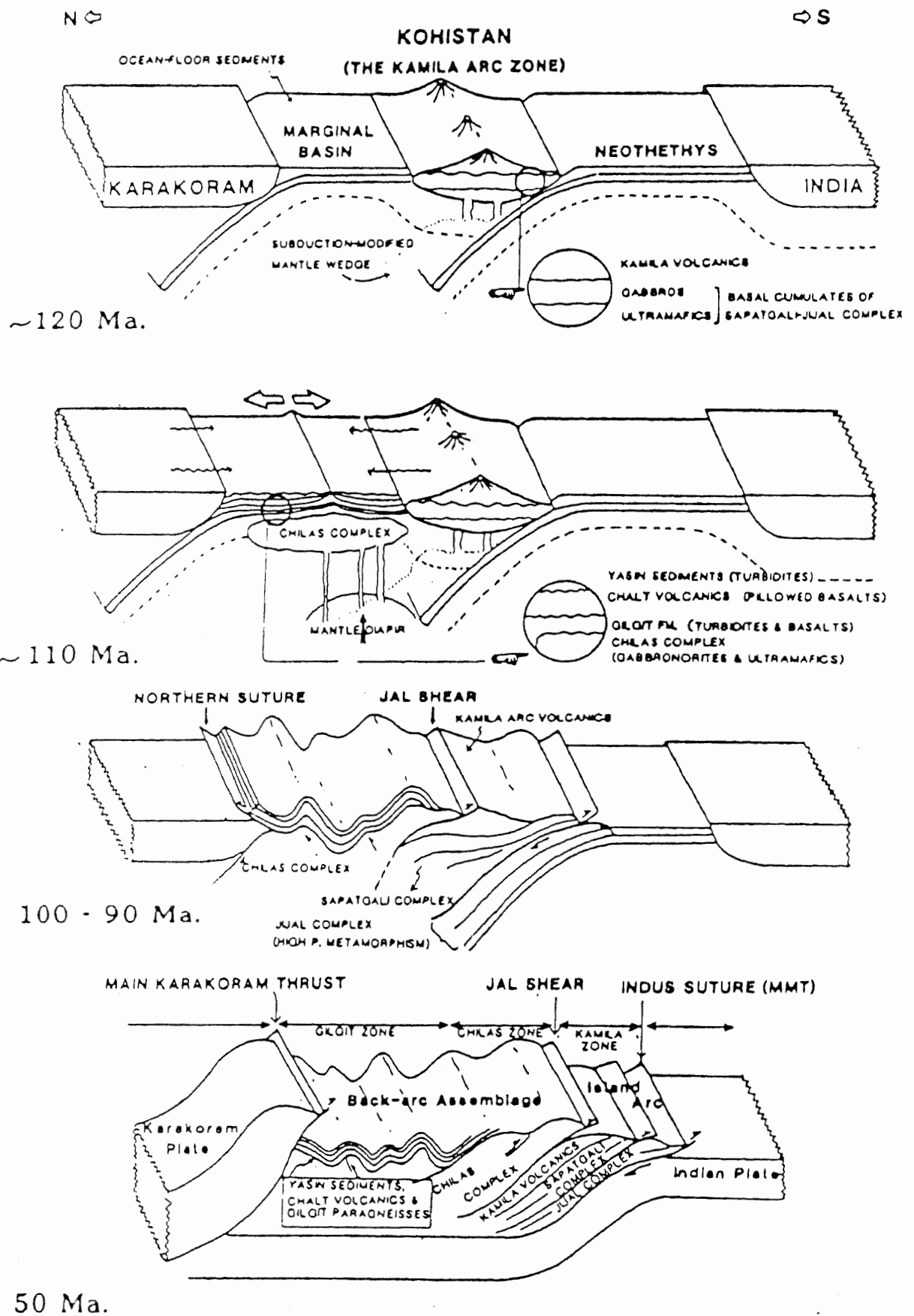


Figure 2.11. A model illustrating the tectonic and petrological evolution of the Kohistan terrane over a span of 120 to 50 Ma (T. Khan, 1994).

the two continuations of the Indus-Tsangpo suture zone. Still they considered it, a megashear and included the ultramafics associated with basic rocks as the bottom part of the Kohistan island arc sequence. Jan et al. (1981) suggested that the rocks of Shangla area represent an oceanic trench melange. Lawrence et al., 1983; Chaudhry et al., 1984 and Chaudhry and Ghazanfar. (1986, 1987) also considered the ultramafics and associated basic rocks along MMT as a trench melange complex and not as the bottom part of Kohistan island arc. Since then information has been added towards a better understanding of the MMT (Lawrence et al., 1983; Zeitler, 1985; Butler, 1986; Kazmer, 1986; Chaudhry and Ghazanfar, 1987; Spencer et al., 1989; Baig, 1989). MMT is now recognized as an overthrust shear towards SSE with an age of 55 Ma (Powell, 1979; Klootwijk, 1992). It is a complex zone with different structural levels of obduction and subduction at different sites due to different uplift (Lawrence et al., 1983), or due to break back faults (Butler, 1986). Mylonites have been reported along MMT at various places.

Fission track and $^{40}\text{Ar}/^{39}\text{Ar}$ cooling ages across the MMT suggests that vertical differential motion along this structure may have continued until as recently as about 20-25 Ma (Zeitler, 1985; Erickson, 1990). Vince and Treloar (1996) and Burg et al. (1996) reported the Miocene north-vergent extensional displacements along the MMT. Cooling histories enable the age of uplift/extension. Cooling ages for zircon and higher temperature chronometers are greater for rocks of the Kohistan arc and the suture zone melange than for the Indian Plate. Although zircon ages are considerably older within Kohistan than within the Indian Plate, apatite ages, at between 16 and 20 Ma (Zeitler, 1985) are similar for both arc rocks on the MMT hanging wall and Indian Plate rocks on the MMT footwall. From this, Vince and Treloar (1996) concluded that extension was completed during the interval of 18 ± 2 Ma over which the Indian Plate rocks cooled between the fission

track annealing temperatures of zircon and apatite of 250 and 120 °C. These data are consistent with the brittle nature of the few extensional features preserved on the Main Mantle Thrust hanging wall, and the transition, during deformation, from ductile to brittle deformation mechanisms recorded on the Main Mantle Thrust footwall.

The Kohistan arc oceanic complex is a major phenomenon, i.e. hundreds of kilometers long and scores of kilometers wide. Only preliminary field studies along selected sections of the Kohistan terrane have been carried out. The present work is a relatively detailed field oriented study in the remote areas of east and southeastern Kohistan. Field work together with petrological and geochemical data proposes a modified tectonic model for the Kohistan terrane. The tectonic evolution of SE Kohistan is still far from clearly understood. Many problems remain unresolved and require more detailed work.

Local Geology

The study area is surrounded by fault structures and shear zones. It is separated from the Indian plate to the south and the Nanga Parbat-Haramosh massif to the east by the Indus suture (MMT), and from the Chilas Complex to the north by the Jal Shear Zone. The area has been mapped in the valleys of Bara gah, Makheli gah, Keo gah, Buto gah, Thak gah, Niat gah and Buner gah during this study. The lithologies, from south to north, are shown in Figure 2.12. The mapped area comprises mafic/ultramafic rocks, amphibolites and metavolcanics, intruded by diorite, granodiorite, granite, trondhjemite and granitic pegmatite. The contacts between the constituent rock units run almost parallel to one another in east-west direction (Figure 2.12). All units are terminated in the eastern part of the

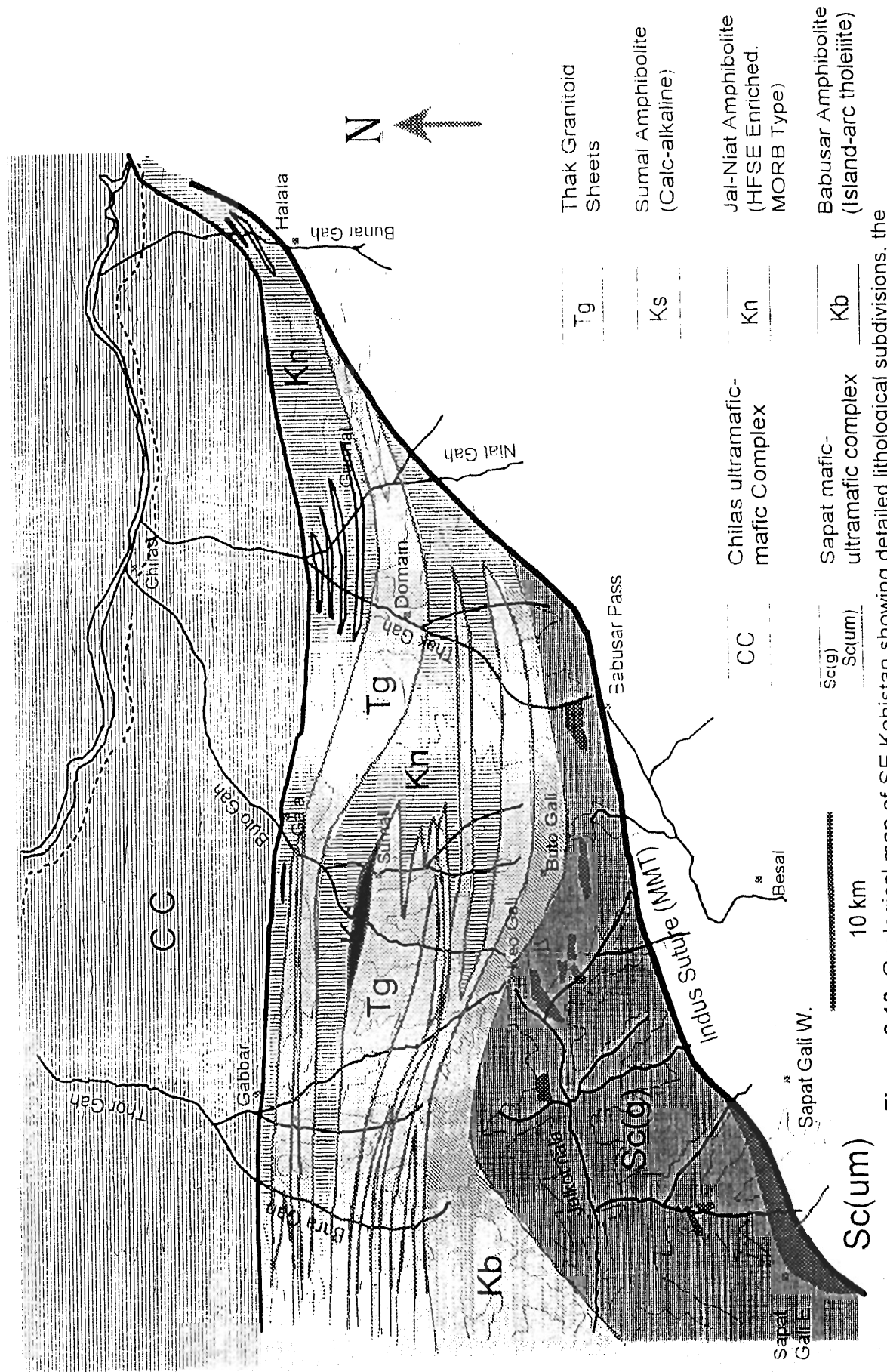


Figure 2.12. Geological map of SE Kohistan showing detailed lithological subdivisions, the Sapat complex, the Kamila amphibolite belt and the Thak granitoid sheets.

study area by the Main Mantle Thrust (MMT). The foliation of the units shows an approximately constant east - west strike with gentle to moderate northerly dips.

The southern part of the area is covered by the mafic-ultramafic rocks. These rocks occupy the immediate hangingwall of the MMT and are exposed in the upper reaches of Thak Gah (i.e., Babusar Pass), Buto Gah, and the tributaries of the Jalkot Nala. To the east, these are truncated by the MMT and are not seen in Niat and Bunar valleys. These mafic-ultramafic rocks are part of the Sapat Complex (Jan et al., 1993). The principal occurrence of the ultramafic rocks of this complex is exposed at the Sapatgali pass in the southwest of the study area, north of Naran. It is a 15 km² ultramafic body which overlies the Indian Plate rocks along the MMT between Parala Sapat and Umar Di Baikh. The body is lensoid in shape, with a maximum thickness of about 750 m, upstream from Ratti Gatti. The body is overlain by a layered sequence of gabbros with sparse pyroxenites and anorthosite. These grade upsection into isotropic gabbros. The ultramafic body at the Sapatgali Pass pinches out immediately to the east of the Umar Di Baikh. Further east occur only the gabbroic rocks in the hanging wall of the MMT. Several small, lensoid bodies of ultramafic composition occur upsection within the gabbros. These bodies are mappable at 1:50,000 scale in the high reaches of Shambaik (between Tuno and Chochargah), southwest of Buto gah gali, north of Kalwan, and near Shotti pass, south of Utla Babusar. The western extension of the complex, towards the Indus valley, is yet to be mapped. The Pattan or Kayal complexes in the Indus valley (Miller et al., 1991; Loucks et al., 1993), Khawzakhela troctolites and gabbros, and ultramafic rocks in Upper Swat, and Tora Tigga complex in western Dir may be western equivalents of the Sapat complex.

The mafic-ultramafic rocks are overlain by a thick sequence of amphibolites in the area. This has been studied to the south of Utla Babusar, at Batsi Sangar, Shikaro

Gah and in the north of Kot Gali. These amphibolites are divided into four units, from south to north, Babusar, Niat, Sumal and Jal amphibolites (Figure 2.12). The Babusar amphibolites occur in the southern part and are best exposed in an east-west belt stretching between the drainage divide of Jalkot Nala and the tributaries of the Indus river at high reaches of Ktai gali, Buto gah gali, Keo gali, Makheli gali, Shikaro gali and Sherman gali. The width of the belt in the Thak valley is 1.5 km while in the western part near Sherman Gali it is 5 km. To the east of Babusar Pass in the Charal gah the belt occurs in the immediate hanging wall of the Main Mantle Thrust. In the north of the belt, diorite occurs with a sharp intrusive contact. The Niat volcanics are exposed as a thick sequence of homogeneous, fine grained amphibolites in the central part of the area. These rocks are not exposed in the eastern part of the area (Bunar valley). These metavolcanics are bounded by two dioritic bodies on both sides (north and south), and invaded by a number of intrusive sheets of different compositions, e.g., diorite, granodiorite and tonalites. The larger of these intrusions are shown on the map, and the two main exposures have been given the names Shai and Khun during this study. A thin slice of Sumal volcanics is separately mapped within the mixed zone of volcanic and intrusive rocks in Buto and Thor valleys. In the northern parts of the study area, the Jal amphibolites form a distinctly different belt due to their striking characteristics. These are well exposed in Thak at Jal and Niat gah, with a thickness of about 3 km. Within these amphibolites a number of thin pegmatitic veins are present. In the extreme eastern part of the study area, these are directly in contact with the gneisses of the Indian plate. These amphibolites are in contact with the Chilas complex to the north. The contact is marked by a strongly sheared amphibolite and granite mylonite zone. This zone, which is 100 meter wide in Thak and 20 meter wide in Thor gah, is termed as the Jal Shear Zone (Coward et al., 1987; Khan,

1988). It is probably an equivalent of the Kamila Shear Zone of Treloar et al. (1990).

Structure

As stated earlier the study area is bounded by two major structures. The Jal Shear Zone in the north separates the study area from the Chilas Complex, and the Main Mantle Thrust in the south and southeast separates it from the gneisses of the Indian Plate. The area contains a number of shear zones from a few centimeters to tens of meter thick. These are heterogeneously distributed and often anastomosing. In these shear zones no consistent attitude could be detected but a large number of these are trending east-west, with steep northerly dips. Layering in the more intense zones and small scale structures including folds and shear bands suggest the up dip and normal fault sense of displacements. The deformational structural trends are expressed in the heterogeneously distributed planar fabric of lenticular amphibole and plagioclase aggregates. This upright to steeply north dipping foliation is associated with a series of large-scale fold structures. Coward et al. (1987) considered that this folding is associated with D3 deformation event, which refolds earlier D2 isoclinal structures, now exposed as downward-facing folds in the core of a D3 anticline. The overturned limbs are particularly more intensely deformed and this intense deformation commonly results in the formation of shear zones.

The sequence comprising metavolcanics of Niat with diorite/ granodiorite sheets is repeated more than once, particularly in the central part of the studied area. This sequence is overthrust onto the Babusar amphibolites which overlie the mafic-ultramafic rocks of the Sapat Complex in the study area. There is evidence that the SW-verging deformation continued subsequent to the main-phase of

deformation, during uplift and unroofing of the southern Kohistan arc. Treloar et al. (1989b) stated that the actinolite-chlorite coated thrusts and the dry brittle thrusts, observed in the Indus valley section, are representative of this deformation episode. The brittle thrusts - dominated deformation is particularly well - pronounced in the Thak , Buto and Bara valleys.

Jal Shear Zone

The contact between the Jal amphibolites and Chilas Complex is marked by the presence of a mylonite zone (Jal Shear Zone of Khan, 1988), which deforms rocks of both the Chilas Complex and Jal amphibolites. The shear zone, oriented E-W and dipping towards north, continues westward as a narrow zone up to the Thor valley, the western part of the study area. Further to the west, in the Indus valley, the equivalent structure is present in the middle sector of the Kamila amphibolite belt (Kamila Shear Zone of Treloar et al., 1989b). Fabric trend of the rocks is E-W with steep dips towards the north in this part of the shear zone. Shear strains are highly variable as compared to the study area. Intensely mylonitised narrow zones show pronounced reduction of grain-size in these rocks. These zones alternate with relatively undeformed rocks.

Chapter 3

THE SAPAT MAFIC-ULTRAMAFIC COMPLEX

Introduction

In northern Pakistan, the Indus suture is known as the Main Mantle Thrust (MMT). It demarcates the Indian plate to the south from the Kohistan terrane to the north (Tahirkheli et al., 1979; Coward et al., 1986). Several ultramafic-mafic plutonic associations occur at a number of localities in the Indus suture zone of N. Pakistan. These are grouped broadly into two genetic types. One group, which is associated with volcanic and sedimentary rocks (e.g., Dargai, Shangla, Allai), occurs in tectonic melanges and probably represents dismembered oceanic ophiolites. The other group defines the deep-crustal base of the Kohistan terrane and overrides the Indian plate in the immediate hanging wall of the suture. These rocks (Tora Tigga, Jijal, Sapat, Babusar) are considered as cumulates to the magmas of the Cretaceous Kohistan island arc (Jan and Jabeen, 1990; Jan and Windley, 1990). The Chilas complex occurs to the north of the presently studied area and is a part of the Kohistan crustal sequence, but without being directly associated with the Indus suture. It consists of gabbro-norites with subordinate ultramafic, troctolitic and anorthositic rocks (Jan et al., 1984).

The southern parts of the thesis area are occupied by gabbroic rocks with eight small ultramafic bodies. At Sapat to the southwest of the area, Jan et al. (1993) reported a big ultramafic body (15 x 2 km) overlain by gabbroic rocks with local pyroxenite pegmatite. Ghazanfar et al. (1991) reported a lenticular body of pyroxenite which occurs upsection of Sapat complex within the gabbros. The ultramafic and gabbroic rocks in the area are hereby considered as eastern

continuation of the Sapat complex. There is a possibility that the Pattan and Kayal complex of Miller et al. (1991) and Loucks et al. (1992) are the westward continuation of the Sapat complex in the Indus valley (Searle and Khan, 1996). The Khwaza Khela body of troctolites and gabbros in the Swat valley (Jan and Karim, 1995) and Tora Tigga ultramafic-mafic complex in Dir (Jan et al., 1983) may be the continuation of the Sapat complex further to the west.

This chapter deals with the description of the ultramafic-mafic plutonic rocks occurring in the hanging wall of the Indus suture and forming part of the presently investigated area in southeast Kohistan. Field relations, petrographic studies and a limited whole-rock geochemistry form the basis of this description.

General Characteristics

At the type locality, i.e., Sapat, the complex is made up of a variety of lithologies including dunite, pyroxenites, peridotites, chromitite, gabbros and anorthosite. Jan et al. (1993) presented details of a ~2 km thick section exposed at and to the north of the Sapatgali Pass, comprising from base upward, serpentinites, massive dunite with abundant thin layers of chromitite, thinly layered dunite and wehrlite, interlayered pyroxenite, peridotite and gabbro, layered gabbro-anorthosite and finally isotropic gabbros with rare pyroxenite and anorthosite.

The part of the Sapat complex exposed in the presently studied area has general geological characteristics common with those described from Sapat by Jan et al. (1993) and Khan et al. (1994). The principal difference is that the base of the complex in the Babusar area is marked by amphibolitized gabbroic rocks, which are in tectonic contact with garnet-mica schists of the Indian plate along the MMT. Unlike the type location at Sapat, the ultramafic rocks do not form the base of the

complex, rather they occur as lenzoid bodies within the layered and isotropic gabbroic rocks.

Eight lenzoid ultramafic bodies are mapped in the studied area (Figure 2.12). These are located at high reaches of Shambaik (between Tuno and Chochargah), southwest of Buto gah gali, north of Kalwan and near Shotti pass, and to the south of Ulla Babusar. These range from 50 m to 200 m in thickness and have a lateral extent between 500 m to 2000 m. The largest body is exposed near Shotti pass. It is 200 m thick and is 1500 m in its lateral extent. The body has concordant relations with the enclosing gabbroic rocks and pinches out gradually at both ends. It comprises mainly dunite and pyroxenite. Pyroxenite occurs both as layers alternating with those of dunite as well as cross-cutting veins. Veins of chromitite are locally observed cross-cutting layered dunite-pyroxenite. The ultramafic body is extensively brecciated and serpentinized, several cross-cutting shear zones cause intense mylonitization and serpentinization. One such shear zone is about 5 m thick and extends oblique to the contact as well as the general strike of the rock body.

The ultramafic rocks in the area are medium- to coarse-grained, and massive to rhythmically layered (Plate 3.1). Some of the smaller bodies are exclusively massive dunites or peridotites. Others contain both massive and layered ultramafic rocks. Layering is primarily defined by variations in mutual proportions of olivine and pyroxene. Most layers are limited in lateral extent, but in rare cases the layers are laterally continuous along the entire length of the bodies. Layers with typical lenticular shapes are abundant.

The gabbroic rocks are dark to medium greenish grey on fresh surface (Plate 3.2). These are mostly medium-grained and range from homogeneous to



Plate 3.1. Rhythmic layering in serpentinized pyroxenite–dunite near Shotti pass. Layering is defined by variation in olivine-pyroxene proportions.



Plate 3.2. Amphibolitized foliated gabbro near Tuno in Jalkot Nala. The rock is massive and dark to medium greenish grey on fresh surface.

very well-layered varieties (Plate 3.3). The homogeneous gabbros are most abundant in the southern part of the complex whereas layered gabbros are mainly exposed in the northern parts. The layers are commonly a centimeter or less in thickness, but in some cases individual layers can attain a thickness of 6 to 10 cm. The layered rocks display size and mineral-graded layering, truncation of earlier layers by later layers, slump folding, syndepositional faults and dykes (Plates 3.4, 3.5 and 3.6). Some layers extend for several meters, but most layers are of limited lateral extent. These features are also reported in the Chilas complex by Khan et al. (1989). In contrast, in the Bushveld, Skaergaard and Stillwater Complexes, even thin layers may persist for a long distances (Jackson, 1967). The short lateral extent of the layers and the ultramafic bodies are the primary features, which are consistent with deposition from a series of small crystal suspensions rather than from convective flow (Irvine, 1980).

The gabbroic rocks are mostly medium-grained but at places these are coarse-grained and are foliated (Plate 3.7). Where involved in the shear zones, they are fine-grained mylonitized. Mylonitization is particularly common in the basal part of the complex along the MMT. Here about 50 meter thick basal part of the gabbroic succession is transformed into fine-grained, strongly foliated, massive to banded amphibolites with well developed stretching lineation typical of mylonites. A number of shear zones do occur upsection in the northern part of the complex in the area between Kalwan, Batsi Sangar, Tuno and south of Shotti Pass. Again ~~The~~ the rocks are highly mylonitized and the xenoliths are also oriented in the direction of shear (Plate 3.8). The xenoliths are fine-grained, show darker shades than gabbros and are mostly found near the contact with amphibolites.



Plate 3.3. Layered in gabbros near Chochargah in Jalkot Nala. Felsic layers reach up to 10 cm in thickness. A 3 cm thick quartz vein cuts the layered rock.



Plate 3.4. Folding in the layered gabbros at Buto gali. Some layers extend for several meters, but mostly the layers are of limited lateral extent.



Plate 3.5. Rhythmic layering in gabbros at Kot gali in Sapat Nala. Faulting in the rock can also be seen. Dark spots in the photograph are due to weathering effect.

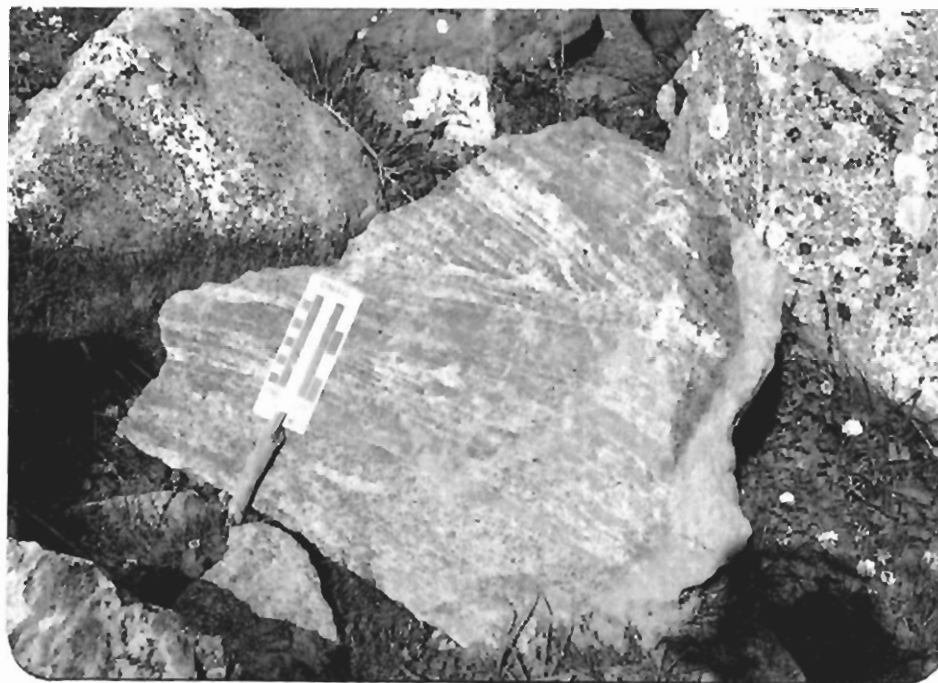


Plate 3.6. Syngenetic faulting is visible in layered gabbros near Kot gali in Thor valley.



Plate 3.7. Foliated gabbro containing medium- and coarse-grained bands. Both bands show foliation in the same direction. Aligned hornblende is very much visible in coarser band.



Plate 3.8. Mylonitized and sheared gabbros in the shear zone near Kalawan. Fine-grained xenoliths of volcanics are aligned in the direction of shear.

In the northern parts, the gabbroic rocks are characterized by the presence of intrusive sills, dykes and sheets of granodiorite and trondhjemite composition. These are especially more abundant towards the northern contact of the complex against the amphibolites. At places abundant veins and sills of quartzofeldspathic rocks occur at regular interval within the amphibolitized gabbros, furnishing a banded appearance. Quartz veins are also very common in these rocks. The veins are 0.2 cm to 6 cm thick (Plate 3.9).

Modal Composition and Petrography

Ultramafic rocks

The ultramafic rocks include dunite, peridotite and pyroxenite. Dunites and peridotites are composed predominantly of medium- to coarse-grained olivine and pyroxene. Olivine and pyroxene occur as rounded and anhedral grains and constitute up to ~ 70 vol% of these rocks. Disseminated chromite is commonly present but rarely exceeds a percent or two in terms of modal percentage. The olivine-rich rocks commonly show varying degrees of alteration to serpentine, magnesite and some minor talc, accompanied by Mg-rich chlorite around chromite. These secondary minerals occur as fine-grained matrix surrounding the relicts of primary minerals like olivine, clinopyroxene and chromite. Serpentinization is particularly intense in the ultramafic bodies nearer the suture. Some ultramafic rocks show deformational features such as granulation of olivine and presence of kink bands in the clinopyroxene. Modal composition of ultramafic rocks is presented in Table 3.1.

Olivine occurs as subhedral crystals some of which display weak undulatory extinction. Olivine grains vary from 0.5 mm to 5 mm in length. It is partially altered to serpentine and magnetite along margins and fractures but complete alteration to

Table 3.1. Modal composition (based on visual estimates) of ultramafic rocks.

Sample Nos.	BA-26	TKA-40	BA-27	BA-28	TKA-48	TKA-41	TKA-49
Serpentine	26	92	50		50	24	12
Pyroxene	15	2	40	4	40	62	80
Magnetite		5	1	6	10	10	6.4
Chromite	3					2	
Ni-Sulphide	tr		tr	tr			0.6
Magnesite			8				1
Amphibole		1		60			
Olivine	56	tr	1				
Chlorite	tr			30	tr	2	
Total	100	100	100	100	100	100	100

Key : BA-26(peridotite); TKA-40 (serpentinite); BA-27 (serpentinized peridotite); BA-28 (hornblende bearing UM); TKA-48 (serpentinized pyroxenite) and TKA-41,49 (pyroxenite).

Tr= Traces, BA= Buto and TKA= Thak valley ultramafics.

serpentine has also been noticed. It is likely that the anhedral texture of olivine grains has a direct relation with the serpentinization. Severely serpentinized parts of peridotite and dunite have clusters of olivine relics in serpentine matrix (Plate 3.10).

Pyroxene occurs as subhedral to tabular crystals displaying ophitic to sub-ophitic texture. It is predominantly clinopyroxene and orthopyroxene is rare. The former is diopsidic, colourless to faint brown, nonpleochroic and forms subhedral to euhedral crystals. The porphyroclasts of clinopyroxene are fractured and corroded at the margins. Some exhibit kink banding and laminar twinning. Clinopyroxene shows partial alteration to serpentine and chlorite and also to fibrous amphibole (Plate 3.11). Serpentinization is dominant over chloritization but chlorite is frequently present in majority of pyroxenites. Microveins of carbonate material cross-cutting the clinopyroxene grains are noticed in some thin sections.

Serpentine is a dominant mineral, occurring together with variable proportions of chlorite, talc, magnetite and, in some cases, magnesite with relics of clinopyroxene, olivine and chromite. In extreme cases no relics of olivine and clinopyroxene are observed and the ultramafic rocks are entirely serpentinized. Serpentine is dominantly antigorite, but some cross-fibres of chrysotile also occur along shear zones. Serpentine forms radial aggregates and small heaps of flakes. Magnetite is the most common ore mineral. It can be seen both as subhedral scattered grains and minute specks arranged in straight parallel rows. A little part of magnetite weathers to limonite. Magnesite occurs as an alteration product in small veinlets. The other accessories are sulphide, chlorite, and secondary iron oxide.



Plate 3.9. Amphibolitized gabbro with medium- and coarse-grained bands showing foliation in the same direction and cut by a 5 cm thick quartz vein. The coarse-grained part shows visible alignment in amphibole crystals.

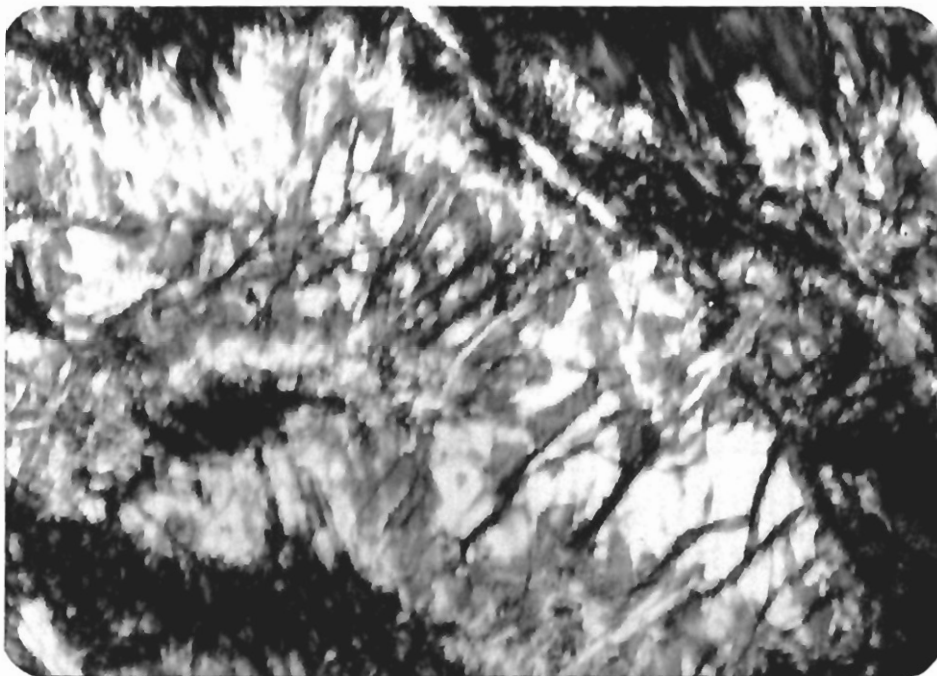


Plate 3.10. Thin section of the ultramafic rock showing olivine relics in serpentine with minor magnetite. Field of view is 4 mm.

The pyroxene-rich ultramafic rocks vary in texture and mineralogy, but most are hypidiomorphic. The clinopyroxene is diopside/diopside augite and orthopyroxene is enstatite. Both the pyroxenes may display exsolution. A few pyroxenites contain appreciable amounts of brown hornblende. The clinopyroxene and brown hornblende commonly form ophitic/poikilitic grains up to 2 cm in length. The pyroxene grains show varying degrees of alteration to amphibole, epidote, serpentine and chlorite. Another amphibole of green colour occurs either as acicular or columnar crystals or as irregular patches. Serpentinization is strong wherever the rock has undergone deformation. Epidote occurs as small prismatic, granular or acicular grains locally forming aggregates. It is clearly related to the alteration of pyroxene.

Gabbroic rocks

The bulk of the Sapat complex consists of gabbroic rocks ranging from homogeneous to very well-layered varieties. The layers are from centimeter to meter-scale in thickness. The rocks are commonly sheared and metamorphosed under epidote-amphibolite facies conditions leading to an abundance of amphibole and epidote. Modal composition of the gabbroic rocks is presented in Table 3.2.

The rocks are generally medium- to coarse-grained, hypidiomorphic and equigranular to subporphyritic. They consist mainly of amphibole, epidote and chlorite with smaller amounts of pyroxene, quartz, sphene, feldspar and magnetite. In one section garnet is also present. It is commonly observed that pyroxene, amphibole and ores tend to be segregated in crude layers, patches and clots. Where sheared, the rock is finer grained and strongly foliated (Plate 3.12). Along fractures carbonate is present but at places both carbonate and chlorite are also seen.

Table 3.2. Modal composition (based on visual estimates) of Gabbros.

Sample Nos.	TKA-32	TKA-34	TKA-45	KA-238	KA-249	KA-253	KA-261	BA-175
Amphibole	30	40	35	48	54	50	45	50
Pyroxene		15	10	4		3		
Chlorite	5	25	12	30	6	10	15	10
Sphene	tr	2	3	tr	2	2	6	7
Quartz	15	5	7	6	7	9	5	1
Plagioclase	15		2		8	15	10	2
Magnetite	10	2	1	2	4	tr	1	2
Calcite					1			
Muscovite	1	1	1	tr		1	1	3
Epidote	24	10	30	10	18	10	15	25
Ilmanite							2	
Apatite	tr	tr	tr		tr	tr	tr	tr
Total	100	100	100	100	100	100	100	100

Key: TKA-32, 34, 45 (Ulla Babusar banded gabbros),

KA-238, 249, 253, 261 (Keo gali gabbros),

BA-175 (Buto gali gabbros), Tr = Traces.

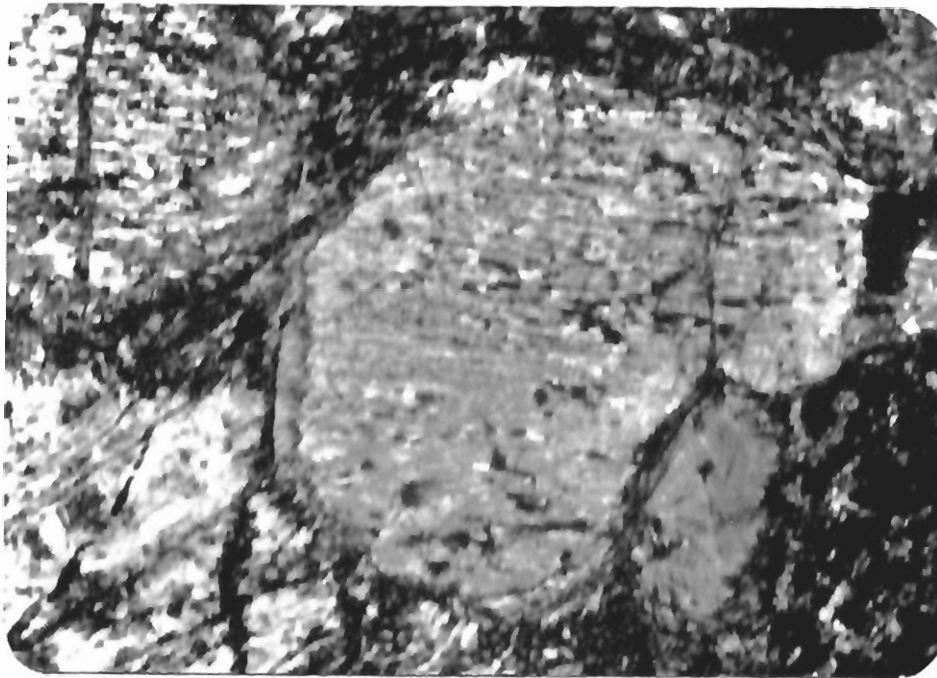


Plate 3.11. Thin section of partially altered pyroxenite showing relics of pyroxene in a matrix of serpentine (white and grey) and chlorite (dark top left). Field of view is 2.5 mm.

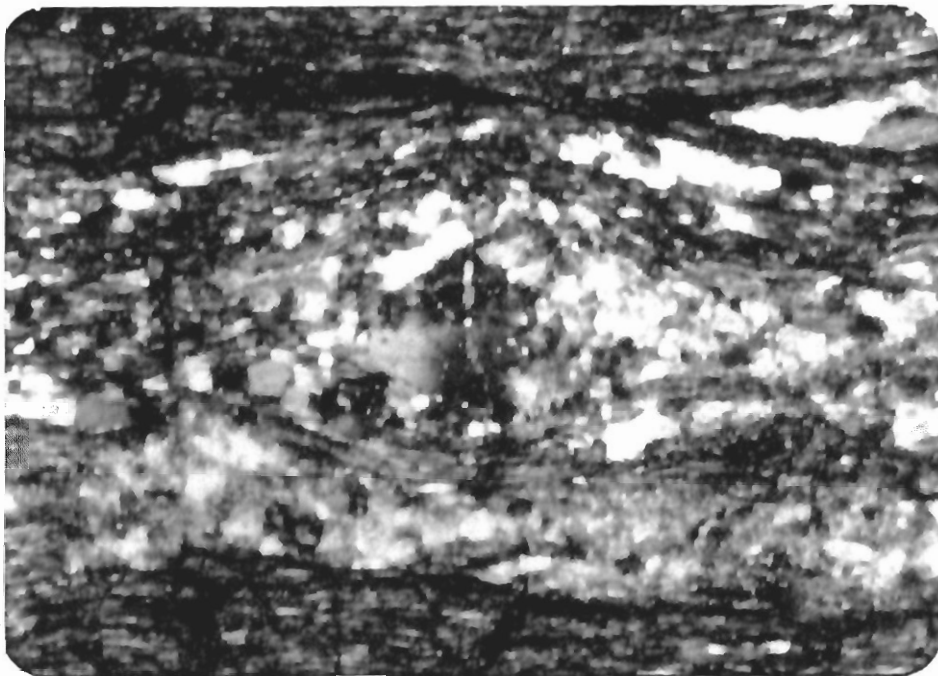


Plate 3.12. Microphotograph showing strongly sheared and mylonitized mafic and felsic bands in the gabbros with augen structure. All the minerals (chlorite, epidote and muscovite), and also quartz are elongated and aligned in the direction of shear. Field of view is 2.5 mm.

Both the pyroxenes are present in the gabbroic rocks. Orthopyroxene is ubiquitous as large, equant or elongated crystals and less commonly as aggregates or clots of small crystals. These are strongly pleochroic from neutral green or pale green to pink or flesh pink. Clinopyroxene is generally present as medium- to coarse-grained crystals, commonly in tabular shapes. The bigger crystals tend to be subhedral and show alteration. The clinopyroxene is commonly mantled by a thin rim of hornblende. Inclusions include quartz and magnetite. Alteration to amphibole, chlorite and sericite is observed along margins, in fractures or in inclusions. Amphibole, when primary, is sub- to euhedral in texture and brown to green in colour. Secondary amphibole, developed at the expense of pyroxenes, is typically light to bluish green and fibrous. The primary amphibole is commonly altered to fibrous amphibole and chlorite.

Plagioclase is cloudy and highly saussuritized. It shows alteration to epidote and chlorite. Epidote is prismatic to subprismatic and forms granular aggregate. At places quartz shows myrmekitic intergrowth with plagioclase. Magnetite and ilmenite are the most common ore minerals. They occur as small grains associated with pyroxene and amphibole. Ilmenite is surrounded by sphene and at places occurs only in tiny relicts. Sphene also occurs as small grains and granular aggregates irregularly distributed in the rock.

Geochemistry

Analyses of ten selected samples of ultramafic and gabbroic rocks from the Sapat complex are presented in Table 3.3. These data are used to decipher the range of internal variations in the studied rocks together with evaluation of their petrogenetic characteristics. As expected, there is a visible difference between the ultramafic and gabbroic rocks. The ultramafic rocks are typically rich in MgO, Ni

Table 3.3. XRF analyses of ultramafic and gabbroic rocks.

Sample	BS13	BS14	BS15	BS16	BS17	A-13	A-16	A-22	A-35	A-38
SiO ₂	45.95	48.64	43.70	47.62	48.00	46.95	47.76	56.62	47.55	49.65
TiO ₂	0.12	0.14	0.07	0.16	0.18	0.33	0.18	0.68	0.18	0.16
Al ₂ O ₃	2.36	0.00	3.32	3.56	2.90	19.50	24.44	16.38	16.00	14.62
Fe ₂ O ₃	12.97	9.92	14.74	12.05	9.24	9.59	6.19	8.40	8.12	8.48
MgO	33.58	28.19	37.37	27.06	19.16	8.92	4.84	5.74	11.51	11.50
CaO	4.56	12.54	0.55	9.17	20.01	14.52	15.40	9.19	16.51	15.00
Na ₂ O	0.27	0.35	0.09	0.18	0.29	0.20	1.15	2.56	0.13	0.60
K ₂ O	0.00	0.02	0.00	0.00	0.00	0.01	0.01	0.31	0.01	0.01
MnO	0.18	0.16	0.16	0.18	0.19	0.00	0.00	0.00	0.00	0.00
P ₂ O ₅	0.02	0.02	0.01	0.01	0.01	0.01	0.03	0.10	0.01	0.01
Total	100.01	99.98	100.01	99.99	99.98	100.03	100.00	99.98	100.02	100.03
Ni	574.70	407.10	667.70	444.70	238.90	75.00	60.00	50.00	71.00	66.00
Cr	1441.50	2324.70	62.30	1696.90	2776.20	55.00	30.00	45.00	73.00	54.00
V	106.60	155.80	149.40	191.70	211.30	0.00	0.00	0.00	0.00	0.00
Sc	41.90	55.70	19.00	72.30	84.90	0.00	0.00	0.00	0.00	0.00
Cu	7.40	6.40	74.80	35.40	126.80	0.00	0.00	0.00	0.00	0.00
Zn	63.80	44.00	83.10	58.60	36.10	0.00	0.00	0.00	0.00	0.00
Ga	3.00	3.10	3.30	3.50	2.50	0.00	0.00	0.00	0.00	0.00
Sr	5.00	9.00	2.50	8.40	7.40	125.00	158.00	227.00	67.00	67.00
Rb	0.20	0.10	0.00	0.00	0.00	0.90	0.87	9.00	0.70	0.89
Ba	6.40	5.20	4.90	6.60	5.80	0.00	0.00	0.00	0.00	0.00
Zr	0.20	0.40	0.30	1.10	1.80	6.00	7.00	69.00	1.00	1.00
Nb	0.10	0.10	0.30	0.00	0.60	0.50	0.50	2.50	0.40	0.30
Th	0.30	0.10	0.50	0.10	0.20	1.80	1.70	3.00	1.90	1.60
Y	2.10	3.40	1.50	4.10	4.60	11.00	11.00	17.00	4.00	5.00
La	0.30	0.30	0.40	0.00	0.10	13.00	14.00	16.00	9.00	10.00
Ce	1.30	1.50	1.70	1.60	0.40	49.00	64.00	70.00	23.00	25.00
Nd	0.40	0.30	0.30	1.30	0.10	126.00	26.00	26.00	27.00	126.00
P	0.00	0.00	0.00	0.00	0.00	43.64	130.93	436.44	43.64	43.64
K	0.00	0.00	0.00	0.00	0.00	83.02	83.02	2573.50	83.02	83.02
Ti	0.00	0.00	0.00	0.00	0.00	1978.38	1079.12	4076.67	1079.12	959.22

Key: BS13, 14, 15, 16 and 17 are ultramafics and A13, 16, 22, 35 and 38 are gabbros.

and Cr relative to the gabbroic rocks. Dunite (BS15) stands distinct by the absence of CaO (< 0.5%), and highest MgO content (~33 wt%). About 3% Al₂O₃ in this rock is, may be, due to the presence of spinel. The rest of the analyzed ultramafic rocks (BS13, 16, 14, 17) contain variable proportions of CaO (4 to 20 wt%) depending upon the content of the clinopyroxene. Al₂O₃ content of all these rocks is less than 4 wt%, suggesting absence of cumulus plagioclase or amphibole. The gabbroic rocks are characterized by the presence of large amounts of Al₂O₃ (14-24 wt%) reflecting high proportions of plagioclase. The values of the molar ratio MgO/(MgO+FeO+MnO) for ultramafic rocks of the studied area are: BS13=0.78; BS15=0.78; BS14=0.79; BS16=0.75 and BS17=0.74. These values for the gabbroic rocks are lower and ranges from 0.49 to 0.66. The MgO/SiO₂ ratio decreases from dunite (BS15=0.86) through peridotite (BS13=0.73) to pyroxenite (BS14=0.58; BS16=0.57 and BS17=0.40), whereas the gabbroic rocks show very low ratios ranging from 0.10 to 0.24.

Geochemical Variations

Compatible Major and Trace Elements

Considering that the ultramafic and gabbroic rocks from the Sapat complex represent cumulates, whole rock geochemistry of the individual rock is expected to be governed by their modal composition. This is particularly so for the elements highly compatible with the constituent minerals, including MgO, CaO, Fe₂O₃ and Al₂O₃. Figure 3.1 displays binary plots involving the major elements. In addition to the analyzed rocks, the minerals like olivine, clinopyroxene, and plagioclase, from the base of the complex at Spatgali, are also plotted in order to evaluate their role on chemical composition of the resultant rocks. The ultramafic samples show accumulation of all these minerals except plagioclase. The samples BS15 and

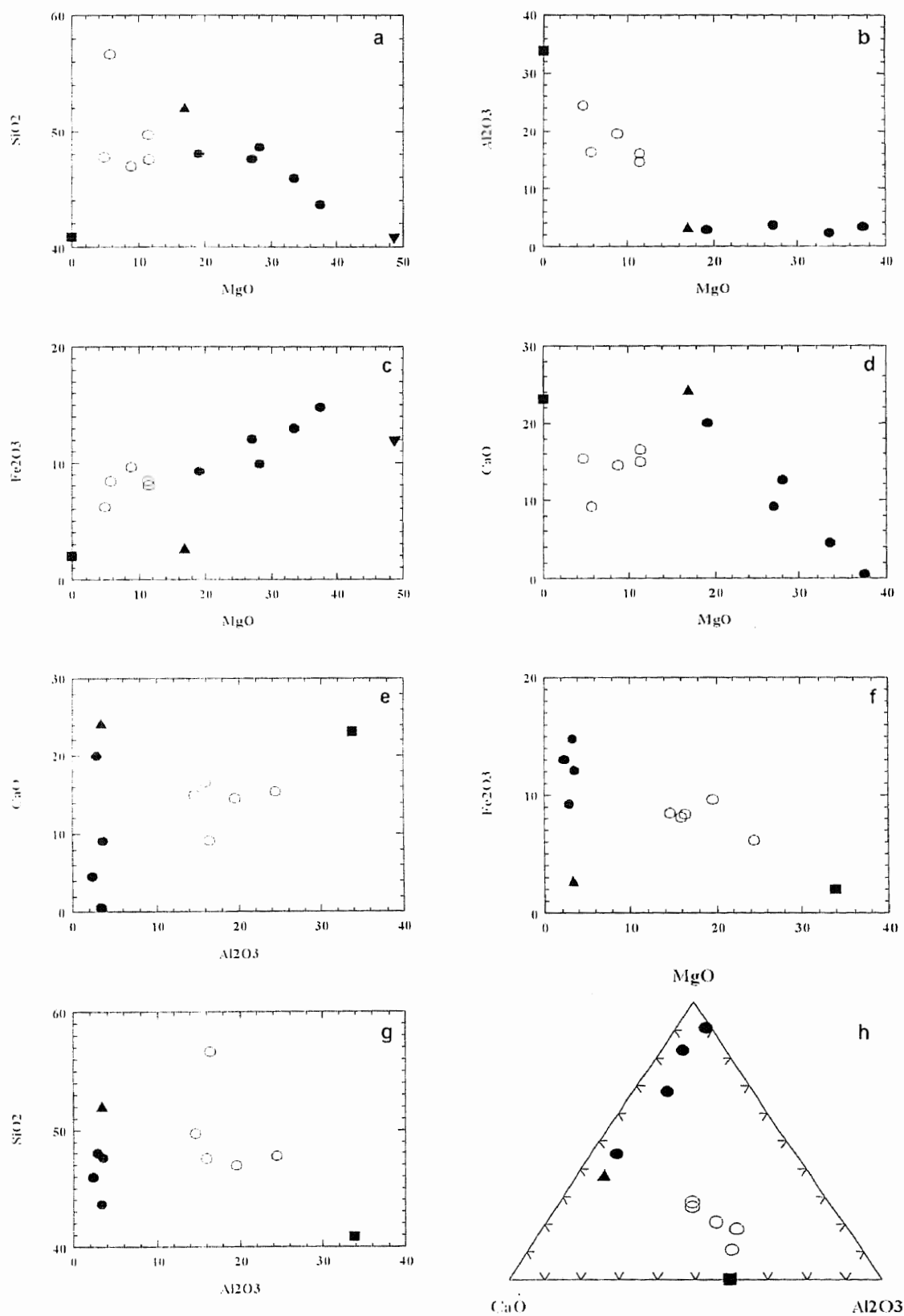


Figure 3.1. Plots of some major oxides of the studied rocks (gabbros: open circles; UM: filled circles), and the cumulates from the base of Sapat complex (olivine:inverted triangle; pyroxene:triangle and plagioclase; square).

BS13 depict a greater control by olivine (and /or orthopyroxene) while BS17, 16 and 14 show control of diopside. Fe_2O_3 in all the ultramafic rocks is higher than the ferromagnesian minerals olivine and clinopyroxene, suggesting control by the presence of some spinel. Likewise the higher Al_2O_3 content of the ultramafic rocks relative to these ferromagnesian minerals can be attributed to the presence of chromian spinel (Figure 3.1b (Al_2O_3 vs MgO) and 3.1c (Fe_2O_3 vs MgO). The gabbroic rocks, on the other hand, show control of cumulus plagioclase and clinopyroxene. The abnormally high content of Al_2O_3 (~ 24 wt%), low MgO (~ 5 wt%) and low SiO_2 (48 wt%) in the gabbroic sample (A16) suggests the presence of appreciable amounts of highly calcic-plagioclase. Sample A22 is the most evolved of the analyzed gabbros, probably approaching cotectic proportions of constituent minerals like plagioclase and clinopyroxene. High content of incompatible trace elements in this sample suggests that it may be non-cumulate in nature (see later).

Amongst the trace elements, Ni, Cr, Sc and Zn are transition-metals which are highly compatible with minerals like olivine, clinopyroxene and spinel. That is why Cr and Ni have distinctly higher proportions in the ultramafic than in the gabbroic rocks. Within the ultramafic rocks dunites and peridotites (BS15 and BS13) are rich in Ni and Zn while pyroxenites and pyroxene-rich peridotites (BS14, BS16 and BS17) are rich in Cr and Sc (Figure 3.2). Higher content of Ni in the peridotites compared to pyroxenites is a common feature in the ultramafic rocks (Fomin and Kozak, 1971), due to preferential accommodation of Ni in olivine than pyroxene. It is noted that the average Ni content (466 ppm) in the studied rocks is lower than those of the peridotite from mid-ocean ridges (about 2300ppm, Vinogradov, 1962; Bonatti, 1968).

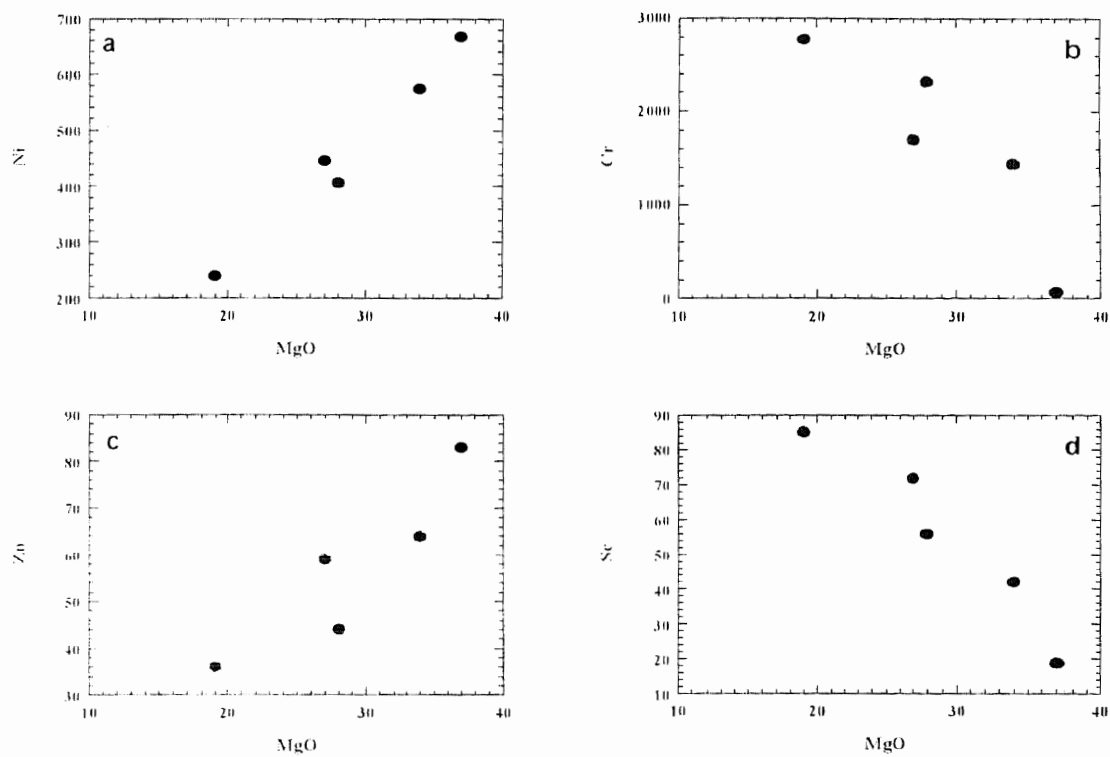


Figure 3.2. Binary plots showing the fractionation of Ni, Zn, Cr and Sc in the ultramafic rocks.

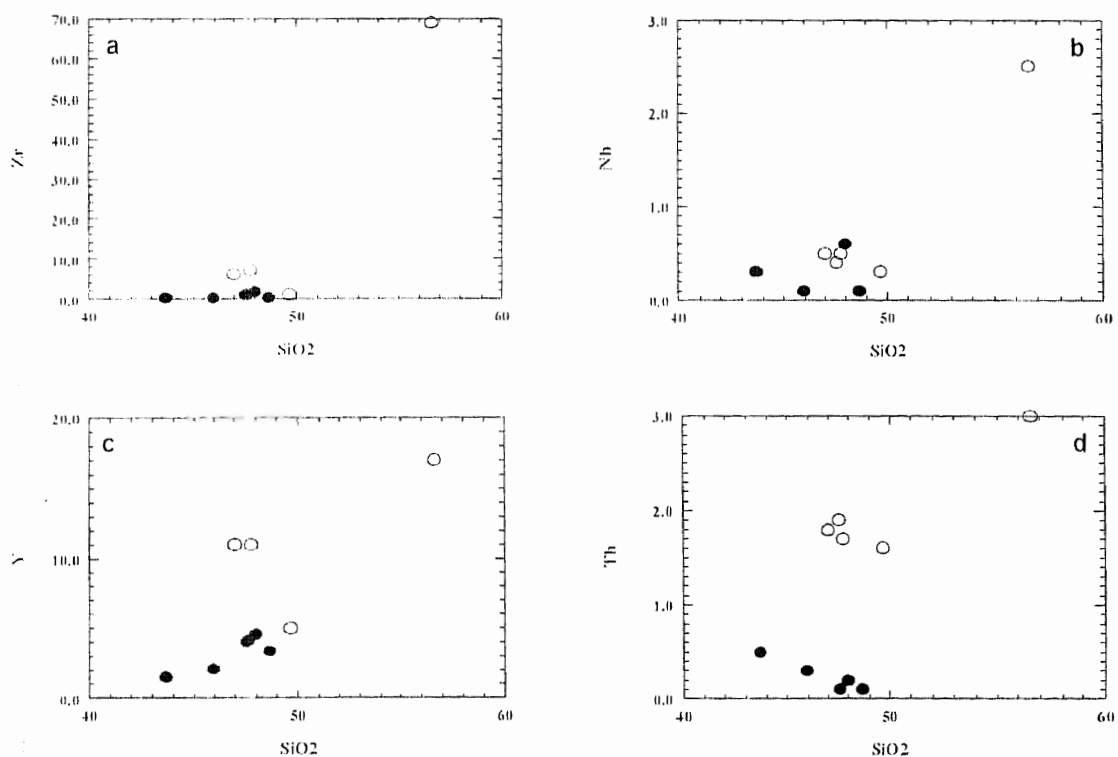


Figure 3.3. Binary plots showing the relationship of the incompatible trace elements in gabbroic rocks (open circles) and ultramafic (filled circles) rocks.

Incompatible Trace-elements

Minor elements like Ti, K, and P, and several of the trace elements like Rb, Ba, Sr, Nb, Y, and Zr (+REE), have low values of distribution coefficients for the constituent minerals (e.g., olivine, clinopyroxene, orthopyroxene and plagioclase) of the ultramafic and gabbroic rocks and are thus classified as incompatible. Absolute concentrations of these elements in cumulates reflect amount of the trapped liquid as inter- or post-cumulus material. Since amounts of liquid trapped between the cumulus crystals is subject highly variability, two rocks with identical modal composition might end up with different absolute concentrations of incompatible trace elements. In general, most cumulate rocks contain low absolute concentrations of incompatible minor and trace elements. The incompatible trace elements in cumulates, however, can be used to determine petrological relations between the rocks. The rocks crystallized from the same magma may have different absolute concentrations but have similar ratios between the incompatible trace elements.

Except for the sample A22, the analyzed rocks from the Sapat complex are all cumulus characterized generally by very low abundances of the incompatible trace elements. Gabbroic rocks have slightly greater abundances of the incompatible trace elements relative to the ultramafic rocks, reflecting a greater liquid/cumulus minerals ratio (Figure 3.3). The gabbroic sample A22 has exceptionally high abundances of incompatible trace elements suggesting a non-cumulus nature of the rock.

Binary plots involving several of the incompatible minor and trace elements show positive trends for both the ultramafic and the gabbroic rocks. The trends are particularly linear for HFSE including Zr, TiO_2 , and Y, and for the REE including La

and Nd, but less so for LILE like K_2O , Rb and Sr. These plots indicate that ratios between incompatible trace elements are mutually similar in the analyzed suite of rocks from the Sapat complex, suggesting their comagmatic nature (Figure 3.4).

Spidergrams involving incompatible trace elements normalized to a standard (e.g., primordial mantle) are an extension of the binary plots with added advantage of being capable of portraying mutual ratios between several incompatible trace elements at a time (Figure 3.5). The spidergrams of the analyzed samples from the Sapat complex reflect strongly cumulus nature of the ultramafic rocks, all the incompatible trace elements are lower than even the primordial concentrations. Zr shows a marked negative anomaly for the ultramafic rocks, less pronounced negative anomaly for most of the gabbroic rocks and a positive anomaly for the sample A22. Again this variation may be attributed to cumulus nature of the rocks except for A22. Sr shows a strong positive anomaly for the gabbroic rocks and a negative anomaly for the ultramafic rocks, reflecting the presence or absence of cumulus plagioclase. Despite these differences the Y-Ti-P for all the rocks yield mutually similar normalized ratios. Since concentrations of the remaining incompatible trace elements (e.g., Rb, K and Nb) are below detection limits for the ultramafic and most of the analyzed gabbroic rocks, the following interpretations about the overall petrogenetic characteristics of the complex are based on trace element pattern of the non-cumulate gabbroic rock (A22). Firstly the pattern has an overall slope towards the right, suggesting a slight enrichment in the large-ion lithophile elements (LILE) relative to the high-field strength elements (HFSE). Secondly, the pattern is marked by a pronounced negative anomaly for Nb and positive anomaly for Sr.

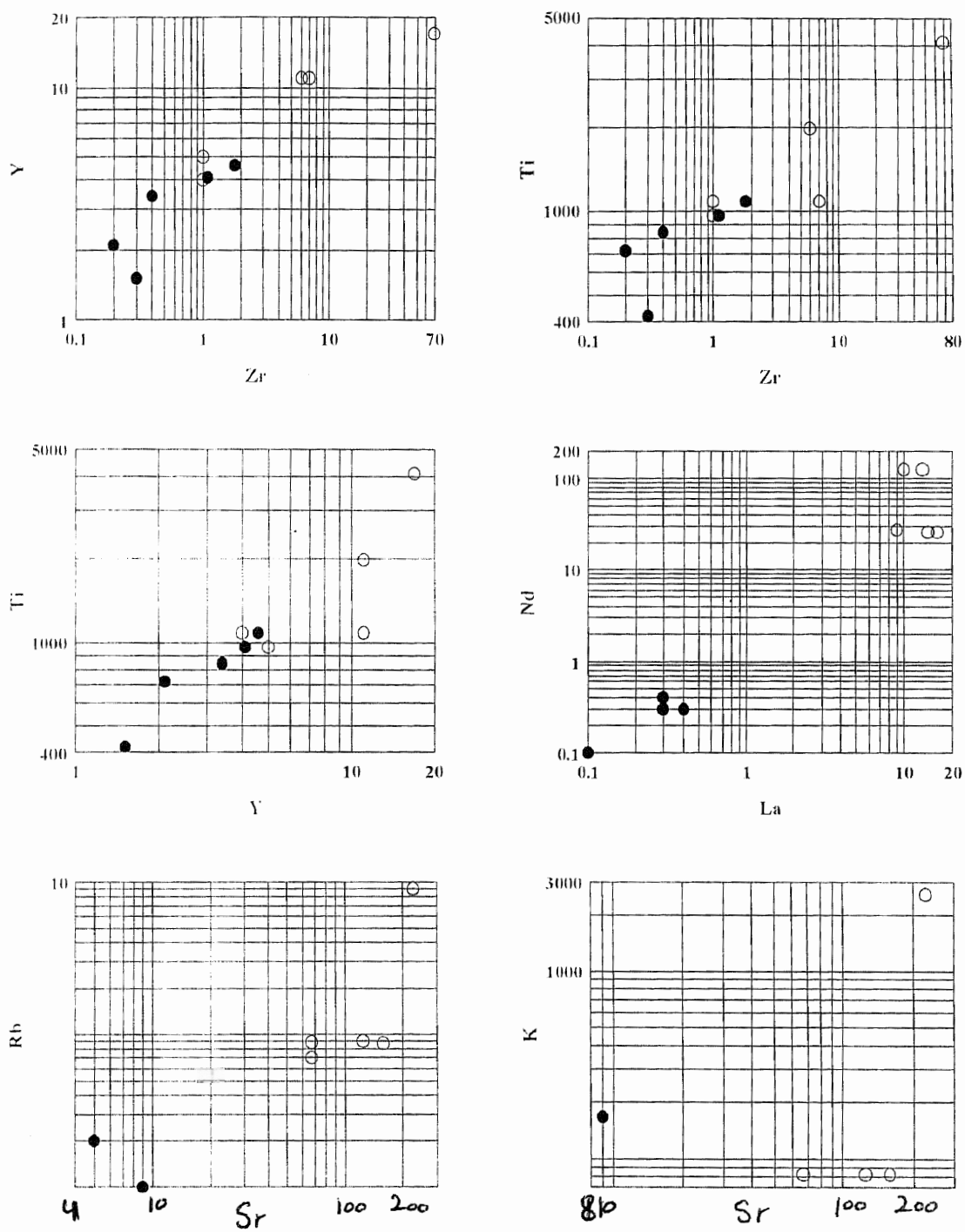


Figure 3.4. Binary plots of incompatible trace elements of gabbros (open circles) and ultramafics (filled circles) of the Sapat Complex. Positive linear trends are suggestive of their comagmatic nature.

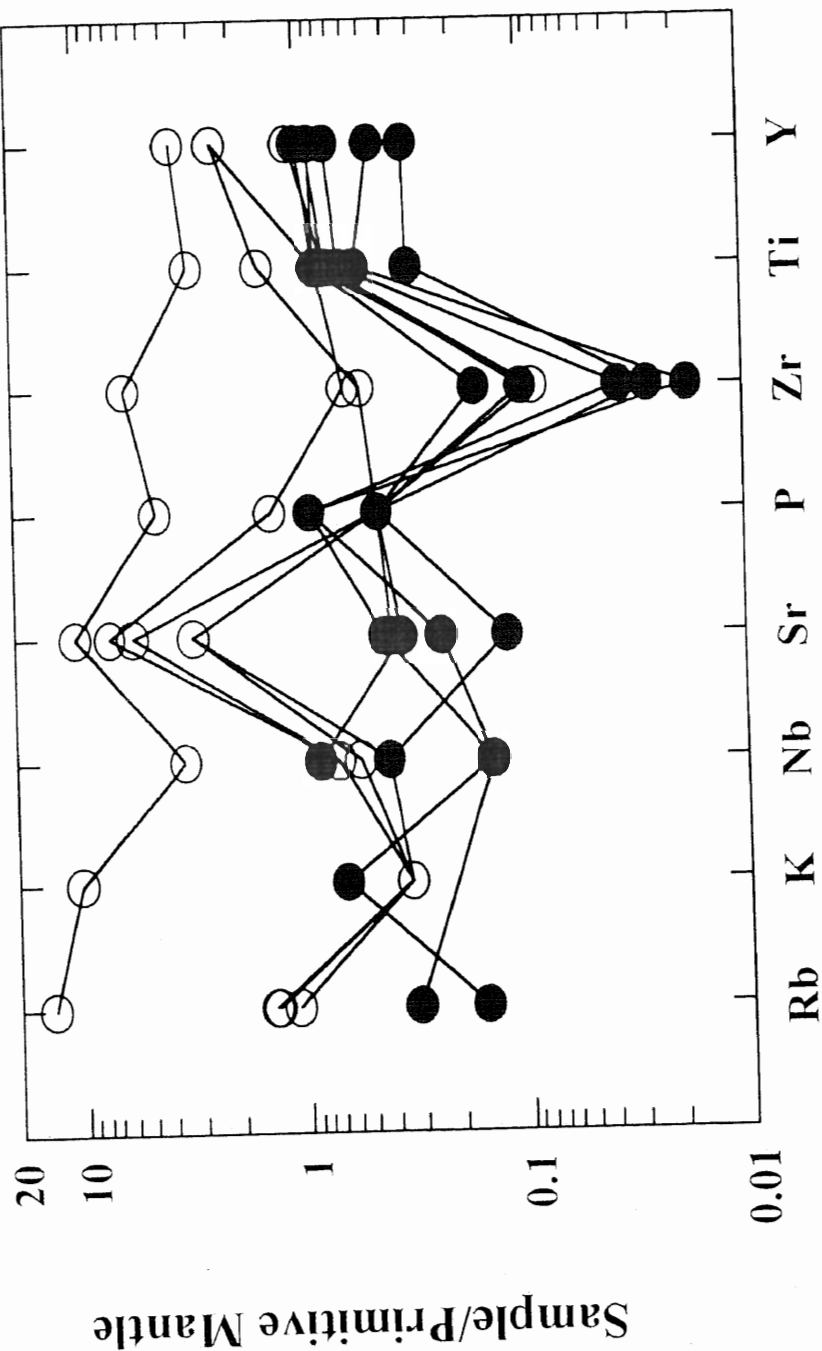


Figure 3.5. Primordial mantle-normalized multi-element patterns of the gabbros (open circles) and ultramafic rocks (filled circles). The segment Y-Ti-P for all the patterns is quite similar yielding similar normalized ratios between these elements. Ultramafic rocks have lower concentrations than the primordial mantle. A rock (A22 i.e., gabbro) showing slight enrichment in LIL elements relative to HFS elements.
Normalizing values of Primordial Mantle: Rb 0.635, K 250, Nb 0.713, Sr 21.1, P 95, Zr 11.2, Ti 1300 and Y 4.55 after Sun and McDonough, 1989.

Petrogenesis

An important aspect of the petrology of the Sapat complex is the cumulus nature of the constituent rocks. It is reflected in: i) diversity of the rock-types (i.e., dunite, peridotites, pyroxenites, chromitite, gabbros and anorthosite), ii) field features like layering, iii) textures showing subhedral cumulus minerals contained in post-cumulus poikilitic and ophitic minerals, and iv) whole-rock geochemistry showing generally high abundances of the compatible elements and low abundances of the incompatible elements. Whereas the concentration of compatible major and trace elements highlight the diversity imparted by the cumulate processes, incompatible minor and trace elements provide a window to see-through this diversity a certain comagmatic relationship, if any. The gabbroic and ultramafic rocks from the Sapat complex display linear positive trends on binary plots involving incompatible trace elements (Figure 3.4). This implies that the gabbroic and the ultramafic rocks are crystallized from a single magma. If not, the magma batches responsible for these two groups of rocks were derived from a single source. Whichever the case, there exists a genetic relation between the ultramafic and the gabbroic rocks suggested by the incompatible trace elements.

The shape of the trace-element patterns involving mantle-normalized incompatible trace elements suggest the presence of a subduction component. Marked negative trough for Nb, low Rb, positive spikes for Sr, combined with a degree of enrichment in LILE relative to the HFSE are some of the characteristics of the trace element patterns of subduction-related magmas (Figure 3.5). In contrast, rocks derived from mantle accompanying subduction, and unaffected by metasomatism are characterized by a lack of Nb anomaly (Pearce, 1982).

An important aspect of investigation of the petrogenesis of the Sapat complex is its relationship with the metavolcanic amphibolites overlying the complex in SE Kohistan (referred to as the Jal-Niat metavolcanics in this study). First noted by Khan et al. (1993), the part of the Kamila amphibolite belt in SE Kohistan is: 1) metavolcanic in origin, 2) has a composition closely approaching that of the type MORB characterized by high TiO_2 (between 0.54 and 2.91 wt%) and higher contents of HFSE relative to the LILE. Since the MORB-type basalts are often underplated by ultramafic-mafic cumulates in ophiolite successions (Coleman, 1971a; Moores and Jackson, 1974), there is a scope for the cogenetic relationship between the Sapat complex and the overlying metavolcanic amphibolites. To investigate this possibility, binary ratios between the incompatible trace elements from the Niat metavolcanics have been compared with those of the Sapat complex. There is a clear difference in the ratios of the two suites, negating any petrogenetic interrelationship. This difference is particularly elaborated by the difference in the shape of the trace-element patterns for the two suites of rocks (Figure 3.6). Khan et al. (1993) pointed out that the Jal-Niat metavolcanics represent the oceanic basement which was intruded by the subduction-related magmas belonging to the Kohistan island arc. The present study supports this view and envisages the Sapat complex was originated in the subduction-related stage, and representing a magma chamber in the basal part of the island-arc crust, rather than being a part of an oceanic basement represented by the Niat volcanics.

Besides the geochemistry, several other features of the Sapat complex suggest a strong link with an island arc or subduction-related environment. Jan et al. (1993) showed that chromite from the type area of the complex to north of Naran is characterized by high Cr No. >60, which is akin to arc-related rocks (Dick

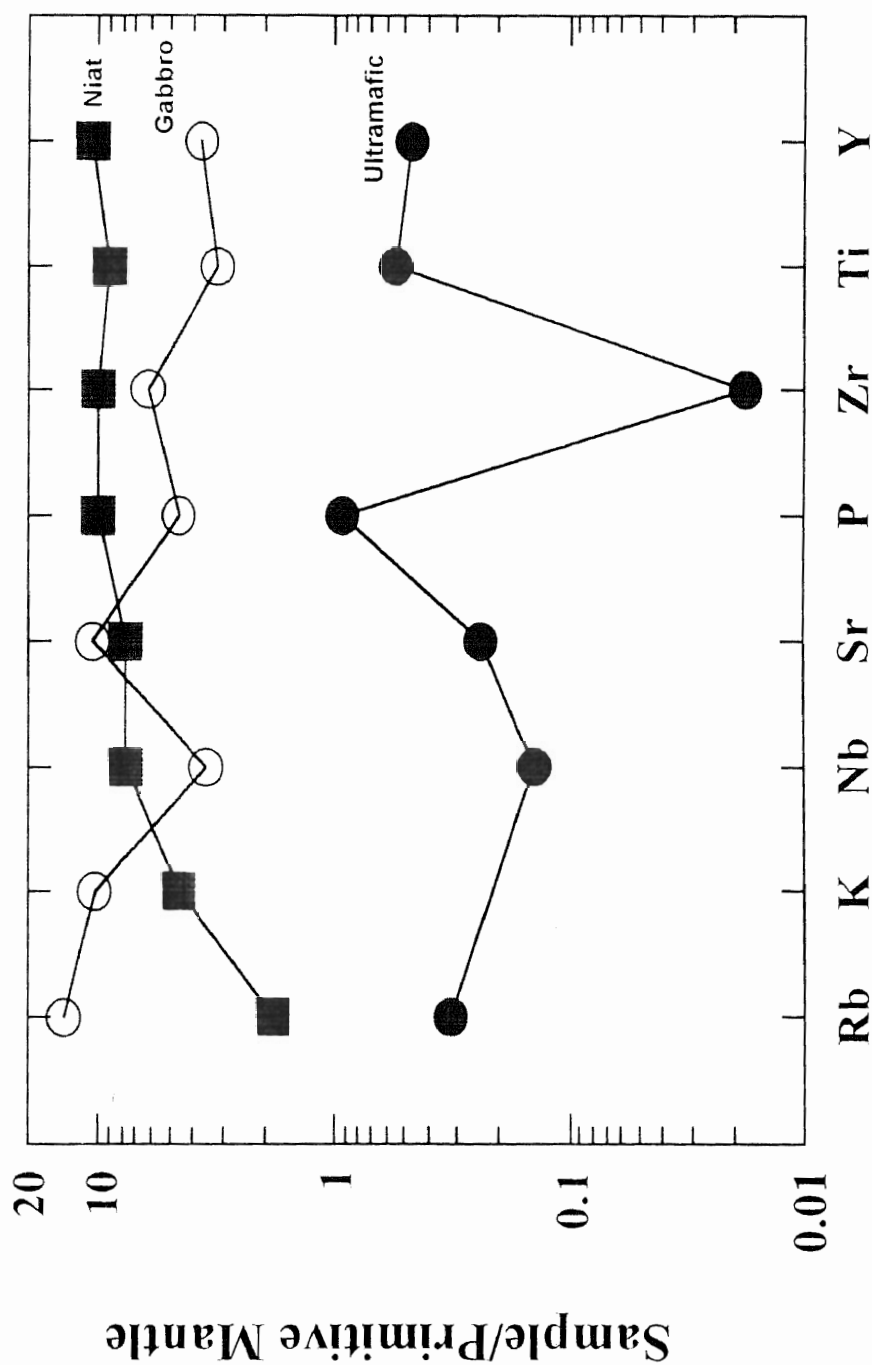


Figure 3.6. Spidergram showing differences in patterns of ultramafic and gabbroic (A22) rocks of Sapat from the MORB-type volcanics of Niata unit.
Normalizing values of Primordial Mantle: Rb 0.635, K 250, Nb 0.713, Sr 21.1, P 95, Zr 11.2, Ti 1300 and Y 4.55 after Sun and McDonough, 1989.

and Bullen, 1984). The clinopyroxene from the Sapat complex is devoid of zoning and shows a consistent composition suggestive of slow-cooling environment akin to the base of an island-arc crust rather than that of normal ocean floor (Flower et al., 1977b). The absence of plagioclase in the studied ultramafic rocks may also be indicative of rather high pressure environment and depth.

Chapter 4

THE AMPHIBOLITE BELT

Introduction

Amphibolites are widespread in the Kohistan sequence and form a prominent belt that extends from Afghanistan in the west, through Bajaur, Dir, Swat, and Indus valley, up to Nanga Parbat in the east. The belt has a maximum width of about 50 km and a length of 300 km. Preliminary studies were performed by Martin et al. (1962) and Davies (1965) in the Swat area. These authors included the Kohistan amphibolites in their "Upper Swat Hornblendic Group" and interpreted them to be a product of metamorphism rather than igneous processes. In contrast, part of the amphibolite belt exposed in the Thak valley was assigned an igneous parentage by Shams (1975), who called them "veined metadiorites". Jan and Kempe (1974) introduced the name "the Kohistan Basic Complex" for the basic rocks of southern Kohistan and for the first time recognised the presence of an extensive suite of amphibolites.

Jan (1979), while working in Swat and along the Karakoram highway in the Indus valley, classified the amphibolites into two varieties: (a) massive and homogeneous, and (b) banded and sheared. Since then, the amphibolites of southern Kohistan have been referred to as the Kamila amphibolite belt (Tahirikheli and Jan, 1979; Coward et al., 1986) or the southern amphibolites (Jan, 1979, 1988; Bard et al., 1980; Bard, 1983 a,b). The true thickness of the Kamila amphibolites is still uncertain due to an abundance of intrusive plutonic bodies and intense ductile-brittle shearing. However, recently, the stratigraphic position of the Kamila amphibolites in the Kohistan sequence has become clearer with the

delineation of its lower stratigraphic contact in the presently studied area and the upper contact in the Dir-Swat area (Sullivan et al., 1993). Therefore the name "Kamila Amphibolite Unit" is used in this study, which carries a stratigraphic conotation.

The Kamila amphibolite unit has a vast distribution in southern Kohistan. Previously, it was considered that the unit occupies the entire southern part of the Kohistan terrane between the Main Mantle Thrust (MMT) in the south and the Chilas Complex in the north (Tahirkheli and Jan, 1979; Bard et al., 1980). In the Indus valley, the unit was considered to overlies the Jijal Complex which occupies the hanging wall of the MMT. Recent mapping (Khan and Jan, 1992; Jan et al., 1993; this study) has revealed that the Kamila amphibolite unit is in direct contact with the MMT only in the extreme eastern (i.e., Bunar valley) and western parts of the Kohistan terrane. In the area between the Babusar Pass in the east and the Indus Valley in the west, the unit is separated from the MMT by a basal ultramafic-mafic layered complex in the hanging wall of the MMT, termed the Sapat Complex (Jan et al., 1993). To the north, the unit is bounded by the Chilas Complex which occupies an axial position in the Kohistan terrane.

In the presently study area of south-eastern Kohistan, the Kamila amphibolite unit does not occur as a single, extensive body. Field relations show that the amphibolites occur in three main linear belts, in addition to small patches and screens within or between plutons. These belts, here named from south to north as Babusar, Niat, and Jal, will be treated separately in the following pages. Within the Niat belt, a thin slice of amphibolites with distinctly different characteristics, is named as Sumal amphibolite. The Sumal amphibolites will be treated in a separate section in the Niat amphibolite unit in terms of their field

relations and petrography. All these amphibolites are intruded by diorites, granodiorites, trondhjemites and granites.

Babusar Amphibolites

Field Features and Relations

These amphibolites are best exposed in the southern part of the study area as east-west belt stretching between the drainage divide of Jalkot Nala and the tributaries of the Indus river at high reaches of Katai gali, Butogah gali, Keo gali, Makheli gali, Shikaro gali and Sherman gali. The width of the belt in the eastern part of the area in the Thak valley is 1.5 km while in the western part near Sherman Gali it is 5 km. The belt has a gradational contact with the basal ultramafic-mafic rocks of Sapat-Babusar Complex to the south. To the north the contact is sharp with intrusive diorites. To the east of Babusar Pass in the Charal gah the belt occurs directly in the hanging wall of the Indus suture. On the fresh surface the rocks are dark grey to dark greenish grey. On weathered surface, they look dark greenish brown.

The amphibolites have a NE strike with gentle dip towards north, but at places to the south instead. The rocks are strongly foliated and commonly banded (Plate 4.1). Foliation is mostly parallel to the banding (Plate 4.2), which is defined by alternate leucocratic and melanocratic bands. The banded aspect of these rocks is due to variations in the proportions of amphibole, epidote and plagioclase \pm quartz in alternate layers. The bands range from centimetric streaks to over half a meter in thickness (Plate 4.3). Most of them are less than two centimeters thick and usually have sharp contacts. In these respects, the rocks are similar to those of Swat and Indus valley (Jan 1979).



Plate 4.1. Babusar amphibolites at Batsi Sangar, south of Keo gali in Jalkot Nala. Felsic and mafic bands are 3 cm to 12 cm thick show change in dip direction.



Plate 4.2. Photograph showing foliation and shearing in the Babusar amphibolites, south of Ulla Babusar (Thak valley). Both mafic and felsic bands are strongly sheared.



Plate 4.3. Quartzofeldspathic bands in Babusar amphibolite with a range in thickness from 0.75 cm to 5 cm.



Plate 4.4. Shear zone in Babusar amphibolites, just north of Buto Gali. The rock is strongly sheared and left side of the photograph is showing the mylonitized part of the rock.

The shear zones in the Babusar amphibolites are typically anastomosing (Plate 4.4, 4.5 and 4.6). Within the shear zones the rocks are blastomylonitic medium-grained and fine-grained, locally difficult to distinguish from the fine-grained variety of the amphibolites (Plate 4.7). The width of the shear zones is highly variable, ranging from centimetric to several tens of meters.

Modal Composition and Petrography

The Babusar amphibolites are generally medium-grained, and hypidioblastic to xenoblastic in textures. Locally they contain poikiloblasts and porphyroblasts with minor inclusions. Foliation and gneissose banding are common (Plate 4.8), in some rocks alternating bands of quartz and plagioclase with fine-grained aggregates of amphibole and epidote are present. In foliated varieties flaky minerals are oriented in one direction, elongation is also seen in quartz and epidote crystals. The banded varieties are mostly finer grained than the homogeneous types some of which are coarse-grained. Variations in texture and mineral proportion are common in both the varieties. Modal composition of eight representative amphibolite samples from this belt is given in Table 4.1. They contain hornblende, epidote and plagioclase as the dominant constituents. Chlorite, quartz, sphene, rutile and opaque minerals occur as accessories, while some samples contain biotite, white mica and garnet and a few have clinopyroxene.

The amphibole is mostly hornblendic in composition and shows a wide range in modal proportion from 20% to 70% except the sample (A18). It occurs as subhedral to anhedral grains of various sizes. The grains are fresh, however, some of the large ones are uralitized at boundaries. It has a sieve-like texture due to abundant inclusions of quartz and opaque minerals (Plate 4.9), suggesting post magmatic growth. In some cases these minerals occur only in the central parts of



Plate 4.5. Ductile shearing in the banded Babusar amphibolites at Buto Pass. Pencil and ball-pen point to folding and deformation in the rock.



Plate 4.6. Shear zone at Sherman Gali. Both the Babusar amphibolite and the white colour granitic intrusion with xenoliths of country rock show shearing and mylonitization.



Plate 4.7. Mylonite zone near Shotti Pass in Babusar amphibolites. Both the mafic and felsic bands are fine-grained due to mylonitization.

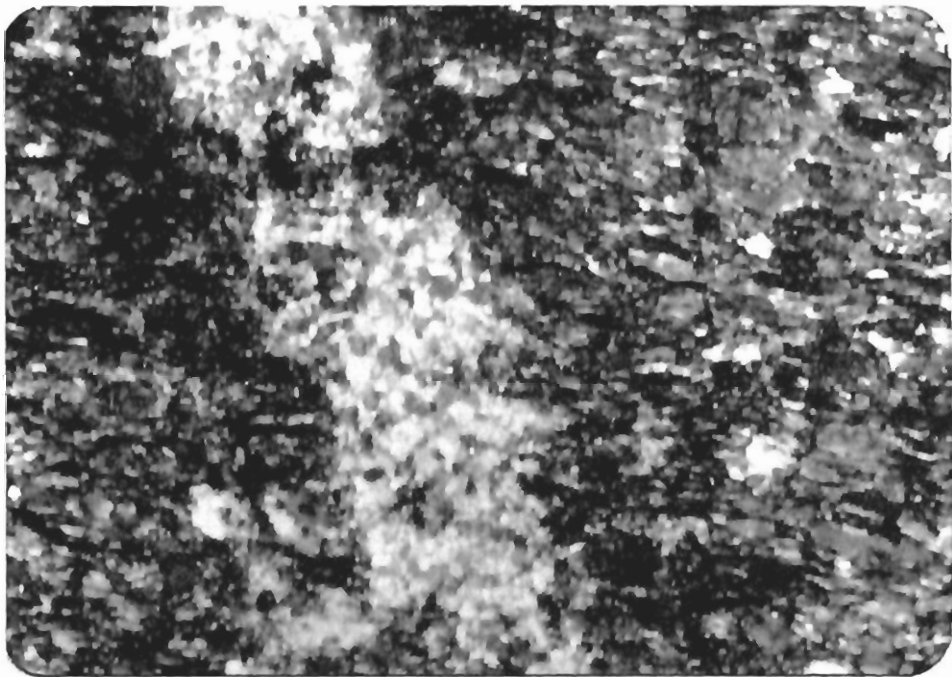


Plate 4.8. Microphotograph of fine-grained, foliated and banded Babusar amphibolites. Kink banding is also present in the rock. A calcite vein cuts the original banding of the rock and parallel to the kink banding. Field of view is 2.5 mm.

Table 4.1. Modal composition (visual estimates) of Babusar Amphibolites.

Sample	A-243	A-241	BS-10	A-31	BS-18	A-56	A-58	A-59
Amphibole	30	40	55	39	7	55	52	70
Plagioclase	4	23		22	4	20	14	6
Epidot	8	22	24	24	40	8	11	9
Quartz	20	6	10	5	3	7	9	6
Chlorite	4	3	8	6	43	2	3	
Magnetite	1	1	1	1		4	5	3
Sphene	3	2	2	1	3	4	6	6
Biotite		1		tr				
Calcite	30			1				
Muscovite	tr	2		1				
Apatite			tr		tr			tr

Key : A-243, 241 (Keo valley); A-7, 31, 187 (Buto valley); A-56, 58, 69, BS-10, 18 (Thak valley) and Tr = Traces

the grains. Blebs and small inclusions of hornblende within large hornblende crystals are also commonly observed (Plate 4.10). In some rocks hornblende encloses or is enclosed by epidote. In the altered rocks, the hornblende is partly replaced by chlorite, less commonly by epidote, sphene and minor chlorite. It is generally pleochroic from light green to brownish green and bluish green. Locally it also displays zoning with bluish green cores and greenish blue margins. Actinolite occurs as long prismatic crystals and in columnar to fibrous aggregates. It is colourless to light green.

The plagioclase ranges from 4% to 23% in these rocks and is generally cloudy due to saussuritization and kaolinization. The composition of the plagioclase, determined from symmetrical extinction angles on albite twins, is in the range of andesine (An_{40-46}) but in rare cases it is sodic labradorite. Some untwinned, anhedral plagioclase grains present in the rock are enclosed by quartz and show myrmakititic intergrowth. Inclusions of sericite are common but in some grains apatite crystals are seen. Some grains are replaced by epidote and albite. Due to mixing with younger and more acidic rocks, the hybrid zones may contain albite or oligoclase.

Epidote is a secondary mineral and present in the rocks from 8% to 40% by volume. It occurs as elongated, subhedral grains as well as anhedral aggregates in amphibole and feldspar aggregate matrix, and has likely formed subsequent to the growth of amphibole. In some rocks inclusions of epidote are seen in hornblende crystals. It is zoned and displays anomalous blue interference colours in cores and greenish or brownish in margins. It is likely that the cores are poorer in Fe than the margins.

Quartz, ranging from 3% to 20%, is anhedral and shows strong strain effects. It occurs in the form of streaky aggregates elongated parallel to the well-

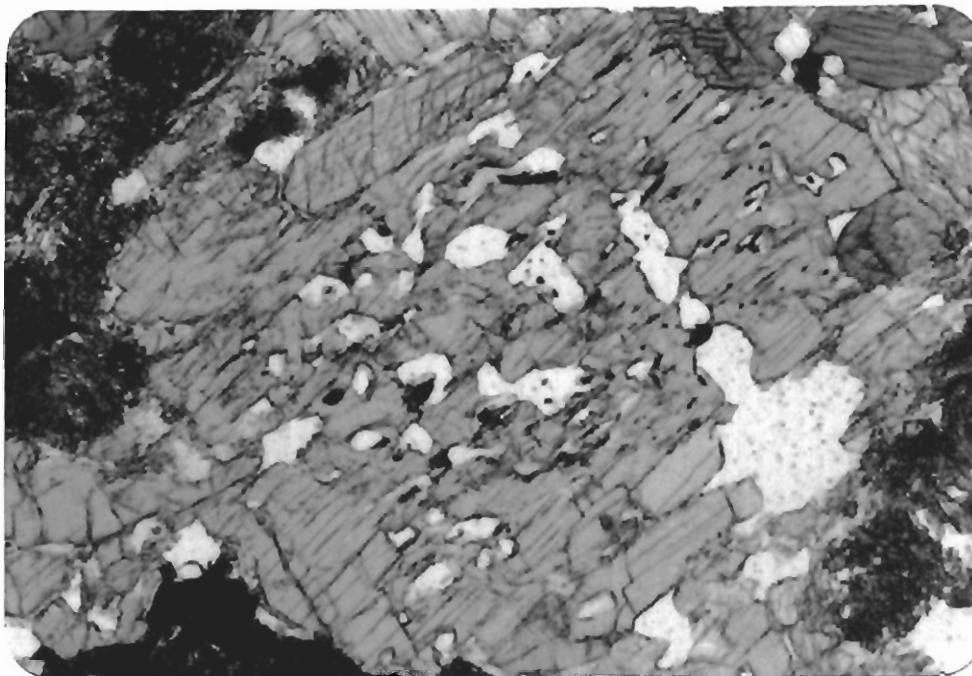


Plate 4.9. A large crystal of amphibole with enclosed quartz, sphene and hornblende. Alteration to chlorite can be seen on the margins of the large amphibole crystal. Top right shows opaque oxide. Field of view is 2.5 mm.

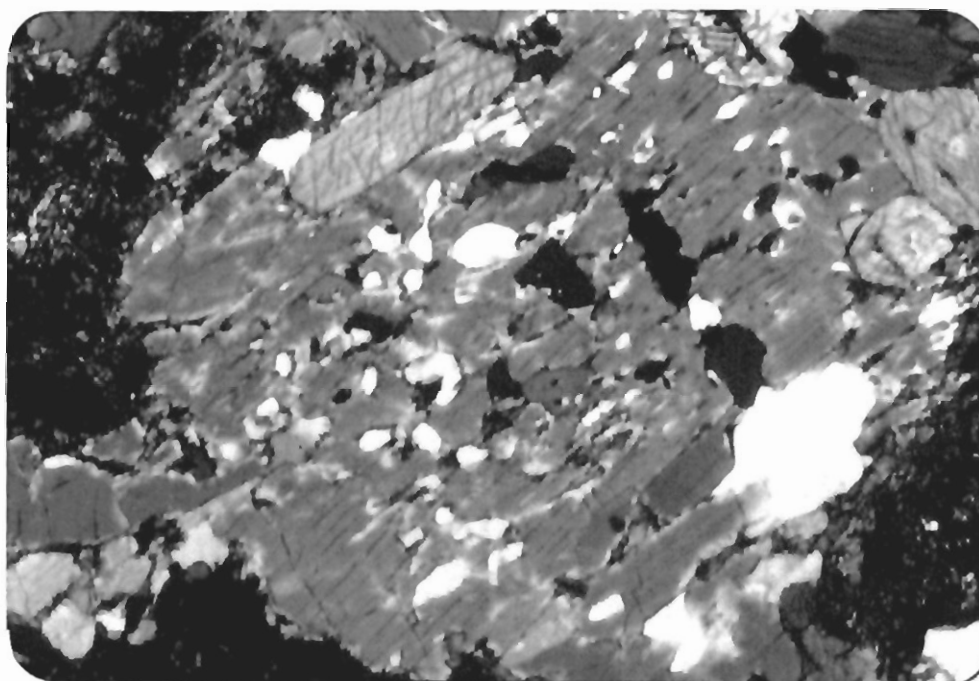


Plate 4.10. Same in cross light.

developed schistosity of the rocks. Its segregation and straining boundaries suggest that the recrystallization occurred during metamorphism. Sphene, biotite, magnetite or ilmenite are common accessories. Sphene is generally developed along the fractures, cleavages and grain boundaries of hornblende. Calcite occurs in minor amounts in a few rocks but in one sample it is 30%. Together with 20% quartz and only 30% amphibole, this may represent a metasediment or a highly altered rock. At places a good zoning in the crystals of calcite is also seen.

Chlorite is generally under 10%, but reaches up to 43% in the more altered rocks. It occurs as bluish green to light green flakes along the margins and within fractures of the hornblende grains. Opaque minerals occur generally in the cores and along grain boundaries of hornblende. Rutile is associated with magnetite, and both may be derived from ilmenite.

Niat Amphibolites

Field Features and Relations

A thick belt of fine-grained amphibolites extends from east to west in the central part of the area. It is bounded on the north by diorites and granodiorites and on the south by diorites. Westward the belt gradationally merges with the Babusar amphibolites, whereas eastward it is truncated by the MMT. The trend of the belt is NW, dipping steeply towards south, but at places the dip direction changes to north. Folding and deformation is common at many places in this unit (Plates 4.11, 4.12, 4.13 and 4.14). The foliation planes show greater enrichment of chlorite and, therefore, appear dark green. At places, a laminated appearance is seen in the rocks due to quartz partings.

These homogeneous amphibolites are intruded by a number of intrusions of diorite, granodiorite and tonalite (Plates 4.15 and 4.16). Small intrusive patches

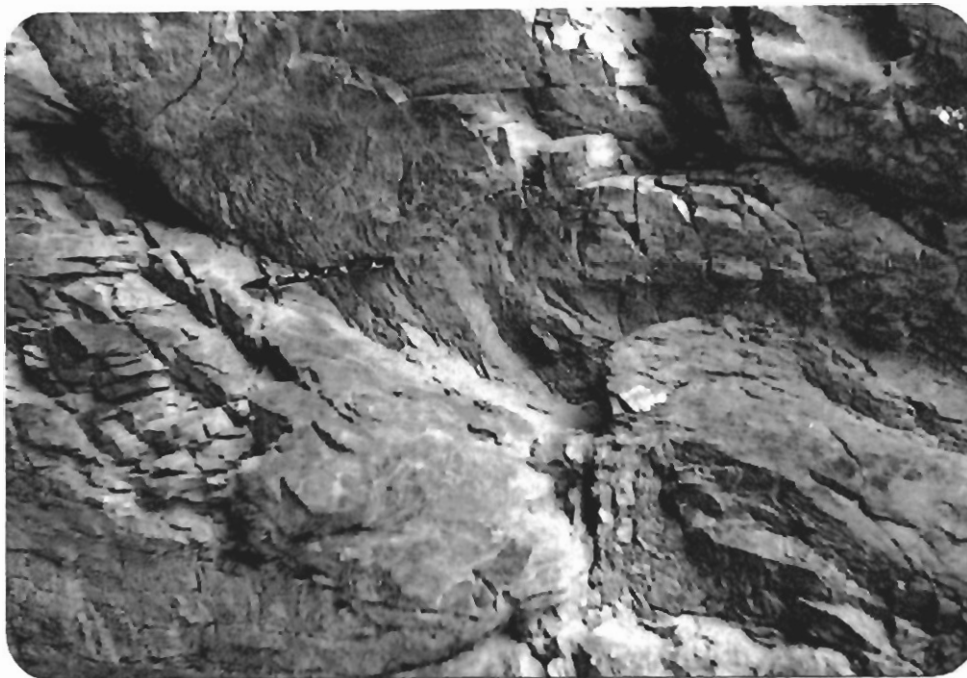


Plate 4.11. Photograph showing folding in the Niat volcanics, near Nigaran in Niat valley. Niat volcanics are fine-grained and grey colouroured.



Plate 4.12. Open folding in the Niat volcanics, near Nigaran in Niat valley.



Plate 4.13. Photograph showing deformation and folding in Niat volcanics in Buto valley.



Plate 4.14. Another view of folding and strong deformation in the rocks of Niat volcanics in Buto valley.



Plate 4.15. 50 cm thick granitic intrusion in the Niat volcanics, just north of Butogal village in Buto valley. The Granitic rock is cream in colour and coarse grained.



Plate 4.16. Photograph showing the contact between Niat volcanics and diorite/ granodiorite north of Tushkal in Keo valley. White brown colour shows the diorite and dark grey/green shows the volcanics.

and lenses of granite and coarse-grained granodiorite are commonly present in these rocks (Plates 4.17 and 4.18). The granodiorite is light brown to light greenish brown in colour, whereas the amphibolites show a darker shade of greenish gray or greenish brown from a distance. The mafic mineral content decreases in the vicinity of diorite and granodiorite intrusions. Locally some rocks of this belt are more mafic and retain pillow structures. The pillows are stretched and locally sheared (Plate 4.19). Some pillows are so strongly sheared that their cores and crusts give the impression of banded amphibolites (Plate 4.20), similar to those of central Kohistan to the south of Jaglot (T. Khan, 1994). Biotite and amphibole schists are locally found intercalated with the amphibolites and are probably derived from tuffs through metamorphism. The rocks are metamorphosed under greenschist to amphibolite facies conditions.

This unit occurs typically in thin (50-100 m), linear bands and slices of amphibolites alternating with intrusive sheets of granitic rocks. These bands and slices can be seen on the map (Figure 2.12). As mentioned earlier in the introductory statement, within these bands a thin (~500 m) tectonic slice of Sumal amphibolites is exposed in Keo and Buto valleys, which will be discussed under a separate heading within this section.

Modal Composition and Petrography

The Niat amphibolites are fine- to medium-grained, strongly foliated and generally non-porphyroblastic to subporphyroblastic. Grains of the constituent minerals are oriented and elongated in one major direction (Plate 4.21). Alternating mafic and felsic bands occur in the rock. The felsic bands do not seem to be oriented or foliated in one direction in some rocks, while the mafic bands are aligned. The rocks have a preponderance of amphibole (64-85%), and substantial

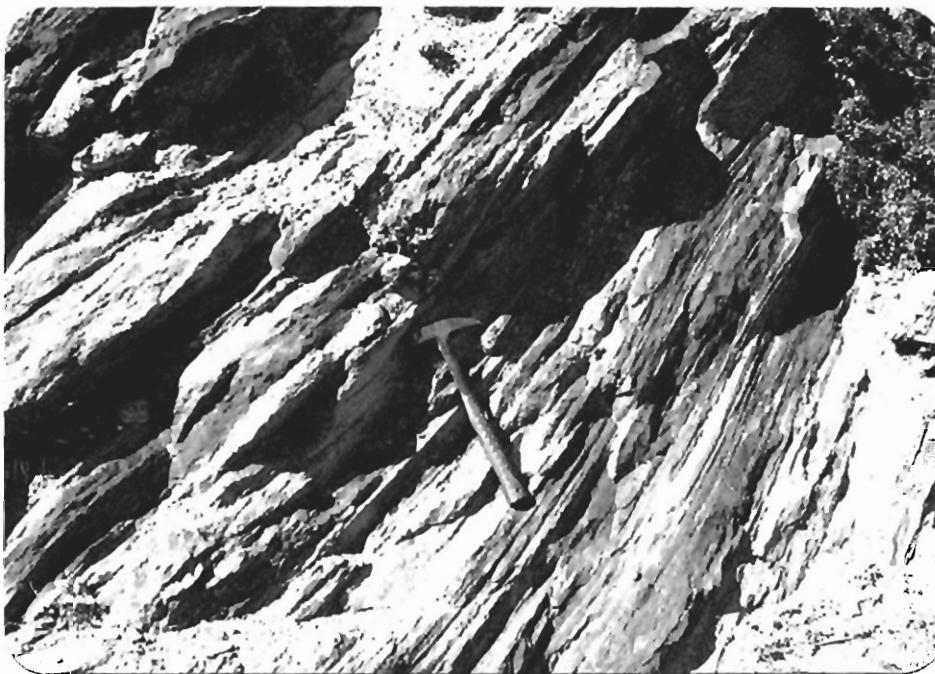


Plate 4.17. Alternate bands of volcanics/amphibolites and diorites in Niat valley. Cream colour represents the diorites and dark grey/green colour shows the amphibolites.



Plate 4.18. Mix zone of alternating diorites and amphibolites in Keo valley. The dioritic bands show a range in thickness from 2 cm to 40 cm in the photograph. Lower center shows some deformation in the rocks.



Plate 4.19. Stretched pillows are seen in Niat volcanics in the front of Dalupar gah in Buto valley. Some pillows show shearing.



Plate 4.20. Strongly sheared pillows in Niat volcanics, giving the impression of banded amphibolites like the Babusar amphibolites (Buto valley).

quartz (8-26%). Plagioclase, epidote and chlorite are subordinate and others are insignificant. Opaque mineral (magnetite), sphene, muscovite, and apatite occur as accessory minerals. Modal composition of representative rocks is given in Table 4.2.

Plagioclase is subhedral to euhedral and ranges from traces to 7% in the rocks. It is highly saussuritized and cloudy and may often be untwinned. Two size populations of plagioclase crystals are present in the rocks. The large crystals show a higher anorthite content (andesine An_{38-44}), whereas the small crystals are albitic (An_{6-10}). The margins of the plagioclase grains are corroded and cores are sericitised (Plate 4.22). These are enclosed by mostly quartz and some epidote. At places the plagioclase is enclosed in chloritised hornblende, imparting sub-poikiloblastic texture to the rock. Apatite is presents in the large (3-4 mm) crystals. The alteration probably occurred hydrothermally.

Amphibole is subhedral, green (pleochroic sometimes to bluish green), and ranges from 64% to 85% in the rocks. Two varieties of amphibole are present: hornblende and actinolite. Hornblende shows light to dark green colour and perfect cleavage. It is aligned and elongated in the major direction of foliation /schistosity but in some cases it shows no deformation. It has sharp boundaries (Plate 4.23) with epidote and quartz, but at places the margins are altered. Actinolite, presents in strongly foliated rocks, occurs mainly as subprismatic crystals in association with epidote and chlorite. It is light green to pale green in colour, and may occur as long prismatic crystals often in columnar aggregates and in parallel intergrowths with hornblende in the direction of deformation.

Epidote forms aggregates of subrounded grains but it may also occur in prismatic to subprismatic crystals elongated parallel to schistosity. It is widely present and grown after hornblende. Sphene occurs as small independent grains

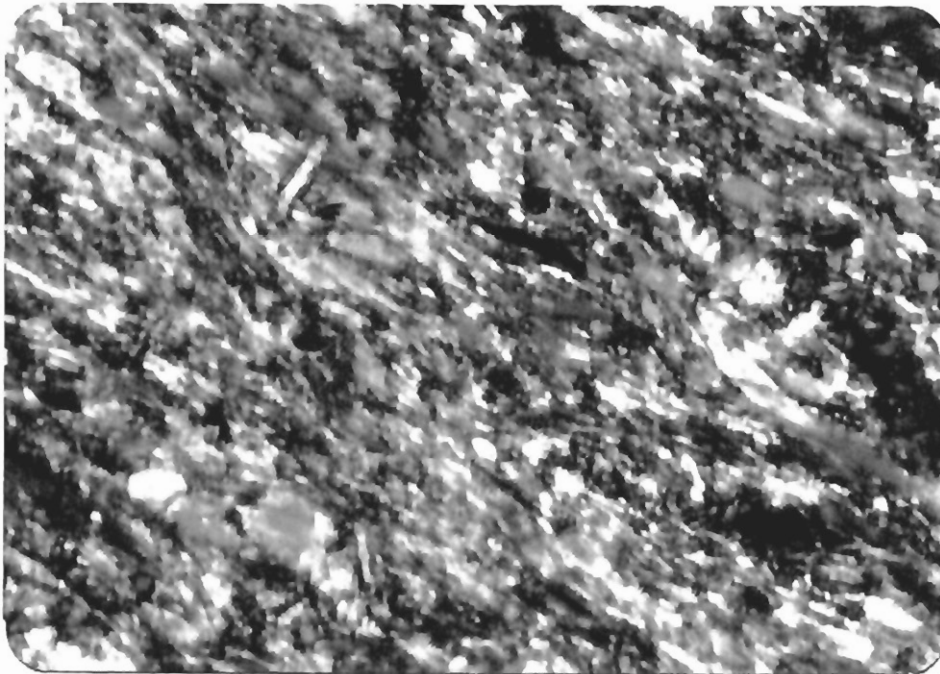


Plate 4.21. Fine-grained and foliated Niat volcanics containing hornblende, chlorite, epidote, quartz, sphenes, muscovite and ore. Field of view is 4 mm.

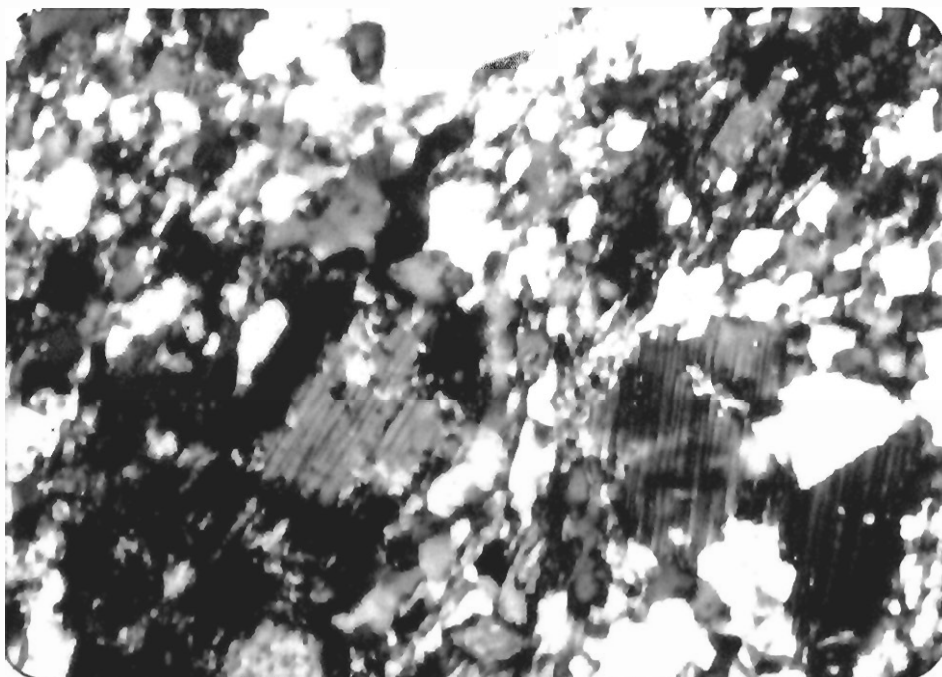


Plate 4.22. Deformed rock containing plagioclase, quartz, chlorite, epidote, muscovite and sphenes. Some chlorite encloses plagioclase which shows alteration to epidote and sericite and is locally corroded on margins. Quartz may be concentrated in crude bands. Field of view is 4 mm.

Table 4. 2. Modal composition (visual estimates) of Niat volcanic rocks.

Sample No	A-82	A-89	A-114	A-200	A-221	A-132	A-134	A-135
Amphibole	84	76	85	78	84	64	70	74
Plagioclase	tr			2		3	4	7
Epidot	1	6	3	1	2	5	3	2
Quartz	15	16	11	14	8	26	16	13
Chlorite				3	4		6	3
Magnetite		2				tr	tr	tr
Sphene	tr	tr	1	tr	1	1	tr	
Biotite								
Calcite								
Muscovite			tr	1	1	1	1	1
Apatite								tr

Key : A-82, 89 (Niat valley); A-114, 200 (Buto valley); A- 221 (Keo valley) and A-132, 134, 135 (Thor valley).

and granular aggregates. It is irregularly distributed and may itself contain iron oxide inclusions. The amount of sphene does not exceed 1 vol%. Chlorite occurs as flaky aggregates. Opaque oxide grains are sparsely disseminated and formed by alteration of hornblende. Magnetite, biotite, and muscovite may occur as accessories. Quartz is presents in alternating bands with the bands of mafic minerals, e.g., amphibole, epidote and chlorite. It is subhedral to anhedral. Mostly the anhedral crystals are cloudy. Some elongation and deformation is also seen in quartz crystals.

Sumal Amphibolites

Field Features and Relations

A succession (~500 m thick) of amphibolites, exposed in the middle reaches of Buto and Bara valleys, with best representative outcrops in the vicinity of the Sumal village, is distinguished from the adjacent Niat amphibolites. In the field, these amphibolites are lighter green in colour compared to the dark green amphibolites of the Niat unit. In terms of geochemical composition, these amphibolites are distinctly different than the rest of the amphibolites of the studied area (see later). The Sumal Amphibolite Belt has tectonic contacts with adjacent rock units. It is bounded by Niat amphibolites in the north and a foliated granite in the south. Because of the tectonic nature of the contacts, the age relationship of the Sumal amphibolites is not clear with its neighbouring lithologies. The granite at the southern margin could have been originally intrusive into the Sumal amphibolites as suggested by the occurrence of amphibolite xenoliths in it.

The Sumal amphibolites are fine-grained and massive to weakly foliated. Unlike the Niat and Jal amphibolites, they are commonly porphyroblastic with medium-sized grains of amphibole. The lighter green colour and porphyroblastic

texture clearly distinguish them from the rest of the amphibolites of the studied area. Part of the belt in the vicinity of the Sumal village contains relict pillow structures which are tectonically stretched without losing their internal geometry. These pillows have epidote-chlorite rich light green cores with dark crust (the colour difference is probably due to difference in grain size). Locally, the amphibolites show weak banding which is suspected to be due to shearing of the pillow structures. The Sumal amphibolite belt is commonly intruded by veins, dykes and sheets of granites, granodiorites and diorites. Quartz veins are also common. The rocks are metamorphosed under greenschist facies conditions.

Modal Composition and Petrography

The Sumal amphibolites are fine- to medium-grained, massive to foliated and mostly porphyroblastic. Most grains are elongated and aligned in one major direction but some are tilted or rotated. Amphibole, epidote and quartz constitute the principal component minerals with small amounts of sphene (locally 5-12%), chlorite, muscovite and biotite. In some rocks minor calcite and apatite are accessory minerals. Modal composition is given in Table 4.3.

Plagioclase is subhedral to anhedral. It ranges from oligoclase (An_{28-30}) to andesine (An_{34-48}). In the less mafic parts of rocks, plagioclase is mostly oligoclase. Laboradorite occurs in a few samples, reflecting a higher metamorphic grade and/or the influence of bulk composition. Polysynthetic twinning is present, and alteration to epidote and sericite is common (Plate 4.24).

Amphibole is subhedral and pleochroic. Compositionally it is mainly hornblende of brownish green to dark green colour. In some cases zoning is present with dark green cores and light green margins. Three types of hornblende grains are present in these rocks; i) small, elongated and oriented with the fine

Table 4.3. Modal composition(visual estimates) of Sumal volcanic rocks.

Sample Nos.	A-187	A-110	A-117	A-122	A-225
Amphibole	54	44	39	37	32
Plagioclase	10	11			
Epidot	19	22	35	38	42
Quartz	12	17	16	15	10
Chlorite	2	4	3		7
Magnetite	tr				
Sphene	2	1	4	7	8
Biotite			2		
Calcite				1	
Muscovite	1	1	1	2	1
Apatite	tr	tr			

Key: A-110, 117, 122, 187 (Buto valley) and A-225 (Keo valley)

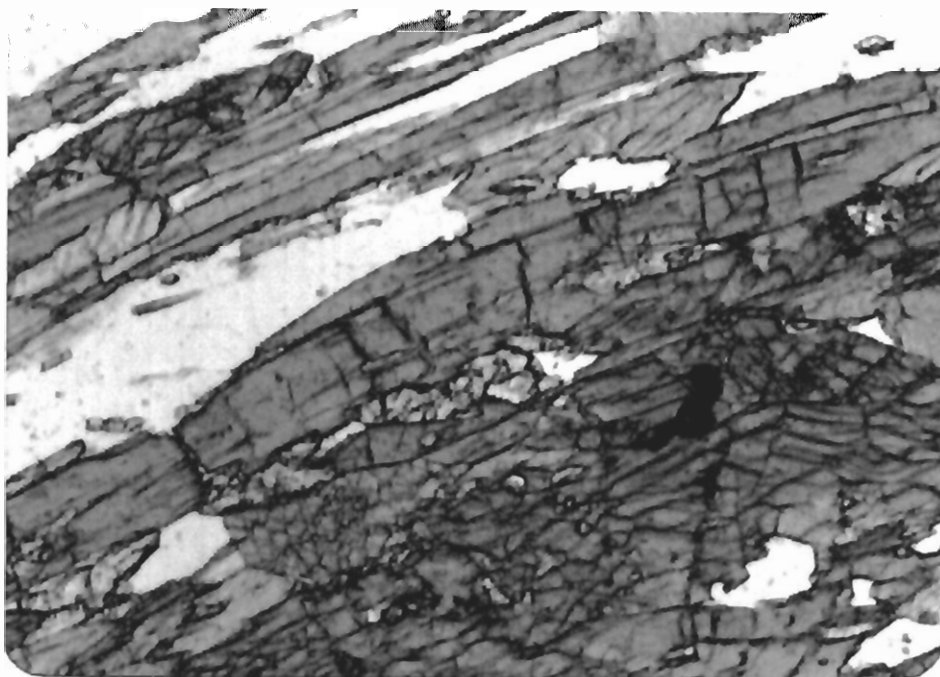


Plate 4.23. Microphotograph showing the perfect cleavage of hornblende and inclusions of sphene in it. Amphibole, epidote and quartz are elongated parallel to schistosity or foliation. Field of view is 4 mm.

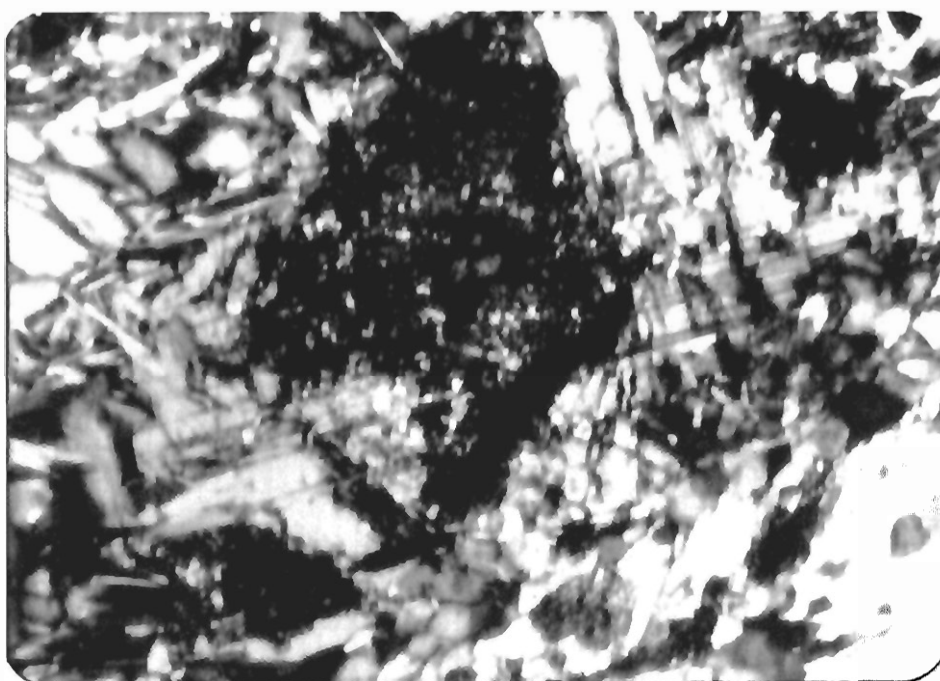


Plate 4.24. Sumal volcanics containing feldspar, hornblende, chlorite, muscovite and sphene. Core of feldspar is altered to chlorite and in the lower right corner amphibole crystal enclose sphene. Field of view is 4 mm.

matrix, ii) oblique and rotated, and iii) undisturbed. Along shear planes, actinolite-tremolite commonly occurs with hornblende and epidote as subprismatic crystals and columnar to fibrous aggregates. It is colourless to light green with light bluish tinge at some places. The margins of the actinolite grains are corroded away.

Epidote occurs in the form of granular aggregates. Some grains form euhedral to subhedral prisms, but most are anhedral. It develops along the margins of the amphibole (both hornblende and actinolite) crystals. Sphene may be enclosed in hornblende (Plate 4.24) and may itself have formed from iron oxides (titanomagnetite/ ilmenite). It occurs as small grains and also as granular aggregates. The amount of sphene varies from sample to sample, depending upon the degree of alteration and modal content of titanium-bearing opaque oxides. Chlorite occurs as flaky aggregates and shows light green colour. It may have grown at the expense of hornblende and/ or epidote. Opaque oxide grains are sparsely disseminated throughout the rock. Magnetite, biotite, and muscovite may occur as accessories. Stretched quartz crystals are visible in the rock.

Jal Amphibolites

Field Features and Relations

The Jal Amphibolite belt is striking because of the presence of leucocratic bands and concordant sheets of granite pegmatite in it (Plates 4.25 and 4.26). The belt is well exposed in Thak and Niat valleys with a thickness of about 3 km. It is in contact with the Chilas complex to the north and Khun diorite to the south (Plate 4.27). In the extreme eastern part of the area (i.e., Buner valley), it is in direct contact with the MMT (Plates 4.28 and 4.29). The contact with the Chilas complex is marked by a strongly sheared amphibolite and granite mylonite zone (Plate



Plate 4.25. Bands of granite, andesitic rock and amphibolite in the Jal amphibolite unit in Thak valley near Jal. Bands varies from 1 cm to 20 cm in thickness.



Plate 4.26. Photograph showing andesitic veins in Jal amphibolites, producing a banded appearance in Thak valley.

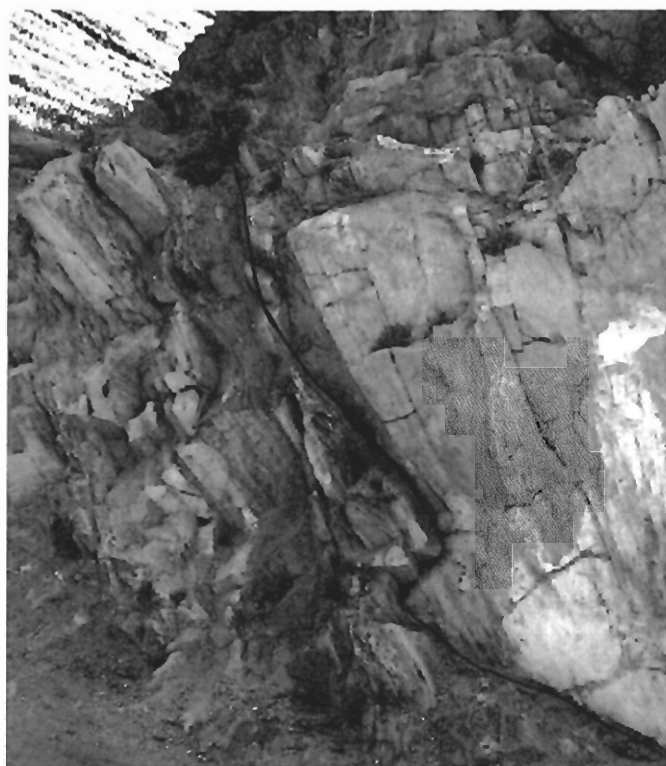


Plate 4.27. The contact of diorite (light colour) and Jal amphibolites (grey) in Thor valley, between Sarin and Gabbar.

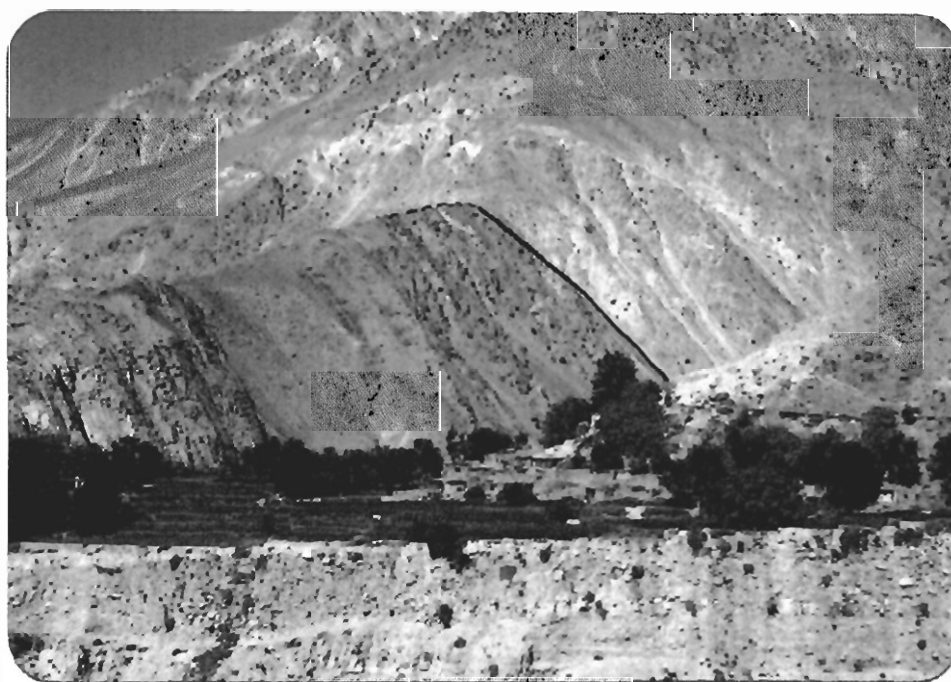


Plate 4.28. Contact of Jal amphibolites with the gneisses of the Indian plate in Bunar valley, the rocks of Indian plate are light in colour. Tall tree marked the contact.

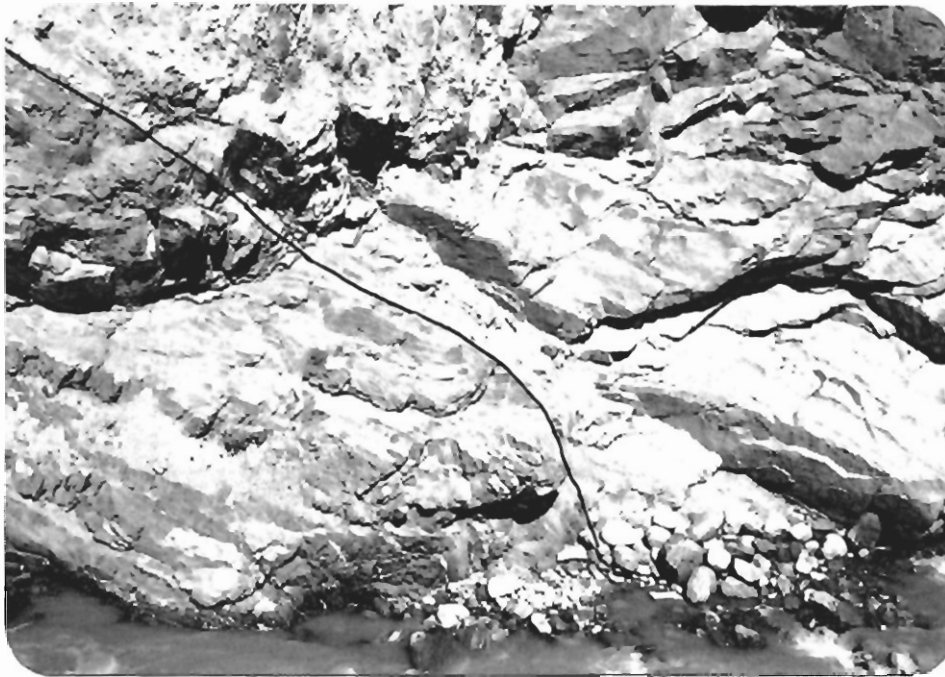


Plate 4.29. Photograph showing the closeup of the contact between the Jal amphibolites and the gneisses of Indian plate at Halala, in Bunar valley.



Plate 4.30. Strongly sheared and mylonitized amphibolites and granite of Jal unit in Thak valley. The shear zone is 100 m wide.

4.30). This zone, which is 100 meter wide at Jal in Thak and 20 meter wide in Thor gah, is termed as the Jal shear zone (Coward et al., 1987; Khan, 1988). It is probably an equivalent of the Kamila shear zone of Treloar et al.(1990).

The granite pegmatite bodies are folded and boudinaged. Ptygmatic folding is the most prominent feature of these rocks (Plates 4.31). Folding is very irregular; every vein has its own individual fold direction without showing any structural relation to the enclosing host rock (Plates 4.32 and 4.33). Another interesting feature of these rocks is the close association of the highly folded veins and those without a single twist. Sometime a single vein is folded at one end and straight at the other.

The quartzofeldspathic veins and granite pegmatites are white to light grey on fresh surface. On weathered surface they become pale white to pale yellow. At places, the two rock-types (quartzofeldspathic bodies and amphibolites) show a greater degree of mixing. The colour on the fresh surface also becomes lighter and gives the shades of green. Due to this, the rock becomes banded in the form of thin and medium layers of green and white appearance (Plate 4.34). This banded appearance is due to regularly spaced felsic veins which are intruded along schistosity that is very prominent. The alternation of felsic material with mafic host rock led Shams(1975) to suggest the term "vein diorite" for the Jal amphibolites. The invading veins are highly variable in thickness and range from a fraction of a centimeter to several meters. The volume of invading felsic material at places may reach to a maximum of 50% of the rock (Plate 4.35). The bands always have a sharp contact and no gradation is observed.

The amphibolite bands are fine-grained, melanocratic and foliated. They are generally dark green, especially along schistosity planes. These planes are marked by the growth of randomly oriented crystals of acicular hornblende. These crystals



Plate 4.31. Ptygmatic folding in Jal amphibolites, Thak valley.

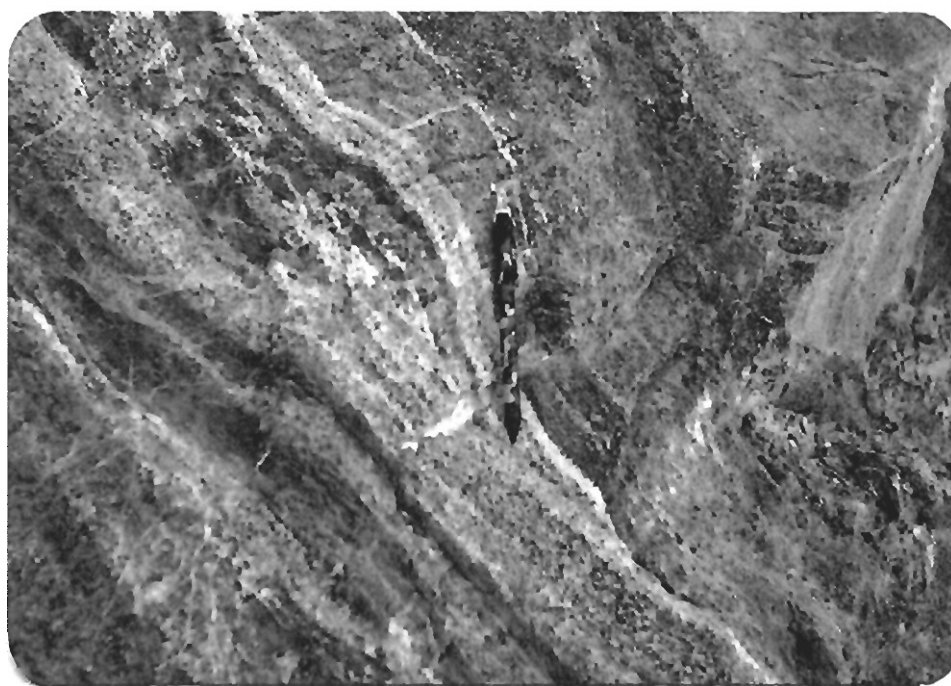


Plate 4.32. Banding, shearing and folding in Jal amphibolites, Bunar valley. Photograph also shows the orientation of minerals in the direction of foliation.

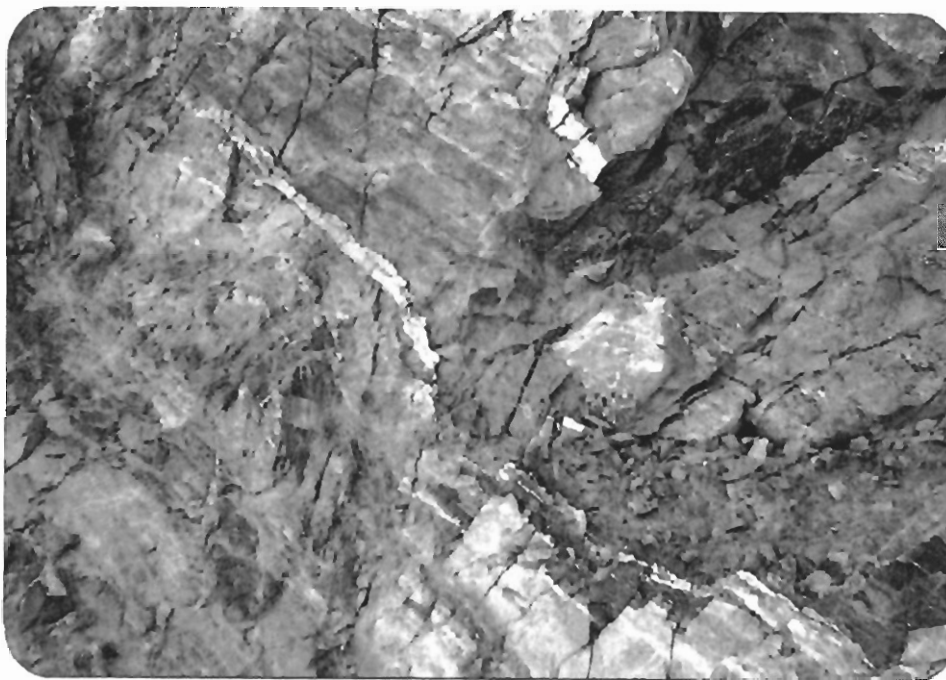


Plate 4.33. Photograph showing the banding and shearing in Jal amphibolites, Bunar valley. The rock is finer-grained than in the photograph 3.32.



Plate 4.34. Bands of amphibolite and granite give the impression of layering in Jal amphibolites at Gabbar, Thor valley. Mylonite zones are very common in the Jal unit, including the present photograph.

represent post-tectonic growth of amphibole during the varying stages of stresses. On weathered surface the amphibolite bands are dark greenish brown, dark brown and dark brownish grey. At many places the dips are nearly vertical which make the dark grey and pale white bands especially distinctive and characteristic.

Modal Composition and Petrography

The Jal amphibolites consist of dark green (rich in mafics) and pale white to white (rich in felsics) bands. The light coloured component of the rock is of three types : 1- *Pegmatitic*, 2- *Thin granitic layers*, and 3- *Quartz veins*

The rock is mainly medium- to coarse-grained and euhedral to subhedral. It is strongly mylonitized, and foliated in one direction. Banding and foliation are due to variations in the amounts of amphibole, plagioclase and quartz (Plate 4.36). In the mafic bands amphibole, chlorite and magnetite are concentrated. In felsic bands plagioclase, quartz and some epidote occur. Sphene, when present, tends to be concentrated in the mafic bands. Modal composition is given in Table 4.4. Twin planes, cleavage traces and crystal faces are bent and kinked at many places.

Hornblende is the most dominant mineral in the rock and ranges from 9 to 76 vol%. It is medium-grained, brown green to dark green and shows perfect cleavage. It shows anomalous colours from yellow, yellowish green, light to dark green in cross light. Grains are elongated and arranged in parallel rows in direction of deformation and impart the rock a schistose texture (Plate 4.37). At places hornblende crystals elongated oblique to schistosity are also seen. Some crystals show inclusions of quartz and sericite. Along the margins, where, hornblende is in contact with plagioclase crystals, a rim of epidote and sphene is present. Magnetite is also presents along the boundaries of hornblende.

Table 4.4. Modal composition (visual estimates) of Jal rocks.

Sample Nos.	A-76	A-156	A-158	A-159	A-69	A-148	A-151	A-89
Amphibole	65	47	54	51	60	76	30	9
Plagioclase	14	17	28	29			49	40
Epidot	3	3	2	2	15	1	6	5
Quartz	16	9	12	13		18	9	5
Chlorite		23			17	4		26
Magnetite		tr	tr	tr	2		5	2
Sphene	1	1	1	1	1	1		
Biotite	1				5			
Calcite								12
Muscovite		1	3	4			1	1
Zircon		tr		tr				

Key : A-76 (Bunar valley); A-89 (Niat valley); A-156, 158, 159, 69 (Thak valley) and A-148, 151 (Thor valley).



Plate 4.35. Bands of amphibolite and granite near the confluence of Chirat gah and Thak gah in the Jal unit. Both the rock types are sheared and mylonitized.

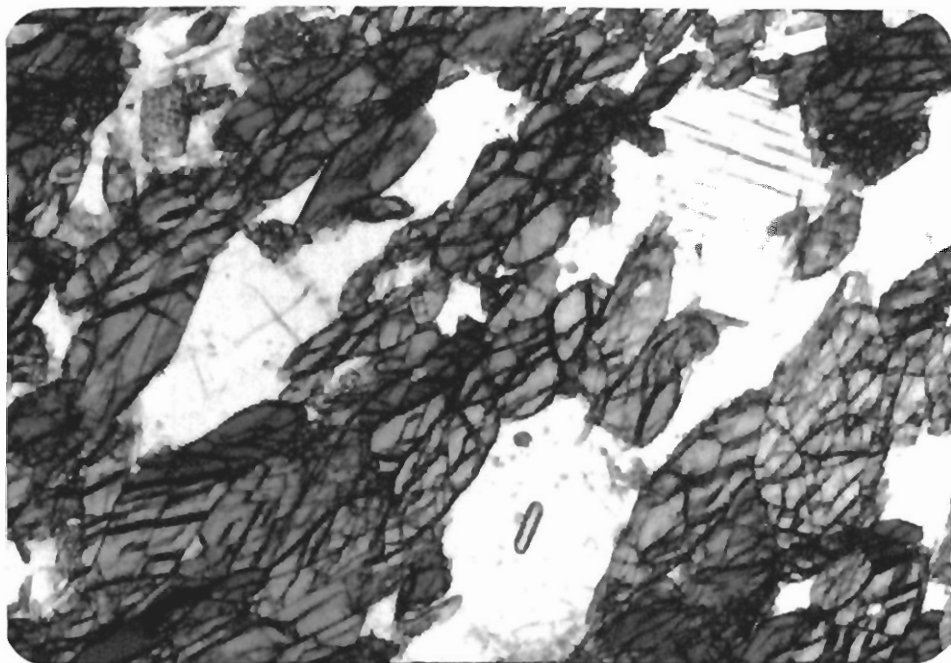


Plate 4.36. Microphotograph showing mafic and felsic bands in parallel rows. Banding and foliation are due to variations in the amounts of amphibole, plagioclase and quartz. Field of view is 2.5 mm.

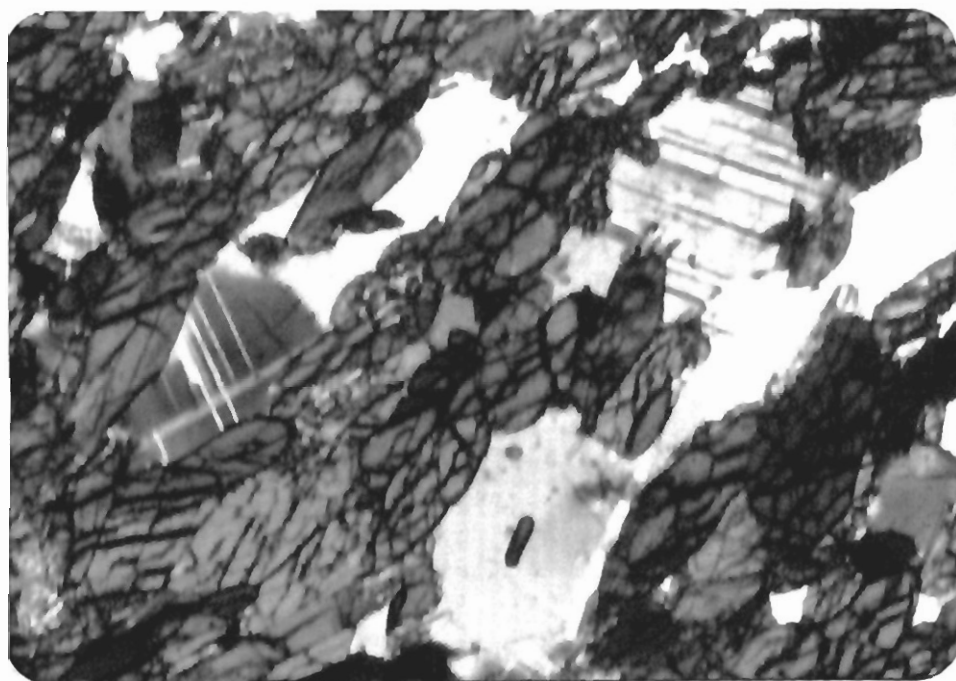


Plate 4.37. The same as 3.36 in crossed polars.

Plagioclase is medium-grained and xenoblastic. Its proportion ranges from 14 to 49 vol% in the studied rock. Its composition ranges from oligoclase through andesine (An_{30-46}) to labradorite (An_{56}). Mostly it is in andesine range. It shows twinning and euhedral to subhedral. A few samples contain minor microcline. Plagioclase is highly saussuritized, especially the more calcic type An_{42-56} . The andesine with low An_{30-42} content is less saussuritized. Myrmekitic intergrowth with quartz is presents in some samples. Quartz is fine- to medium-grained and subhedral to anhedral. Its grains are interdigitating with hornblende and plagioclase and forming notched boundaries.

Whole-rock Geochemistry

The four units (Jal, Niat, Babusar and Sumal) of the amphibolites show a lot of mineralogical, textural and structural variations. But interestingly, three (Jal, Niat and Babusar) of them show a similar geochemical behaviour except Sumal unit. All these rocks will be discussed in terms of their geochemistry in this section. Forty nine rock samples from the four groups of amphibolites were selected for whole-rock geochemistry including both major and trace elements. The analyses were performed only on homogeneous samples devoid of low-temperature alteration. In the case of banded amphibolites, samples were collected from the interior parts of thick mafic bands in an attempt to avoid possible effects of magma mixing. The analyses were obtained using XRF. Details of the analytical techniques and limits of detection for the analyzed elements are given in Chapter 1, whilst the analyses are given in Tables 4.6, 4.7, 4.10 and 4.11.

Alteration during solidification

Mineralogical retrogression is widespread in these rocks and where evidences exist for secondary mineral growth, the chemical abundances and ratios

may have been modified to a greater or lesser extent. Therefore, it is very important to determine the extent of element mobility and redistribution. The elements considered mobile in aqueous fluids, namely the large-ion lithophile elements (LILE) Ba, Rb, K and Sr, are redistributed, depleted or enriched by alteration processes (Floyd and Winchester, 1975; Pearce and Cann, 1973, Pearce, 1982; 1983). Light rare earth elements can also be affected in a similar manner (Ludden and Thompson, 1979; Terrell et al., 1979). On the other hand, high-field strength elements (HFSE) such as Ti, P, Zr, Y, Nb and heavy rare-earth elements have better chances of retaining primary petrogenetic characteristics, as such forming the basis of diagrams used in discrimination of tectonic settings (e.g. Pearce and Cann, 1973; Meschede, 1986).

The studied rocks are altered and affected by greenschist /amphibolite facies metamorphism with common chlorite, epidote and quartz. Under these metamorphic conditions, certain elements, especially the low field strength and alkali elements (K, Rb, Ba, Sr) may be prone to secondary mobility. To ascertain how mobile the elements have been, data may be plotted against a relatively immobile element such as Ti, Nb or Zr (Macdonald et al., 1988). Several elements from the studied rocks are plotted against Zr. These plots give a qualitative assessment about the relative mobility of these elements. High field strength elements P and Y display excellent correlations with Zr. Nb is increasing with increase of Zr and show good correlation. Correlation is less pronounced for Sr suggesting that this element was mobile to some degree. Weakest correlation is seen with K_2O pointing to changes in its original magmatic proportions through alteration and metamorphism.

Grouping

Table 4.5 displays the average concentration of major and trace elements in the amphibolites of the different units. Although in the field the amphibolites have been divided into four units depending on their field characteristics, Babusar, Jal and Niat display remarkable resemblance in their geochemistry (tholeiitic) while the Sumal amphibolites stand out because of their calc-alkalic chemical characteristics (Figure 4.1). The tholeiitic amphibolites are further divided into two groups on the basis of their chemical composition and trends.

I) A great majority of the analyzed samples (25 of 30 samples, including five anomalous ones) have distinctly high TiO_2 i.e., 1-3 wt%; mean 1.56% for Jal amphibolites (JA) and 1.99% for Niat amphibolites (NA) and low K_2O (mean 0.2 for JA and 0.14 for NA). When plotted against Zr, these samples show distinct enrichment in TiO_2 and Fe_2O_3 suggesting a tholeiite trend for the magmatic evolution. Additionally there is a negative correlation of Al_2O_3 and Sr with Zr, suggesting plagioclase fractionation control. This group includes both Jal and Niat metavolcanic amphibolites and thus are hereafter referred to as the Jal-Niat Group.

II) Eight samples from Babusar amphibolites (BA) show higher Fe_2O_3 (mean) and low K_2O (mean 0.08 wt%) suggesting a tholeiitic trend for the magmatic evolution of the rocks, but they contain low TiO_2 (mean 0.8%) and very low Zr (mean 8.68ppm) as compared to the tholeiitic amphibolites of Jal-Niat group. There is a negative correlation of Al_2O_3 and positive correlation of Sr with Zr, whereas the Jal-Niat amphibolites show negative correlation of Sr with Zr. Additionally, the oxides Al_2O_3 , Na_2O_3 , CaO, MgO, TiO_2 and P_2O_5 show very steep variation trends of these rocks as compared with the gentle trends shown by the amphibolites of

Table 4.5. Average composition of the analyzed volcanic / amphibolite rocks.

Samp. No.	JAL	NIAT	BABU	SUMAL
SiO ₂	50.64	49.36	49.50	50.26
TiO ₂	1.56	1.99	0.80	0.68
Al ₂ O ₃	15.53	14.99	18.46	17.41
Fe ₂ O ₃	11.91	13.22	11.39	9.06
MgO	6.82	6.46	5.60	7.99
CaO	10.50	10.57	11.74	10.36
Na ₂ O	2.64	3.00	2.02	3.38
K ₂ O	0.20	0.14	0.08	0.66
P ₂ O ₅	0.16	0.22	0.18	0.17
Total	99.96	99.95	99.77	99.97
Nb	3.92	5.44	0.77	2.70
Zr	94.00	112.00	8.69	36.60
Y	33.30	48.38	15.34	15.00
Sr	198.46	163.00	182.36	235.60
Rb	2.61	1.15	0.99	13.80
Th	2.00	2.00	0.74	2.00
Pb	2.00	2.00	1.53	2.00
Ga	19.53	21.84	16.43	16.00
Zn	107.00	81.53	100.29	68.40
Cu	99.92	34.23	62.14	54.40
Co	55.61	55.38		53.00
Ni	61.69	48.54	18.71	90.00
Ti	9352.36	11930.25	4796.08	4076.67
K	1660.32	1162.22	675.99	5479.06
P	698.30	960.17	791.83	741.95
Mg	41132.10	38960.91	33782.78	48188.49

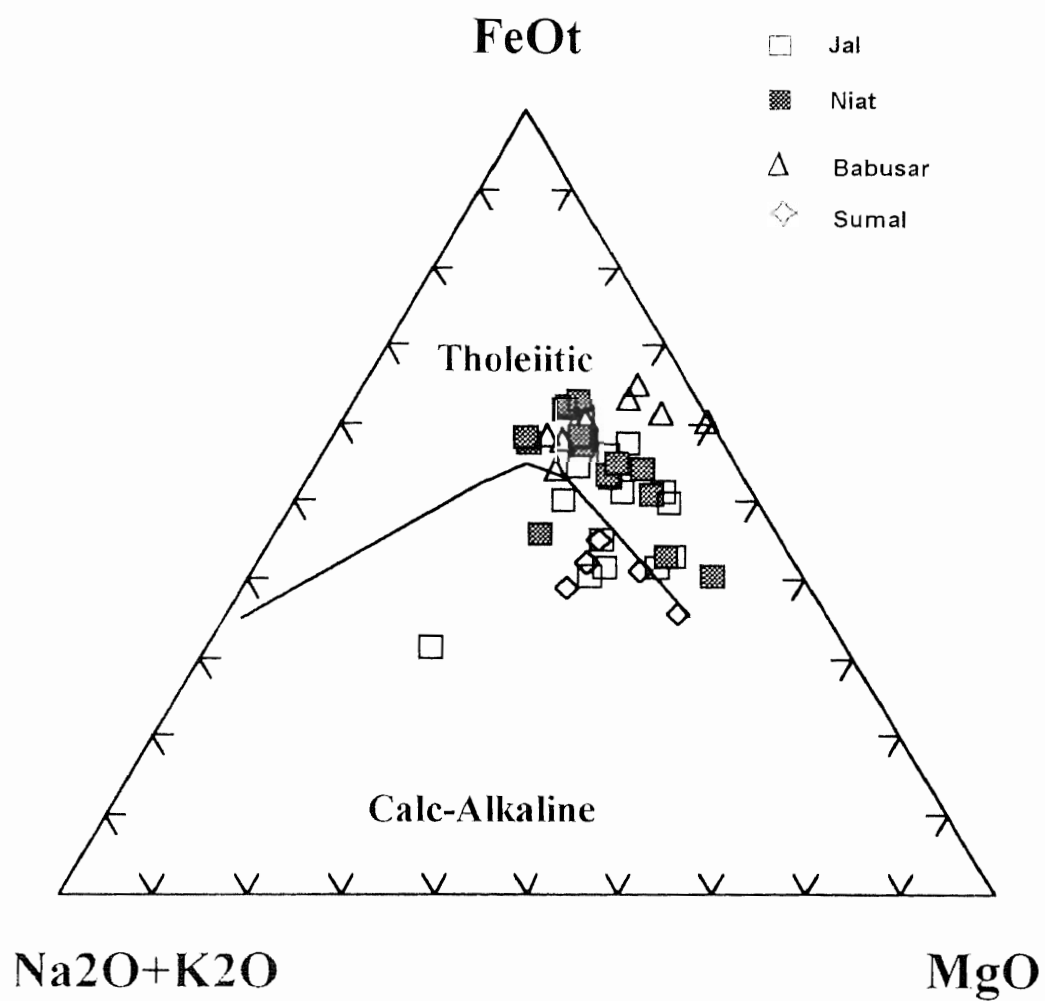


Figure 4.1. An AFM ternary plot differentiating the studied amphibolites into tholeiites (Babusar, Niat and Jal) and calc-alkaline (Sumal) suites.

Jal-Niat group with Zr. On the basis of compositional variations and trends, the geochemistry of this suite of samples is discussed separately as the Babusar Group.

III) A limited number of samples (only five), collected from a coherent tectonic slice of amphibolite from the Buto Gah shows compositional characteristics of type calc-alkaline suite. They contain low TiO_2 (mean 0.68%) and Fe_2O_3 (9.06%), high Al_2O_3 (17.41%) and K_2O (0.66%). This group shows Fe-Ti depletion and alumina enrichment with fractionation, suggesting the role of iron-bearing minerals (possibly spinels) from the onset of crystallization and absence of the control of plagioclase from the fractionation assemblage. This group of samples belongs to Sumal metavolcanic amphibolites.

Inter-relationship between Jal and Niat Amphibolites

The inter-element ratios involving essentially incompatible elements remain unaffected by the magmatic processes and fractionation (Weaver et al., 1981). This implies that the three components of a crystallizing magma, i.e., partial melt, crystallized minerals and residual liquid, should have identical incompatible inter-element ratios. When the trace-element variation of the two units of amphibolites of the study area are treated together, the binary inter-element plots yield mainly one type of patterns. In the case of trace-elements which are incompatible, the rocks of the two units define mutually coherent trends, with identical inter-element ratios. The whole rock analyses data are given in Tables 4.6 and 4.7 for Jal and Niat respectively.

Like the incompatible trace elements, most of the compatible elements (e.g. Ti and Y), when plotted against Zr, also yield the same trend for the two units. This gives an impression that, the two units collectively define a continuous "Liquid

Table 4.6. Major and trace element concentration of Jal Amphibolites.

Sample Nos.	A-69	A-72	A-78	A-74	A-98	A-101	A-105
SiO ₂	49.33	50.13	51.89	50.19	50.11	50.72	51.79
TiO ₂	1.13	1.64	0.73	1.52	2.91	1.15	2.39
Al ₂ O ₃	16.74	14.68	20.19	14.55	13.40	15.49	13.89
Fe ₂ O ₃	9.65	11.87	9.25	12.19	16.42	11.14	14.61
MgO	9.00	7.30	4.86	6.81	5.63	7.69	5.65
CaO	11.57	11.34	9.52	11.68	7.61	11.83	8.49
Na ₂ O	2.34	2.76	3.32	2.69	3.44	1.70	2.85
K ₂ O	0.14	0.13	0.17	0.23	0.13	0.15	0.08
P ₂ O ₅	0.10	0.15	0.06	0.13	0.35	0.12	0.25
Total	100.00	100.00	99.99	99.99	100.00	99.99	100.00
Nb	2.80	3.10	0.70	3.10	8.00	3.10	6.50
Zr	68.00	85.00	20.00	85.00	168.00	64.00	160.00
Y	22.00	34.00	11.00	34.00	59.00	28.00	50.00
Sr	164.00	185.00	475.00	185.00	162.00	176.00	144.00
Rb	1.00	1.00	1.00	1.00	1.00	2.00	1.00
Th	2.00	2.00	2.00	2.00	2.00	2.00	2.00
Pb	2.00	2.00	2.00	2.00	2.00	2.00	2.00
Ga	16.00	20.00	20.00	20.00	22.00	19.00	23.00
Zn	64.00	99.00	78.00	99.00	210.00	119.00	180.00
Cu	5.00	18.00	28.00	18.00	814.00	76.00	179.00
Co	57.00	59.00	54.00	59.00	50.00	69.00	49.00
Ni	129.00	50.00	7.00	50.00	25.00	94.00	33.00
Ti	6774.46	9831.96	4376.42	9112.55	17445.74	6894.37	14328.29
K	1162.22	1079.21	1411.27	1909.37	1079.21	1245.24	664.13
P	436.44	654.66	261.86	567.37	1527.54	523.73	1091.10
Mg	54279.90	44027.03	29311.15	41071.79	33955.09	46379.16	34075.72

Table 4.6 continued

Sample Nos.	A-147	A-148	A-151	A-154	A-156	A-157
SiO ₂	49.08	49.42	54.77	50.17	51.90	48.90
TiO ₂	1.15	2.03	0.54	2.13	1.93	1.10
Al ₂ O ₃	15.41	14.25	18.27	13.99	15.00	16.06
Fe ₂ O ₃	11.57	13.34	8.62	13.43	12.91	9.83
MgO	8.55	6.64	4.47	6.31	6.54	9.24
CaO	12.16	11.29	9.99	9.96	9.49	11.58
Na ₂ O	1.54	2.52	2.87	3.56	1.97	2.88
K ₂ O	0.45	0.30	0.32	0.24	0.07	0.32
P ₂ O ₅	0.09	0.20	0.15	0.21	0.18	0.10
Total	100.00	99.99	100.00	100.00	99.99	100.01
Nb	3.00	5.40	2.10	5.60	5.00	2.60
Zr	76.00	126.00	51.00	135.00	118.00	66.00
Y	28.00	43.00	17.00	45.00	40.00	22.00
Sr	173.00	153.00	250.00	128.00	227.00	158.00
Rb	15.00	4.00	1.00	2.00	1.00	3.00
Th	2.00	2.00	3.00	2.00	2.00	2.00
Pb	2.00	2.00	4.00	2.00	2.00	2.00
Ga	19.00	21.00	18.00	21.00	19.00	16.00
Zn	104.00	95.00	80.00	98.00	98.00	68.00
Cu	2.00	54.00	47.00	33.00	23.00	2.00
Co	67.00	54.00	36.00	52.00	56.00	61.00
Ni	97.00	64.00	17.00	40.00	42.00	154.00
Ti	6894.37	12170.05	3237.35	12769.56	11570.54	6594.61
K	3735.72	2490.48	2656.51	1992.38	581.11	2656.51
P	392.80	872.88	654.66	916.52	785.59	436.44
Mg	51565.91	40046.50	26959.02	38056.24	39443.39	55727.36

Table 4.7. Major and trace element composition of Niat volcanics.

Sample Nos.	A-80	A-83	A86	A-92	A-93	A-109	A-112
SiO ₂	50.25	51.19	47.98	49.21	48.76	46.71	48.37
TiO ₂	2.13	2.24	2.13	1.72	1.86	1.74	2.52
Al ₂ O ₃	14.75	14.31	14.44	15.23	14.71	15.11	17.96
Fe ₂ O ₃	14.67	14.67	14.08	11.91	13.06	12.55	14.30
MgO	6.32	5.11	6.11	6.51	6.90	8.38	2.69
CaO	8.33	9.63	11.64	12.39	11.82	12.98	8.35
Na ₂ O	3.11	2.40	3.09	2.73	2.66	2.25	5.18
K ₂ O	0.23	0.26	0.32	0.14	0.08	0.09	0.06
P ₂ O ₅	0.21	0.19	0.21	0.16	0.17	0.19	0.58
Total	100.00	100.00	100.00	100.00	100.02	100.00	100.01
Nb	5.20	4.80	6.20	4.10	4.30	0.90	1.60
Zr	150.00	139.00	149.00	113.00	114.00	25.00	6.00
Y	57.00	53.00	52.00	37.00	40.00	21.00	37.00
Sr	172.00	150.00	137.00	165.00	169.00	193.00	247.00
Rb	1.00	2.00	2.00	1.00	1.00	1.00	1.00
Th	2.00	2.00	2.00	2.00	2.00	2.00	2.00
Pb	2.00	2.00	2.00	2.00	2.00	2.00	2.00
Ga	24.00	22.00	23.00	18.00	20.00	17.00	32.00
Zn	110.00	93.00	101.00	70.00	78.00	63.00	102.00
Cu	8.00	14.00	12.00	78.00	15.00	13.00	43.00
Co	51.00	54.00	54.00	60.00	60.00	58.00	48.00
Ni	32.00	22.00	75.00	67.00	58.00	136.00	8.00
Ti	12769.56	13429.02	12769.56	10311.57	11150.89	10431.47	15107.65
K	1909.37	2158.42	2656.51	1162.22	664.13	747.14	498.10
P	916.52	829.24	916.52	698.30	741.95	829.24	2531.35
Mg	38116.55	30818.92	36850.02	39262.46	41614.59	50540.62	16223.66

Table 4.7 continued

Sample Nos.	A-114	A-115	A-116	A-132	A-133	A-135
SiO ₂	46.59	51.58	48.49	55.56	52.09	44.94
TiO ₂	1.73	2.38	1.20	1.91	1.75	2.58
Al ₂ O ₃	15.21	14.24	15.75	15.40	14.82	13.04
Fe ₂ O ₃	12.45	13.63	10.41	11.76	12.52	15.93
MgO	8.43	4.65	11.61	4.03	5.76	7.60
CaO	12.95	10.43	10.20	7.18	8.55	13.05
Na ₂ O	2.36	2.68	2.19	3.74	4.14	2.56
K ₂ O	0.08	0.20	0.06	0.08	0.16	0.09
P ₂ O ₅	0.20	0.21	0.09	0.34	0.21	0.22
Total	100.00	100.00	100.00	100.00	100.00	100.01
Nb	4.90	4.60	2.10	19.00	7.80	5.20
Zr	134.00	140.00	79.00	142.00	203.00	63.00
Y	55.00	49.00	26.00	98.00	57.00	47.00
Sr	183.00	138.00	175.00	146.00	132.00	114.00
Rb	1.00	1.00	1.00	1.00	1.00	1.00
Th	2.00	2.00	2.00	2.00	2.00	2.00
Pb	2.00	2.00	2.00	2.00	2.00	2.00
Ga	22.00	22.00	15.00	23.00	23.00	23.00
Zn	15.00	25.00	71.00	107.00	106.00	119.00
Cu	2.00	2.00	67.00	23.00	67.00	101.00
Co	43.00	53.00	55.00	57.00	61.00	66.00
Ni	22.00	22.00	25.00	34.00	57.00	73.00
Ti	10371.52	14268.34	7194.12	11450.64	10491.43	15467.36
K	664.13	1660.32	498.10	664.13	1328.26	747.14
P	872.88	916.52	392.80	1483.90	916.52	960.17
Mg	50842.17	28044.62	70021.07	24305.33	34739.14	45836.36

line of descent". The concentration of Nb, Y and Ga increases and Sr decreases with the increase of Zr.

Jal and Niat Amphibolites

Scrutiny of the Data

Whole-rock analyses are used for a variety of objectives like nomenclature, classification, chemical variations (to evaluate processes like fractional crystallization, partial melting, contamination, magma mixing, etc.), and petrogenesis. One of the fundamental requirements for meeting most of these objectives is that the analyzed samples should approach the composition of the melt from which they crystallized. The chemistry of the samples can deviate from that of the melt through the effect of several factors: fractional crystallization, contamination of wall-rock or xenoliths, and hydrothermal alteration.

One of the simplest approach for evaluation of the data involves usage of binary plots (i.e., XY variation). The analyzed data for the amphibolites of the present study show a moderately high scatter when plotted on binary plots involving compatible elements, e.g. SiO₂, MgO. The scatter is reduced, however, when the data are plotted against an incompatible element like Zr (Figure 4.2). It may be noted that Zr is not only an incompatible element, it is the least susceptible to mobilization during metamorphism and hydrothermal alteration (e.g., Pearce and Cann, 1973; Floyd and Winchester, 1975; and Weaver and Tarney, 1981). In these diagrams, a large proportion of the samples plot as two groups. There is a particularly good correlation between Zr and the group of incompatible minor and trace elements such as TiO, P₂O₅, Nb, Y and Sr (Figure 4.2). This high correlation can be taken as an evidence for the immobility of these elements in the presently studied rocks (Weaver et al., 1982). The same cannot be said with certainty about the nature of K, Rb, Pb and Th because these elements have concentrations either

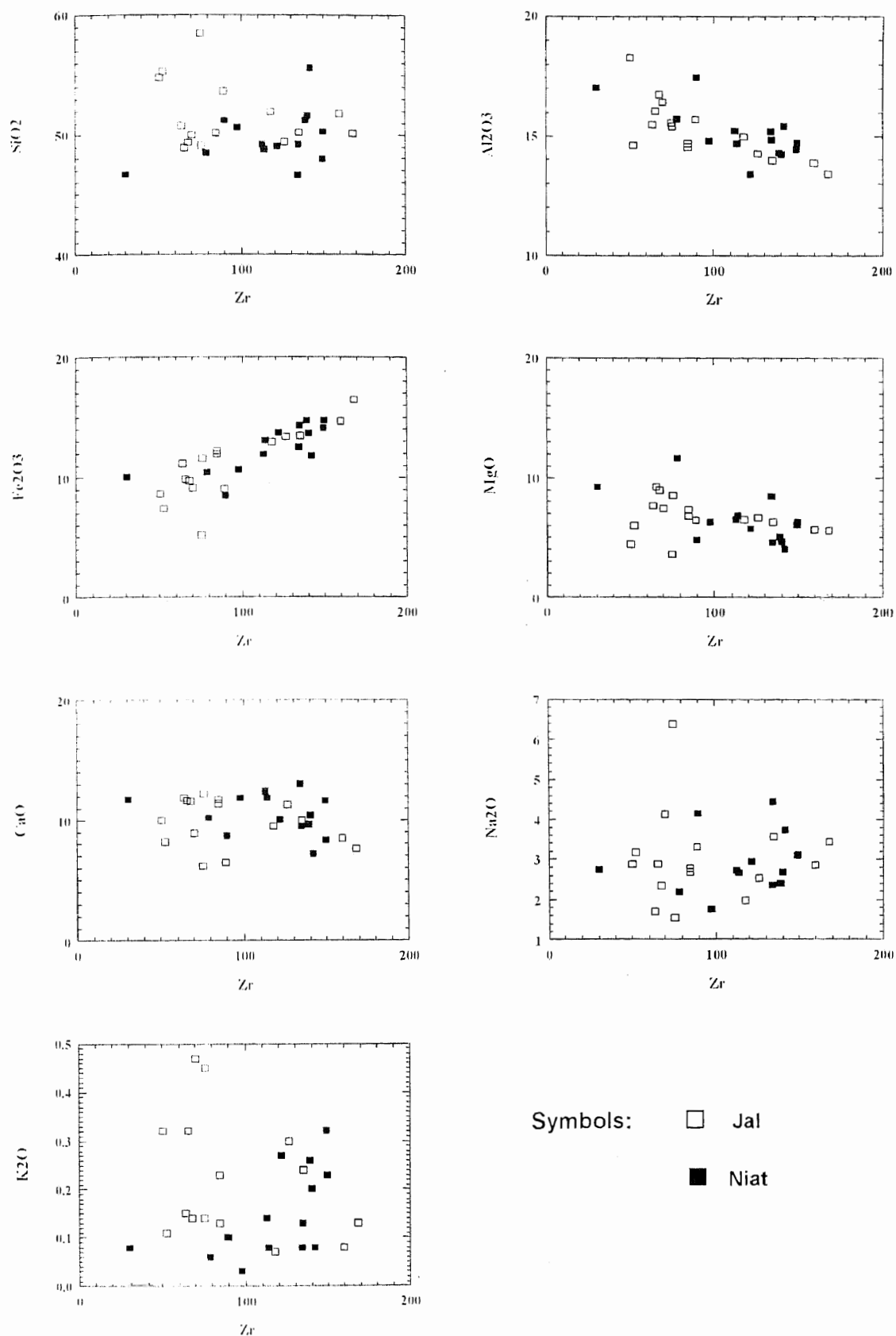
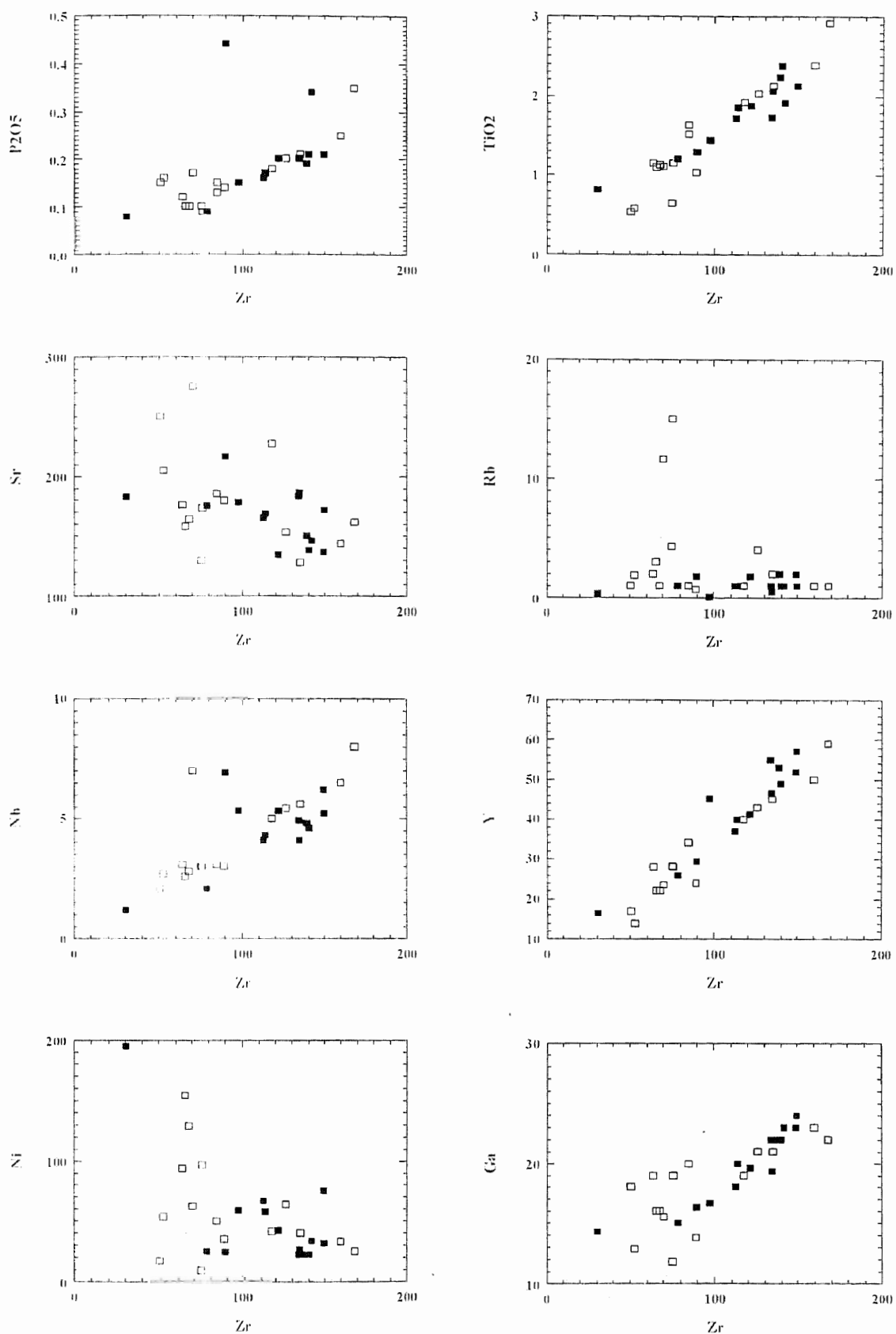


Figure 4.2. Binary plots of major oxides and trace elements versus Zr.

Figure 4.2 continued



below the detection limit of XRF or only marginally above. It is interesting to note that the major elements, like MgO , CaO , Fe_2O_3 , Al_2O_3 and SiO_2 , also have coherent trends on these plots suggesting preservation of original concentrations. A further degree of check can be applied by comparing the mutually compatible trace and major elements like Ti and Fe and, Sr and Ca. Like Ti, Fe_2O_3 also shows a positive correlation with the Zr, while CaO and Sr display a negative correlation with Zr. This suggests that not only the incompatible trace elements have retained their original magmatic concentrations in the analyzed rocks, major elements too have done so.

Figure 4.2 represents the binary plots of analyzed amphibolites. All the analyzed elements are plotted against Zr, except K, Rb, Th and Pb which have concentrations below the detection limit of XRF. There are, however, five samples which deviate from the main-stream trends in terms of several elements (e.g., A-78, A-109, A-112, A-133 and A-135). All samples show enrichment in Fe_2O_3 and TiO_2 with increase of Zr but these anomalous samples are enriched in these elements without increase of Zr. In case of MgO , all the samples show a decrease but it is reverse in the anomalous ones. In an attempt to check if this scatter is due to the effect of cumulus (phenocrysts) phases, mineral analyses of major constituent phases in basalts (e.g., olivine, plagioclase, clinopyroxene, orthopyroxene and amphibole) were plotted on the binary plots along with the whole-rock data (figures not given). None of the anomalous samples show any tendency of plotting towards or close to the lines joining these mineral phases, negating any role of cumulus phases in causing scatter of these samples. This leads to interpretation that these samples might have acted as open systems during metamorphic or hydrothermal alteration or, alternatively, modified chemically by mixing or contamination with associated magmas or rocks.

Therefore, these five samples are not included in evaluation and interpretation carried out later in this chapter.

Classification

The amphibolites of this study are classified as basalts (thirty samples) and basaltic andesites (four samples) on the SiO_2 - ($\text{Na}_2\text{O} + \text{K}_2\text{O}$) plot of Le Maitre et al. (1989) (Figure 4.3). One sample plots in the field of trachyandesite. Since there is a suspicion that total alkalis might have been remobilized during metamorphism, two additional classification schemes, i.e., De la Roche et al. (1980) and Jensen (1976), are used. The R1-R2 diagram of De la Roche et al. (1980) has certain advantages over the other classification schemes, like:

- (1) the entire major element chemistry of the rock is used in the classification;
- (2) the scheme is sufficiently general to apply to all types of igneous rocks;
- (3) mineral compositions can also be plotted on the diagram, allowing a broad comparison between modal and chemical data; and
- (4) the degree of silica saturation and changing feldspar compositions can be shown.

A majority of the studied samples plot in the field of basalt, but six samples fall in the field of andesite-basalt, and two in andesite field (Figure 4.4). The Jensen cation plot supports the above classification of the studied amphibolites. Three samples plot in the field of andesite and the rest classify as basalt. The Jensen cation plot is a classification scheme for subalkaline volcanic rocks and it can be used successfully with metamorphosed volcanic rocks which have suffered mild metasomatic loss of alkalis.

Tholeiitic Nature

The Jal-Niat Amphibolites plot in the field of tholeiites in the diagram of Irvine and Barager (1971) but the variation is limited which hides the iron-

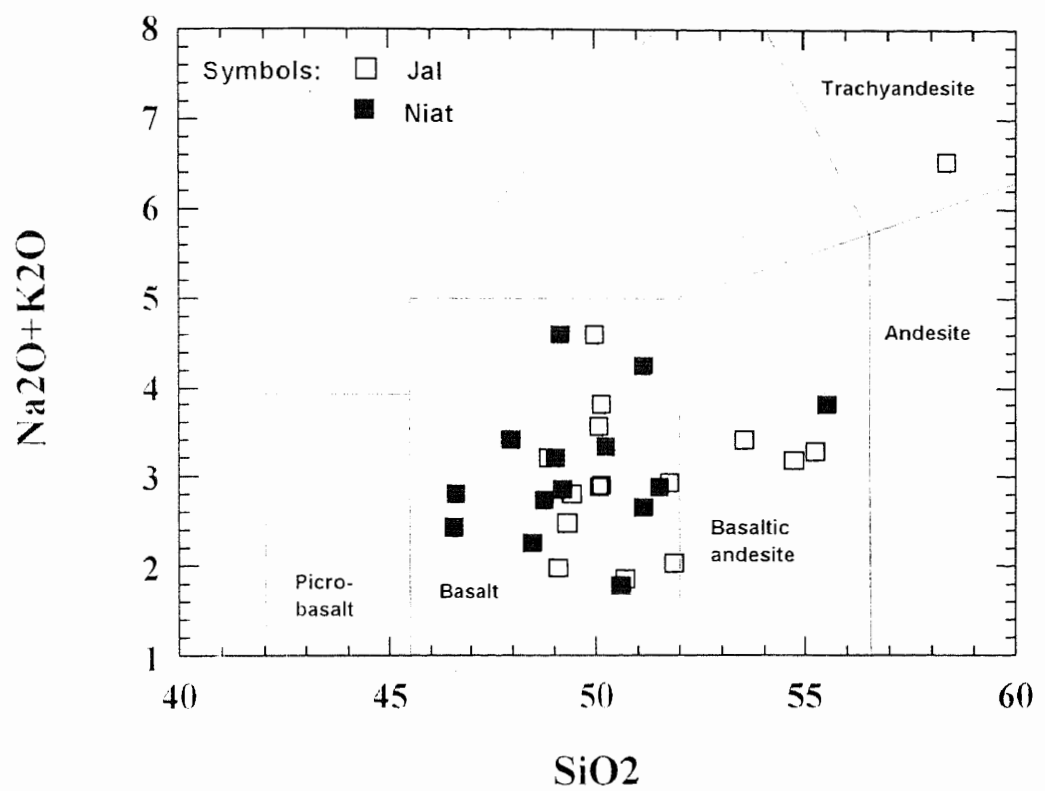


Figure 4.3. The chemical classification and nomenclature of the studied rocks using the total alkalis versus SiO_2 (TAS) plot (after Le Maitre et al., 1989)

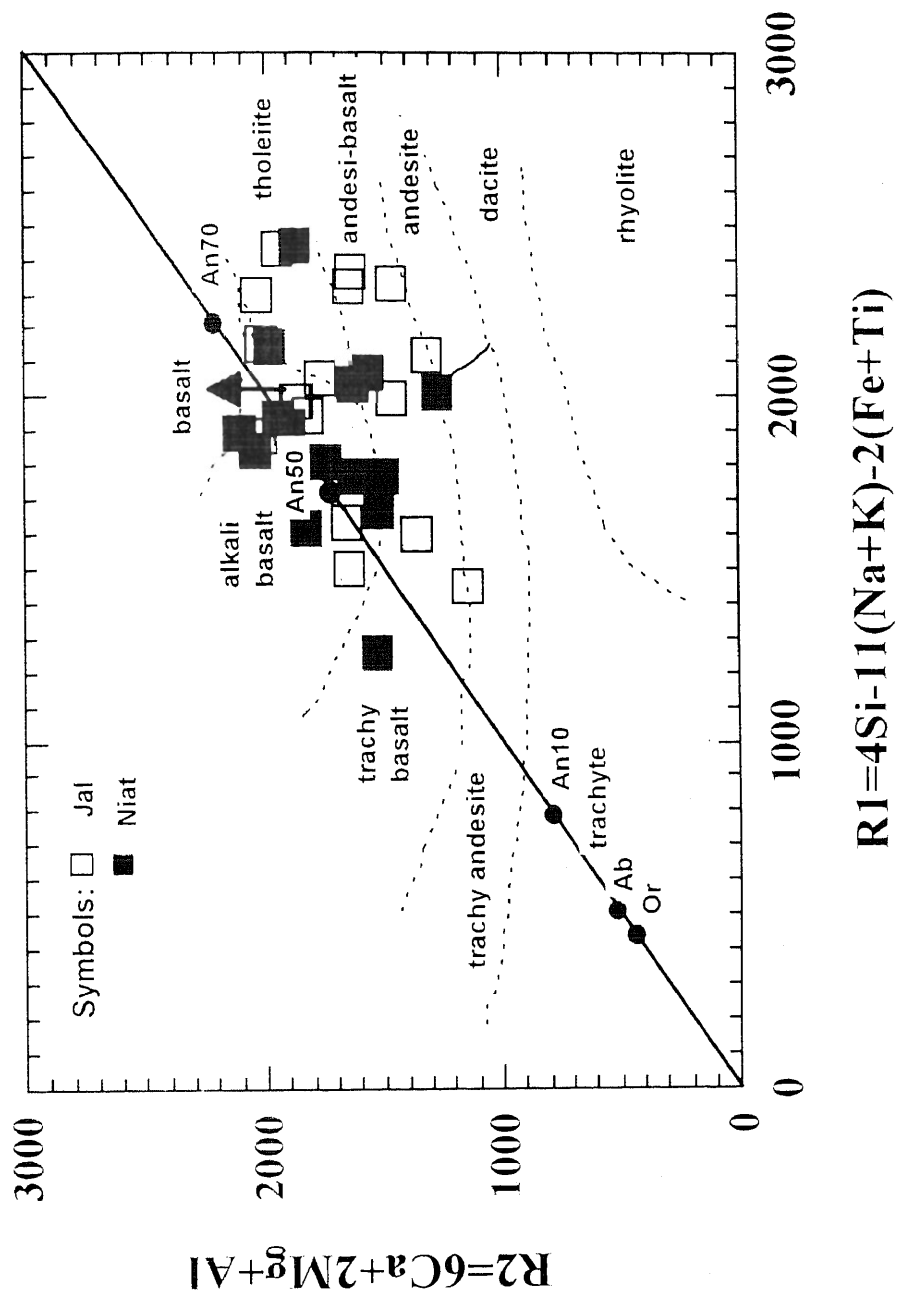


Figure 4.4. The classification of studied rocks using the parameters R1 and R2 (after de la Roche et al., 1980), calculated from millication proportions. $R1 = 4Si-11(Na+K)-2(Fe+Ti)$; and $R2 = 6Ca+2Mg+Al$.

enrichment trend (Figure 4.5). Other binary plots, e.g., %An- Al_2O_3 and SiO_2 -FeO/MgO (Irvine and Barager, 1971 and Miyashiro, 1974, respectively) support the tholeiitic nature of the rocks (Figure 4.6 and 4.7). The tholeiitic character of the group becomes readily apparent when plotted on a bivariate plot involving a fractionation index such as Zr (Figure 4.2). On these plots Fe_2O_3 shows a distinct negative correlation against Zr. A mirror-image relationship is portrayed by TiO_2 against Zr. These relations suggest a clear tholeiitic character for the Jal-Niat amphibolites.

Fractionation Assemblage

Metamorphosed rocks do not retain intact magmatic mineralogy and textures, inhibiting interpretation regarding the fractionating assemblages and order of crystallization of minerals. In such cases, variation diagrams provide an alternative tool for such an assessment. Olivine is commonly an early crystallizing mineral in basalts. Depletion of MgO with advancing fractionation (using Zr as a fractionation index; Figure 4.2), is indicative of early crystallization of olivine and for the pyroxene in the studied Jal-Niat rocks. Fe_2O_3 and TiO_2 show a good mutual correlation and an enrichment with increasing proportions of Zr, suggesting a lack of crystallization of iron-rich minerals such as magnetite and ilmenite (Figure 4.2). CaO shows depletion with advancing fractionation. A similar trend is exhibited by Al_2O_3 . This points out the possibility that plagioclase and perhaps clinopyroxene too started crystallizing in the early stages of fractionation. Iron enrichment trend together with early crystallization of plagioclase in the fractionation history are typical features of MORB tholeiites (Wilson, 1989).

Trace-element Variations

The Jal-Niat Amphibolites are generally poor in large-ion lithophile elements like Rb, Pb, Th and K. The first three elements are lower than even the detection

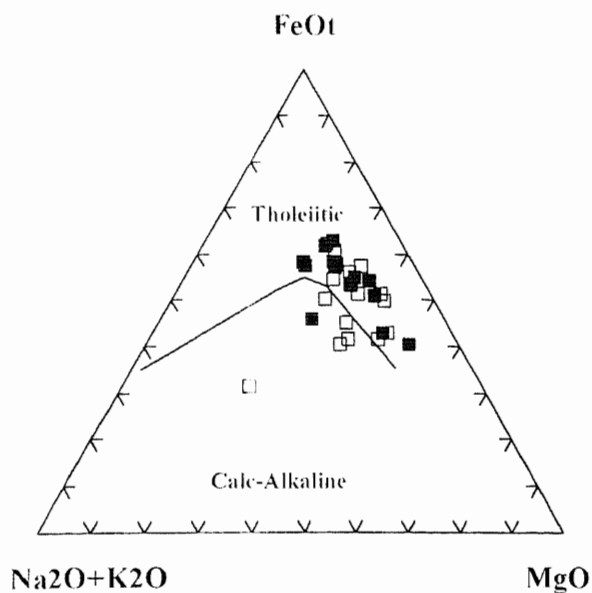


Figure 4.5. AFM diagram with boundry between tholeiite and calc-alkaline rocks after Irvine and Barager 1971, most of the Jal (□) and Niat (■) rocks plot in tholeiite field.

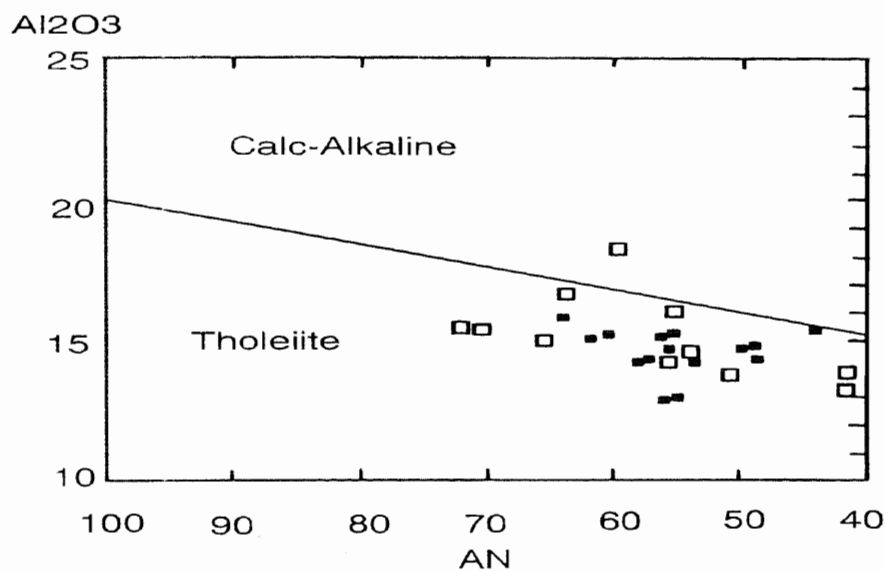


Figure 4.6. Bivariate plot of %AN versus Al₂O₃ showing the tholeiitic nature (after Irvine and Barager, 1971).

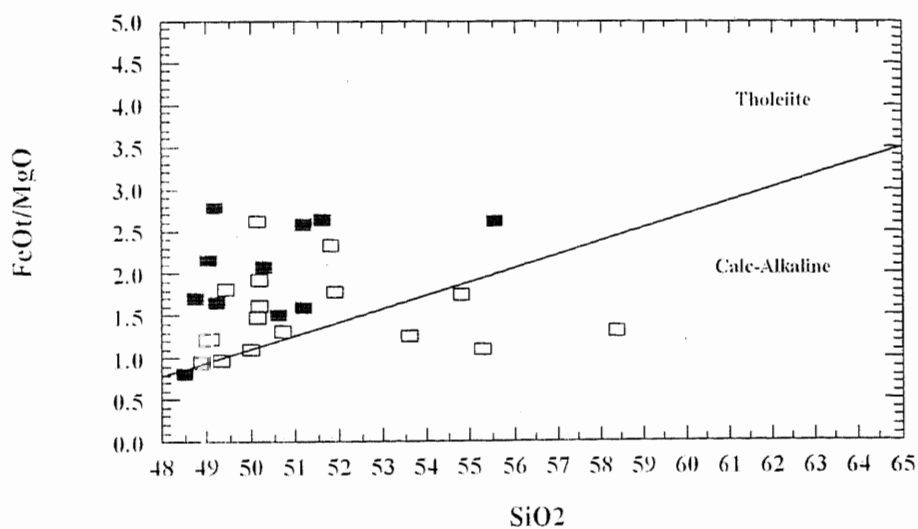


Figure 4.7. Bivariate plot of SiO₂ versus FeO/MgO showing the tholeiitic nature (after Miyashiro, 1974).

limit of the XRF used for the analysis. Sr concentration is controlled by the fractionation of plagioclase, in the initial stages, and by both plagioclase and clinopyroxene, in the later stages. This is shown by its inversely proportional relationship against Zr (Figure 4.2). Amongst the high-field strength elements (HFSE) Ti concentration is controlled by a lack of crystallization of a Ti phase in tholeiites of the studied suite. Other HFSE like Zr, Y, and P are truly incompatible and suitable for use in petrogenesis of the studied Jal-Niat rocks. Their concentrations are about ten times higher than those in the chondrites.

Ferromagnesian Elements

Crystal-liquid distribution coefficient data indicate that Ni and Co will partition into olivine during partial melting and fractional crystallization processes, while Sr, Cr and V will enter clinopyroxene. Thus a knowledge about the amounts of these elements should be useful in studying petrogenetic processes. Ni abundances in MORB are strongly controlled by olivine fractionation. Ni ranges from >300 ppm in primitive glassy basalts to 25 ppm in highly evolved basalts and correlates well with MgO content. In the studied rocks Ni ranges from >150 to <10. This shows the middle character of the rocks, which is neither highly evolved nor primitive. When plotted against Zr, the elements like Ni, Co, Sr and Cr display decrease in concentration with increasing contents of Zr (Figure 4.2). This decrease with increasing Zr abundance implies that much of the chemical variation in these rocks may be attributed to crystal fractionation processes. Assuming a possible parental amphibolite with 60 ppm Zr, 150 ppm Ni, 60 ppm Co and 160 ppm Sr in studied suite, such amphibolites have low Zr with TiO₂ (1.10%) and Y (22 ppm) abundances. These rather depleted incompatible element characteristics are not due to cumulation effects, because, if significant olivine and /or pyroxene

accumulation had occurred then low abundances of Ni and Cr would be expected in these primary amphibolites.

Inter-element Ratios

Ratios between truly incompatible trace elements are of great significance in petrogenetic studies. They provide a tool to see through the effects of processes like fractional crystallization and partial melting, and reflect the composition of not only the parent melt but also that of the source (Weaver et al., 1981). The inter-element ratios of incompatible trace elements in the studied suite of amphibolites and the different tectonic environments are listed in Table 4.8 and graphically portrayed in terms of XY scatter plots (Figure 4.2). The element ratios K/Rb (i.e. 668 for Jal and 1027 for Niat) and Sr/Rb (i.e. 76 for Jal and 142 for Niat) are characteristically higher for these amphibolites like MORB. Zr abundances range from 20 to 203 ppm in these amphibolites, with an average of 94 and 112 ppm for Jal and Niat amphibolites respectively. Figure 4.2 shows good colinear trends between Zr and Ti, Y, and P, and the average ratios of Ti/Zr, Zr/Y and Zr/P₂O₅ for Jal-Nait Amphibolites are 99, 2.5 and 548 respectively, which are very close to those of N-MORB.

Trace-element Patterns as Spidergrams

Two types of trace element plots are used for the investigation of element mobility. Firstly, the MORB normalized multi-element diagram of Pearce (1983) was constructed to show the difference in behavior between elements which are mobile and those which are not. Brewer and Atkin (1989) found that this diagram successfully differentiates between the behaviour of mobile elements such as Sr, K, Rb and Ba, and the immobile elements Nb, Ce, P, Zr, Ti and Y during the greenschist facies metamorphism of basalt. A second approach is to use the enrichment-depletion diagram. This type of diagram can only be used when the

Table 4.8. Average composition of major and trace elements for all studied volcanic / amphibolite suites compared with various tectonic settings.

Samp.No	JAL	NIAT	SUM	BAB	N-MORB	P-MORB	IAT	BAT	OIT
SiO ₂	50.64	49.36	50.26	49.50	50.55	49.72	49.20	50.36	50.51
TiO ₂	1.56	1.99	0.68	0.80	1.27	1.00	0.52	1.46	2.63
Al ₂ O ₃	15.53	14.99	17.41	18.46	16.38	15.81	15.30	16.36	13.45
Fe ₂ O ₃	11.91	13.22	9.06	11.39	1.27	1.66		9.07	1.78
MgO	6.82	6.46	7.99	5.60	7.80	7.90	10.10	7.36	7.41
CaO	10.50	10.57	10.36	11.74	11.62	11.84	13.00	10.84	11.18
Na ₂ O	2.64	3.00	3.38	2.02	2.79	2.35	1.51	3.39	2.28
K ₂ O	0.20	0.14	0.66	0.08	0.07	0.25	0.17	0.43	0.49
P ₂ O ₅	0.16	0.22	0.17	0.18	0.12	0.14	0.06	0.20	0.28
Total	99.96	99.95	99.97	99.77					
Nb	3.92	5.44	2.70	0.77	2.33	8.33	0.70	8.00	17.00
Zr	94.00	112.00	36.60	8.69	74.00	73.00	22.00	130.00	115.00
Y	33.30	48.38	15.00	15.34	28.00	22.00	12.00	30.00	25.00
Sr	198.46	163.00	235.60	182.36	90.00	155.00	200.00	212.00	371.00
Rb	2.61	1.15	13.80	0.99	0.56	5.04	4.60	6.00	9.20
Th	2.00	2.00	2.00	0.74	0.12	0.60	0.25		1.64
Pb	2.00	2.00	2.00	1.53	0.30				5.00
Ga	19.53	21.84	16.00	16.43				15.00	
Zn	107.00	81.53	68.40	100.29				68.00	
Cu	99.92	34.23	54.40	62.14					
Co	55.61	55.38	53.00						
Ni	61.69	48.54	90.00	18.71	138.00	32.00		64.00	
Ti	9352.36	11930.25	4076.67	4796.08	7607.78	6007.09	3117.45	8752.85	15767.11
K	1660.32	1162.22	5479.06	675.99	597.72	2092.00	1411.27	3569.69	4067.78
P	698.30	960.17	741.95	791.83	510.63	624.11	261.86	872.88	1222.03
Mg	41132.10	38960.91	48188.49	33782.78	47042.58	47645.69	60914.11	44388.90	44690.45
Ti/Zr	99.49	106.52	111.38	551.91	102.81	82.29	141.70	67.33	137.11
Zr/Y	2.82	2.32	2.44	0.57	2.64	3.32	1.83	4.33	4.60
Zr/P ₂ O ₅	587.50	509.09	215.29	48.28	632.48	510.49	366.67	650.00	410.71

Source of data: N-Morb and P-Morb (Sun and McDonough, 1989); IAT (Sun, 1980); BAT (Saunders and Tarney, 1979) and OIT (Basaltic volcanism study project, 1981). The total is not 100% here, because some oxides are excluded.

composition of the unaltered rock is known. Due to the alteration and metamorphic effects on the rocks of the study area preference is given to the use of the multi-element diagrams.

Whereas XY scatter plots are very usefull for portraying ratios between two elements, the spidergrams provide an effective method of portraying mutual ratios between several elements at a time. A set of incompatible trace elements for each sample is normalized to a standard (commonly either an average chondrite, primordial mantle or MORB) and plotted in a specific order (Rollinson, 1993). It is the comparison of the shape of the pattern between various samples which determines their petrogenetic relationship.

Trace-element patterns for four samples from the studied suite of Jal-Niat amphibolites, covering the range from most primitive through intermediate to most evolved compositions, are presented in Figure (4.8). In the primitive composition (A-69, A-157), trace-element patterns show their low concentration from primordail mantle abundances. It is increasing successively through intermediate (A-93) and more evolved compositions (A-86) to most evolved sample (A-105) and reaching 20' primordial mantle. The overall patterns of truly incompatible trace elements (Zr, Y, P and Nb), implying inter-element ratios of the four samples plotted are identical, suggesting a close petrogenetic realtionship and a common source.

Conventional spidergrams (Pearce, 1983) include a greater number of trace elements including Rb, K, Sr and Ti which, though incompatible with respect to the mantle minerlogy, behave compatibly during fractional crystallization. The four selected samples, when plotted on such a spidergram (Figure 4.9) do not show matching shapes for the patterns. For instance, Ti is low in primitive compositions but shows higher concentrations in the evolved samples. This is probably a reflection of the iron-enrichment trend as deduced from the major-element

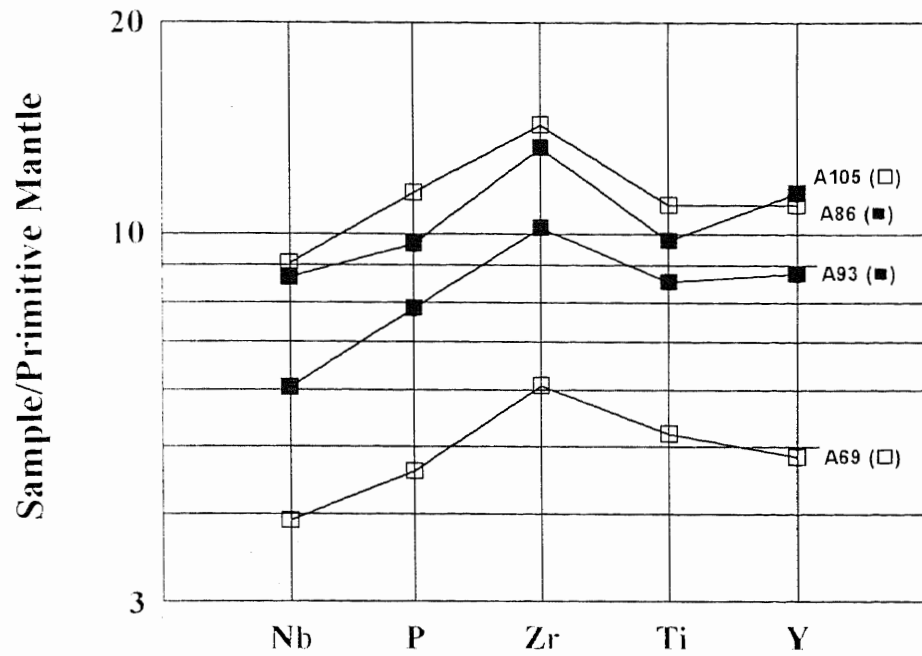


Figure 4.8: Spidergrams of selected truly incompatible trace elements (Nb, P, Zr, Ti and Y) for four samples of Jal-Niat amphibolites showing the range from primitive, through intermediate, to most evolved compositions.

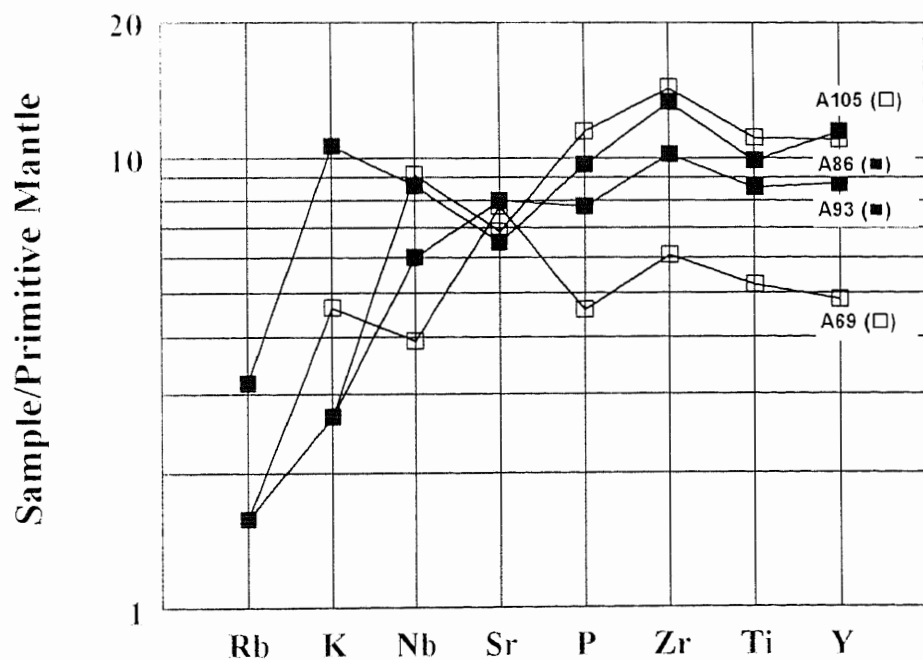


Figure 4.9. Conventional spidergram for the samples of Figure 4.8 showing variations.

Normalizing values of Primordial Mantle: Rb 0.635, K 250, Nb 0.713, Sr 21.1, P 95, Zr 11.2, Ti 1300 and Y 4.55 after Sun and McDonough, 1989.

variations. Sr shows opposite of the relationship shown by Ti. Primitive samples have high Sr while the evolved ones are marked with a negative Sr anomaly, reflecting the role of plagioclase fractionation. K and Rb variations, to some extent follow variations in Sr, but a combination of factors (low concentrations either below or only marginally above the detection limit of the analyzing instrument, and possibility of remobilization during metamorphism) cause discrepancies in their ratios relative to HFS elements. However, when the elements (Rb, K and Sr) with very low concentrations or suspected of remobilization are excluded, the four selected samples have mutually similar trace elements patterns suggesting cogenetic origin (Figure 4.8).

Estimation of Parent Magma

Two approaches are in practice for the estimation of parental magma compositions. If the chilled margins of the igneous bodies are available for sampling, parental magma compositions can directly be estimated. Chilled margins are commonly not available for a variety of reasons, such as lack of exposure, shearing and metamorphism. In such cases indirect methods are used for estimation of parent magma. If the igneous mineralogy is intact, composition of the most magnesian olivine can yield magnesium number of the melt with which it was in equilibrium during crystallization. Alternatively, rocks with most primitive composition are evaluated for their parental characters.

The studied amphibolites neither retain the chilled margins nor their igneous mineralogy is intact. The most primitive rocks of the analyzed Jal-Niat suite (selected on the basis of high Mg number, high Ni and low concentrations of incompatible trace elements) are listed in (Table 4.9) and compared with primitive MORB compositions. Initially, these selected samples (A-69, A-109 and A-157) show similarity with N-MORB. The MgO versus Zr plot (Figure 4.2) shows the

Table 4.9. Major and trace element composition of primitive samples from Jal-Niat suite are compared with various tectonic settings.

Sample Nos.	A-69	A-109	A-157	N-MORB	P-MORB	IAT	BAT	OIT
SiO ₂	49.33	46.71	48.90	50.55	49.72	49.20	50.36	50.51
TiO ₂	1.13	1.74	1.10	1.27	1.00	0.52	1.46	2.63
Al ₂ O ₃	16.74	15.11	16.06	16.38	15.81	15.30	16.36	13.45
Fe ₂ O ₃	9.65	12.55	9.83	1.27	1.66		9.07	1.78
MgO	9.00	8.38	9.24	7.80	7.90	10.10	7.36	7.41
CaO	11.57	12.98	11.58	11.62	11.84	13.00	10.84	11.18
Na ₂ O	2.34	2.25	2.88	2.79	2.35	1.51	3.39	2.28
K ₂ O	0.14	0.09	0.32	0.07	0.25	0.17	0.43	0.49
P ₂ O ₅	0.10	0.19	0.10	0.12	0.14	0.06	0.20	0.28
Total	100.00	100.00	100.01					
Nb	2.80	0.9	2.60	2.33	8.33	0.70	8.00	17.00
Zr	68.00	25	66.00	74.00	73.00	22.00	130.00	115.00
Y	22.00	21	22.00	28.00	22.00	12.00	30.00	25.00
Sr	164.00	193	158.00	90.00	155.00	200.00	212.00	371.00
Rb	1.00	1	3.00	0.56	5.04	4.60	6.00	9.20
Th	2.00	2	2.00	0.12	0.60	0.25		1.64
Pb	2.00	2	2.00	0.30				5.00
Ga	16.00	17	16.00				15.00	
Zn	64.00	63	68.00				68.00	
Cu	5.00	13	2.00					
Co	57.00	58	61.00					
Ni	129.00	136	154.00	138.00	32.00		64.00	
Ti	6774.46	10431	6594.61	7607.78	6007.09	3117.45	8752.85	15767.11
K	1162.22	747	2656.51	597.72	2092.00	1411.27	3569.69	4067.78
P	436.44	829	436.44	510.63	624.11	261.86	872.88	1222.03
Mg	54279.90	50541	55727.36	47042.58	47645.69	60914.11	44388.90	44690.45

Source of data: N-Morb and P-Morb (Sun and McDonough, 1989); IAT (Sun, 1980); BAT (Saunders and Tarney, 1979) and OIT (Basaltic volcanism study project, 1981). The total is not 100% here, because some oxides are excluded.

entire range of this suite of rocks from the primitive three samples (A-69, A-109 and A-157), through intermediate (A-93, A-80 and A-86), to most evolved compositions (A-98, A-105 and A-133).

A cation normative $An/(An + Ab + Or)$ versus $Mg/(Mg + Fe_2O_3)$ diagram is also used to calculate the fractional crystallization (Figure 4.10). The crystallization of olivine, plagioclase and clinopyroxene from basaltic liquids near the primitive end will produce evolved basaltic liquids near the evolved end. The fields for basaltic glasses from the Mid-Cayman Rise spreading centre (Thompson et al., 1980) and data from O' Donnell and Presnall (1980) are shown with large arrow and with the slopes calculated for the liquid lines of descent. The primitive samples (A-69 and A-157) and the evolved samples (A-98 and A-105) plot along the trend of fractional crystallization. It is considered from above-mentioned diagrams that the magma which produced the Jal-Niat amphibolites was of MORB characters.

Tectonic Environment

The majority of mid-ocean ridge basalts are sub-alkaline and tholeiitic. They show characteristically low concentrations of incompatible elements, including Ti and P and LIL elements (K, Rb, Ba). Low K_2O contents appear to be a particularly useful discriminant in distinguishing MORB from basalts erupted in other tectonic settings (Pearce 1976). A majority of the studied samples have concentration of TiO_2 (1-3 wt%; mean 1.56 wt%JA; 1.99 wt%NA) and K_2O (mean 0.2 wt%JA; 0.14 wt%NA) similar to MORB. Floyd and Winchester (1975) and Winchester and Floyd (1976) proposed a series of diagrams based upon immobile high field strength (HFS) elements which discriminate between tholeiitic and alkali basalts. These are most useful in altered volcanic rocks and effectively discriminate between magma series. The rocks of Jal-Niat amphibolite group follow the tholeiitic trend (figures not given). Winchester and Floyd (1976) report that the Y/Nb ratio is constant

MgO/MgO+Fe₂O₃

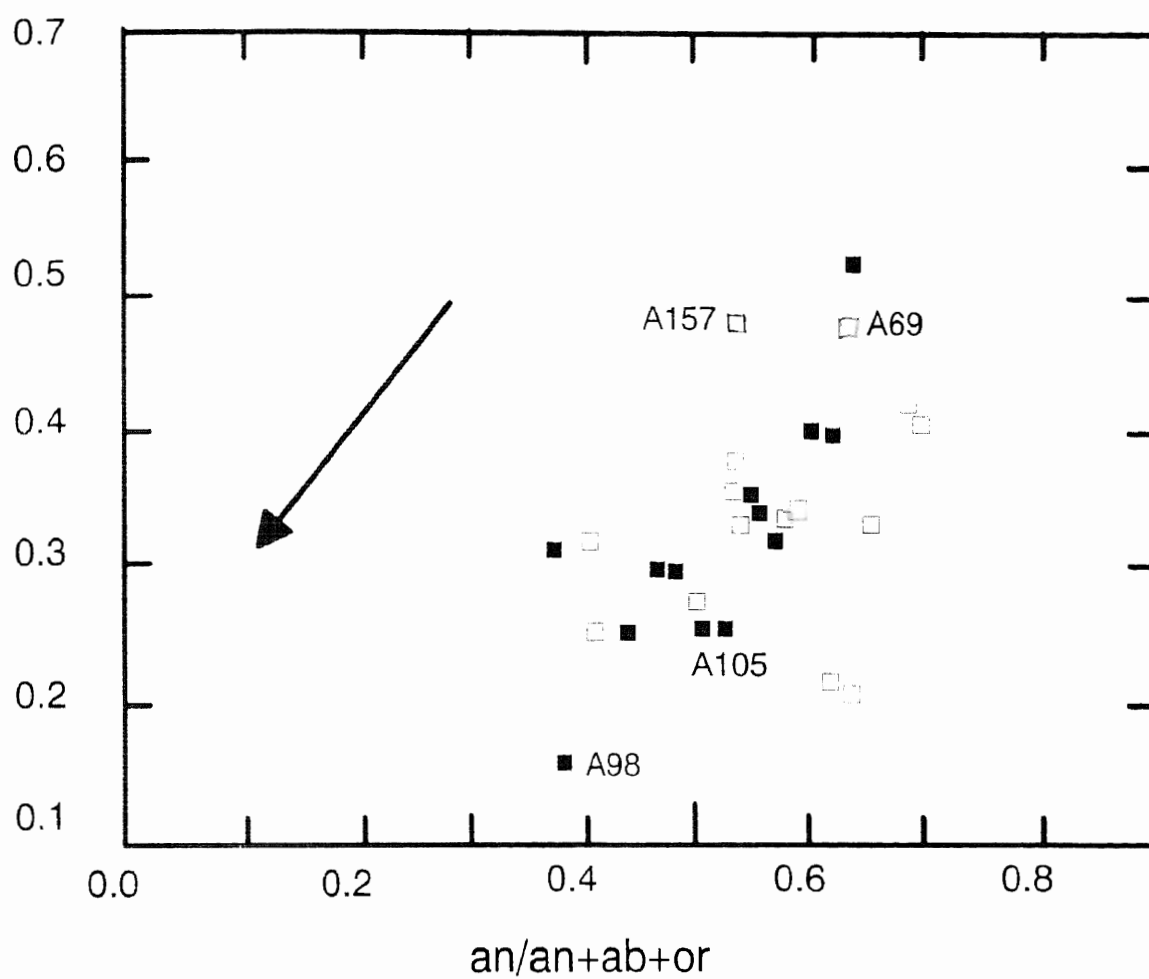


Figure 4.10. Binary plot of the Mg/(Mg+Fe₂O₃) versus An/(An+Ab+Or) showing the fractional crystallization path for the Jal-Niat amphibolites. Arrow showing perfect fractional crystallization path is after Ghiorso (1985).

during metamorphism and alteration. The average Y/Nb ratio for Jal and Niat is 8.4 and 8.9, respectively, which is close to N-MORB(12) and much higher than P-MORB(2.64).

The rocks show a closer correspondence to the MORB (mid-ocean ridge basalts) than the IAT (island arc tholeiites) or CAB (Calc alkali basalts). Various established discrimination diagrams were applied to the studied rocks to know their magmatic affinity and tectonic environment (Figure 4.11). In majority of cases the rocks plot in the field of ocean floor basalts. A plot of Zr/Y vs Zr (Pearce and Norry, 1979) discriminates effectively between basalts from ocean island arcs, MORB and within plate environments (Figure 4.11d). This plot can also be used to subdivide island-arc basalts into those belonging to oceanic arcs, where only oceanic crust is used in arc construction, and arcs developed at active continental margins. All the samples plot in the field of MORB. Meschede (1986) suggested that the immobile trace element Nb can be used to separate the different types of ocean-floor basalt. A triangular plot of Zr/4, 2 x Nb and Y displays the rocks of the study area in the field of N-type MORB (Figure 4.11a). From these discriminant diagrams, it is concluded that the Jal-Niat amphibolites of the study area are essentially tholeiitic in nature and developed in mid-ocean ridge setting.

Petrogenesis

Amphibolites and volcanic rocks cover a considerable thickness along MMT. Both the volcanic and plutonic features, including pillow structures, cumulate layering and textures have been noticed at several localities. The field relations and petrography of the Jal and Niat units have already been described in the preceding pages of this chapter. Now an attempt is made to discuss the probable genetic and tectonic configuration of the units. The rocks underwent greenschist to amphibolite facies metamorphism. They are fine-grained, foliated /schistose and

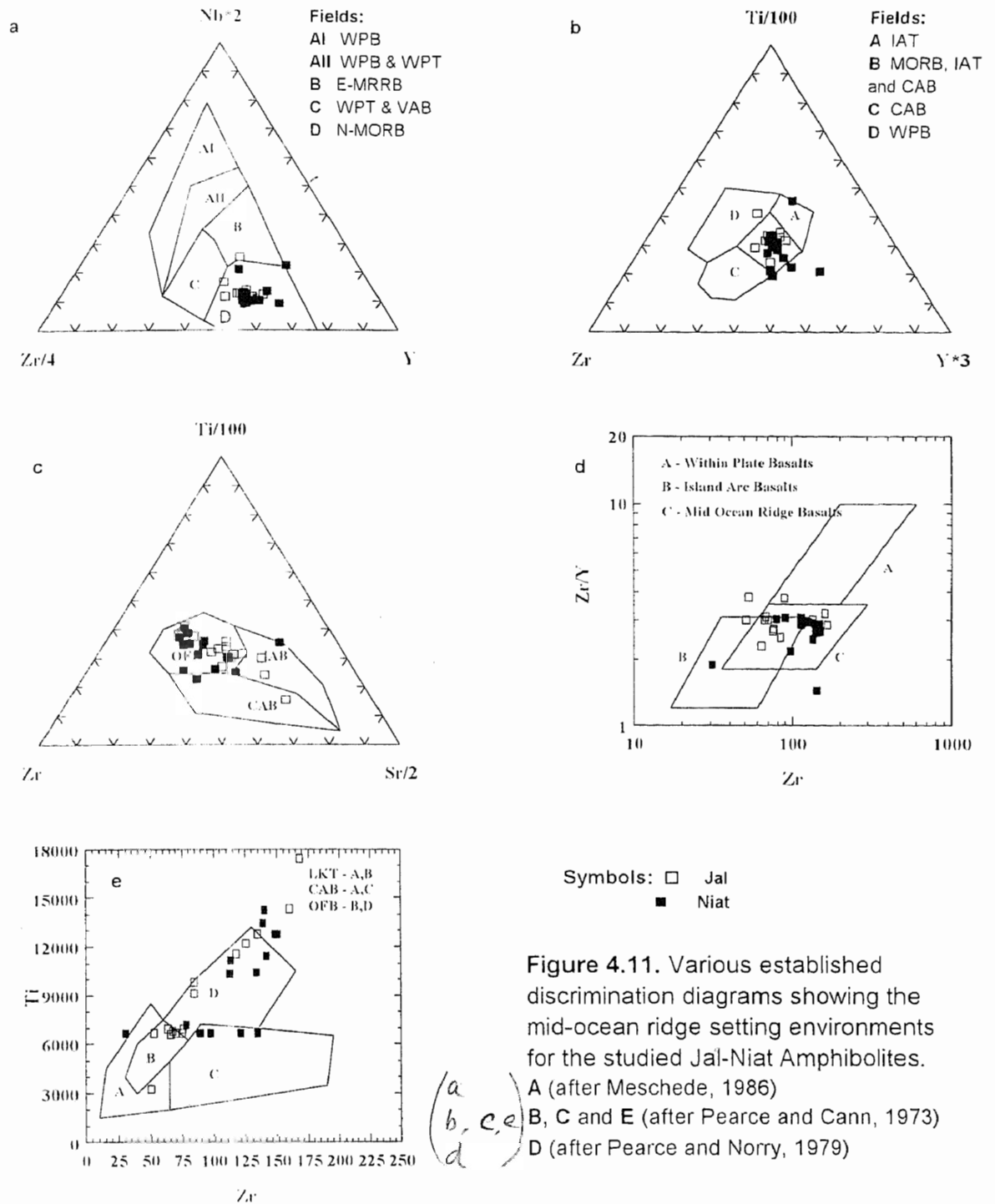
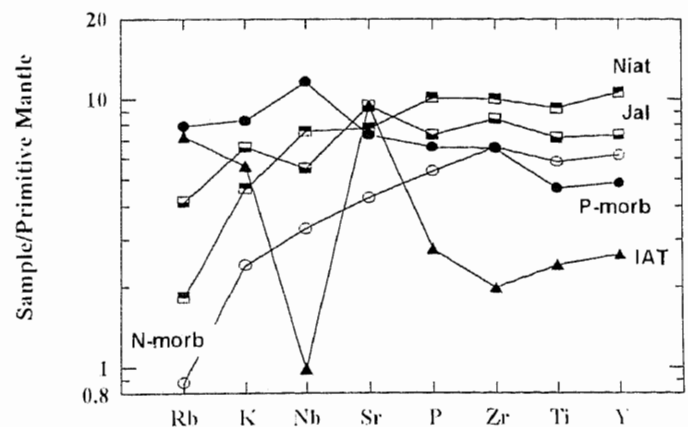


Figure 4.12. Primordial mantle normalized diagram showing the patterns of studied average Jal and Niat amphibolites compared with other tectonic settings.

Normalizing values of Primordial Mantle: Rb 0.635, K 250, Nb 0.713, Sr 21.1, P 95, Zr 11.2, Ti 1300 and Y 4.55 after Sun and McDonough, 1989.



contain hornblende, epidote, quartz, plagioclase, chlorite, biotite, magnetite, and sphene.

In the previous pages, a detailed account of the geochemical characteristics of the rocks has been presented. The major and trace element variations have been evaluated in order to deduce the fractionating mineral assemblage. Suggestions have been made regarding the relationships between the rocks in terms of fractional crystallization. The bulk-rock geochemical data were compared with the known affinities / environments. These pages are aimed at investigating the tectonic setting of the rocks in light of the geochemical characteristics presented in the previous pages.

The rocks display a broad range in chemical composition and are depleted in Nb and Zr. This depletion may be due to: (i)-crystallization of mafic phases (Pearce and Norry,1970), (ii)- retention or stability of these elements in minor mineral phases (e.g., Zr in zircon and Nb in rutile) at source, and (iii)-contamination by fluids enriched in LIL elements.

The chemistry of the rocks shows flat patterns and transitional characters from N-type MORB to humped patterns of P-type MORB. Zr/Nb ratios (mean= 24 and 21 for Jal and Niat, respectively) of the studied rocks also support their transitional behavior because N-MORB have high ratios (>30) whereas P-MORB have low ratios (<10). The patterns are unaffected by subduction (Pearce et al,1984). Since the shape of these patterns is little affected by differences in partial melting and fractional crystallization histories (Pearce,1983), the variations between the patterns are best explained in terms of heterogeneities in mantle source (Pearce et al.,1984). The geochemical patterns of rocks are similar to the tholeiites but enriched in Nb, Zr, Sr, Rb, Th and Pb elements. This enrichment may

possibly be due to contamination or mixing of a more depleted source by enriched mantle.

The enhanced LILE / HFS ratios in the rocks may be due to incorporation of slab derived material within the depleted mantle source (Hawkesworth et al., 1977; Pearce and Norry, 1979; Saunderson and Tarney, 1979, 1991; Green, 1982; Wyllie, 1982, 1984; Arculus and Powell, 1986; Wilson, 1989). This feature results in selective enrichment in certain elements (Rb, Ba, K, Sr, +Ce+Sm+P) and a relative lack of enrichment in others (Nb, Zr, Ti, Y) (Pearce et al., 1984). Table (4.8) shows selected trace element ratios of the studied rocks compared with the mid ocean ridge basalt (MORB), island arc tholeiites (IAT), and oceanic island tholeiites (OIT). The average concentration of these selected trace elements shows flat patterns with slight increase in slope pattern towards HFS elements and compared with different tectonic environments (Figure 4.12). The studied rocks show their resemblance with the N type MORB. The enrichment in HFS elements like MORB indicating that these rocks are developed from a more heterogeneous and enriched mantle source.

Babusar Amphibolites

Eight selected samples from the Babusar amphibolites are used for the evaluation of the geochemical characteristics of these rocks. The data are presented in Table 4.10. All the samples have low TiO_2 (mean 0.8 wt%) and MgO (mean 5.6 wt%) compared to Jal-Niat amphibolites. All the trace elements also are depleted in these rocks as compared with Jal-Niat amphibolites, but the elements like Nb (0.7ppm), Y (15.3ppm), Zr (8.6 ppm) and Ni (18.7ppm) are particularly depleted.

Table 4.10. Major and trace element composition of Babusar Amphibolites.

Samp. No	BS-3	BS-7	BS-8	BS-9	BS-10	BS-11	BS-18	BS-19
SiO ₂	49.43	47.86	56.09	54.34	43.21	46.54	49.32	45.13
TiO ₂	1.25	0.86	0.85	0.63	0.72	1.00	0.79	0.68
Al ₂ O ₃	15.80	20.36	15.83	17.70	19.05	17.82	18.21	18.76
Fe ₂ O ₃	13.98	11.95	10.89	9.67	13.47	14.75	12.50	14.25
MgO	5.72	4.25	4.26	4.20	7.88	6.19	4.93	7.06
CaO	12.38	10.81	8.88	9.98	15.37	11.81	11.48	12.93
Na ₂ O	0.87	3.28	2.76	3.00	0.04	1.50	2.45	0.95
K ₂ O	0.21	0.12	0.15	0.18	0.02	0.04	0.04	0.01
MnO	0.24	0.26	0.19	0.19	0.23	0.28	0.21	0.22
P ₂ O ₅	0.11	0.24	0.10	0.10	0.02	0.06	0.07	0.01
Total	99.99	99.99	100.00	99.99	100.01	99.99	100.00	100.00
Nb	0.70	1.70	1.00	0.50	0.60	0.20	0.90	0.20
Zr	15.40	25.10	8.70	11.90	1.00	5.00	5.50	3.60
Y	23.10	28.90	16.80	17.30	6.30	12.50	14.80	10.80
Sr	252.00	296.50	154.70	167.40	148.60	167.40	200.30	141.60
Rb	1.20	0.50	1.10	1.50	1.50	1.00	0.90	0.40
Th	0.40	0.20	-0.50	0.30	-0.10	0.10	-0.10	-0.50
Pb	4.20	2.10	1.70	2.40	1.10	1.50	1.00	0.90
Ga	17.90	19.00	14.50	15.40	14.80	17.20	18.00	15.80
Zn	115.30	110.10	92.40	85.00	88.80	126.40	100.00	99.50
Cu	96.50	17.00	38.80	35.30	49.70	103.40	123.20	67.50
Ni	21.80	6.30	14.00	16.60	36.40	17.90	16.60	23.00
Cr	28.60	4.70	34.70	36.20	82.30	41.70	36.80	88.40
V	498.10	148.70	299.70	247.10	464.50	414.10	395.80	439.00
Sc	51.40	26.10	39.10	41.50	60.10	59.90	49.00	65.10
Ba	29.50	31.50	55.30	67.60	17.60	21.60	28.50	16.90
La	0.60	2.90	1.50	1.30	-1.40	0.10	-0.20	-1.30
Ce	6.10	10.20	3.60	4.30	1.40	2.60	2.90	3.50
Nd	5.50	10.40	3.60	3.90	0.60	0.60	2.70	1.10

Classification

The amphibolites classify as basalts (five samples) and basaltic andesites (BS-8 and BS-9) on the SiO_2 –($\text{Na}_2\text{O}+\text{K}_2\text{O}$) plot of Le Maitre et al. (1989) (Figure 4.13). One sample (BS-10) plot in the field of microbasalt. On the classification scheme of De La Roche et al. (1980) the analyses range from olivine basalt through tholeiite to andesite basalt. One sample (BS-8) plots in the field of andesite (figure not given). The Jensen cation plot (Jensen, 1976) supports the above classification of the studied amphibolite rocks (Figure 4.14). Four samples BS7, 8, 9 and 18) plot in the field of andesite and the rest of the four samples show an affinity with high-Fe tholeiite basalt. On AFM diagram of Irvine and Barager (1971), the amphibolites classify as tholeiites but they display an alkali-enrichment trend (Figure 4.15). The K_2O content in all the analyses is low (< 0.2 wt%) and the rocks classify on this basis as low-K tholeiites (compare Le Maitre et al., 1989).

Fractionation Assemblage

To evaluate the crystallization sequence of Babusar amphibolites, variation diagrams (using SiO_2 as a fractionation index; Figure 4.16) are plotted. Depletion of MgO and Ni with advancing fractionation in the studied rocks is indicative of early crystallization of olivine. The depletion of these two elements together with that of Cr, increasing degree of fractionation suggests the igneous parentage of these rocks. The low TiO_2 and low Zr/TiO_2 ratios also confirm the igneous past of these amphibolites. The depletion of iron and CaO increasing fractionation warrants the crystallization of an iron oxide and clinopyroxene. Na_2O and Sr variation trend supports this sequence of fractionation. Na_2O , K_2O and P_2O_5 show an enrichment with increasing proportions of SiO_2 . Depletion in Al_2O_3 suggests plagioclase crystallization started early in the sequence. Sr is highly compatible with plagioclase and shows enrichment in early fractionation and at ~ 50 wt%, Sr

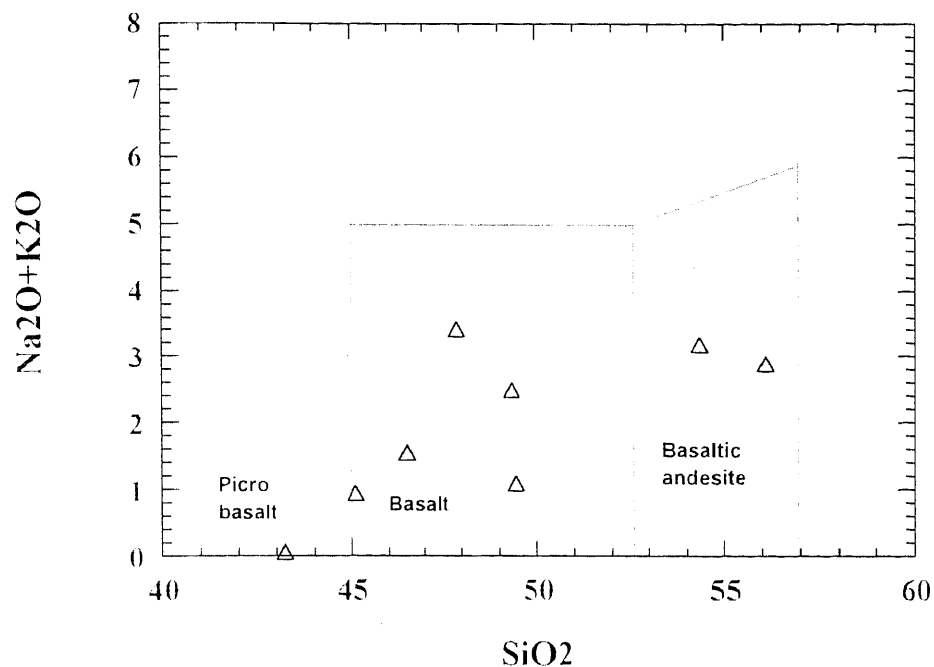


Figure 4.13. The chemical classification and nomenclature of the Babusar amphibolites using the total alkalies versus SiO_2 (TAS) plot (after Le Maitre et al., 1989).

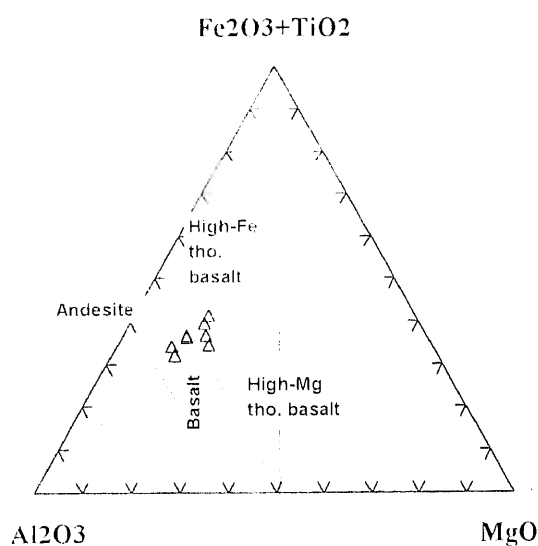


Figure 4.14. Ternary plot of classification according to the cation percentages of Al, (Fe+Ti) and Mg. It also showing the tholeiite and calc-alkaline fields (after Jensen, 1976).

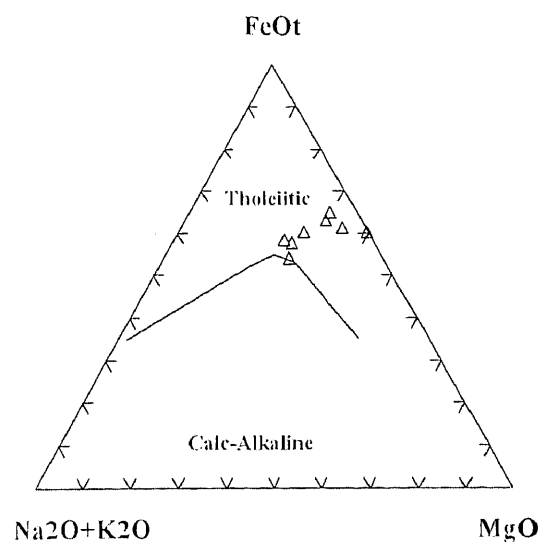


Figure 4.15. An AFM diagram showing the tholeiitic trend of studied rocks (after Irvine and Barager, 1971).

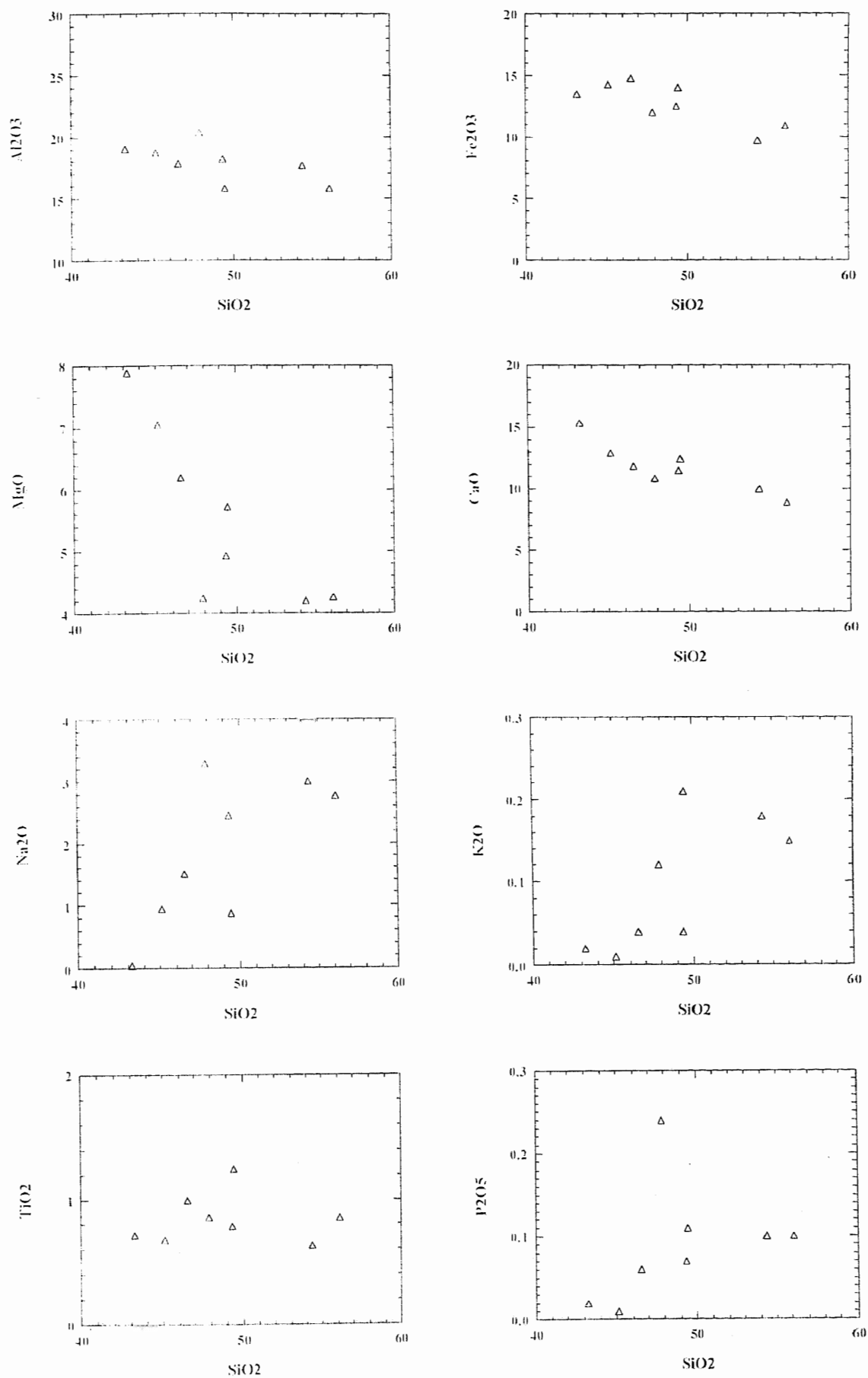


Figure 4.16. Binary plots of major oxides versus SiO₂.

trend becomes negative (Figure 4.17). It is likely that the plagioclase crystallizing earlier was calcic to accomodate much Sr, but at ~50 wt% of SiO₂, it probably changed its composition. TiO₂ shows some enrichment in early fractionation and then, because of probable crystallization of ilmanite, shows a decline. On the basis of major and trace element variations it is considered that olivine, clinopyroxene and iron oxide were the earliest crystallizing minerals and joined subsequently by plagioclase. This sequence of crystallizing minerals is mainly responsible for the compositional diversity in the Babusar amphibolites. The crystallization of plagioclase after clinopyroxene in the crystallizing sequence is a characteristic of subduction-related settings than that of mid-ocean ridges (Perfit et al., 1980).

Trace-element Variations

The Babusar amphibolites are generally depleted in large-ion lithophile elements like Rb, Pb, Th and K. The contents of these elements show an increase with fractionation. Amongst the high-field strength elements (HFSE) Ti concentration is controlled by tholeiitic trend of the studied suite. The amounts of Zr and Y are about eight times higher than those in the chondrites. In some samples the Zr concentration is equal or less than chondrites.

Ferromagnesian Elements

Ni ranges from 6 ppm to 36 ppm and Cr from 5 ppm to 88 ppm in the studied rocks. When plotted against SiO₂, the elements like Ni, V, Sc and Cr display decrease in concentration with increasing contents of SiO₂ (Figure 4.17). Decrease in Ni with increasing SiO₂ may be attributed to olivine fractionation and that in Cr to clinopyroxene and Cr-spinel separation.

Trace-element Patterns as Spidergrams

The Babusar amphibolites have highly spiked trace element pattern characterized by positive peaks for Ba, K, Sr, Ti, and negative anomalies for Rb,

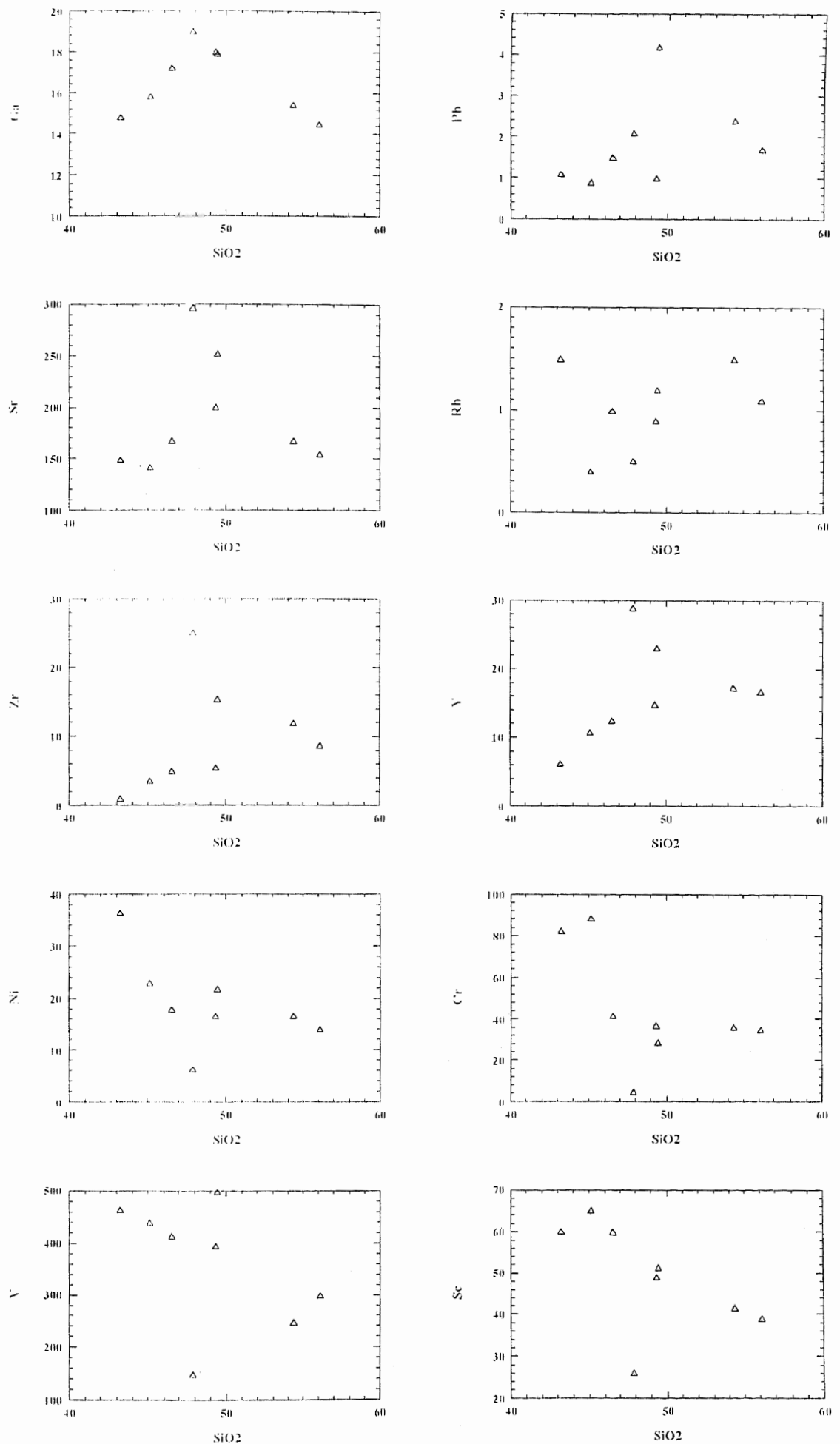


Figure 4.17. Binary plots of trace elements versus SiO₂ for Babusar amphibolites.

Nb and Zr. The patterns have a peculiar shape which is resembling the alphabet "W" (Figure 4.18). These patterns are different from that of the ocean-floor tholeiites and are matching with the island arc tholeiites (Figure 4.18h). The peaks and troughs of arc tholeiites are, in general, corresponding with the amphibolites of this group.

Tectonic Environment

The Babusar amphibolites are tholeiitic and are depleted in large ion lithophile (LIL) elements which is a characteristic feature of tholeiitic rocks from mid-ocean ridge and subduction-related environments (island arcs and Andean-type continental margins). Tholeiitic basalts can occur in all the major tectonic settings of magma generation. The depleted contents of LIL elements in the Babusar amphibolites clearly indicate their affinity with within-plate oceanic or continental settings. The Jal-Niat amphibolites of the studied area and the surrounding rocks are characterized by their affinity with oceanic environments, so the Babusar amphibolites are may be related to either oceanic- or island arc/continental margin environments. The tholeiite series is considered to be the earliest and in some cases dominating phase of magmatism in island arc /continental margin environments. The island arc basalts are characterized by selective enrichment of elements of low ionic potential (Sr, K, Rb, and Th) and low abundances of elements of high ionic potential (Nb, P, Zr, Ti, and Y) compared to N-type MORB (Figure 4.19). The enrichment in low ionic potential elements has been attributed to metasomatism of the mantle source of arc basalts by fluids released from the subducted slab. In contrast, the relative depletion in high ionic potential elements has been variably attributed to higher degrees of partial melting and to the stability of residual mantle phases (Pearce, 1982). N-Morb normalized values of the Babusar amphibolites and oceanic island arc basalts clearly show enrichment in

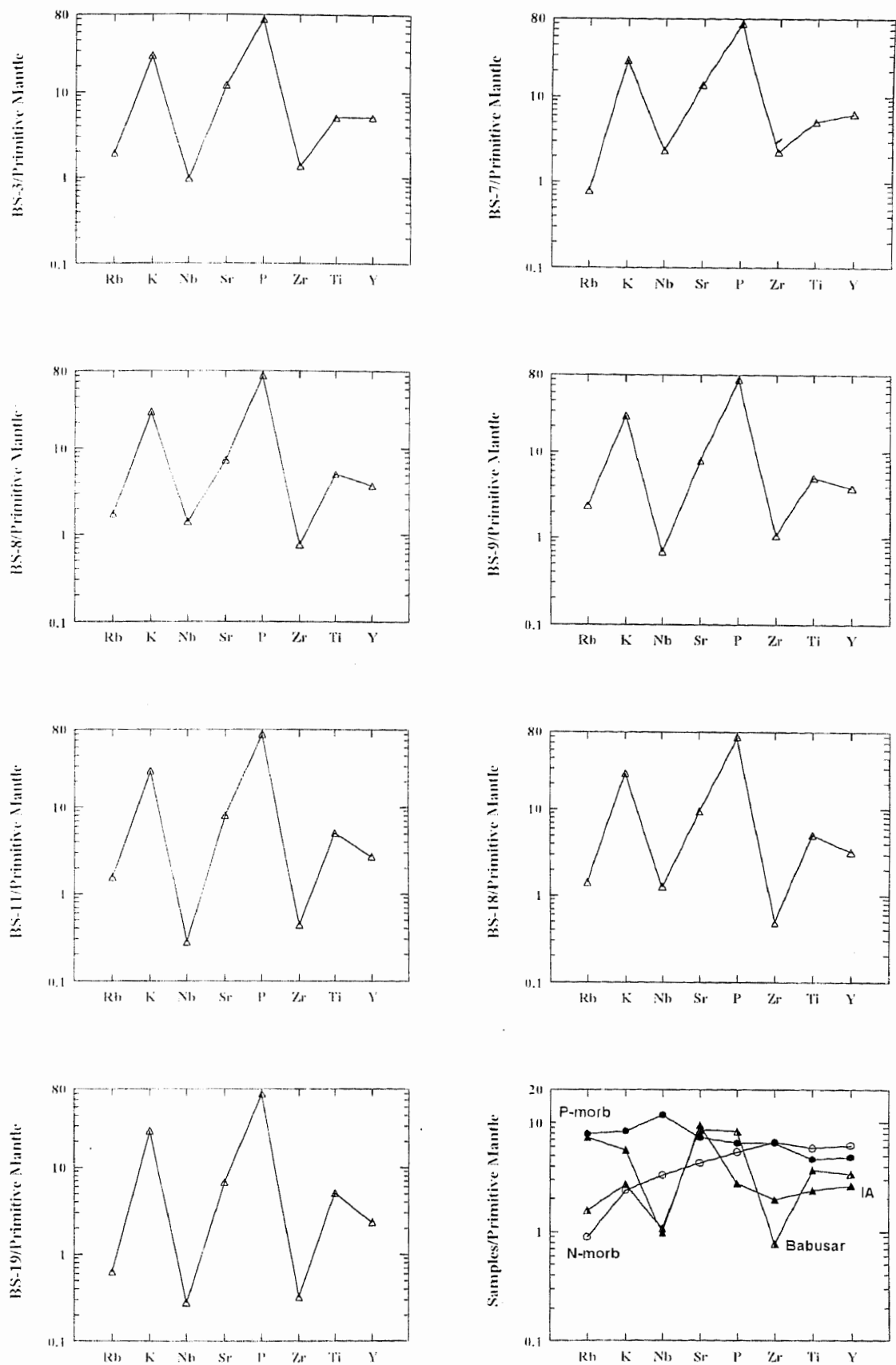


Figure 4.18. Primordial mantle normalized diagrams of the Babusar amphibolites showing the spiked trace element patterns and also compared with various tectonic settings.

Normalizing values of Primordial Mantle: Rb 0.635, K 250, Nb 0.713, Sr 21.1, P 95, Zr 11.2, Ti 1300 and Y 4.55 after Sun and McDonough, 1989.

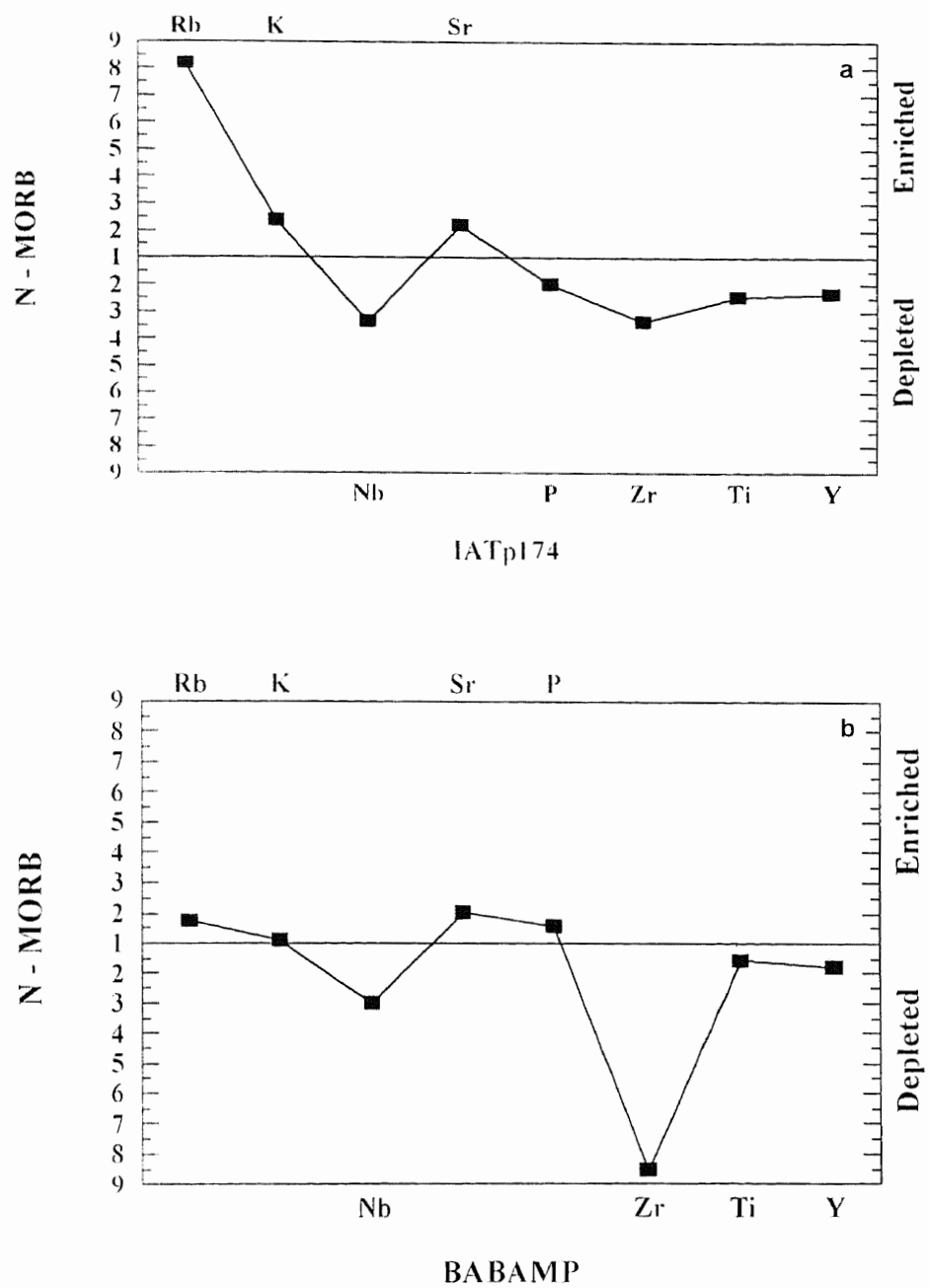


Figure 4.19. Diagram showing enrichment of low ionic potential elements (Sr, K, P and Rb) and depletion of high ionic potential elements (Nb, Zr, Ti and Y) in island arc tholeiites and Babusar amphibolites as compared to N-type MORB.

elements of low ionic potential (Rb, K, Sr and P) and depletion in high ionic potential (Nb, Zr, Ti and Y) (Figure 4.19b). The only difference in the studied rocks and the island arc rocks is that the Babusar amphibolites are highly depleted in Zr and Rb, and show some enrichment in P, but the patterns are broadly the same.

The Babusar amphibolites show the distinctive spiked pattern with peaks at Th, Sr and Y, and negative anomalies for Rb, Nb and Zr. These patterns are a characteristic of all subduction related magmas, attesting to the involvement in their petrogenesis of subduction zone fluids enriched in Sr and Th. The peaks and troughs in the Babusar amphibolites show a general resemblance with the low-K island arc tholeiites.

Sumal Amphibolites

Classification

Major and trace element composition of five samples is presented in Table (4.11). According to the classification scheme of Le Maitre et al. (1989), based on SiO_2 vs $(\text{Na}_2\text{O}+\text{K}_2\text{O})$, four of the five samples from the Sumal amphibolites classify as basalts and one is basaltic trachy-andesite (Figure 4.20). The data are also plotted on other diagrams (e.g., Irvine and Barager, 1971 and Cox et al., 1979). In all these schemes the rocks classify as basalts. The Jensen cation plot (Jensen, 1976) supports the above classification of the studied rocks.(Figure 4.21).

On the total alkalis versus silica diagram of Le Maitre, (1989), all the samples plot in the field of subalkaline magma series except (A-117), which falls just at the border line of these two magma series. All rocks fall in the field of medium-K calc-alkaline series on the SiO_2 vs K_2O diagram (Figure 4.22), which differentiate them from the amphibolites of Niat and Jal with very low concentration of K_2O . The calc-alkaline character of these rocks is evident from their plot on AFM diagram (Figure 4.23) of Irvine and Barager(1971). The Al_2O_3 versus %An binary

Table 4.11. Major and trace element concentration of Sumal amphibolites.

Sample Nos.	A-117	A-119	A-121	A-122	A-125
SiO ₂	49.94	49.54	50.26	52.85	48.72
TiO ₂	0.88	0.69	0.47	0.60	0.75
Al ₂ O ₃	18.59	15.90	16.36	17.11	19.11
Fe ₂ O ₃	9.62	9.08	8.93	8.54	9.15
MgO	7.27	11.17	8.18	6.85	6.50
CaO	8.92	9.83	12.28	8.77	12.01
Na ₂ O	3.85	3.22	2.81	4.52	2.52
K ₂ O	0.71	0.38	0.57	0.59	1.06
P ₂ O ₅	0.22	0.19	0.12	0.17	0.17
Total	100.00	100.00	99.98	100.00	99.99
Nb	3.90	2.60	1.00	1.00	5.00
Zr	60.00	41.00	23.00	6.00	53.00
Y	21.00	18.00	13.00	8.00	18.00
Sr	155.00	233.00	268.00	265.00	257.00
Rb	18.00	9.00	10.00	5.00	27.00
Th	2.00	2.00	2.00	2.00	2.00
Pb	2.00	2.00	2.00	2.00	2.00
Ga	16.00	14.00	14.00	19.00	17.00
Zn	76.00	60.00	59.00	77.00	70.00
Cu	86.00	26.00	49.00	69.00	42.00
Co	56.00	54.00	53.00	52.00	51.00
Ni	90.00	207.00	56.00	14.00	83.00
Ti	5275.69	4136.62	2817.70	3597.06	4496.33
K	5894.14	3154.61	4731.91	4897.94	8799.70
P	960.17	829.24	523.73	741.95	741.95
Mg	43846.10	67367.39	49334.40	41313.04	39202.15

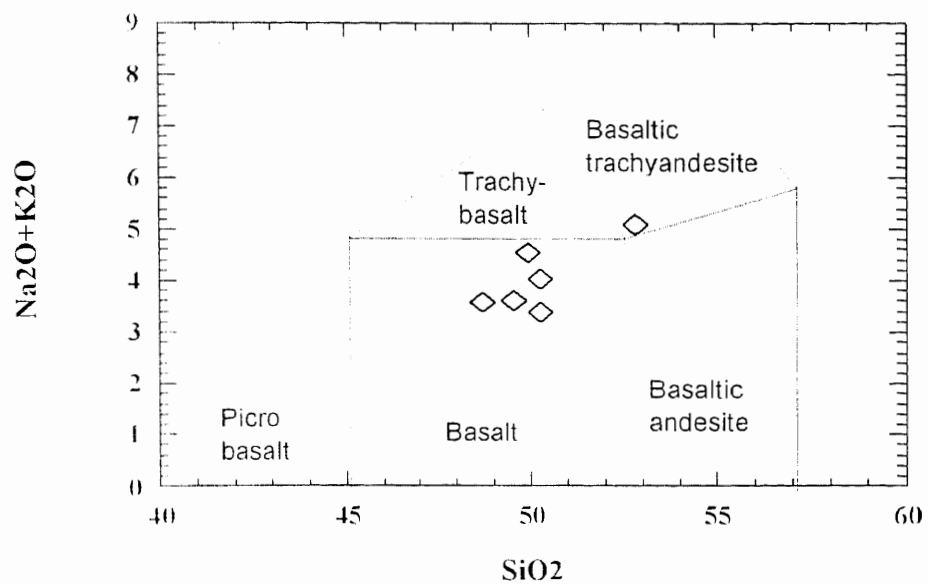


Figure 4.20. The chemical classification and nomenclature of the Sumal amphibolites using the total alkalis versus SiO₂ plot of Le Maitre et al. (1989).

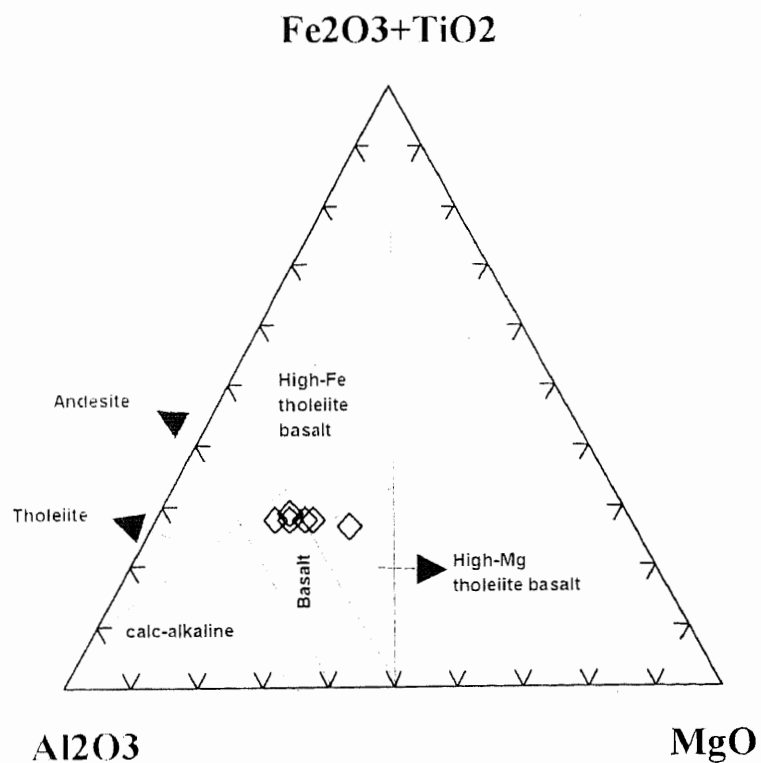


Figure 4.21. Classification of the Sumal amphibolites according to the cation percentages of Al, (Fe total + Ti) and Mg. It also shows the tholeiite and calc-alkaline fields (after Jensen, 1976).

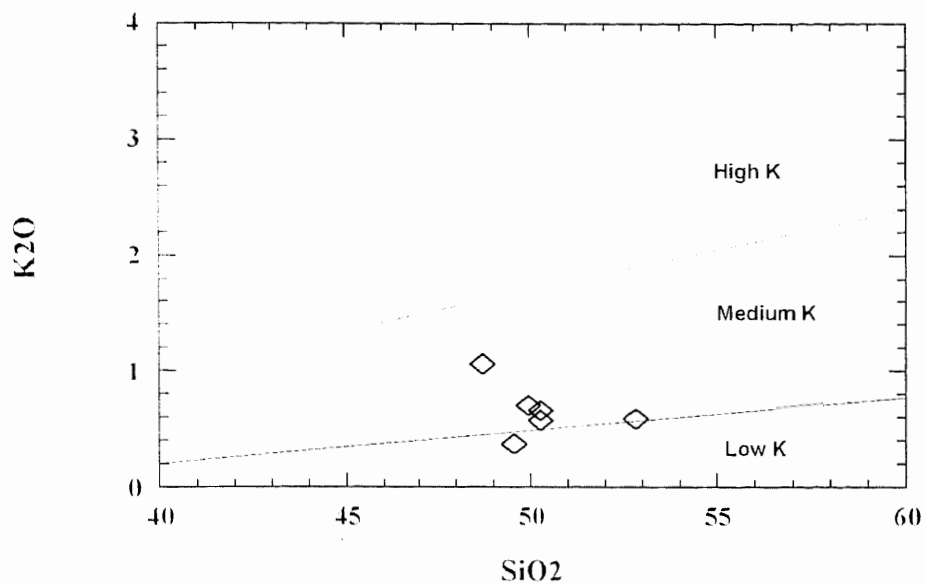


Figure 4.22. Subdivision of Sumal amphibolites on the K₂O versus silica diagram of Le Maitre et al. (1989).

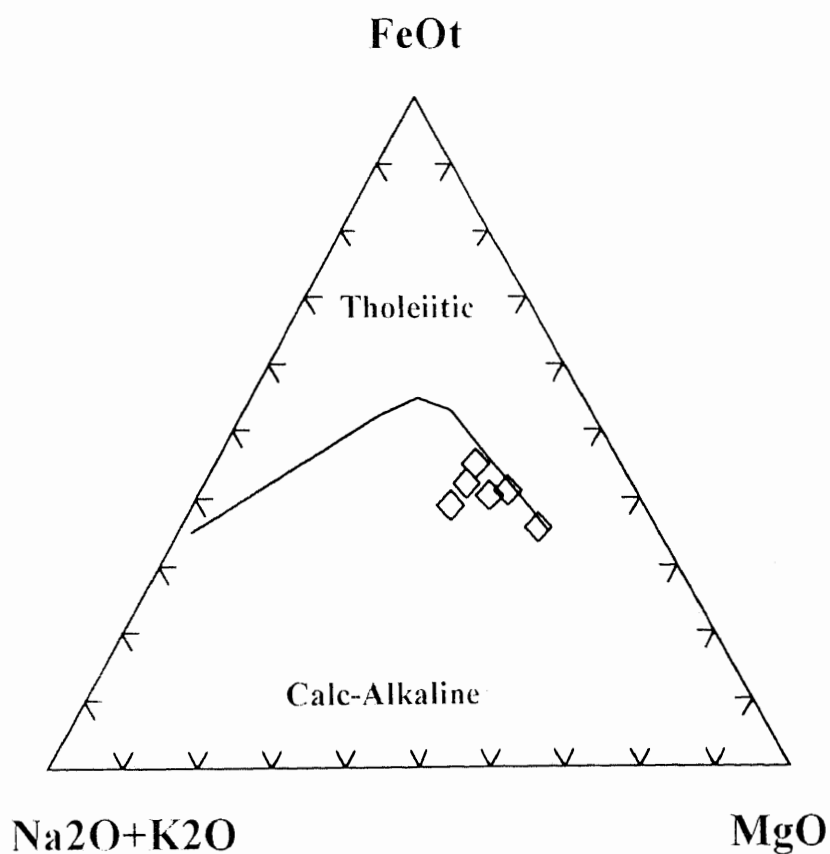


Figure 4.23. AFM diagram showing the calc-alkaline trend of the studied rocks (after Irvine and Barager, 1971).

plot (Irvine and Barager, 1971), also supports the calc-alkaline character of these rocks.

Major-element Variation Diagrams

Plot of the major elements using SiO_2 as abscissa show a considerable scatter. The volcanic rocks of this unit are enriched in Al_2O_3 and K_2O and depleted in TiO_2 and Fe_2O_3 as compared with the tholeiitic rocks of Babusar, Jal and Niat units. Table 4.8 shows the average composition of major and trace element of studied rocks compared to those from mid ocean ridge basalts (MORB) and island arc basalts (IAB). A similarity can be seen in the composition of the studied rocks of this unit and IAB. Only TiO_2 appears to be distinctive, being characteristically low in the rocks of this unit and in island arc basalts from the studied tholeiitic rocks and MORB.

Amongst the major elements e.g., TiO_2 , CaO , K_2O , and Fe_2O_3 show a consistent decrease, while Al_2O_3 shows slight decrease with increasing degree of fractionation. MgO shows enrichment upto ~50 wt%, and then showing slight decrease with increasing degree of fractionation. Na_2O shows enrichment with increasing SiO_2 . The depletion of Fe_2O_3 and TiO_2 indicate that iron-bearing minerals crystallized early in the history of fractionation. Decoupled relation of CaO and Al_2O_3 suggests role of clinopyroxene rather than plagioclase in the fractionation because CaO is much depleted than Al_2O_3 in these rocks. In general, it is considered that fractionation under reducing conditions suppresses the crystallization of magnetite, thus promoting iron enrichment in the early stages (tholeiitic trend). In contrast, under oxidising conditions magnetite crystallizes from the outset, rapidly depleting residual liquids in iron (calc-alkaline trend: Osborn, 1962; Miyashiro, 1974). The major element variations in the studied rocks support

crystallization under oxidising conditions and the calc-alkaline nature of the Sumal amphibolites as deduced earlier from the AFM and other diagrams.

Trace-element Variations

The distribution of some selected minor and trace elements (Ti, Zr, Y and Nb) can be used to classify the volcanic rocks. These trace elements have more or less similar concentration levels in the studied rocks. Trace element variations are shown on binary plots involving Zr as fractionation index (Figure 4.24). Nb and Y increase and Sr decreases with the increase of Zr. Sr concentration is controlled by the fractionation of plagioclase and clinopyroxene. These trends are similar with the tholeiitic rocks (Jal & Niat units) of the study area. The ferromagnesian elements (Ni and Co) show a positive correlation with Zr. A negative correlation of Sr with Zr implies that these elements are characterized by a bulk distribution coefficient $D > 1$ with respect to the fractionation assemblage involved. Ni and Co values reflect compatibility in early crystallizing minerals and these are presumed to be pyroxene and spinel.

When we compare the average concentration of these volcanic rocks with the tholeiitic volcanic rocks of Jal and Niat units, these are enriched in Sr, Rb and Ga and depleted in Nb, Zr, Y, and Ni (Table 4.5). Overall, these volcanic rocks are depleted in HFS elements and enriched in LIL elements. Low abundances of most incompatible elements are highly significant in terms of the source magma. It is reverse in the case of tholeiitic rocks of the study area.

Spiderdiagrams

The Sumal metavolcanic rocks display negative anomalies for Nb and positive for K. Spidergrams of these rocks do not show flat patterns like those of Jal-Niat Amphibolites; rather they display spikes with low magnitude. The rocks show a general enrichment trend in LIL elements compared to the HFS elements

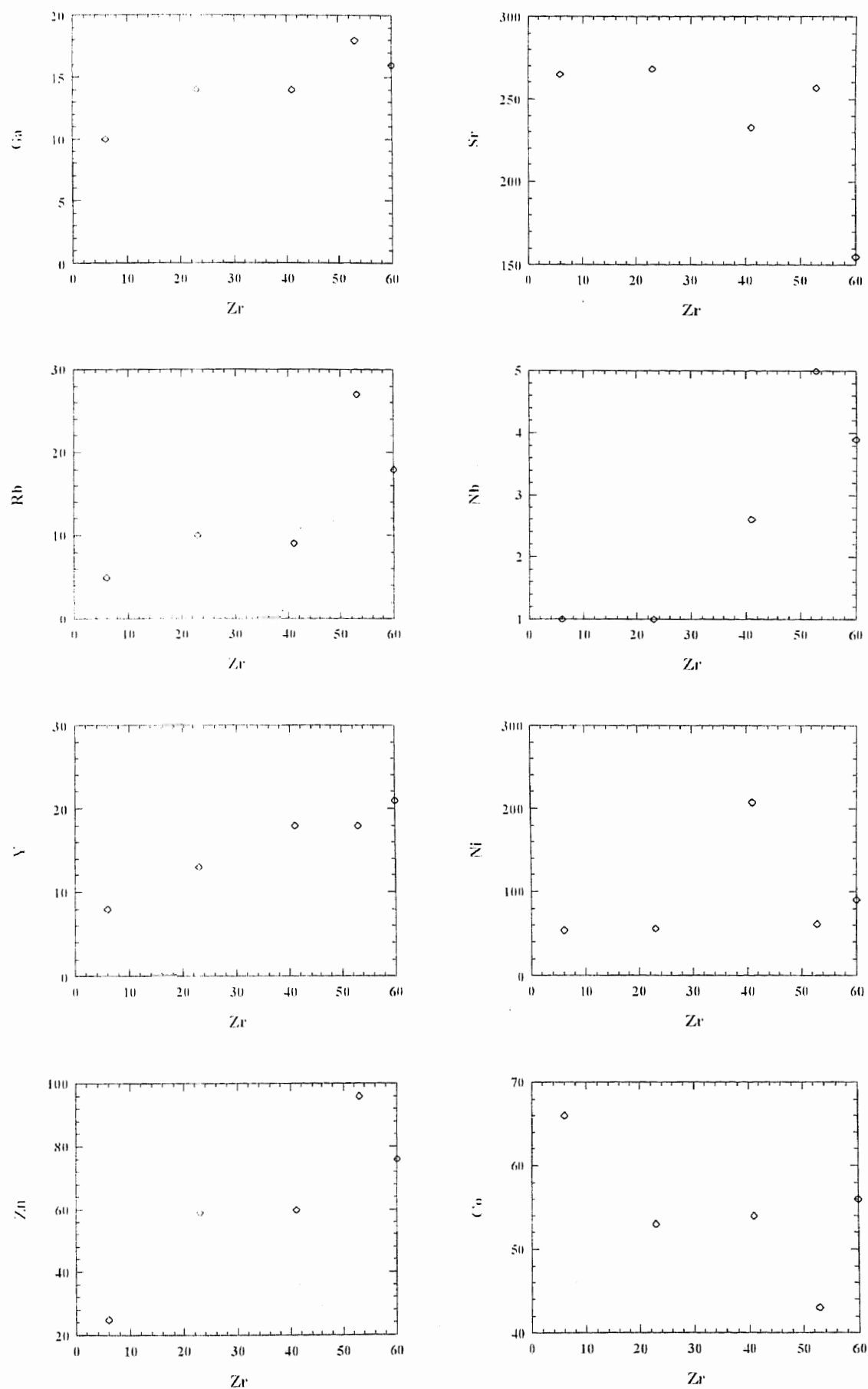


Figure 4.24. Binary plots of trace elements versus Zr for Sumal amphibolites.

and patterns are sloping towards the right (Figure 4.25). The patterns are very similar to the magmas of subduction zones, displaying an enrichment in LILE relative to HFSE. Since the LILE may have been modified in the studied rocks through alteration and metamorphism, the similarity may be superficial. However the resemblance in the rest of the pattern based on HFSE is also close, and the presence of Nb anomaly is particularly indicative of affinity with subduction related magmatic environment.

Binary inter-element plots and mantle-normalized multi-element plots show that some of the elements such as Zr and Nb have good mutual correlation and more or less constant inter- element ratios (Figure 4.24 and 4.25). As discussed in the previous pages such variation trends depict a generally incompatible relationship of these trace elements with the minerals involved in the fractionation.

Trace-element Characteristics of Subduction-related Magmas

When intra-oceanic island-arcs initiate on the oceanic lithosphere, the chemical characteristics of the magmas would be quite similar to MORB. However, arc magmas do differ from MORB in a number of important respects. An enrichment in the LIL elements (Ba, Rb, Th, K and Sr) relative to the HFS elements (Nb, Zr, Ti and Y) is seen in the studied rocks. The distinguishing feature of the enriched elements in these rocks is their low ionic potential and hence their greater tendency to be mobilized by aqueous fluids, which are supposed to be driven off from subducting oceanic crust. These fluids would contain the alkali and alkaline earth elements, which are added to the upper part of the oceanic crust during sea-floor weathering processes and are released into the aqueous phase by dehydration of secondary minerals (Saunders et al., 1980; Gill, 1981; Pearce, 1982). In contrast, the remaining HFS elements are relatively immobile in aqueous fluids and remain in the residual phases within the mantle wedge. Thorium is

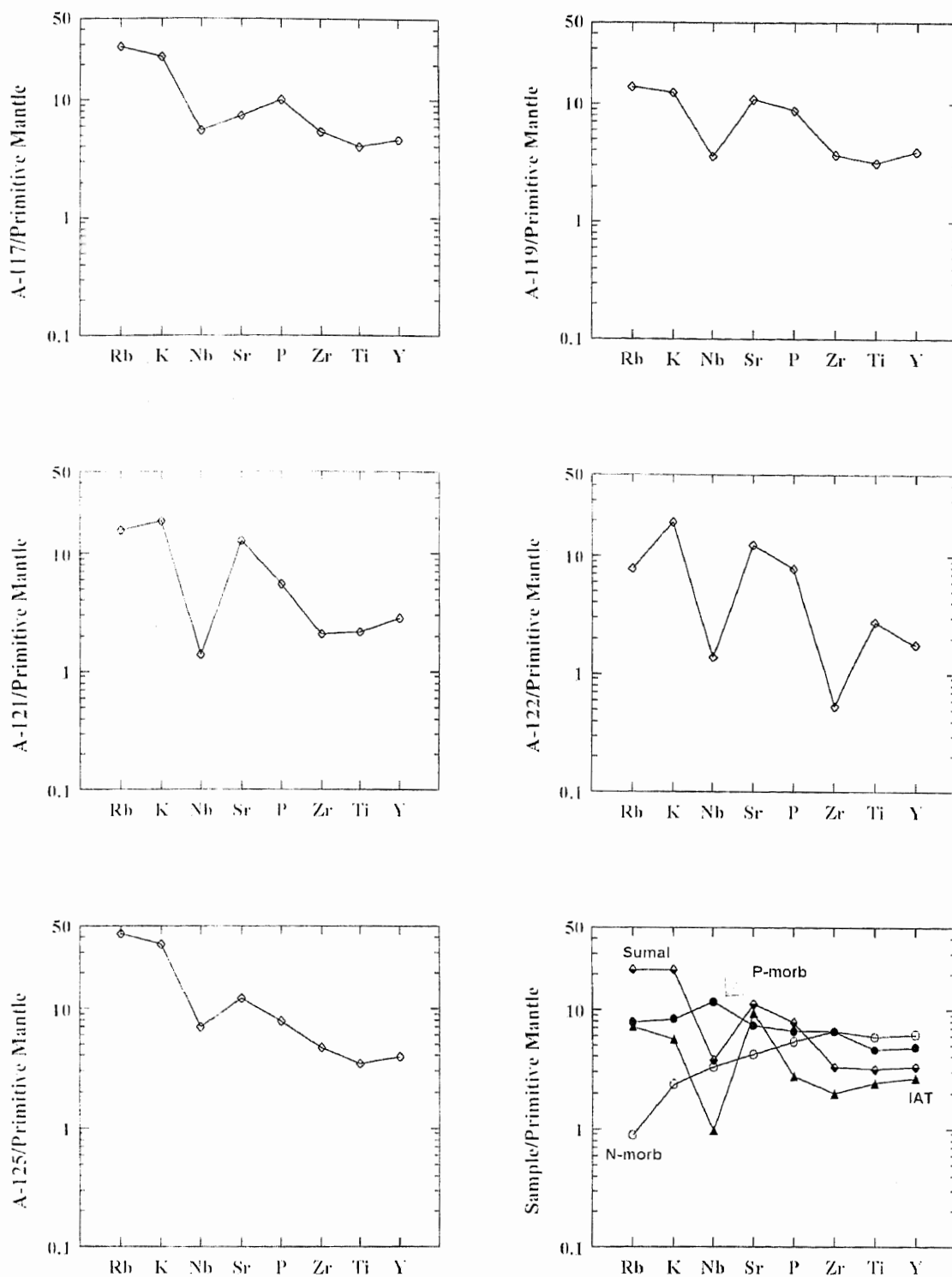


Figure 4.25. Primordial mantle normalized diagrams of the Sumal amphibolites. Lower right figure shows comparison of average values of Sumal amphibolite with basalts from mid ocean ridges and island arcs.

Normalizing values of Primordial Mantle: Rb 0.635, K 250, Nb 0.713, Sr 21.1, P 95, Zr 11.2, Ti 1300 and Y 4.55 after Sun and McDonough, 1989.

transitional in this respect and may behave as a mobile or immobile element depending on pressure, temperature and fluid composition (Wood et al., 1979).

The second notable feature displayed by these rocks is the low abundance of the HFS elements relative to MORB (Figure 4.26). Low Ni contents suggest that the rocks have undergone considerable olivine fractionation en route to the surface. This type of fractionation would tend to increase the incompatible element concentrations in the primary magma. The rocks formed from this type of magma are depleted in certain HFS incompatible elements. Explanations of this phenomenon include: the presence of stable incompatible rich minor phases such as rutile, sphene and zircon in the residue (Saunders et al., 1980; 1988); a higher degree of partial melting (Pearce and Norry, 1979), magma-mantle interactions (Kelemem et al., 1990) and remelting of already depleted mantle (Green, 1972; Saunders et al., 1991).

Tectonic Environment

Sumal amphibolites are medium-K and calc-alkaline in nature. Various established discrimination diagrams have also been used for these rocks to know their magmatic affinity and tectonic environment. Ti-Zr-Sr, Ti-Zr-Y, and Ti vs Zr discrimination diagrams (Pearce and Cann 73 and Pearce, 1982) are used systematically to decipher the origin of Sumal amphibolites (Figure 4.27). The Ti-Zr-Y plot discriminates between within-plate basalts, i.e., ocean-island or continental flood basalts, island-arc tholeiites plot in field A and calc-alkaline basalts in field C, whereas, MORB, island-arc tholeiites and calc-alkaline basalts all plot in field B. Four of the studied samples plot in field B and one falls in field A. Same results are seen in Ti-Zr plot. These two plots are not clearly discriminating the origin of the rocks in terms of island-arc tholeiites or calc-alkali basalts and MORB. The Ti-Zr-Sr plot subdivides the rocks plotting in field B of the Ti-Zr-Y

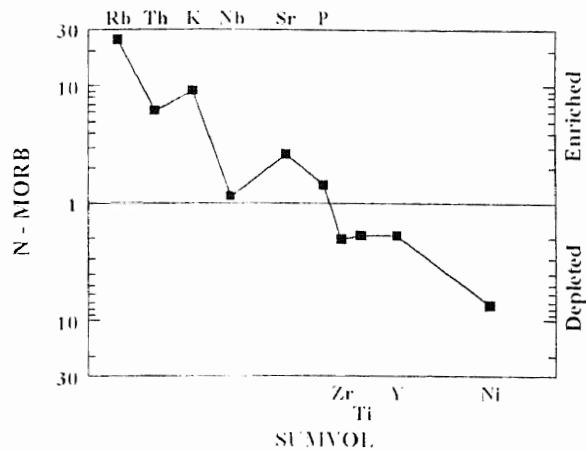


Figure 4.26. Diagram showing the low abundance of high field strength elements (Zr, Ti, Ni and Y) in Sumal amphibolites relative to N-type MORB.

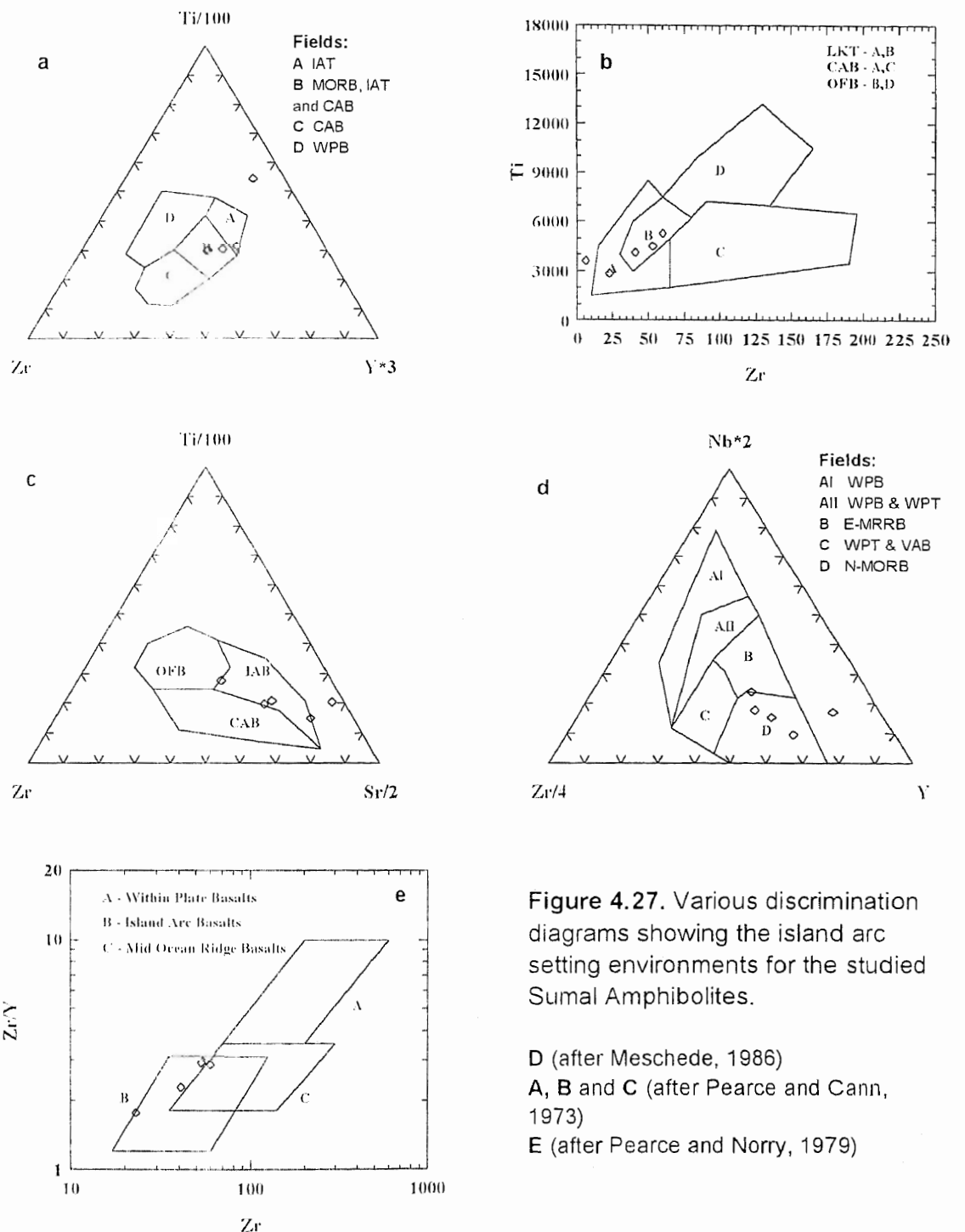


Figure 4.27. Various discrimination diagrams showing the island arc setting environments for the studied Sumal Amphibolites.

D (after Meschede, 1986)
A, B and C (after Pearce and Cann, 1973)
E (after Pearce and Norry, 1979)

diagram into the three different tectonic settings; island-arc tholeiites, calc-alkaline basalts and MORB. Sumal amphibolites fall in the field of island-arc tholeiites indicating their affinity with island-arc environments (Figure 4.27c).

The average major and trace elements data of the studied rocks is compared with basaltic composition from various tectonic environments in Table 4.8. More diagrams are also used to understand the origin of the studied rocks. Meschede (1986) suggested that the immobile trace element Nb can be used to separate the different types of ocean-floor basalt. When the rocks are plotted on a triangular plot of $Zr/4-2*Nb-Y$, they show their presence in the field of IAB and N-type MORB. A trend of these above mentioned diagrams indicating that these rocks show a great correspondence to IAB (island arc basalts) than the MORB (mid-ocean ridge basalts). A further confirmation was made to use a plot of Zr/Y vs Zr (Pearce and Norry, 1979), which discriminates effectively between basalts from ocean island arcs, MORB and within plate basalts. This plot can also be used to subdivide island-arc basalts into those belonging to oceanic arcs, where only oceanic crust is used in arc construction, and arcs developed at active continental margins. The studied samples occupy the field of IAB. From the above mentioned diagrams it is concluded that the rocks of the Sumal group of the study area have calc-alkaline trend of oceanic environments and predominantly, if not entirely, made up of subduction related island-arc setting.

Petrogenesis

Because of insufficient data on these rocks of the study area, a true petrogenetic model is difficult to construct. However, an attempt has been made to discuss their genesis and petrogenetic comparisons. It is understood that partial melting of mantle lherzolite and peridotite generates basaltic magma which is later on injected through tensional fissures to form large and small intrusions or surface

flows (Wilson,1989). Partial melting of a metasomatized mantle source may be suggested to have produced these rocks.

The low abundances of the trace elements particularly the high ionic potential elements such as Nb, Zr, Ti and Y relative to MORB have been variously attributed to (i) higher degree of partial melting of the mantle source, (ii) stability of the minor residual phase (rutile, zircon and sphene), and (iii) the remelting of the already depleted mantle source (Pearce,1982). However, crustal contamination can also cause such a depletion (Wilson,1989). As depicted by the geochemical signatures, these rocks show a strong to moderate degree of partial melting of a depleted but metasomatized mantle source. The higher values of MgO (11.17 wt%) and Ni (207ppm) in sample A-119 indicate low degree of fractional crystallization (Table 4.11). The other samples show low Ni contents, which suggest that they are not primary magma and have undergone olivine fractionation en rout to the surface.

The geochemical spidergram patterns of these rocks are more or less horizontal approaching those found in the tholeiites of Jal and Niat units. The flat trend of immobile elements (Nb, Zr, Ti, and Y) of Sumal rocks which is relatively parallel to the MORB pattern, is presumably reflecting the pre-subduction characteristics of the mantle wedge. The spiked trace element signatures in Sr and K are presumably derived from the subducted lithospheric slab, to the lherzolite of the mantle wedge. The marked trough at Nb may not actually reflect a real depletion in Nb as its cocentration is close to that in MORB (Table 4.8). The apparent sharpness of the trough is in fact a consequence of the marked enrichment of the adjacent elements Sr and K in the spiderdiagram. Variations in the parental basalt composition, from tholeiitic to calc-alkaline to alkaline, must

reflect the relative proportions of LIL (large-ion lithophile) enriched component and normal mantle lherzolite phases entering subsequent partial melts.

The rocks are less fractionated and enriched in Al_2O_3 and Ni as compared to the rocks of Jal and Niat units. This enrichment may be considered in terms of "cumulus enrichment" (Cox et al., 1979). These calc-alkaline magmatic rocks may be produced due to partial melting of the metasomatized mantle or from a heterogeneous mantle source. The basaltic liquid migrated from the source and solidified during the initial subduction related processes within magma chamber. This magmatism may be occurred before the closure of the Northern suture.

Chapter 5

THE THAK GRANITOID SHEETS

Introduction

Intrusive rocks of predominantly granitic composition, but including gabbros, diorites and tonalites, occur in large proportions in the northern half of the Kohistan terrane. Many workers, e.g., H.H.Hyden (1916), Ivanac et al. (1956), Davies (1965), Chaudhry et al. (1970), Jan and Mian (1971), Tahirkheli and Jan (1979), Butt et al. (1980), Jan and Khan (1983), Petterson and Windley (1985) and Ghazanfar et al. (1991) described these rocks from different parts (Dir, Swat, Gilgit and Indus valleys) of the Kohistan terrane. Jan et al. (1981) included these rocks in their Ladakh-Kohistan granitic belt, while Petterson and Windley (1985) and Coward et al. (1986) introduced the term Kohistan batholith for these intrusive rocks. The Kohistan batholith is commonly considered to be restricted to the northern half of the Kohistan terrane (see maps by Tahirkheli and Jan, 1978; Searle and Khan, 1996). On a relatively limited scale, intrusive rocks of gabbro, diorite, tonalite and granite composition, however, do occur in the southern parts of the Kohistan terrane. These rocks are characteristically associated with the Kamila amphibolite belt, and are reported from Dir (Butt et al., 1980), Swat (Jan and Mian, 1971) and Indus (Jan, 1970; Treloar et al, 1990) valleys.

A sizeable proportion of the presently investigated area in SE Kohistan comprises plutonic igneous rocks intruding the Kamila amphibolite belt. These are predominantly dioritic in composition, but include gabbros, granodiorites, granites and trondhjemites and are considered to constitute the equivalent of the Kohistan batholith in southern Kohistan. In this chapter, the granitoid sheets of the studied

area are described in terms of field relations, petrography and geochemistry. In the end, an attempt is made to evaluate their petrogenesis.

Previous Studies

Wadia (1932), for the first time, reported occurrence of diorites from SE Kohistan in his regional geological map, which was included in his study on general account of the Nanga Parbat region and Chilas. However, it was Shams (1975), who described the occurrence of diorites from the Thak valley, with a geological sketch map. He delineated two diorite units, one to the north (downstream) and the other to the south (upstream) of Jal (i.e., the Thak-Niat confluence). Chemical analyses for major elements were presented for thirteen samples and he concluded that the rocks of Thak valley were formed in two stages. In the first stage, norite magma was intruded which gave rise to various basic to ultrabasic rocks and the set of basic pegmatites. During the second stage, diorite magma was intruded and gave rise to rocks ranging from meladiorite to granodiorite, acid pegmatites and veins. Ironically, later studies (Khan, 1988) showed that none of the two diorite units of Shams (1975) were actually diorites; the rocks to the north of Jal confluence are gabbro-norite to hypersthene diorites and form an integral part of the Chilas Complex (Khan et al., 1989), while those to the south of the Jal confluence (the veined metadiorites of Shams, 1975) are basic metavolcanic amphibolites belonging to the Kamila amphibolite belt (Khan et al., 1993; this study). Ahmed and Chaudhry (1978) reported several sheet-like masses of dioritic rocks from the middle and upper reaches of Thak valley alternating with greenschist-facies metavolcanics. These authors presented a detailed account on petrography and chemical analyses of major elements for ten samples. They concluded that the dioritic rocks of the Thak valley were emplaced in five episodes;

(i) intrusion of intermediate to basic rocks and some simple pegmatites in the northern part of the area, (ii) intrusion of basic dykes and sills, mainly in the south, (iii) intrusion of a peridotite body, (iv) intrusion of ultramafic, basic and intermediate rocks belonging to the Thak Valley Igneous Complex in the north of the area, and (v) injection of some simple pegmatites. The first two episodes of intrusion are metamorphosed. Ghazanfar et al. (1991) have mapped several lenticular masses of diorites, granodiorites and granites from southern Kohistan together with a detailed petrographic account.

Ahmed, Z. (1985) presented a sketch geological map of a small part of Niat Gah between Jal and a little upstream from Lumar. However, none of the geological units identified by Ahmed (1985) could be located during this study; particularly, no evidence was found for the extension of the Salkhala Formation of the India plate as north as the lower reaches of the Niat Gah.

Field Relations

The granitoid rocks of SE Kohistan comprise a number of large to small bodies comprising gabbros, diorites, tonalites, granodiorites, granites and trondhjemitites. Two modes of occurrence are characteristic; 1) large sheet-like lenticular masses, and 2) minor intrusives in the form of veins, sills or dykes. The sheet-like bodies are up to 5 km thick, and stretch east-west for a distance over 40 km in the mapped area alone. They are typically composite, comprising gabbros, diorite/tonalite, granodiorite and granite. Deformation has obscured contact relations between what would have been cross-cutting sequential phases. The minor intrusions, forming veins, sills and dykes are abundantly present in the studied part of Kohistan terrane, but are characterised by variance in distribution and composition. Minor intrusions are predominantly granitic or trondhjemitic in

composition with aplitic as well as pegmatitic textures. In the following, the intrusive rocks of the SE Kohistan terrane are described in terms of observations in the Niat, Thak, Buto and Thor valleys.

Niat Gah

A principal mass of granitic rocks occurs at Lumar-Niat confluence, separating the Niat metavolcanic unit from the Jal amphibolite unit. It is not a cohesive body, and comprises sheets of granites alternating with those of amphibolites belonging to the Niat metavolcanic unit (Plate 5.1). The granite sheets are generally one to two meters thick, but some are several meters in thickness, while those of the host amphibolites are rarely thicker than a meter. The granites and amphibolites are strongly foliated, and commonly mylonitized. The pervasive deformation has obliterated the intrusive relations, but amphibolites occur as xenoliths in the granites. The contact between the granites and the Jal amphibolites is marked by strong shearing and folding. Even a minor brittle fault filled with gouge is observed at the contact.

To the north, several minor sheets, dykes and veins of the granitic rocks occur within the Jal amphibolite unit. Sheets comprising medium- to coarse-grained gabbroic diorites form a minor but important part of the amphibolite sequence. These are strongly sheared and appear to have undergone the same phase of deformation and metamorphism which affected the host metavolcanics. The rest of the granitic component in the Jal amphibolite unit is in the form of dykes and veins. These intersect the fabric in the amphibolites, but are themselves commonly foliated, suggesting a syntectonic to rarely post-tectonic origin. There is a considerable variation in grain size, ranging from pegmatitic, through granitic to aplitic. Two rock types are represented. Predominantly, the rocks are



Plate 5.1. Photograph showing the alternating bands of diorites (light) and Niat volcanics/ amphibolites (dark) at Gurmali in Niat valley.



Plate 5.2. Photograph showing fine-grained xenoliths of different shapes and sizes in diorites. The largest xenolith is 10 cm in breadth.

garnetiferous two-mica trondhjemites. A few of the fine-grained dykes are andesitic in composition. In one case, about a meter thick trondhemitic pegmatite contains a 4 cm thick andesite dyke running along its medial axes.

Thak Gah

Three sheet-like cohesive bodies of granitoids are encountered in the Thak Gah. Additionally, there are minor intrusions in the forms of veins and dykes within the Niat and Jal metavolcanic units. A granitoid body in the uppermost reaches of the Thak Gah is exposed in the vicinity of the Babusar Rest House. It is a > 1.5 km thick sheet, extending east-west with dips of 30-50° to the south. The body has experienced a thorough ductile shearing resulting in a penetrative foliation (70-100°/ 30-40° S). Locally, the rock is transformed into mylonites. Sheets of fine-medium grained amphibolite are locally found intercalated with the gneissose diorites. Though some of them are laterally extensive beyond the limits of the outcrops, most are discontinuous due to incorporation of masses of the host rock, stretched and transposed during deformation of the diorites. Compositionally, the body is a homogeneous diorite. The fabric is defined by chlorite and tremolitic amphibole. This body of foliated diorites corresponds to the chlorite gneiss unit of Ahmed and Chaudhry (1976).

The second body of granitoids occurs in the vicinity of village Shai. It is some 400 m thick sheet. Again the attitude is about east-west, with northerly dips at moderate angles. The body is diorite in composition with pervasive foliation defined by amphibole.

The principal granitoid body occurs in the Thak valley, between the Loshi and Khun convertible bridge. This body is about 5 km in thickness and extends for ~ 40 km. The constituent rocks are foliated but deformation is distinctly less

intense than that in the two bodies to the south. In essence, the deformation is more intense in its marginal parts. Whereas the northern 200 metres from the contact are strongly sheared, the shearing in the southern margin is pervasive up to a km from the contact. The interiormost part of the body between the Khun bridge and the village Domain has escaped deformation. Compositionally, this body is relatively more mafic than the two southerly bodies. Gabbroic diorite in the interiors and diorites in the marginal parts are the principal constituents. Gabbros, with a distinct smoky appearance, form a subordinate but important component of the body in the vicinity of the village Domain. The intrusive relations between the various compositional types could not be observed due to vegetation/debris cover. The gabbroic and dioritic rocks of this body are characterized by the occurrence of xenoliths. Two varieties are noticed; fine-grained, amphibole-rich xenoliths resemble the metavolcanics of the Niat unit. Other xenoliths are microdiorite in composition and represent precursors of the host gabbros and diorites. The shape of the inclusions varies from almost spherical to much flattened ellipsoids (Plate 5.2), the latter showing a perfect alignment (Plate 5.3).

The minor intrusions in the form of dykes and veins are characterized by four compositional types; diorites, andesites, granites and trondhjemites. Strongly foliated gneissose diorites occur intercalated with greenschist-amphibolite metavolcanics of the Niat unit. Andesites, occur as thin veins (up to 4 cm thick) cross-cutting the fabric in the amphibolites. Granites occur as dykes, some as thick as 5 meter, intruding the Niat metavolcanic unit. The trondhjemites are restricted to the Jal amphibolite unit; they occur as veins and dykes. Locally they are so abundant that they furnish a banded appearance to the amphibolites. This led Shams (1975) and Ahmed (1985) to use the name "veined metadiorites" for the Jal



Plate 5.3. Photograph shows a perfect alignment of elongated and flattened fine-grained xenolith along foliation in the diorites. Length of inclusion is 25 cm.



Plate 5.4. Photograph showing the sharp contact between the diorites (lighter middle right) and Niat volcanics (darker upper left) near Chakkar in Buto valley.

amphibolite unit defined in this study. The trondhjemite veins and dykes cross-cut the fabric in the amphibolites, but are mostly deformed themselves, suggesting a syntectonic origin.

Buto Gah

The upper reaches of the Buto Gah contain several sheet-like granitoid bodies, of which the southerly two are probably a direct continuation of the granitoid bodies exposed in the upper reaches of the Thak Gah, i.e., Babusar Rest House and Shai. The granitoids at and around the Katai-Buto confluence have a limited easterly extension and comprise medium- to coarse-grained and strongly foliated gabbroic diorites. There are veins and up to one meter thick dykes of trondhjemite composition intruding the diorites and Niat metavolcanic unit which are equally deformed. These trondhjemites are porphyritic with phenocrysts of feldspar. Rare dykes, in this area, are fine-grained and dacitic in composition.

A thick body of medium-coarse grained granitic composition is exposed at the mouth of the Chakkar confluence, separating Jal amphibolite unit in the north from the Niat metavolcanic unit in the south (Plate 5.4). This body is about 3 km thick and is a westerly continuation of the granitoid body exposed between Loshi and Khun bridge in the Thak Gah. The body is typically composite, comprising gabbro-diorite in its southern parts and coarse-grained pegmatitic trondhjemite in its northern parts. The trondhjemites are clearly younger than the gabbro-diorite as suggested by the cross-cutting field relations between the two in the southern part of the body near the Chakkar confluence.

Thor Gah

Two major bodies of granitoid composition occur in the Thor Gah, to the north and to the south of the village Makheli. These bodies comprise gabbroic

diorites or diorites with intruding dykes of andesite and granite composition. As in the Niat Gah, the minor intrusions in the form of veins and dykes comprise trondjemites, and are restricted to the Jal amphibolite unit.

Summary

The geology of the southeastern part of Kohistan is known to host granitoid bodies of dioritic composition (Shams, 1975; Ahmed and Chaudhry, 1976; Ahmed, 1985; Khan and Thirlwall, 1988; Ghazarfar et al., 1991). This study has revealed that about one-third of the area between the Chilas Complex in the north and MMT in the south comprises granitoids. Some important observations concerning the geology of these rocks are as under:

- 1) Compositionally, tonalite/diorite forms the principal component of the granitoids in SE Kohistan. Relatively more mafic rocks (e.g., gabbros) also form a significant proportion of these bodies. Trondjemites, granites, andesite and dacite occur as dykes and veins. Of these, the trondjemites are the most abundant, granites are subordinate, while andesite and dacite are uncommon.
- 2) Almost all the granitic intrusive complex is younger than the host metavolcanic amphibolites. Amongst the various constituent lithologies the order of intrusion appears to be as follow:
 - i) high Ti-diorite gneisses intercalated with Niat metavolcanic unit. These diorites have composition very close to the host metavolcanics and share the same phase of metamorphism and deformation, suggesting an early stage of intrusion.
 - ii) gabbros, diorites and tonalites.
 - iii) trondjemites, granites and andesite/dacite dykes and veins.

3) Trondhjemites have a preferred distribution in SE Kohistan, restricted to the northern parts of the amphibolite belt. In Niat and Thak valleys, they are restricted to the Jal amphibolite unit, whereas to the west, in the Butto and Thor, they, in addition, intrude the diorite body immediately to the south of the Jal amphibolite unit. The only exception is the upper reaches of Buto Gah (Katai-Buto Confluence), where trondhjemites have been noticed in the south-central parts of the amphibolite belt.

4) All the granitoid rocks in SE Kohistan are ductily deformed. The deformation is particularly strong in the most southerly bodies (e.g., Babusar RH), where the rock is transformed into blastomylonite gneisses. Smoky gabbros and gabbroic diorites to the south of the Khun bridge (Thak Gah) are the least deformed rocks in SE Kohistan. These rocks escaped deformation due to their location in the interior of the 5 km thick sheeted body, rather than being post tectonic. Even the trondhjemites which cross-cut fabric in the amphibolites are syntectonic in origin. The presence of foliation in the granitoid rocks of SE Kohistan enables their correlation with stage-I Kohistan batholith of Petterson and Windley (1985).

Modal Composition and Petrography

The granitoids of the studied area in SE Kohistan are broadly divisible into three groups on the basis of petrography and modal composition. The Shai group includes sheet-like bodies exposed in the southern parts of the studied area, at the middle and upper reaches of Niat-Thak-Buto-Thor valleys. The Khun group includes granitoid body separating Jal amphibolite unit from the Niat metavolcanic unit, in the northern parts of the studied area. The third group includes minor intrusions in the form of veins and dykes scattered throughout the area.

Shai Granitoid Group

This group is characterized by diorite/tonalite rocks which are strongly foliated and often transformed into balstomylonite gneisses (Plate 5.5). Foliation follows the general trend of the host rock. Shearing is particularly strong in the sheet-like body exposed around Babusar Rest House (Plate 5.6). Where shearing is less intense, xenoliths are present and are mostly aligned to the foliation (Plate 5.7). There is a strong mixing between the diorites and host metavolcanics. Incorporated xenoliths and screens of metavolcanics are strongly transposed along with the host diorites giving rise to this tectonic mixing. The foliation is defined by plagioclase, quartz, amphibole and chlorite which are mutually parallel and preferentially oriented. The gneissic texture is marked by quartz ribbons, eye shape feldspar/clinozoisite aggregates, amphibole and chlorite. Banding is defined by segregation of quartz and feldspar in bands alternating with bands rich in epidote+amphibole±chlorite. Modal compositions for the diorite/tonalite rocks of this group are given in Table 5.1.

Plagioclase mainly occurs as short, stumpy, euhedral/subhedral crystals and shows a range in anorthite (An_{30-46}) content. In some cases, it is labradorite, but andesine (An_{36-42}) is the most common composition in these rocks. All plagioclase grains are invariably saussuritized but in some rocks they are completely cloudy (Plate 5.8). Irregular and patchy zoning is seen in some rocks.

Green amphibole is an important constituent in the rocks of the Shai group. It is mainly tremolite-actinolite amphibole, but hornblende is encountered in the relatively basic varieties. Amphibole contains inclusions of epidote and quartz and shows alteration to chlorite. At places the whole amphibole crystal is altered and consumed by chlorite and only a small relict of it with marginal reaction rim is seen



Plate 5.5. Photograph showing the medium and coarse-grained diorite which is strongly foliated and sheared. The upper dark part represents the fine-grained metavolcanics.



Plate 5.6. Photograph showing the shearing with double deformation in a sheet-like dioritic body exposed around Babusar Rest House, Thak valley.



Plate 5.7. Photograph showing the xenoliths of varying sizes aligned to the foliation in diorite. Thickness of xenoliths vary from 1 cm to 4 cm.

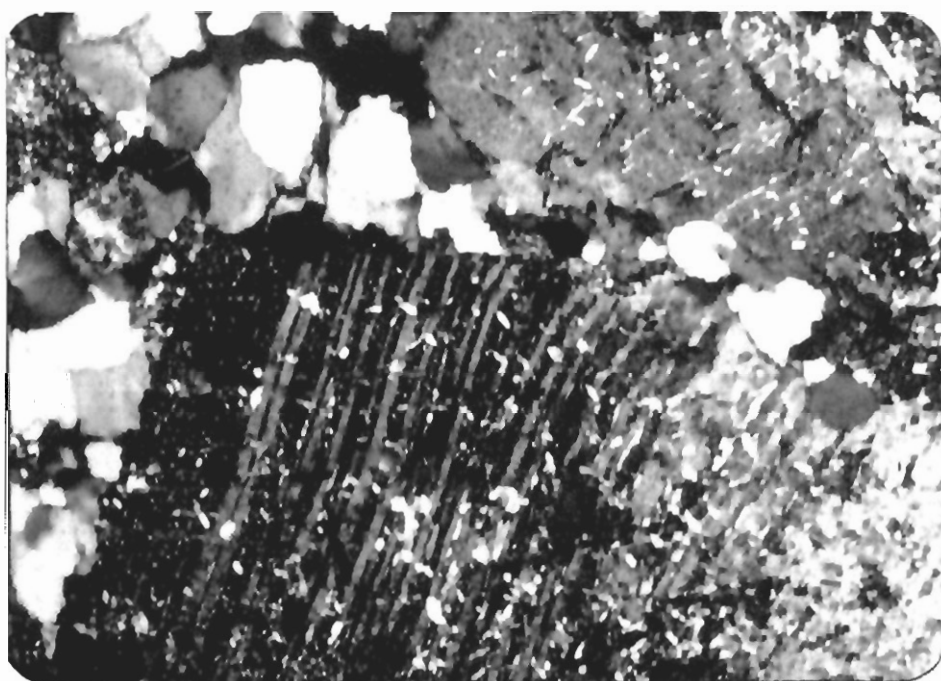


Plate 5.8. Microphotograph showing saussuritized plagioclase in Shai diorites. Quartz occupies spaces between the plagioclase crystals. Field of view is 2.5 mm.

Table 5.1. Modal Composition of intrusive rocks of Shai group.

Sample Nos.	A-249	A-179	A-175	A-173	A-191	A-246	A-185	A-256	A-255	A-254
Feldspar	30	25	20	5	7	45	10	50	48	40
Amphibole	40	21	20	8	50	10	6	10	12	15
Quartz	10	8	10	40	15	30	35	20	25	20
Epidote	5	10	8	10	5	13	5	6	8	3
Chlorite	12	30	40	35	20		40	10	5	15
Sphene	2	1	1	2	1		2	1	tr	
Iron Ore	1			tr	tr	2		2		tr
Muscovite/ Sericite		tr	1	tr	2		2	1	2	2
Calcite		5								5

Key: A249 (gabbro-Keo valley); A179, 175, 173 (gabbro diorite-Buto valley); A191, 246 (diorite-Buto and Keo); A185 (quartz diorite-Buto valley) and A256, 255, 254 (granodiorite-Keo valley).

in the middle of chlorite aggregate. Chlorite is characteristically light green and non pleochroic. Low birefringence, parallel extinction, optically negative character of flaky crystals and interlocking aggregates helped the identification.

Epidote is fine to medium-grained and forms anhedral to euhedral six sided crystals. Its population may belong to two distinct compositional groups, one of which shows bright and the other shows grey interference colours. Epidote with bright colours in crossed polars occurs mostly in the mafic part of the rock, whereas the grey epidote is present in felsic part. A complex zoning with a peculiar twinning is seen in euhedral grains. Sphene and magnetite are present as accessory minerals. Sphene is present mainly along the borders of mafic minerals (amphibole, chlorite and epidote) with quartz (Plate 5.9). In the aggregate of sphene, central part looks darker and ilmenite may be formed probably in it. In the aggregates of chlorite, epidote and sphene, quartz is also present locally. Quartz is medium- to coarse-grained and subhedral to euhedral. Minor calcite is developed along the margins of quartz and plagioclase in some rocks.

Khun Granitoid Group

The undeformed varieties of gabbros, diorites and tonalites in the interiors of the sheet-like plutons are more or less equigranular with coarse- to medium-grained textures. Rarely, diorites are very coarse-grained with amphibole crystals approaching 7.5 cm in length. Primary mineral alignment is prominent at the margins of the diorite bodies. The rock is usually mottled black and white except at the margin, where the mottled appearance cannot be seen due to a marked decrease in hornblende content. Different sets of quartz veins are commonly seen in these rocks, with thickness ranging < 1 to 5 cm (Plates 5.10 and 5.11). In the western part of the area in Thor valley, quartz veins are very prominent in these

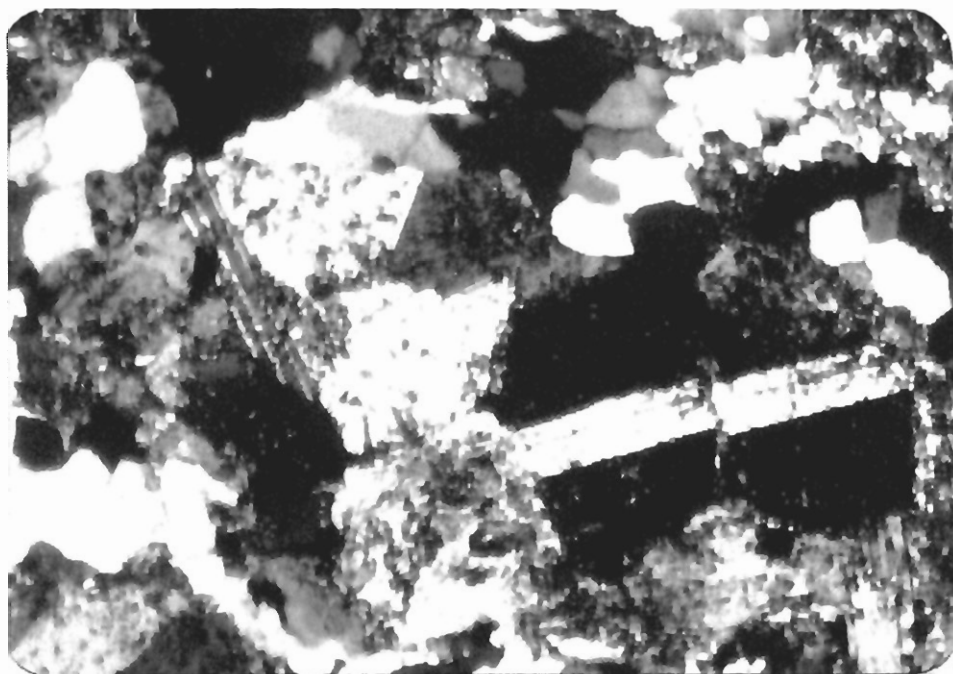


Plate 5.9. Microphotograph of quartz diorite showing the distribution of sphene mainly along the borders of mafic minerals (amphibole, chlorite and epidote) with quartz and plagioclase. Field of view is 2.5 mm.



Plate 5.10. Photograph showing quartz veins in fine-grained diorite, Keo valley. Thickness of the veins varies from < 1 to 3 cm.

rocks. Modal compositions of the gabbros and diorite/tonalite rocks of this group are given in Table 5.2.

The principal constituents of the rocks of this group are plagioclase, hornblende, quartz, and chlorite, whereas biotite, muscovite, magnetite, sphene and apatite are the accessory minerals. Epidote and chlorite is present as secondary minerals (Plates 5.12 and 5.12a). In hornblende, relicts of pyroxene are found rarely. The rocks are mostly medium- to coarse-grained.

Plagioclase is generally andesine in composition, rarely ranging into labradorite in the case of gabbros. It occurs as euhedral to subhedral and medium- to coarse-grained crystals. Alteration to kaolin, sericite, epidote and calcite is common. The plagioclase with high content of anorthite (An_{40-54}) shows a lot of inclusions of secondary epidote, sericite and also apatite (Plate 5.13) as compared with the plagioclase of low anorthite content (An_{28-40}). Epidote and muscovite present along the margins of andesine of low anorthite content (Plate 5.14). Some inclusions of apatite are also present in andesine. Large crystals of plagioclase show myrmekitic intergrowth with quartz.

Hornblende is pleochroic from pale green to dark green. It varies widely in proportion in the rocks and occurs generally as subhedral prismatic crystals. The poikiloblasts often contain inclusions of quartz, epidote and apatite. Quartz and epidote are also present along the margins of amphibole crystals. Amphibole shows alternation to biotite and chlorite.

Epidote, both zoisite and clinozoisite, occur as discrete grains as well as granular aggregates (Plate 5.15). Hybrid zones are specially rich in epidote. It is a secondary in nature and produced by alteration of plagioclase and hornblende. Chlorite is often associated with epidotization, develop in the hybrid zones. It

Table 5.2. Modal Composition of granitoid rocks of Khun Group.

Sample Nos.	A-110	A-167	A-96	A-139	A-140	A-143	A-163	A-118
Feldspar	40	42	45	16	35	22	45	10
Amphibole	7	5	10	15	15	20	10	22
Quartz	25	23	30	35	23	25	25	30
Epidote	2	4	5	20	10	15	5	20
Chlorite	20	20	2	10	15		12	15
Biotite	2	2	7			15		
Sphene	1	2	tr	1	1	2	1	1
Iron Ore		1		1			1	
Muscovite/ Sericite	3	1	1	2	1	1	1	2
Apatite						tr		
Garnet			tr	tr				

Sample Nos.	A-170	A-197	A-81	A-219	A-90	A-61	A-60	A-226
Feldspar	40	50	30	40	50	20	40	45
Amphibole	7	7	25	27	2	5		3
Quartz	25	22	30	23	30	25	20	20
Epidote	10	4	8	9	7	3	6	10
Chlorite	13	16				45	30	20
Biotite			2		8		2	
Sphene	2				1	1	1	1
Iron Ore	1		3	tr				
Muscovite/ Sericite	2	1	2	1	2	1	1	1

Key: A110, 167 (gabbro-Buto and Thak respectively); A96, 139, 140, 143, 163, 118, 170 (diorite-Niat, Thor, Thak, Buto and Thak respectively); A197, 81, 90, 219, (granodiorite-Buto, Niat and Buto) and A61, 60, 226 (granite- Thak and Buto).



Plate 5.11. Photograph showing network of quartz veins in medium-grained diorite near Makheli in Thor valley. Coin on left side for scale is 2 cm.

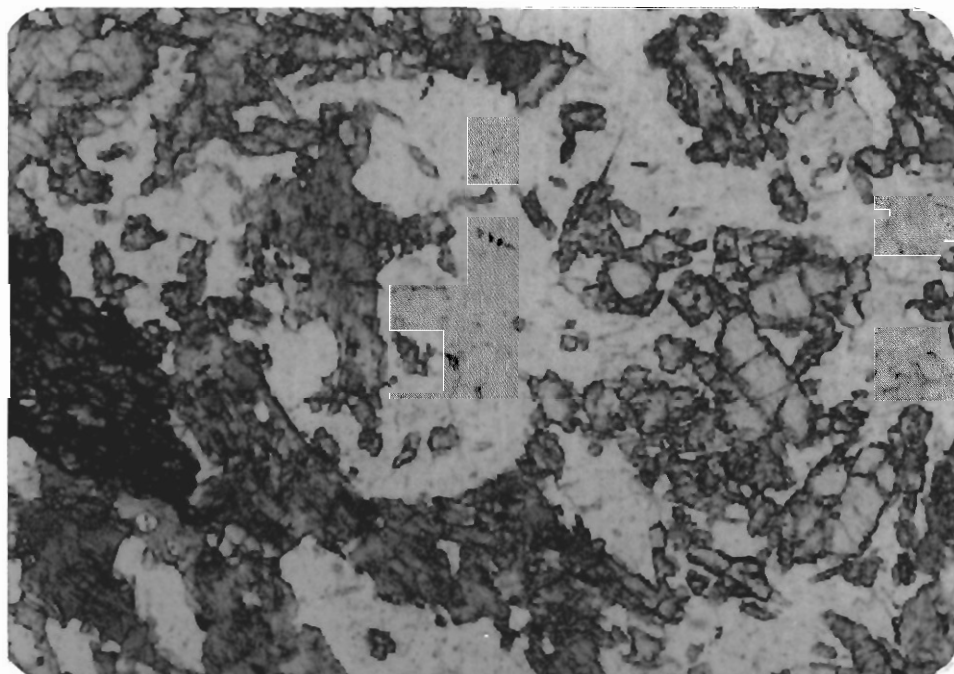


Plate 5.12. Microphotograph of diorite from south of Gabbar showing light green colour chlorite and colourless epidote, quartz, feldspar and dark brown aggregate of sphene. Field of view is 2.5 mm.

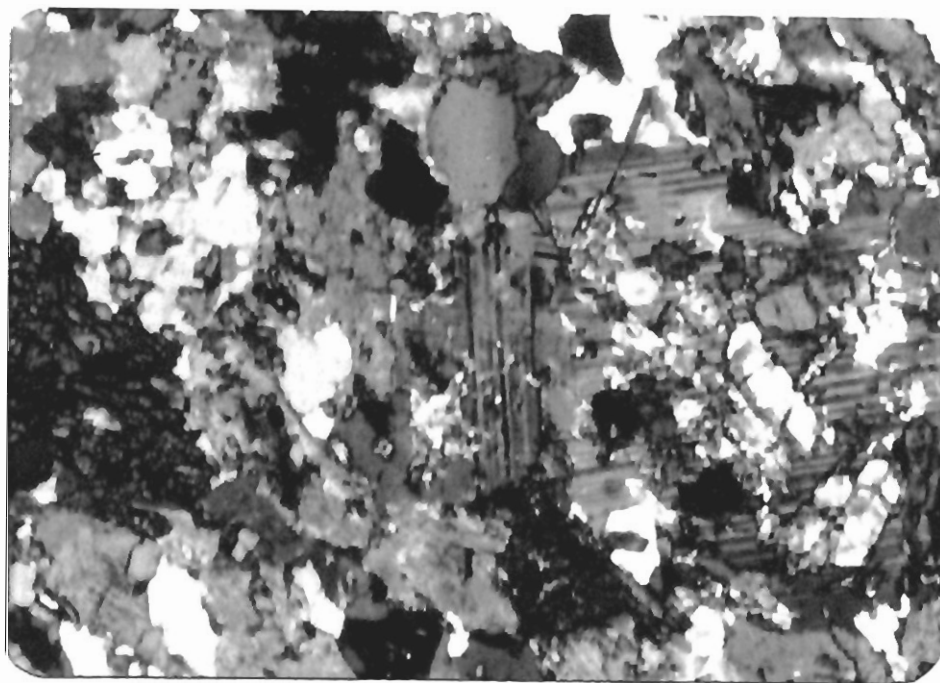


Plate 5.12a. The same in crossed polars.

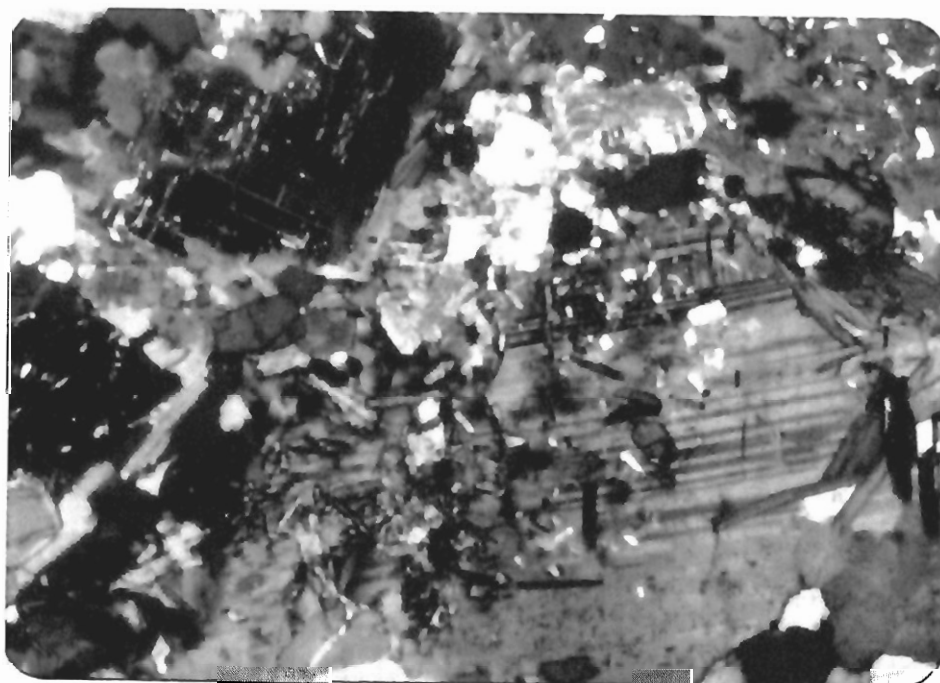


Plate 5.13. Photograph showing plagioclase with a lot of inclusions of epidote, apatite and sericite. Amphibole, chlorite and quartz present along the margins of plagioclase crystals. Field of view is 2.5 mm.



Plate 5.14. Microphotograph of a foliated diorite consisting of plagioclase, quartz, muscovite and epidote. Zoned epidote is prominent. Field of view is 4 mm.

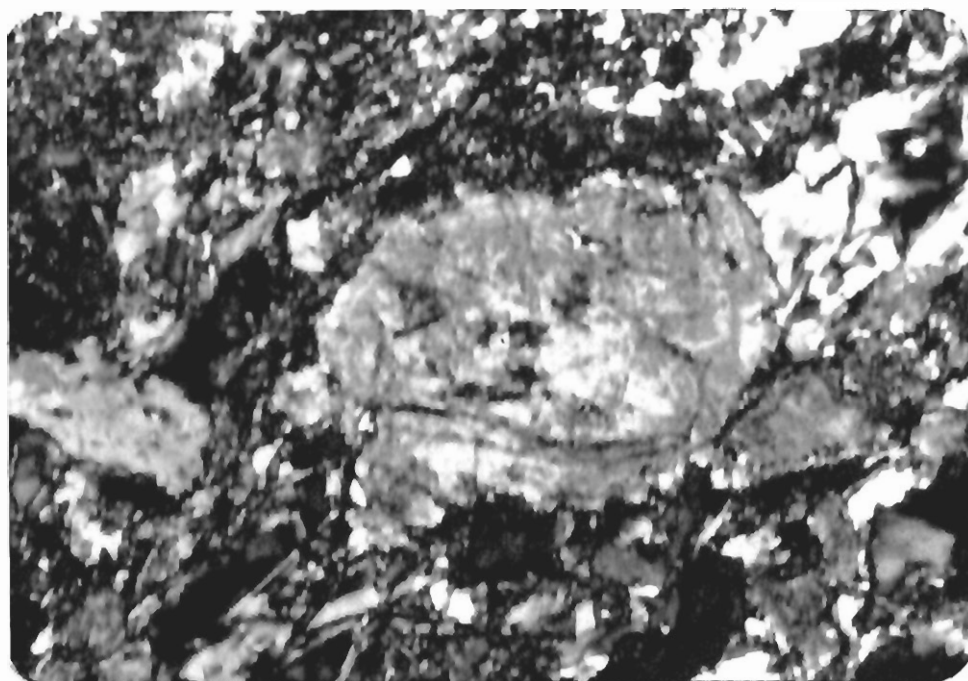


Plate 5.15. Photograph showing large grains of epidote with discrete zoning of different colours. Small grains of epidote are present in aggregate. Other minerals include quartz, feldspar, chlorite, amphibole, muscovite and sphene. Field of view is 4 mm.

occurs as a secondary mineral after both hornblende and biotite. It is light green, pleochroic and sometimes shows inky blue anomalous interference colours (Plate 5.16). Biotite and chlorite flakes are largely responsible for gneissose texture of the rock. They are observed to bend around euhedral epidote. They occur in patches where hornblende is seen in the process of alteration. Biotite is usually brown, pleochroic from pale to dark brown and shows birds eye texture when extinct. Wavy extinction and bent lamellae are common. Subhedral to anhedral biotite occurs in all facies of this intrusive group. Its amount increases in quartz-diorites and it becomes a ubiquitous minor to accessory mineral in tonalites. Some biotite grains contain ilmenite inclusions.

Quartz occurs either in little pools of granules or as an interstitial mineral. It is invariably anhedral and often shows wavy extinction (Plate 5.17). It also occurs as inclusions in hornblende and in biotite at some places. Sphene, calcite, apatite, magnetite, and hematite are the accessory minerals. Occasionally ilmenite may form lamellar intergrowths in hematite. Few rocks contain garnet in traces.

Minor Intrusions

Dioritic Pegmatoids

Dioritic pegmatites occur as sills, dykes, pods, lenses and irregular patches in both tabular and irregular shapes. They are coarse-grained rocks with uneven segregation of constituent minerals. They range in thickness from one centimeter to one meter or even more. The dioritic pegmatoids are veined in diorite and show coarsened dioritic mineralogy. These bodies show all gradations to the surrounding rocks. Plagioclase and hornblende make the principal constituents of all these rocks. Biotite, sphene and apatite make the accessory minerals, while

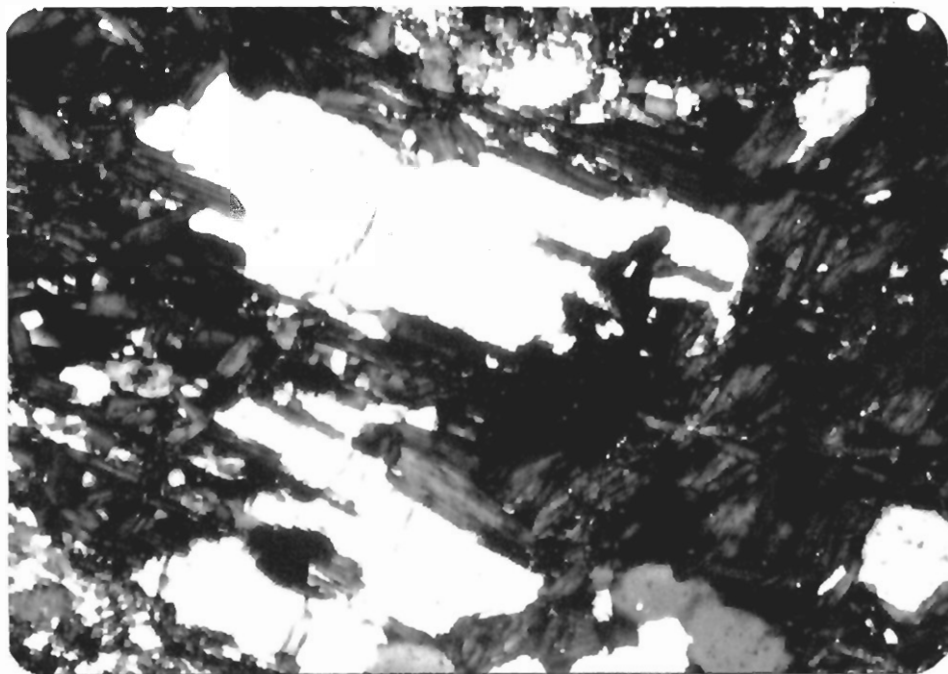


Plate 5.16. Photograph of diorite from Khun group consisting amphibole, chlorite, quartz, and muscovite. Chlorite shows light green to dark green colour in general with inky blue anomalous colour. Field of view is 4 mm.

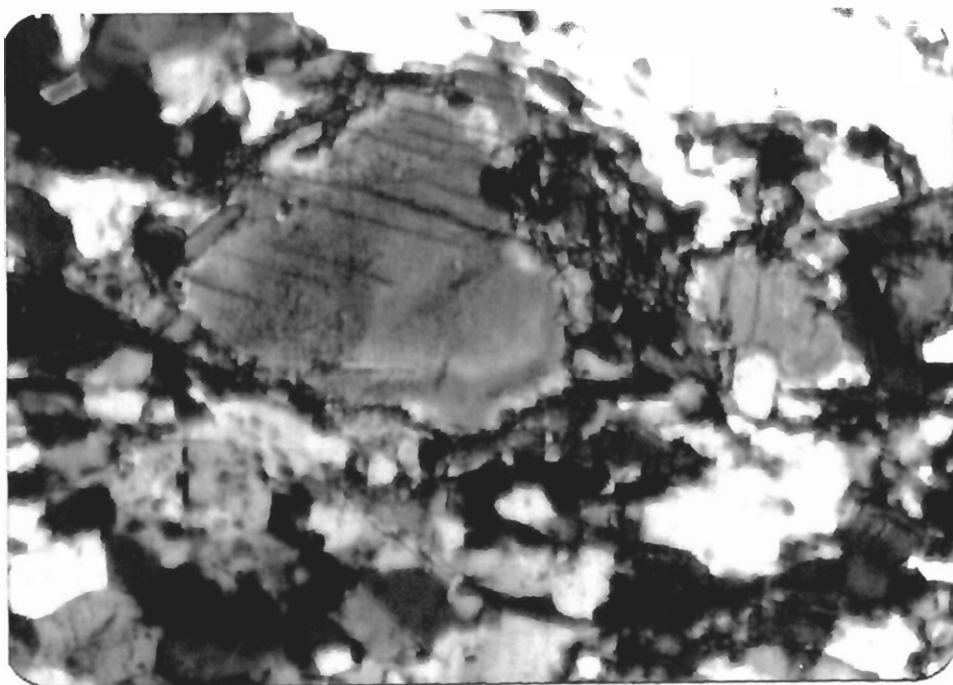


Plate 5.17. Diorite consisting of a feldspar, quartz, amphibole, epidote, biotite and sphene. Quartz is anhedral and shows wavy extinction. Field of view is 4 mm.

epidote and chlorite are secondary minerals. Modal composition of the minor intrusions are given in Table 5.3.

The dioritic pegmatoids are often accompanied by patches of coarse-grained, hornblendite pegmatoids. In highly coarse portions the hornblende may reach 25 cm in length. The hornblendite pegmatoids are composed essentially of black amphibole with accessory plagioclase. Very often, the pegmatites and hornblendites grade into one another. The rocks of minor pegmatites show variation in their textures and some rocks show foliation and deformation.

Hornblende is coarse-grained and pleochroic from brownish green to dark green (Plate 5.18). In some rocks its boundaries are corroded away and accompanied by epidote and chlorite. Plagioclase crystals range in size from very coarse- to medium-grained and they are invariably anhedral. It is mainly andesine in composition but some is labradorite or, rarely, oligoclase. All the grains with high anorthite content (An_{40-60}), are large in size, highly clouded with epidote and sericite, and show poor twinning. On the other hand, the plagioclase with low anorthite content (An_{26-40}) is fresh, shows good twinning and its crystal size is small (Plate 5.19). Inclusions are not present in it but epidote and sericite are present along the boundaries. It shows myrmekitic intergrowth with quartz. It is possible that the former are igneous relics and the latter are metamorphic.

One sample (A152) in which plagioclase ranges from An_{32} to An_{36} , and shows inclusions of fine-grained mineral with high relief, likely epidote. Biotite also shows similar inclusions. Crystal boundaries of plagioclase are visible and demarcated by black lines in this sample. Quartz occurs in the form of milky white finely crystalline aggregates (Plate 5.20). It is medium- to coarse-grained and anhedral to subhedral. In some rocks it shows undoluse extinction.

Table 5.3. Modal Composition of dioritic and granitic pegmatoids.

Sample Nos.	A-231	A-161	A-194	A-107	A-152
Feldspar	25	40	45	50	40
Amphibole	2	10	8		2
Quartz	18	30	10	40	45
Chlorite	8	1	20		tr
Epidote	45	4	5	5	2
Biotite		8	5	2	5
Sphene			2	1	1
Iron Ore	1	2	1	tr	3
Muscovite/ Sericite	1	4	4	2	1
Apatite		tr	tr		
Garnet		1			

Key: A231, 194 (diorite-Buto); A161 (granodiorite-Thak) and A107, 152 (granite- Buto and Thor respectively).

Table 5.4. Modal Composition of Trondhjemites.

Sample Nos.	A-209	A-62	A-124	A-59	A-211
Feldspar	48	50	60	30	53
Amphibole	11	12	10	40	5
Quartz	25	30	25	20	30
Chlorite	7				
Epidote	2	5	1	7	5
Biotite	1		2		5
Sphene	1				
Iron Ore	2	2	tr		
Muscovite/ Sericite	2	1		1	2
Apatite				1	
Garnet	1		2	1	

Key: A209, 124, 211 (Buto) and A62, 59 (Thak)

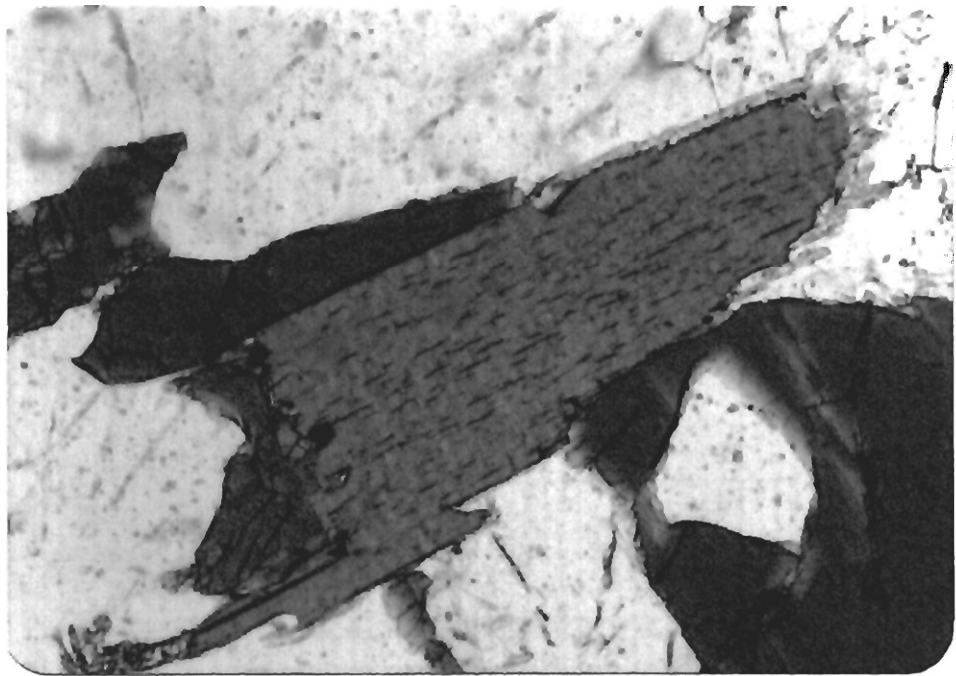


Plate 5.18. Diorite from the south of Thak consisting of feldspar, quartz, hornblende and biotite. Field of view is 4 mm.



Plate 5.19. Photograph from the same rock of Plate 5.18 consisting of plagioclase, quartz with amphibole and biotite. Field of view is 2.5 mm.

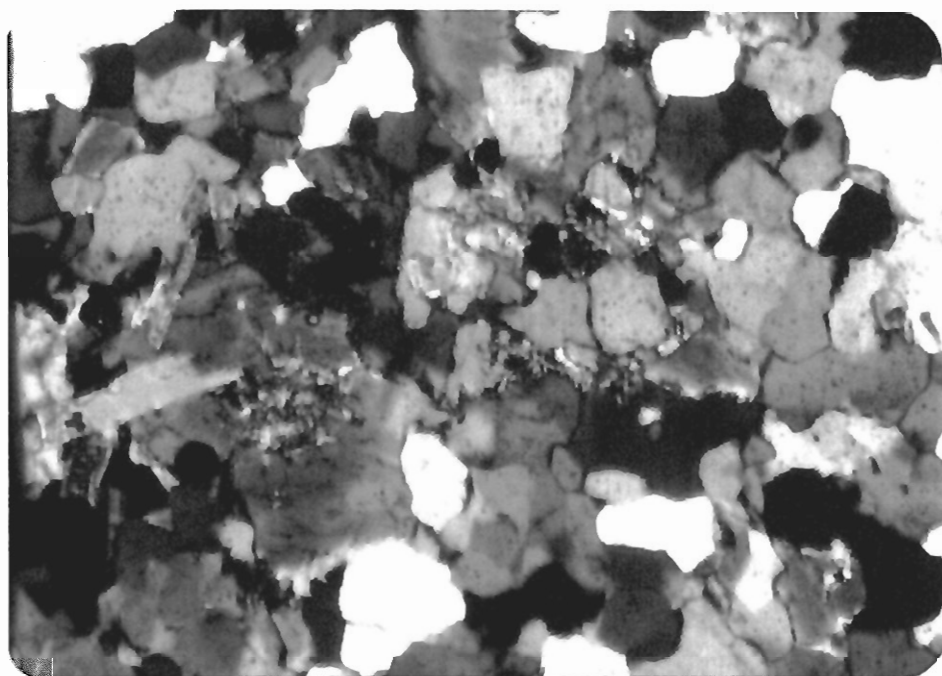


Plate 5.20. Granite from minor body at Gabbar consisting of quartz, feldspar, biotite, muscovite and sphene. Feldspar shows inclusion in the core. Quartz is medium- to coarse-grained and anhedral to subhedral quartz. Field of view is 2.5 mm.

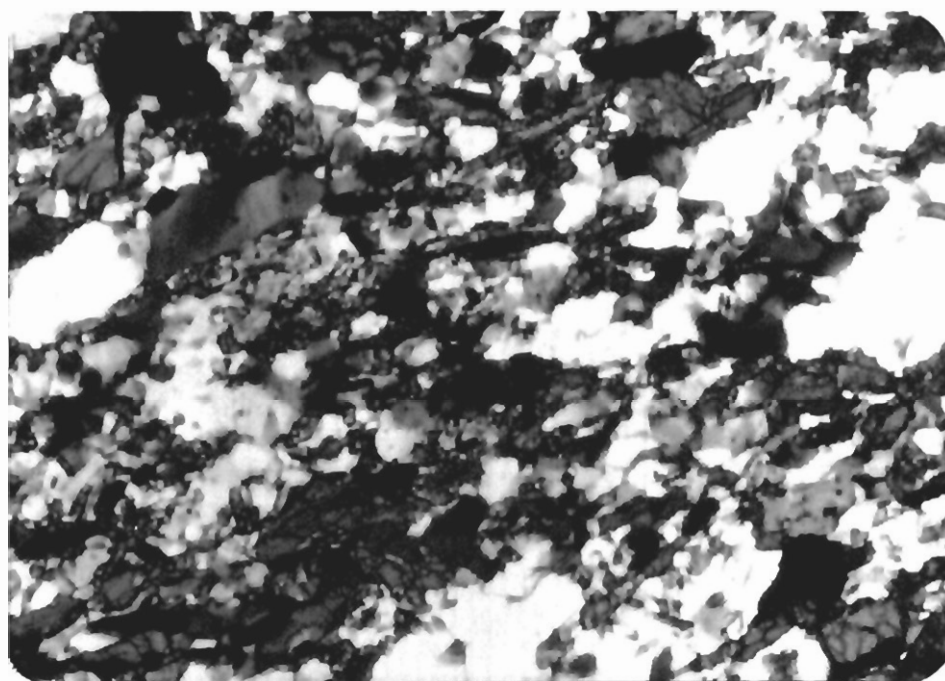


Plate 5.21. Trondhjemite from north of Ulla Babusar consisting of feldspar, quartz, amphibole and epidote. All the minerals show parallel alignment in one major direction. Field of view is 4 mm.

Granitic and Trondhjemitic Pegmatites

These contain alternating bands of quartz and amphibole, and show parallel alignment of mineral grains in one major direction. Quartz and amphibole grains show elongation and rotation (Plate 5.21). Overall the rocks are looking fresh but contain inclusions of sericite and epidote in plagioclase. Feldspar, amphibole and quartz are the main constituents of the rocks with minor epidote, muscovite, biotite, sphene, garnet and ore. Modal compositions of the trondhjemitic rocks are given in Table 5.4.

Plagioclase is the most abundant phase in these lithologies and as a whole comprises from 30% to 70% volume in the rocks. Two types of plagioclase crystals are recognized in these rocks. One are distinctly coarser-grained, subhedral to euhedral and with inclusions of epidote, sericite and at places biotite in cores (Plate 5.22). The content of anorthite ranges from 26% to 42% in most of the rocks. Andesine is prominent but in some rocks oligoclase is also present. One sample (A124) also contains labradorite and shows a higher content of anorthite (up to 64%). Plagioclase is generally unzoned but in sample (A209) it displays a strong normal zoning (An_{38} core to An_{30} rim) (Plate 5.23). The other type of crystals are fine-to medium-grained and usually in mutual contact with perthite + myrmekite. They are always unzoned and have an average composition of $An_{26 \pm 2}$ (Plate 5.24). They show a lot of inclusions of sericite but at places where, they are present in the aggregate of quartz are without inclusions. Epidote, biotite and muscovite are present along the margins of all the plagioclase crystals irrespective of their crystal size. In some rocks plagioclase with average $An_{50 \pm 2}$ gives blue tinge in cross light.

Hornblende is prismatic, subhedral to euhedral and medium-grained. It shows dark green colour in plain light with different anomalous colours (yellow



Plate 5.22. Trondhjemite from south of Rehmal consisting of feldspar, quartz, amphibole, biotite, epidote and sphene. Coarse-grained and subhedral to euhedral plagioclase show inclusions of epidote, sericite and at places biotite in cores. Field of view is 2.5 mm.



Plate 5.23. Trondhjemite consisting of feldspar, quartz, amphibole, biotite and epidote. Plagioclase shows a strong normal zonation. Anorthite decreases from core to margins (An_{38} to An_{30}). Some cores are altered and contain inclusions. Field of view is 2.5 mm.

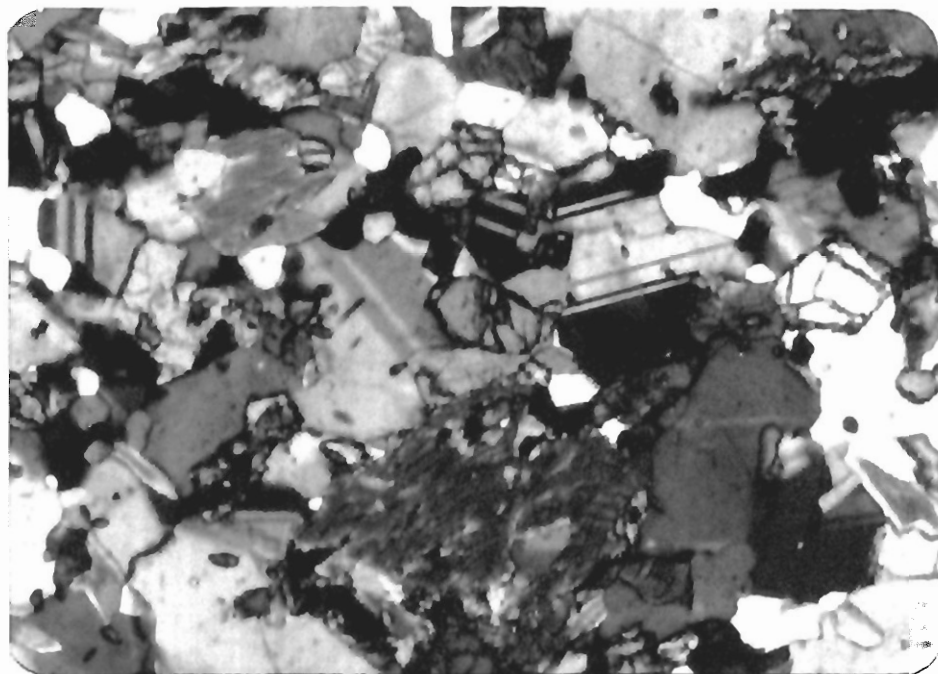


Plate 5.24. Trondhjemite from north of Halala showing plagioclase and hornblende (lower center), biotite (top left), epidote (center, grey) and quartz. Plagioclase is unzoned $An_{26} \pm 2$. Field of view is 2.5 mm.

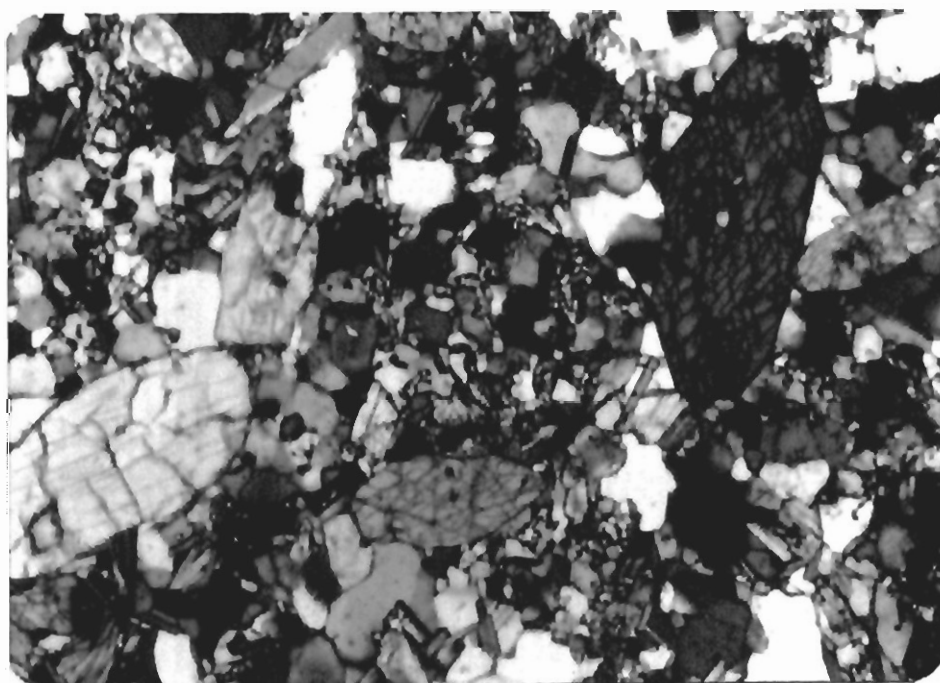


Plate 5.25. Trondhjemite from Uta Babusar showing the prismatic, subhedral to euhedral and medium-grained hornblende crystals with perfect cleavage. Other minerals are quartz, feldspar, epidote and muscovite. Field of view is 4 mm.

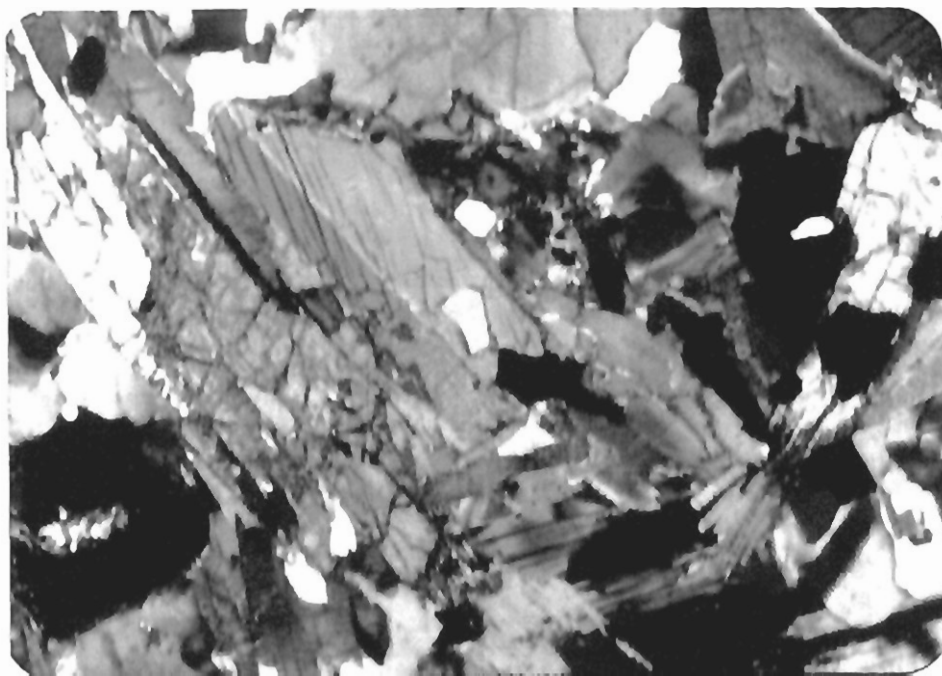


Plate 5.26. Trondhjemite from north of Tushkal showing plagioclase (locally cloudy), quartz, biotite and epidote. Note some of the biotite is elongated oblique to schistosity. Field of view is 2.5 mm.

green, yellow, and green) in cross light and perfect cleavage (Plate 5.25). It is commonly found within a biotite and epidote assemblage (Plate 5.26). In some rocks, euhedral sphene occurs as inclusions in the hornblende. Quartz makes up approximately 25 volume percent of the granitic and trondhjemitic rocks and varies from 0.2 to 3 mm in diameter. It is generally anhedral in shape and exhibits a highly undulose extinction. Epidote, sphene and magnetite represent the accessory phases in these rocks. Sphene occurs as discrete brown euhedral crystals, but is also common as inclusions in biotite and hornblende. Epidote occurs as euhedral to subhedral grains of uniform size.

Geochemistry

Major and trace element data have been obtained for fifty-three representative rocks from granitoid sheets. The data are presented in Table (5.5).

Classification

Several schemes based on chemical composition have been applied for the classification and nomenclature of the studied rocks.

I. A version of the binary plot involving SiO_2 vs Total Alakalis (Cox et al., 1979; Le Bas et al., 1986; Le Maitre et al. 1989) adopted for plutonic rocks (e.g., Wilson, 1985) shows that the rocks of the intrusive complex have a wide compositional variation spanning the fields of ultrabasic, basic, intermediate and acidic igneous rocks (Figure 5.1). According to this scheme the studied rocks classify as gabbro (7 samples), gabbroic-diorite (6 samples), diorite (13 samples), granodiorite (14 samples) and granite (13 samples). Additionally, this diagram portrays a subalkaline character of the studied suite of samples.

II. The classification scheme of De La Roche et al. (1980) involving recasting the whole-rock chemical composition into cationic proportions yields

Table 5.5. Geochemical data of selected rock types from the Thak granitoid sheets.

SAMPLE	A-128	A-126	A-110	A-97	A-136	BS04A	A-164	BS39
SiO ₂	43.33	46.62	47.04	48.56	49.50	50.80	51.92	52.17
TiO ₂	0.77	0.40	0.81	0.87	0.34	1.00	1.14	0.56
Al ₂ O ₃	20.60	21.46	20.00	18.36	16.13	15.17	18.81	20.04
Fe ₂ O ₃	13.06	11.16	7.72	11.28	6.92	12.56	10.72	8.50
MgO	6.40	5.36	10.15	6.86	10.60	8.19	4.33	4.97
CaO	14.34	12.28	11.71	11.70	14.81	9.44	9.25	10.01
Na ₂ O	1.33	2.33	2.43	2.10	1.64	2.01	3.42	3.21
K ₂ O	0.16	0.25	0.07	0.19	0.04	0.39	0.24	0.24
P ₂ O ₅	0.01	0.14	0.06	0.08	0.01	0.09	0.18	0.12
Total	100.00	100.00	99.99	100.00	99.99	99.65	100.01	99.82
Ti	4616.00	2398.00	4856.00	5216.00	2038.00	5995.00	6834.00	3357.00
K	1328.00	2075.00	581.00	1577.00	332.00	3238.00	1992.00	1992.00
P	44.00	611.00	262.00	349.00	44.00	393.00	786.00	524.00
Nb	1.00	2.60	0.80	2.90	1.00	6.00	3.10	2.50
Zr	6.00	58.00	50.00	48.00	9.00	70.50	70.00	31.80
Y	9.00	16.00	17.00	27.00	13.00	48.30	28.00	12.90
Sr	219.00	436.00	209.00	210.00	128.00	148.40	256.00	269.00
Rb	1.00	11.00	1.00	2.00	1.00	7.60	1.00	4.30
Th	2.00	2.00	2.00	2.00	2.00	0.30	2.00	
Pb	2.00	2.00	2.00	2.00	2.00	1.40	2.00	2.30
Ga	18.00	15.00	14.00	18.00	13.00	17.00	25.00	17.00
Zn	64.00	51.00	52.00	75.00	37.00	183.00	69.00	77.00
Cu	46.00	102.00	33.00	61.00	65.00	1097.00	5.00	33.00
Co	67.00	49.00	62.00	69.00	63.00		49.00	
Ni	2.00	57.00	232.00	36.00	117.00	187.00	8.00	23.00
Cr						485.00		53.00
V						217.00		161.00
Sc						33.00		25.00
Ba						72.00		101.00
La						7.00		3.50
Ce						28.30		9.70
Nd						20.40		6.00
Simcation	721.45	776.22	783.22	808.52	824.18	845.82	864.47	868.63
Ti	10.00	5.00	10.00	11.00	4.00	13.00	14.00	7.00
Al	404.00	421.00	392.00	360.00	316.00	298.00	369.00	393.00
Fe	164.00	140.00	97.00	141.00	87.00	157.00	134.00	106.00
Mg	159.00	133.00	252.00	170.00	263.00	203.00	107.00	123.00
Ca	256.00	219.00	209.00	209.00	264.00	168.00	165.00	178.00
Na	43.00	75.00	78.00	68.00	53.00	65.00	110.00	104.00

Figure 5.5 continued

SAMPLE	A-106	BS01	A-165	A-130	A-160	BS38	A-163	A-141
SiO ₂	52.60	53.92	54.59	54.79	55.08	56.63	56.91	56.94
TiO ₂	0.91	0.36	0.67	1.26	1.14	0.57	0.57	0.40
Al ₂ O ₃	15.15	20.28	18.11	15.79	18.05	18.92	19.16	16.75
Fe ₂ O ₃	8.57	7.46	8.86	11.72	9.89	7.49	7.34	6.56
MgO	8.60	3.37	5.60	4.13	3.82	3.65	3.44	5.87
CaO	10.13	8.53	9.42	8.40	8.50	8.80	8.29	9.82
Na ₂ O	3.67	5.83	2.53	2.94	3.02	3.32	3.77	2.51
K ₂ O	0.25		0.15	0.83	0.32	0.30	0.40	1.06
P ₂ O ₅	0.16	0.09	0.07	0.13	0.18	0.15	0.13	0.09
Total	100.04	99.84	100.00	99.99	100.00	99.83	100.01	100.00
Ti	5456.00	2158.00	4017.00	7554.00	6834.00	3417.00	3417.00	2398.00
K	2075.00		1245.00	6890.00	2657.00	2490.00	3321.00	8800.00
P	698.00	393.00	306.00	567.00	786.00	655.00	567.00	393.00
Nb	6.90	1.90	3.50	4.10	4.70	2.60	2.30	1.50
Zr	160.00	30.50	74.00	68.00	104.00	55.50	51.00	37.00
Y	49.00	11.70	38.00	26.00	44.00	13.10	13.00	13.00
Sr	211.00	261.00	245.00	269.00	219.00	267.00	259.00	234.00
Rb	2.00	0.50	2.00	19.00	3.00	6.90	7.00	30.00
Th	2.00	0.60	2.00	2.00	2.00	0.30	2.00	2.00
Pb	2.00	2.30	2.00	2.00	2.00	2.00	2.00	4.00
Ga	18.00	14.00	20.00	18.00	20.00	17.00	18.00	13.00
Zn	69.00	57.00	87.00	88.00	96.00	71.00	76.00	55.00
Cu	9.00	20.00	32.00	17.00	6.00	17.00	21.00	19.00
Co	48.00		58.00	42.00	46.00		40.00	53.00
Ni	113.00	7.00	24.00	2.00	6.00	16.00	7.00	43.00
Cr		4.00				32.00		
V		100.00				135.00		
Sc		15.00				20.00		
Ba		28.00				126.00		
La		2.30				3.80		
Ce		6.40				8.60		
Nd		4.20				5.00		
Simcatio	875.79	897.77	908.92	912.25	917.08	942.89	947.55	948.05
Ti	11.00	5.00	8.00	16.00	14.00	7.00	7.00	5.00
Al	297.00	398.00	355.00	310.00	354.00	371.00	376.00	329.00
Fe	107.00	93.00	111.00	147.00	124.00	94.00	92.00	82.00
Mg	213.00	84.00	139.00	102.00	95.00	91.00	85.00	146.00
Ca	181.00	152.00	168.00	150.00	152.00	157.00	148.00	175.00
Na	118.00	188.00	82.00	95.00	97.00	107.00	122.00	81.00

Figure 5.5 continued

SAMPLE	A-162	A-102	BS26	BS37	A-143	A-139	A-100	A-166
SiO ₂	58.20	58.67	59.46	60.59	60.84	60.97	60.98	62.14
TiO ₂	0.58	0.59	1.30	0.49	0.71	0.31	0.64	0.52
Al ₂ O ₃	18.80	19.06	13.83	18.03	16.87	19.00	18.23	17.52
Fe ₂ O ₃	7.08	6.42	10.52	5.99	7.36	5.59	5.65	5.98
MgO	3.25	3.34	2.81	2.96	3.34	1.69	2.60	2.47
CaO	7.96	6.17	7.50	7.48	6.27	7.85	5.59	6.61
Na ₂ O	3.80	5.04	3.95	3.70	3.37	3.23	5.71	3.71
K ₂ O	0.20	0.61	0.06	0.49	1.07	1.25	0.43	0.94
P ₂ O ₅	0.13	0.11	0.45	0.13	0.17	0.12	0.17	0.11
Total	100.00	100.01	99.88	99.86	100.00	100.01	100.00	100.00
Ti	3477.00	3537.00	7794.00	2938.00	4257.00	1858.00	3837.00	3117.00
K	1660.00	5064.00	498.00	4068.00	8883.00	10377.00	3570.00	7804.00
P	567.00	480.00	1964.00	567.00	742.00	524.00	742.00	480.00
Nb	2.20	3.00	10.10	3.10	3.10	2.40	2.80	4.90
Zr	66.00	65.00	475.00	130.00	75.00	59.00	77.00	121.00
Y	16.00	15.00	108.10	22.20	24.00	18.00	14.00	24.00
Sr	286.00	393.00	226.00	258.00	180.00	359.00	420.00	219.00
Rb	3.00	28.00	0.70	11.00	27.00	44.00	20.00	26.00
Th	2.00	2.00	1.70		3.00	3.00	2.00	3.00
Pb	2.00	6.00	0.60	1.80	2.00	2.00	2.00	2.00
Ga	17.00	21.00	21.00	17.00	17.00	17.00	19.00	16.00
Zn	63.00	114.00	34.00	64.00	65.00	51.00	111.00	79.00
Cu	5.00	101.00	85.00	19.00	2.00	9.00	83.00	5.00
Co	46.00	36.00			34.00	28.00	24.00	47.00
Ni	7.00	19.00	16.00	16.00	17.00	2.00	10.00	7.00
Cr			24.00	39.00				
V			90.00	96.00				
Sc			17.00	15.00				
Ba			20.00	151.00				
La			8.00	4.50				
Ce			29.30	12.40				
Nd			27.20	8.80				
Simcatio	969.03	976.86	990.01	1008.83	1012.99	1015.15	1015.32	1034.63
Ti	7.00	7.00	16.00	6.00	9.00	4.00	8.00	7.00
Al	369.00	374.00	271.00	354.00	331.00	373.00	358.00	344.00
Fe	89.00	80.00	132.00	75.00	92.00	70.00	71.00	75.00
Mg	81.00	83.00	70.00	73.00	83.00	42.00	64.00	61.00
Ca	142.00	110.00	134.00	133.00	112.00	140.00	100.00	118.00
Na	123.00	163.00	127.00	119.00	109.00	104.00	184.00	120.00

Figure 5.5 continued

SAMPLE	A-161	A-96	BS30A	BS36	BS29	A-167	A-62	BS28
SiO ₂	62.23	62.78	62.86	62.98	63.45	63.49	63.86	64.80
TiO ₂	0.67	0.52	0.29	0.49	0.29	0.48	1.21	0.24
Al ₂ O ₃	16.93	17.37	18.02	16.95	17.53	17.58	14.05	17.72
Fe ₂ O ₃	7.21	5.69	4.98	5.86	4.90	5.67	9.09	3.96
MgO	2.75	2.26	1.85	2.34	1.84	2.31	2.24	1.57
CaO	6.65	6.50	7.16	6.61	7.12	6.45	4.16	6.50
Na ₂ O	3.09	4.08	3.22	3.67	3.21	2.99	5.11	4.00
K ₂ O	0.36	0.68	1.28	0.85	1.34	0.94	0.01	0.95
P ₂ O ₅	0.12	0.12	0.16	0.12	0.16	0.10	0.29	0.12
Total	100.01	100.00	99.82	99.87	99.84	100.01	100.02	99.86
Ti	4017.00	3117.00	1739.00	2938.00	1739.00	2878.00	7254.00	1439.00
K	2989.00	5645.00	10626.00	7056.00	11124.00	7804.00	83.00	7887.00
P	524.00	524.00	698.00	524.00	698.00	436.00	1266.00	524.00
Nb	4.50	4.30	4.30	4.90	4.00	4.30		5.90
Zr	160.00	132.00	59.40	113.00	57.50	108.00		53.10
Y	36.00	27.00	14.30	23.90	14.10	23.00		11.70
Sr	237.00	236.00	470.00	236.00	458.00	229.00		441.00
Rb	8.00	18.00	47.70	22.40	50.90	26.00		34.10
Th	2.00	2.00	6.40	1.30	6.80	2.00		6.20
Pb	3.00	2.00	4.40	2.80	5.40	2.00		3.90
Ga	18.00	17.00	17.00	17.00	16.00	16.00		16.00
Zn	77.00	68.00	55.00	73.00	55.00	71.00		55.00
Cu	17.00	19.00	7.00	20.00	7.00	33.00		9.00
Co	67.00	46.00				43.00		
Ni	3.00	5.00	7.00	13.00	7.00	3.00		5.00
Cr			9.00	36.00	24.00			5.00
V			67.00	97.00	67.00			49.00
Sc			7.00	13.00	7.00			6.00
Ba			772.00	239.00	787.00			578.00
La			14.00	5.60	15.90			12.20
Ce			25.00	14.80	27.00			23.30
Nd			10.70	9.60	11.20			8.70
Simcatio	1036.13	1045.29	1046.62	1048.62	1056.44	1057.11	1063.27	1078.92
Ti	8.00	7.00	4.00	6.00	4.00	6.00	15.00	3.00
Al	332.00	341.00	354.00	333.00	344.00	345.00	276.00	348.00
Fe	90.00	71.00	62.00	73.00	61.00	71.00	114.00	50.00
Mg	68.00	56.00	46.00	58.00	46.00	57.00	56.00	39.00
Ca	119.00	116.00	128.00	118.00	127.00	115.00	74.00	116.00
Na	100.00	132.00	104.00	118.00	104.00	96.00	165.00	129.00

Figure 5.5 continued

SAMPLE	BS2	BS1	BS25	A-87	A-113	A-65	A-144	A-146
SIO2	65.47	65.76	67.25	68.78	68.92	70.42	70.66	70.82
TIO2	0.38	0.42	0.60	0.49	0.13	0.15	0.41	0.51
AL2O3	17.71	17.45	13.37	15.29	17.36	16.91	14.66	15.15
FE2O3	3.94	3.97	8.43	4.30	2.42	2.60	3.92	2.79
MGO	1.31	1.37	0.53	1.32	0.73	0.93	0.94	0.97
CAO	5.54	5.85	4.45	3.65	4.44	4.07	3.15	4.06
NA2O	4.86	4.51	5.17	3.97	5.21	2.97	4.12	5.35
K2O	0.55	0.46	0.02	2.06	0.70	1.89	2.04	0.25
P2O5	0.16	0.13	0.16	0.14	0.09	0.06	0.09	0.11
Total	99.92	99.92	99.98	100.00	100.00	100.00	99.99	100.01
Ti	2278.00	2518.00	3597.00	2938.00	779.00	899.00	2458.00	3058.00
K	4566.00	3819.00	166.00	17101.00	5811.00	15690.00	16935.00	2075.00
P	698.00	567.00	698.00	611.00	393.00	262.00	393.00	480.00
Nb	1.70	1.60	21.40	7.10	3.30		5.60	6.70
Zr	78.20	81.00	707.00	112.00	71.00		62.00	151.00
Y	9.50	9.10	204.00	22.00	9.00		9.00	29.00
Sr	497.00	525.00	182.00	190.00	287.00		677.00	204.00
Rb	11.30	9.90		75.00	29.00		63.00	4.00
Th	3.20		2.20	7.00	2.00		3.00	6.00
Pb	2.90	3.20	1.10	6.00	3.00		5.00	2.00
Ga	18.00	18.00	27.00	16.00	14.00		16.00	15.00
Zn	66.00	64.00	14.00	58.00	35.00		64.00	26.00
Cu	3.00	5.00	3.00	9.00	4.00		5.00	2.00
Co				24.00	20.00		25.00	30.00
Ni	6.00	5.00	6.00	3.00	2.00		2.00	2.00
Cr	7.00	8.00	3.00					
V	56.00	55.00	3.00					
Sc	7.00	8.00	8.00					
Ba	204.00	197.00	15.00					
La	19.10	2.20	13.10					
Ce	40.00	3.60	47.30					
Nd	16.30	4.60	46.20					
Simcatio	1090.08	1094.91	1119.71	1145.19	1147.52	1172.49	1176.49	1179.15
Ti	5.00	5.00	8.00	6.00	2.00	2.00	5.00	6.00
Al	347.00	342.00	262.00	300.00	341.00	332.00	288.00	297.00
Fe	49.00	50.00	106.00	54.00	30.00	33.00	49.00	35.00
Mg	32.00	34.00	13.00	33.00	18.00	23.00	23.00	24.00
Ca	99.00	104.00	79.00	65.00	79.00	73.00	56.00	72.00
Na	157.00	145.00	167.00	128.00	168.00	96.00	133.00	173.00

Figure 5.5 continued

SAMPLE	A-88	A-103	A-91	A-155	A-104	A-99	A-108	A-124
SiO ₂	70.96	70.99	71.66	72.89	73.02	73.21	73.54	73.98
TiO ₂	0.40	0.11	0.36	0.33	0.11	0.08	0.35	0.33
Al ₂ O ₃	14.75	16.88	14.64	16.15	15.70	15.67	13.70	14.04
Fe ₂ O ₃	3.37	1.43	3.33	1.24	1.34	1.18	3.59	2.77
MgO	1.00	0.48	0.93	0.39	0.55	0.43	0.68	1.01
CaO	3.21	3.17	2.99	3.91	3.23	2.53	2.65	2.07
Na ₂ O	4.12	6.25	3.96	4.74	5.79	6.56	4.31	2.97
K ₂ O	2.09	0.68	2.03	0.35	0.24	0.31	1.10	2.79
P ₂ O ₅	0.10	0.01	0.10	0.01	0.02	0.03	0.08	0.04
Total	100.00	100.00	100.00	100.01	100.00	100.00	100.00	100.00
Ti	2398.00	659.00	2158.00	1978.00	659.00	480.00	2098.00	1978.00
K	17350.00	5645.00	16852.00	2906.00	1992.00	2573.00	9132.00	23161.00
P	436.00	44.00	436.00	44.00	87.00	131.00	349.00	175.00
Nb	6.20	1.20	6.40	2.90	1.90	2.30	4.00	19.00
Zr	93.00	44.00	98.00	375.00	56.00	23.00	198.00	239.00
Y	19.00	14.00	22.00	9.00	4.00	7.00	12.00	41.00
Sr	167.00	236.00	150.00	338.00	336.00	265.00	172.00	123.00
Rb	67.00	22.00	89.00	6.00	26.00	11.00	27.00	68.00
Th	8.00	2.00	8.00	2.00	2.00	4.00	4.00	6.00
Pb	2.00	3.00	2.00	4.00	4.00	5.00	4.00	5.00
Ga	15.00	14.00	13.00	11.00	13.00	12.00	14.00	15.00
Zn	41.00	34.00	29.00	25.00	44.00	30.00	46.00	57.00
Cu	2.00	5.00	2.00	2.00	18.00	12.00	2.00	16.00
Co	45.00	32.00	31.00	37.00	30.00	37.00	24.00	34.00
Ni	2.00	2.00	2.00	2.00	2.00	2.00	2.00	2.00
Cr								
V								
Sc								
Ba								
La								
Ce								
Nd								
Simcatio	1181.49	1181.99	1193.14	1213.62	1215.78	1218.95	1224.44	1231.77
Ti	5.00	1.00	5.00	4.00	1.00	1.00	4.00	4.00
Al	289.00	331.00	287.00	317.00	308.00	307.00	269.00	275.00
Fe	42.00	18.00	42.00	16.00	17.00	15.00	45.00	35.00
Mg	25.00	12.00	23.00	10.00	14.00	11.00	17.00	25.00
Ca	57.00	57.00	53.00	70.00	58.00	45.00	47.00	37.00
Na	133.00	202.00	128.00	153.00	187.00	212.00	139.00	96.00

Figure 5.5 continued

SAMPLE	A-129	A-149	A-123	A-127	A-71
SiO ₂	74.68	75.07	75.28	75.37	75.99
TiO ₂	0.06	0.04	0.02	0.04	0.09
Al ₂ O ₃	15.21	15.09	14.66	15.22	15.04
Fe ₂ O ₃	0.64	0.70	0.56	0.99	0.73
MgO	0.21	0.48	0.17	0.34	0.33
CaO	2.77	1.55	1.03	1.47	3.30
Na ₂ O	5.80	3.36	5.34	4.78	4.16
K ₂ O	0.61	3.68	2.92	1.67	0.36
P ₂ O ₅	0.01	0.03	0.02	0.03	0.02
Total	99.99	100.00	100.00	99.91	100.02
Ti	360.00	240.00	120.00	240.00	540.00
K	5064.00	30550.00	24241.00	13864.00	2989.00
P	44.00	131.00	87.00	131.00	87.00
Nb	1.20	8.90	15.00	5.80	
Zr	104.00	27.00	54.00	9.00	
Y	3.00	20.00	29.00	23.00	
Sr	260.00	94.00	25.00	167.00	
Rb	24.00	89.00	71.00	55.00	
Th	2.00	5.00	2.00	2.00	
Pb	5.00	15.00	12.00	8.00	
Ga	12.00	15.00	17.00	17.00	
Zn	25.00	27.00	22.00	43.00	
Cu	2.00	2.00	2.00	2.00	
Co	35.00	38.00	36.00	36.00	
Ni	2.00	2.00	2.00	2.00	
Cr					
V					
Sc					
Ba					
La					
Ce					
Nd					
Simcatio	1243.42	1249.92	1253.41	1254.91	1265.24
Ti	1.00	1.00		1.00	1.00
Al	298.00	296.00	288.00	299.00	295.00
Fe	8.00	9.00	7.00	12.00	9.00
Mg	5.00	12.00	4.00	8.00	8.00
Ca	49.00	28.00	18.00	26.00	59.00
Na	187.00	108.00	172.00	154.00	134.00

Symbols: ○ gabbro; ■ diorite; ◇ granodiorite; ▲ tonalite; ▼ trondhjemite;
× andesite and ▴ dacite

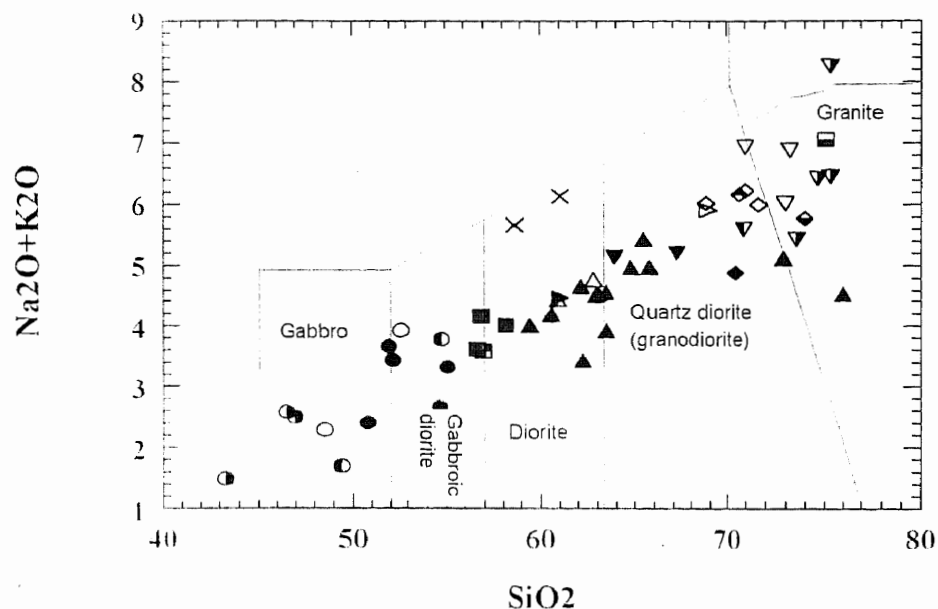


Figure 5.1. Chemical classification and nomenclature of granitoid rocks using the total alkalis versus silica (TAS) diagram (after Le Bas et al., 1986).

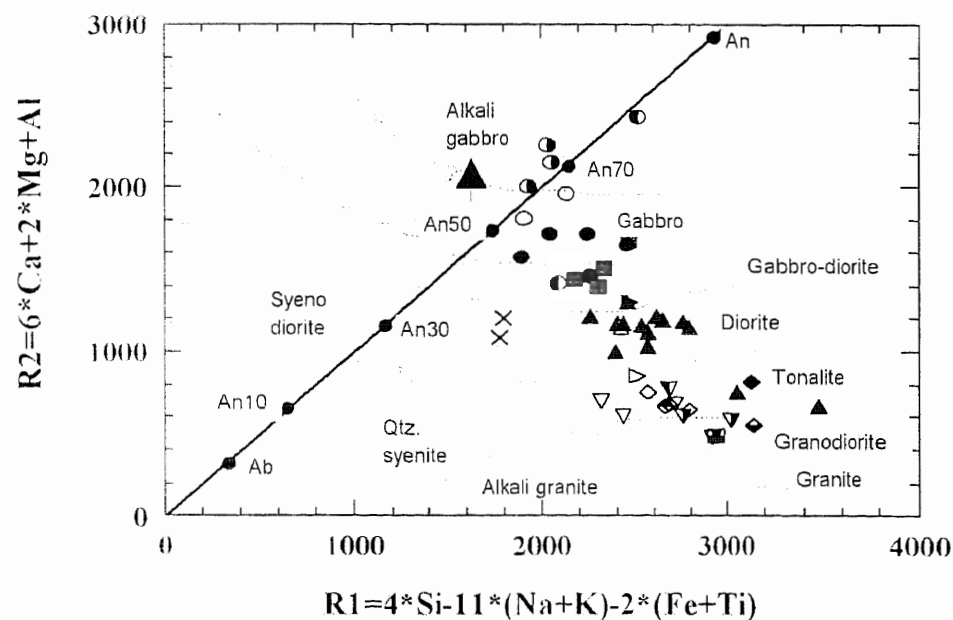


Figure 5.2. Classification of plutonic rocks using the parameters of De la Roche et al. (1980), calculated from milli cation proportions.

mixed results. The regrouping of cations is such that the x-axis (R1) of the diagram portrays variation in quartz content while the y-axis (R2) portrays variations in Mg/Fe ratio and An content of the constituent plagioclase. For basic rocks with common assemblages (plagioclase, pyroxenes and olivine), this classification scheme portrays their compositions satisfactorily. However, for basic and intermediate rocks containing cumulus amphibole, the R2 becomes unrealistically high, resulting in the classification of gabbroic rocks as ultrabasic and those of diorites as gabbros. For the same reason, a greater number of studied diorite and gabbroic samples classify as gabbros and ultrabasics in this classification scheme (Figure 5.2). This classification scheme is, however, useful in distinguishing tonalites from diorites, granodiorites and granites, which is not possible in SiO_2 vs Total Alkalis plot. Fifteen of the studied samples are plotted in the field of gabbro/olivine gabbro, seventeen in different fields of diorite (e.g., monzonite, monzodiorite and diorite), nine in tonalite, two in quartz monzonite, five in granodiorite and five in granite.

III. The classification scheme of DeBon and LeFort (1983) involves recasting of whole-rock major element composition into milications in a fashion very similar to that of De La Roche et al. (1980). Like the scheme of De La Roche et al. (1980), this classification scheme subdivides intermediate to acidic rocks into diorites, tonalites, granodiorites and granites (or adamalites) (Figure 5.3). In this scheme studied intrusive rocks are classified in the fields of gabbro (7 samples), quartz-diorite (13 samples), tonalite (14 samples), granodiorite (17 samples) and adamellite (3 samples).

IV. None of the above three classification schemes discriminate trondhjemites from granites, granodiorites and tonalites. This distinction may be

effectively achieved using An-Ab-Or diagram of O'Connor (1965), modified by Barker (1979). This diagram applies to felsic rocks with more than 10% normative quartz. Thirty five of the samples containing 10% or more normative quartz are classified using this scheme. Ten of the studied samples classify as trondhjemites, one as granite (A149), six as granodiorite and the rest as tonalite (Figure 5.4).

Table (5.6) summarizes classification and nomenclature of the analyzed samples from Thak granitoids using the four classification schemes outlined above. Although some of the samples are assigned similar nomenclature by most of these classification schemes, a great majority are assigned different names by different schemes. For instance, the sample A-99 with a SiO_2 content of 73.21% is classified as granite by TAS, granodiorite by R1-R2, tonalite by Q-B-F and trondhjemite by Ab-An-Or schemes. Since the studied intrusive rocks include both K_2O -rich and K_2O -poor rocks, the classification scheme of O'Connors (1965) is here preferred for the rocks containing greater than 10% normative quartz (Table 5.6; Column 5). One of these samples (A162) contains normative quartz in excess of 10%, but $\text{SiO}_2 < 60\%$, and is classified as diorite. The rest of the samples are classified into gabbros and diorites (Table 5.6, Column 2) as suggested by TAS scheme of classification. Five of the samples from the granitoids are fine-grained and thus assigned names andesite (A100, A102, BS01 and A139) and dacite (A113).

Geochemical Characteristics

In the preceding section, a detailed treatment has been given to the classification and nomenclature of the rocks constituting the Thak granitoid sheets. In the following, geochemical characteristics are evaluated to ascertain petrogenetic relations amongst the various rock types identified in the sheets. The

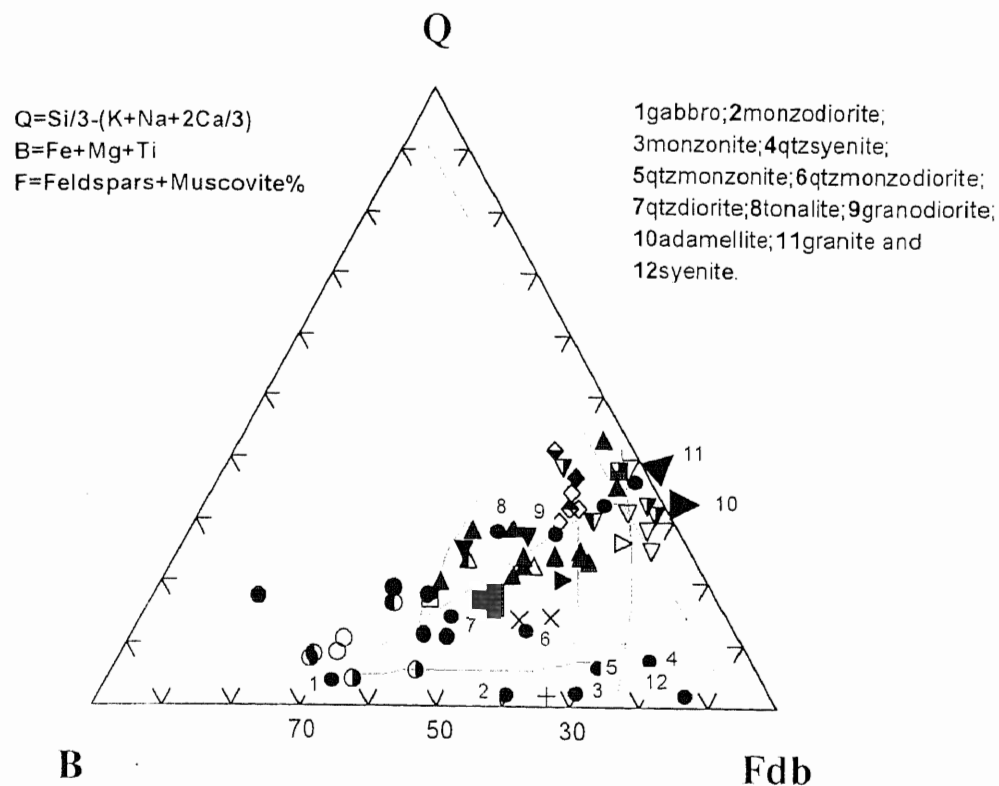


Figure 5.3. Q-B-F diagram (after Debon and Le Fort, 1983) classifying the different types of granitoid rocks

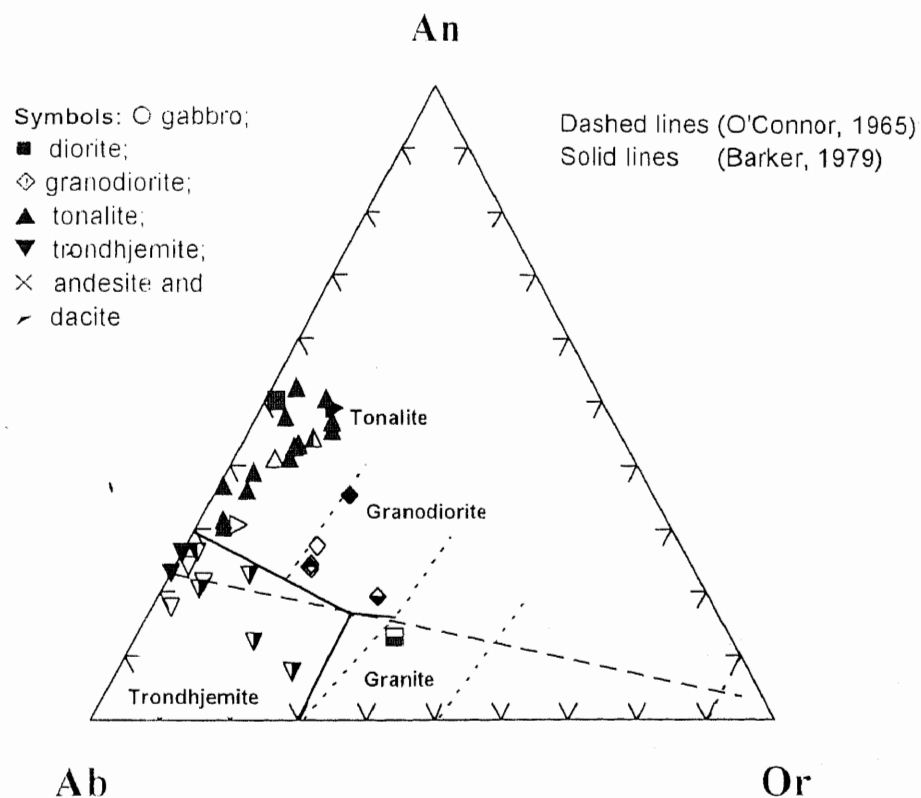


Figure 5.4. Ab-An-Or ternary plot classifying the silicic rocks (> 10% modal quartz) of Thak granitoids.

Table 5.6. Studied rocks showing different names in various classification schemes and in this study

Sample	Cox et al	De La Roche et al.	Debon & LeFort	O'Connor 1965	This Study*
A-128	Gabbro	Olivine gabbro	Gabbro		Gabbro
A-126	Gabbro	Olivine gabbro	Gabbro		Gabbro
A-110	Gabbro	Olivine gabbro	Gabbro		Gabbro
A-97	Gabbro	Olivine gabbro	Gabbro		Gabbro
A-136	Gabbro	Olivine gabbro	Gabbro		Gabbro
BS04A	Gabbro	Olivine gabbro	Gabbro		Gabbro
A-164	Gabbro diorite	Gabbro	Quartz diorite		Gabbro
BS39	Gabbro diorite	Gabbro	Quartz diorite		Gabbro
A-106	Gabbro diorite	Gabbro	Gabbro		Gabbro
BS01	Granite	Tonalite	Tonalite		Andesite
A-165	Gabbro diorite	Gabbro	Quartz diorite		Gabbro
A-130	Gabbro diorite	Gabbro	Quartz diorite		Gabbro
A-160	Gabbro diorite	Gabbro	Quartz diorite		Gabbro
BS38	Diorite	Gabbro	Quartz diorite		Diorite
A-163	Diorite	Gabbro	Quartz diorite		Diorite
A-141	Diorite	Gabbro	Quartz diorite		Diorite
A-162	Diorite	Diorite	Quartz diorite	Tonalite	Diorite
A-102	Diorite	Diorite	Quartz diorite		Andesite
BS26	Diorite	Diorite	Quartz diorite	Tonalite	Tonalite
BS37	Diorite	Diorite	Quartz diorite	Tonalite	Tonalite
A-143	Diorite	Monzodiorite	Granodiorite	Tonalite	Tonalite
A-139	Diorite	Monzodiorite	Tonalite	Tonalite	Andesite
A-100	Diorite	Monzonite	Quartz diorite		Andesite
A-166	Diorite	Diorite	Tonalite	Tonalite	Tonalite
A-161	Diorite	Tonalite	Tonalite	Tonalite	Tonalite
A-96	Diorite	Tonalite	Tonalite	Tonalite	Tonalite
BS30A	Granodiorite	Diorite	Tonalite	Tonalite	Tonalite
BS36	Granodiorite	Diorite	Granodiorite	Tonalite	Tonalite
BS29	Granodiorite	Diorite	Granodiorite	Tonalite	Tonalite
A-167	Granodiorite	Tonalite	Granodiorite	Tonalite	Tonalite
A-62	Granodiorite	Diorite	Tonalite	Trondhjemite	Trondhjemite
BS28	Granodiorite	Diorite	Tonalite	Tonalite	Tonalite
BS2	Granodiorite	Diorite	Granodiorite	Tonalite	Tonalite
BS1	Granodiorite	Diorite	Granodiorite	Tonalite	Tonalite
BS25	Granodiorite	Diorite	Granodiorite	Trondhjemite	Trondhjemite
A-87	Granodiorite	Tonalite	Granodiorite	Granodiorite	Granodiorite
A-113	Granodiorite	Tonalite	Tonalite	Tonalite	Dacite
A-65	Granodiorite	Tonalite	Granodiorite	Granodiorite	Granodiorite
A-144	Granite	Tonalite	Granodiorite	Granodiorite	Granodiorite
A-146	Granite	Tonalite	Tonalite	Trondhjemite	Trondhjemite
A-88	Granite	Tonalite	Granodiorite	Granodiorite	Granodiorite
A-103	Granite	Quartz monzonite	Tonalite	Trondhjemite	Trondhjemite
A-91	Granite	Granodiorite	Granodiorite	Granodiorite	Granodiorite
A-155	Granite	Granodiorite	Tonalite	Tonalite	Andesite
A-104	Granite	Granite	Tonalite	Trondhjemite	Trondhjemite
A-99	Granite	Granodiorite	Tonalite	Trondhjemite	Trondhjemite
A-108	Granite	Granite	Granodiorite	Trondhjemite	Trondhjemite
A-124	Granite	Granite	Adamallite	Granodiorite	Granodiorite
A-129	Granite	Granite	Tonalite	Trondhjemite	Trondhjemite
A-149	Granite	Granite	Adamallite	Granite	Granite
A-123	Granodiorite	Quartz monzonite	Adamallite	Trondhjemite	Trondhjemite
A-127	Granodiorite	Granite	Granodiorite	Trondhjemite	Trondhjemite
A-71	Granodiorite	Granodiorite	Tonalite	Tonalite	Tonalite

*Note: For adoption of names here, see details in text.

approach adopted here is to initially treat the samples collected from each of the four major traverses separately and then to attempt a synthesis for the entire complex.

Niat Gah

A total of eleven samples were analyzed from the Niat valley. These include two gabbros (A97 and A106), a tonalite (A96), three granodiorites (A87, A88 and A91), two andesites (A100 and A102) and three trondhjemites (A103, A104 and A99). Samples with numbers between 96 and 104 are from those intruding the Jal amphibolite unit, while the rest are from the sheets intrusive in the Niat metavolcanic unit. All the samples are foliated to varying extents, although trondhjemites and the andesite dykes are syn- to post-tectonic in nature as suggested by their cross-cutting field relations with the other rocks.

Several of the major and minor elements display a linear variation trends against SiO_2 for the granitoid samples from Niat Gah (Figure 5.5). These include TiO_2 , Fe_2O_3 , CaO and MgO . Other elements like Al_2O_3 , Na_2O , K_2O and P_2O_5 display scatter. Gabbros have lower Al_2O_3 than the tonalite and andesites but have the highest MgO . On Na_2O - SiO_2 plot trondhjemites and andesites are distinguished from the rest of the samples due to higher Na_2O contents. K_2O is distinctly higher in granodiorites than the rest of the samples. Amongst the trace elements, Nb and Zr, when plotted against SiO_2 , display a positive trend for the group of samples including tonalite-andesites-granodiorites, while gabbros and trondhjemites show no particular trend either mutually or with this group. Y is enriched in gabbros, has intermediate concentrations in tonalite, andesites and granodiorites, and is lowest in trondhjemites. These and all other trace elements display a considerable scatter when plotted against SiO_2 .

Symbols: ○ gabbro; × andesite; △ tonalite; ◇ granodiorite; ▽ trondhjemite

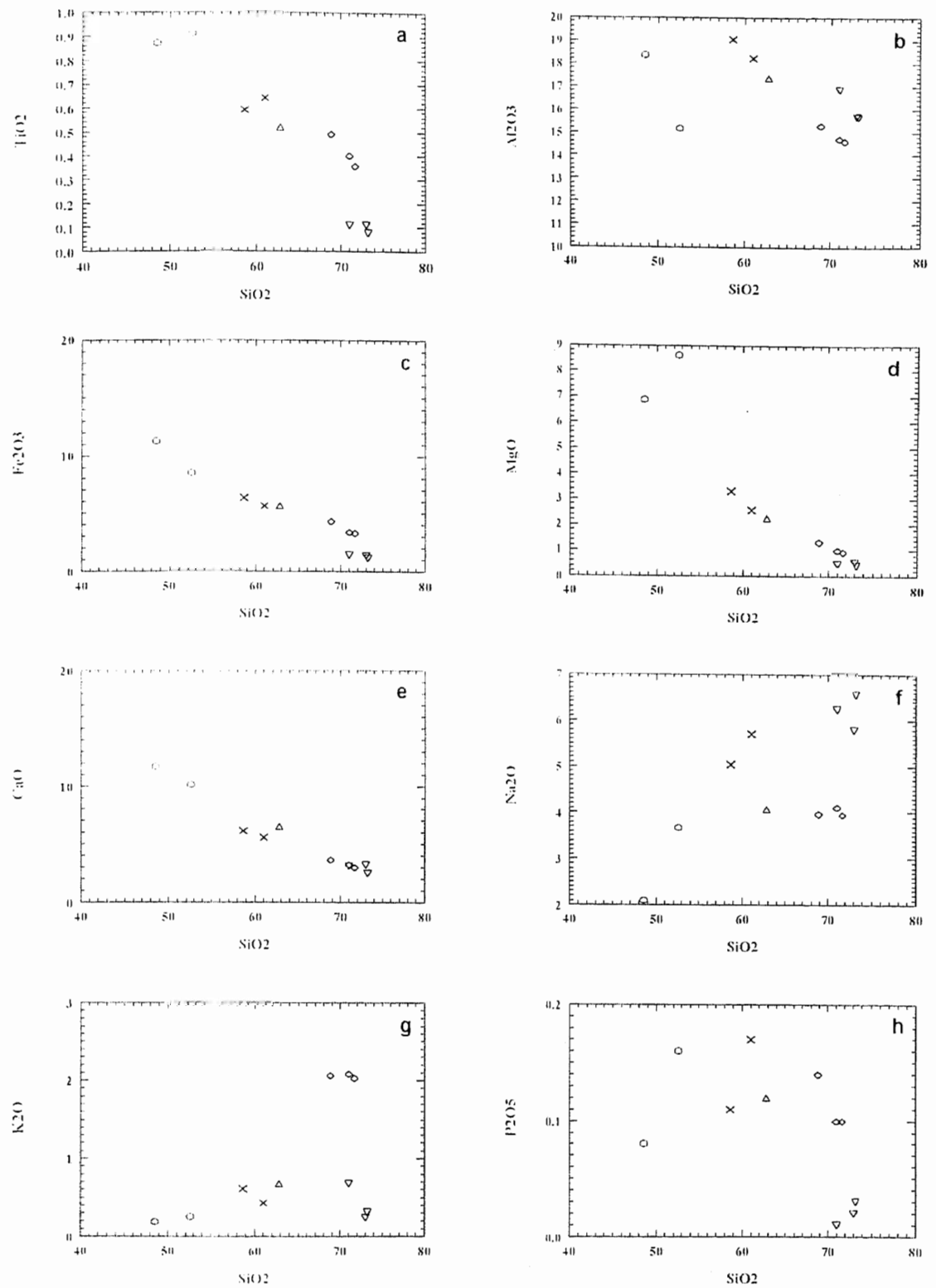
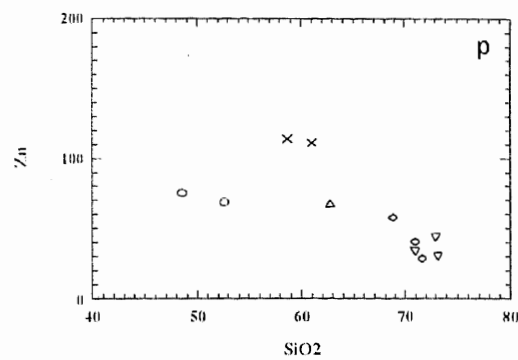
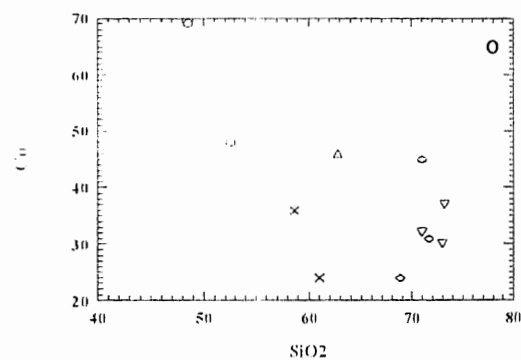
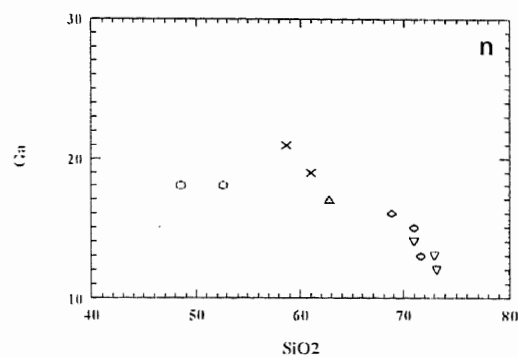
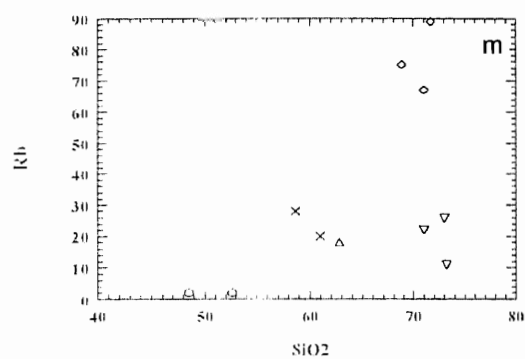
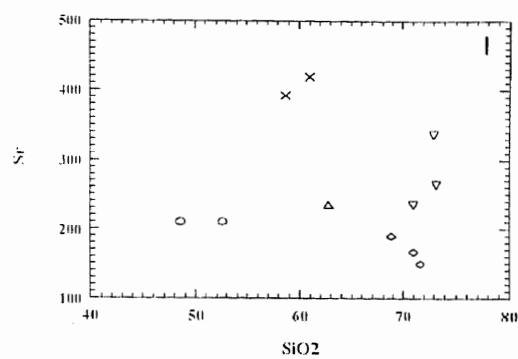
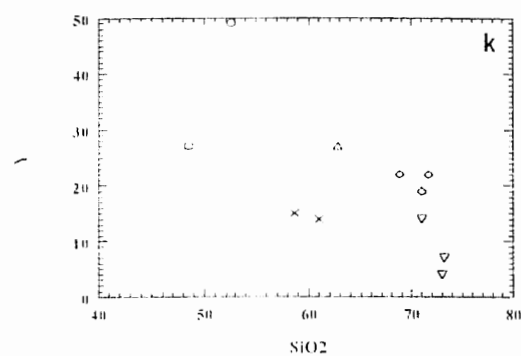
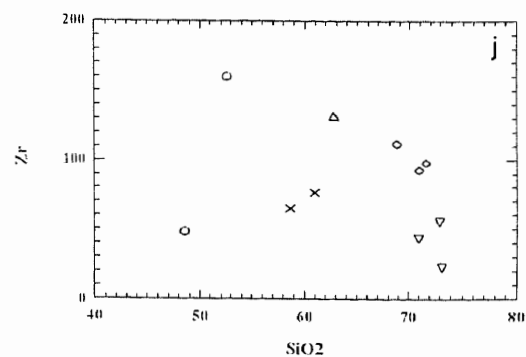
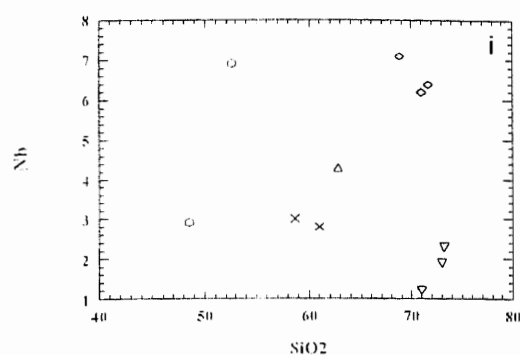


Figure 5.5. Binary plots showing the behaviour of intrusive rocks against SiO₂ from Niat Gah

Figure 5.5 continued



Thus, whereas, some elements exhibit a coherent linear trend suggesting a possibility of co-magmatic relationship between the granitoid samples from Niat Gah, a great majority of them display considerable scatter. Major and trace element variations clearly suggest that the trondhjemites are not comagmatic with the rest of the granitoid rocks, and so is the case, probably, with the gabbro. Tonalite and granodites are probably co-magmatic, but their genetic relationship with andesites, suggested by several of the binary plots may be ruled out on the basis of relative age difference evidenced by field relations.

Petrogenetic relationship amongst the granitoid rocks from Niat may be best evaluated using multi-element variation diagrams involving incompatible trace elements (Figure 5.6).

I. The sample A106 is a foliated and metamorphosed gabbro intercalated with Jal amphibolites. This sample has incompatible trace element concentrations eight to ten times higher than that of the primordial mantle (Figure 5.6a). The pattern is mostly flat or slightly inclined towards left, with HFSE (Zr and Y) slightly enriched relative to LILE (K and Rb). Negative Nb anomaly, considered to be a characteristic of the subduction-related rocks, is missing from this sample. The trace element pattern for this rock is closely comparable with that of the host Jal amphibolites (Figure 5.6c). The sample A97 is a foliated gabbro. The trace element pattern for this rock is comparable to that of A106, particularly in terms of K and Rb (Figure 5.6b). This sample, however, has a small negative Nb anomaly and a positive anomaly for Sr.

II. The sample A96 is a foliated tonalite (Figure 5.6d). The trace-element pattern is inclined towards right; LILE are relatively enriched and negative Nb anomaly is present. Two samples from the andesite dykes (A100 and A102)

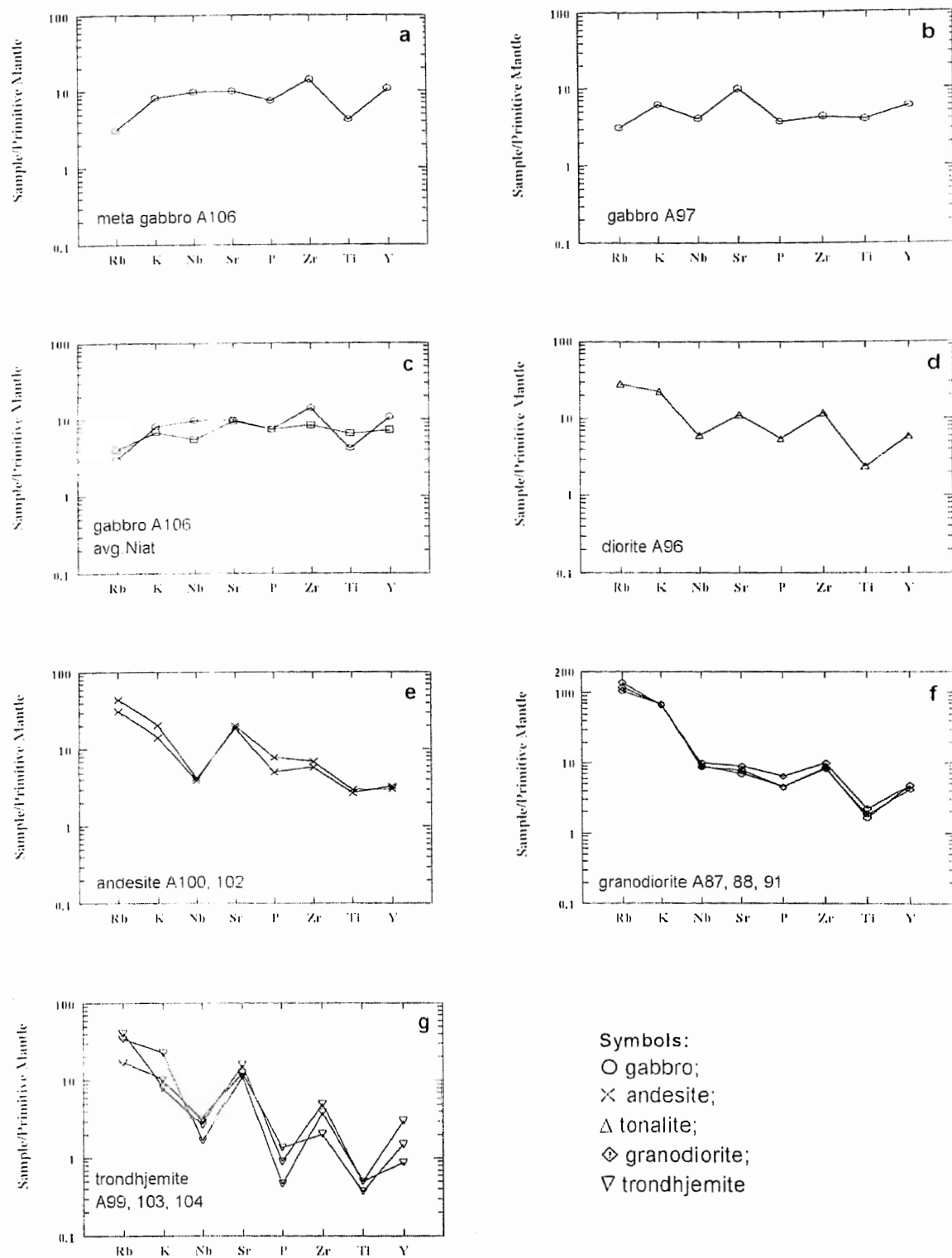


Figure 5.6. Primordial mantle normalized multi element patterns for the granitoids of Niat Gah. Data plotted in this figure are provided in Table 5.5.

Normalizing values of Primordial Mantle: Rb 0.635, K 250, Nb 0.713, Sr 21.1, P 95, Zr 11.2, Ti 1300 and Y 4.55 after Sun and McDonough, 1989.

have patterns closely matching with that of A96 (Figure 5.6e). The trace element patterns for all these three rocks are closely similar to the subduction-related plutonic rocks from Kohistan (e.g., Chilas Complex and Kohistan batholith).

III. The samples A87, A88 and A91 are from sheets intrusive in the northern parts of the Niat metavolcanic unit and are granodiorite in composition. The trace-element patterns for these rocks are strongly inclined towards right, with strong enrichment in K and Rb, and depletion in HFSE (Figure 5.6f).

IV. The samples A99, A103 and A104 are from trondhjemite dykes concentrated in the Jal amphibolite unit. The trace element patterns for these rocks are highly spiked with overall inclination towards the right (Figure 5.6g).

The trace element patterns for the intrusive rocks from Niat show considerable diversity. Considering that the trace element patterns are based on elements which are believed to be incompatible, the observed diversity in the shape of these trace element patterns has strong implications for their petrogenesis. In principal, rocks which are crystallized from the same magma are expected to have mutually similar trace-element patterns, irrespective of the role of fractional crystallization or degree of partial melting. The diversity in the shapes of trace-element patterns is primarily related with the differences in source composition unless the concentration of the trace elements is disturbed by processes like contamination, metamorphism, metasomatism and alteration. Assuming that the studied rocks have escaped remobilization of the incompatible trace-element patterns during weak deformation they have undergone, diversity in the trace element patterns suggests lack of a co-magmatic relationship between

them. The trace-element patterns of the studied granitoid samples from Niat suggests the following three petrogenetic groups.

- 1) The gabbro, represented by A106 is a plutonic counterpart of the metavolcanics constituting the Jal-Niat units, and thus predates the rest of the granitoid sheets. There is a close similarity between the trace element pattern of A106 and that of the metavolcanics, characterized by a pattern which is flat or slightly inclined towards left, lack of negative Nb anomaly, and an enrichment of the HFSE relative to K and Rb.
- 2) The gabbro (A97), tonalite (A96) and andesites (A100 and A102) have trace element patterns typical of subduction-related magmas, and are considered here to be mutually related. They are probably equivalent of the stage-I of the subduction-related Kohistan batholith (Pettersson and Windley, 1985). The granodiorites (A87, A88 and A91) are broadly similar to this group (e.g., A-96), but have; **a)** strong enrichment in Rb and K, and **b)** a slight depletion in HFSE, relative to A106. In the absence of rare-earth elements, the detailed petrogenetic differences cannot be ascertained between these two.
- 3) The trondhjemites (A103, A104 and A99) have trace element patterns which slope towards right but show stronger depletion in incompatible trace elements than all other studied rocks. Moreover the pattern is highly spiked. For these reasons they are considered to represent a discrete petrogenetic group.

Thak Gah

Twenty five samples belonging to the Thak granitoid sheets have been analyzed from the Thak (Babusar) valley. Of these 14 samples are from the principal granitoid body termed Khun group and eleven samples are from Shai group. The analyzed rocks include five gabbros (A160, A164, A165, BS4A and

BS39), three diorites (A162, A163 and BS38), thirteen tonalites (A71, A155, A161, A166, A167, BS1, BS2, BS26, BS28, BS29, BS30, BS36 and BS37) and one granodiorite (A65). Amongst the tonalites, two samples (BS28 and BS29) are from the Shai group and two (BS1 and BS2) from the sheared granitoid body in the vicinity of the Babusar Rest House. Two samples (BS25 and BS26) are trondhjemite and tonalite, respectively, intercalated with the Niat metavolcanics and have undergone the same phase of metamorphism and deformation as that of their host rocks. One sample (BS01) is from an andesite dykes intruding Niat metavolcanics and one sample (A62) is from a trondhjemites intrusive in the Niat amphibolite unit.

The granitoids from the Thak Gah show a wide variation in SiO_2 content from 51 wt% to 76 wt%, but samples have less than 66 wt% SiO_2 . A majority of the samples contain TiO_2 less than 0.7 wt%. Only four samples (A164, A160, BS26 and A62) contain TiO_2 in excess of 1 wt%. The samples with $\text{SiO}_2 < 60$ wt% show scatter in terms of their TiO_2 content. There is an inflection point at SiO_2 60 wt%; samples with higher SiO_2 content show a general decrease in their TiO_2 content with increasing SiO_2 . Al_2O_3 shows a good inverse proportional relationship with increasing SiO_2 resulting in a linear trend inclined towards right. Three samples (A62, BS25 and BS26) deviate from the mainstream trend and contain relatively lower Al_2O_3 wt% and higher Fe_2O_3 wt%. Good linear trends are shown by major elements Fe_2O_3 , MgO and CaO relative to SiO_2 . All these three elements show a progressive decrease in their concentrations with increasing SiO_2 (Figure 5.7). Na_2O , K_2O and P_2O_5 show a general increase in their concentrations relative to increasing SiO_2 contents, although they do not define coherent linear trends.

Symbols: ● gabbro; ■ diorite; ◇ granodiorite; ▲ tonalite; ▼ trondhjemite; + andesite

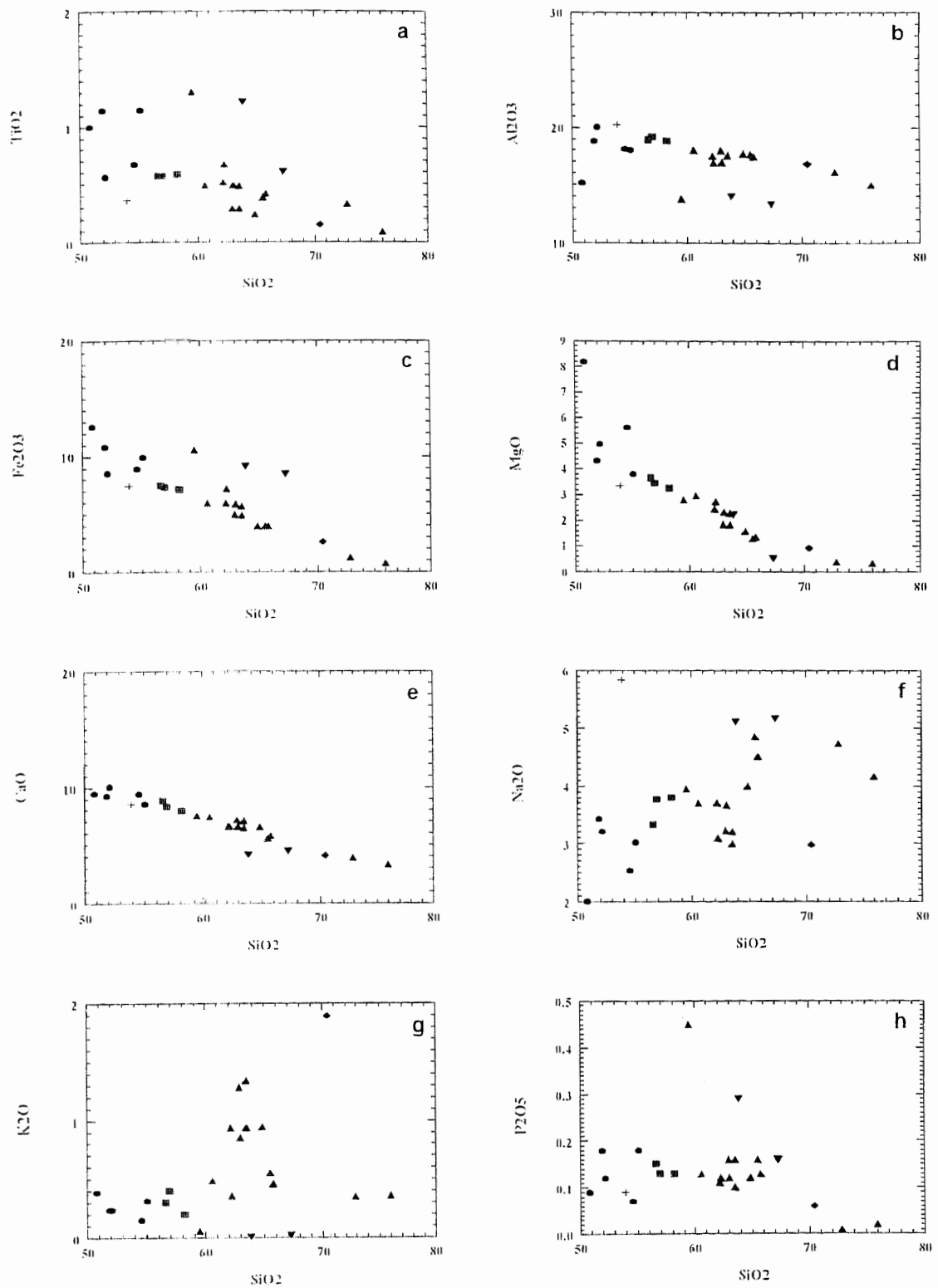
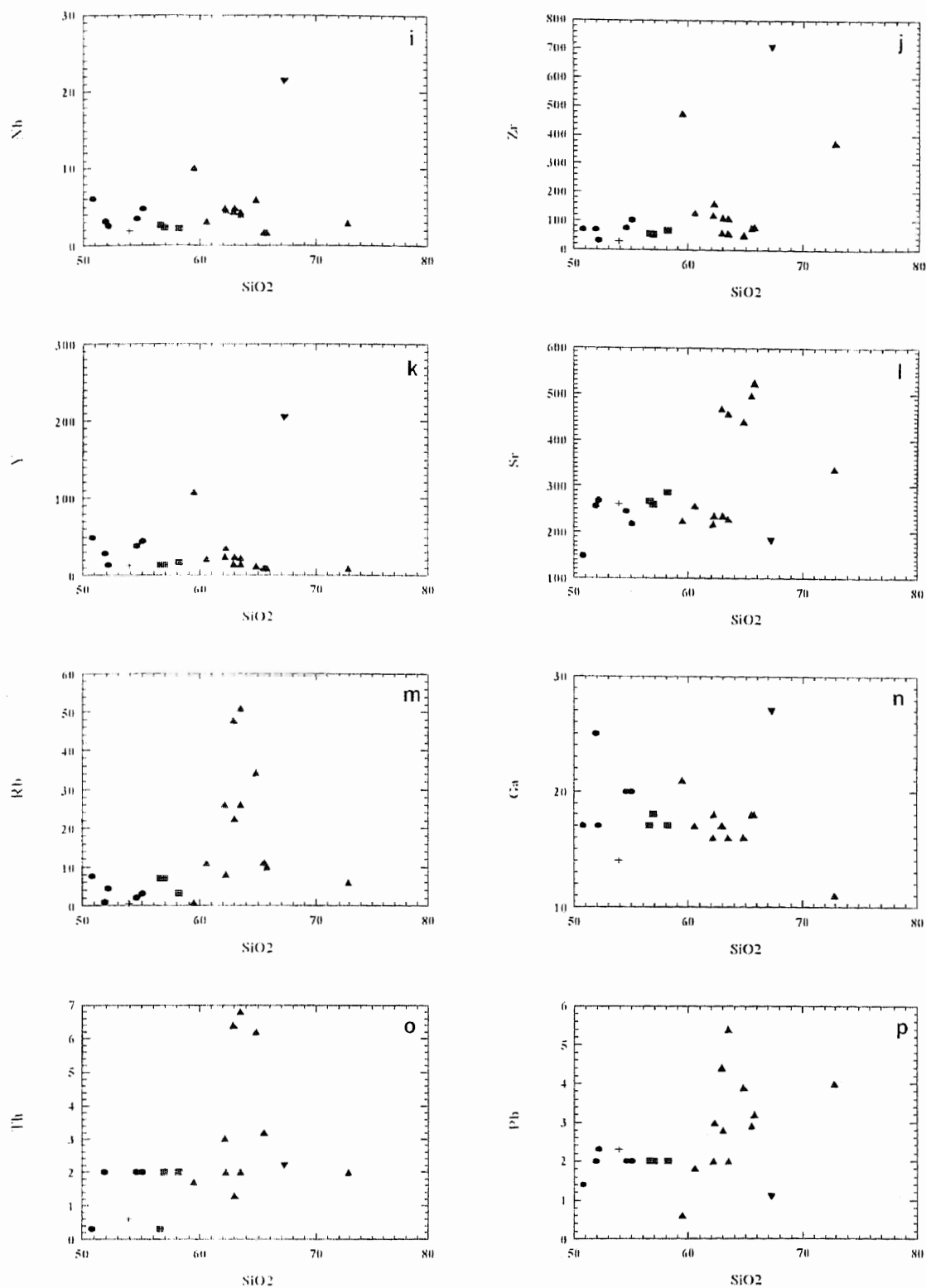


Figure 5.7. Binary plots showing the behaviour of major elements against SiO_2 in granitoid rocks from Thak Gah.

Figure 5.7 continued



Samples like A62, A71, A155 and BS25 contain very low K_2O even though SiO_2 contents are higher than 60 wt%, suggesting their trondhjemitic nature.

Amongst the trace elements, Nb and Zr show only a slight enrichment in their concentrations with respect to increasing SiO_2 (Figure 5.7i and j). Two samples (BS25 and BS26) deviate from the mainstream trend in all these plots with distinctly high concentrations for these HFSE. Samples A155, BS1 and BS2 have relatively low concentrations of Nb and Y compared to the rest of the samples. Trace elements like Rb, Th, Pb and Sr have variations similar to K_2O , with trends showing a marked increase in their concentrations at SiO_2 ~60 wt%. Some samples like A155, BS1, BS2, BS25 and BS26 show deviations from the mainstream trends in terms of one or more of these trace elements. Transitional elements like Ni, Co, Cr, V, Cu, Zn and Sc all show a general depletion with increasing SiO_2 , suggesting their mutual compatibility (Figure 5.8).

Patterns involving incompatible trace elements are used to ascertain petrogenetic relations amongst the samples analyzed from Thak Gah. Samples from the gneissose granitoids belonging to the body exposed at the Babusar Rest House are characterized by a trace element pattern which is slightly inclined towards right, with high positive Sr and negative Nb spikes (Figure 5.9a). An almost similar pattern is exhibited by the samples from the Shai body, though K and Rb are distinctly higher in these rocks (Figure 5.9b). The trace element patterns from various compositional types from the principal granitoid body at Khun are shown in Figure 5.10. The gabbros from this body have trace element patterns which are flat to only slightly inclined towards right, while Sr and Nb define positive and negative spikes, respectively (Figure 5.10a). Diorites and tonalites from this group have trace element patterns similar to the gabbros, though the general slope

Symbols: ● gabbro; ■ diorite; ◇ granodiorite; ▲ tonalite; ▼ trondhjemite; + andesite

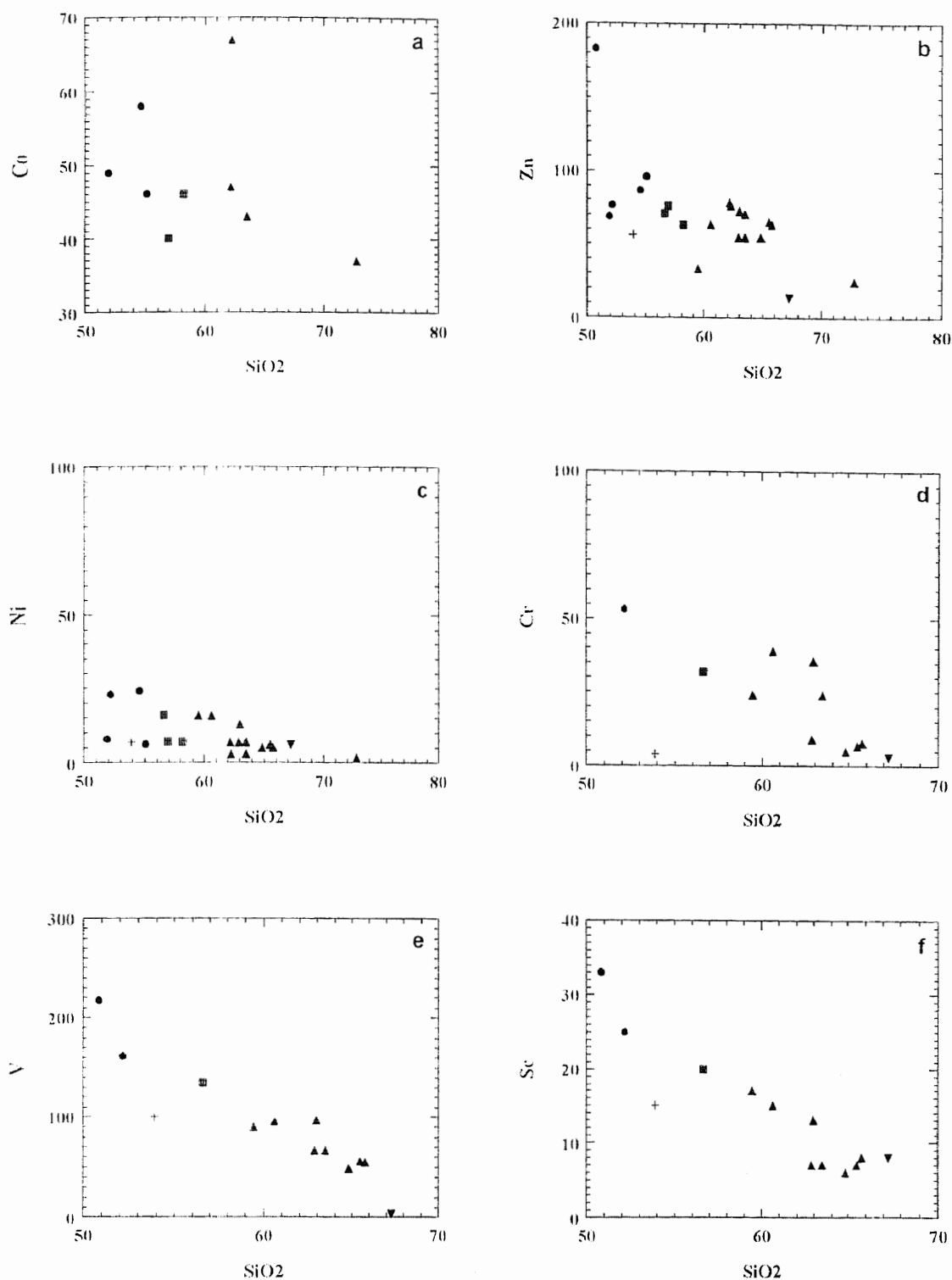


Figure 5.8. Binary plots of transitional elements against SiO₂ showing negative trends for intrusive rocks of Thak Gah.

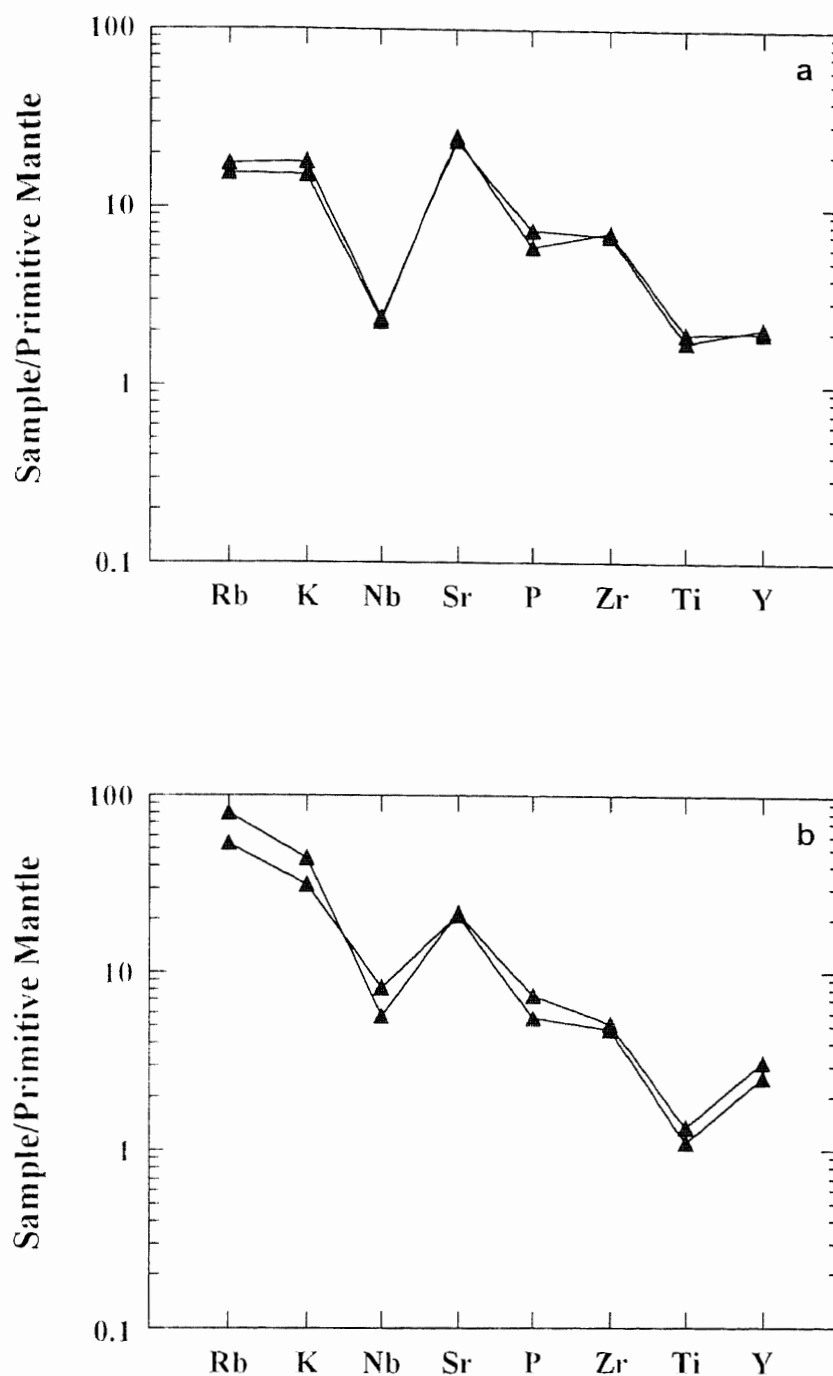


Figure 5.9. Spidergram showing the similar patterns of Shai body tonalites (BS28 and 29) and gneissose tonalites (BS1 and 2) exposed near Babusar Rest House. a) Gneissose tonalites, b) Shai body tonalites.

Normalizing values of Primordial Mantle: Rb 0.635, K 250, Nb 0.713, Sr 21.1, P 95, Zr 11.2, Ti 1300 and Y 4.55 after Sun and McDonough, 1989.

is relatively more steeply inclined towards the right due to higher concentration of K and Rb. Additionally, there is a selective enrichment in Y and Zr and depletion in Ti and P, resulting in a pattern which is more spiked than the gabbros (Figure 5.10b, c).

Two samples A71 and A155 represent highly felsic sheets of granitic/tonalitic composition intruding the Jal amphibolite unit. These rocks exhibit trace element patterns which are highly spiked. These rocks are enriched in Zr and Sr, and strongly depleted in Ti, P and Nb. These rocks have low K and Rb contents almost comparable to the gabbros of the Khun group. The sample BS26, representing plutonic intercalations within the Niat metavolcanics, displays differences with the rest of the samples from Thak Gah even on Harker-type diagrams. The differences are highlighted by trace element patterns (Figure 5.10d). It has the highest Y, Zr and Ti, and least K and Rb, resulting in a trace element pattern which is generally inclined towards left. Figure (5.10f) displays the distinct patterns of A155 and BS26. The trondhjemite (BS25) shows a similar pattern to the BS26 (tonalite) with slightly higher concentration enrichment in Zr, Y and Nb and slightly depletion in Ti and K. The andesite (BS01) intruding the Niat metavolcanic unit has similar general characteristics (Figure 5.10e) suggesting a petrogenetic interrelationship with BS25 and BS26.

Buto Gah

A total of nine samples were analyzed from the rocks belonging to the Thak granitoid sheets exposed in the Buto Gah. Of these, three rocks are gabbros (A110, A126 and A128), one granodiorite (A124) and four trondhjemites (A108, A123, A127 and A129). One sample is from a dacite dyke (A113) intruding the Niat metavolcanic unit.

Symbols: ● gabbro; ■ diorite; ◇ granodiorite; ▲ tonalite; ▼ trondhjemite; + andesite

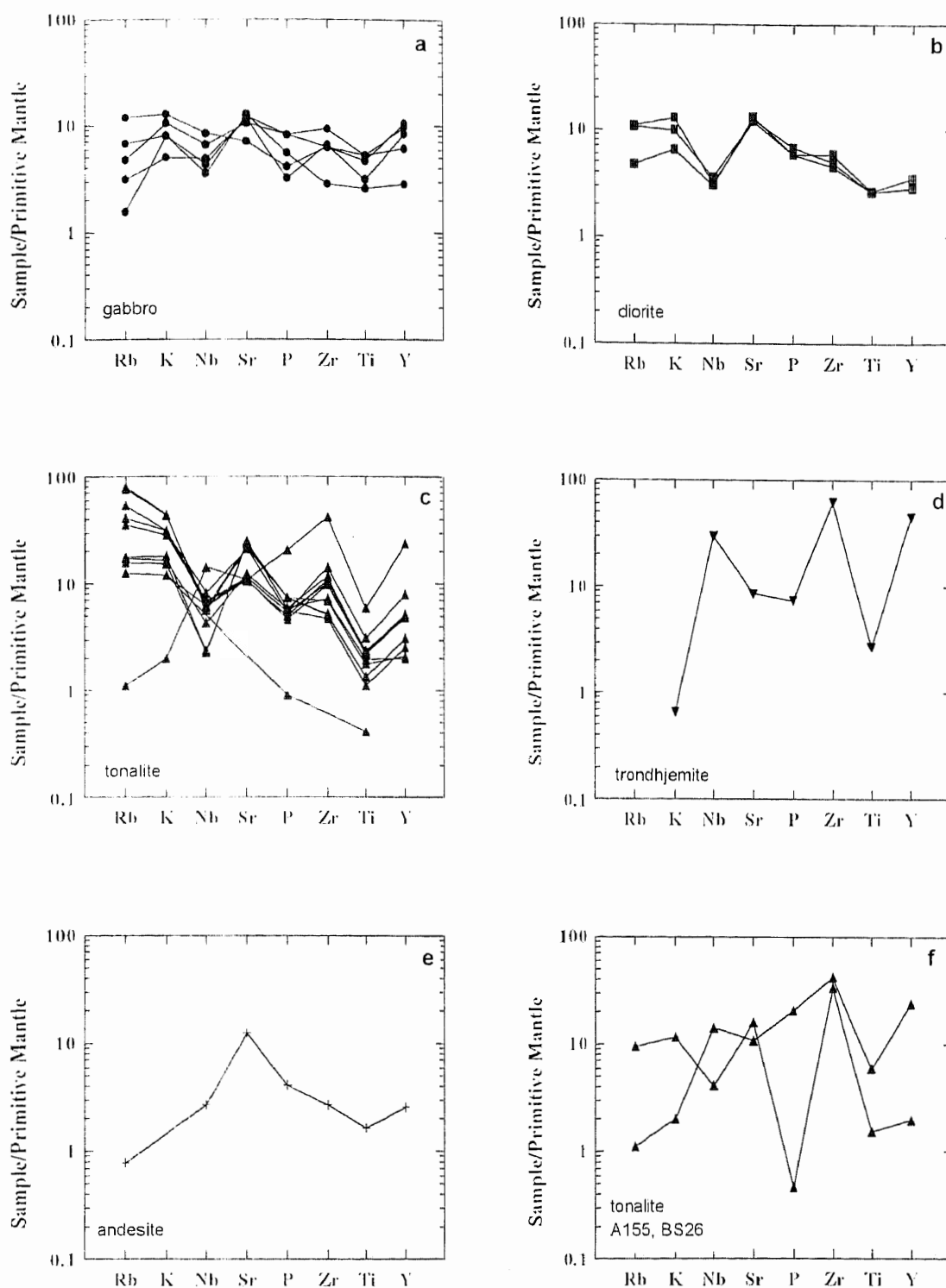


Figure 5.10. Spidergrams showing the patterns of granitoid rocks from Thak Gah.

Normalizing values of Primordial Mantle: Rb 0.635, K 250, Nb 0.713, Sr 21.1, P 95, Zr 11.2, Ti 1300 and Y 4.55 after Sun and McDonough, 1989.

The gabbros from the Buto Gah have major and trace element characteristics matching closely with the gabbroic rocks from the Khun Group (Figure 5.11). The trace element patterns for these rocks are mutually similar with strong positive spike for Sr and negative spike for Nb. When compared with the gabbroic rocks from the Khun group, the overall concentrations of the incompatible elements are slightly lower, and Sr and Nb spikes are stronger, yet overall patterns are mutually similar (Figure 5.11).

The granodiorite sample (A124) has major and trace element composition very similar to that of the trondhjemites from this valley, except for the relatively high K_2O . Trace element patterns for this rock and the trondhjemites (A108, A123, A127 and A129) are mutually similar, characterized by slopes inclined towards right and highly spiked shape of the patterns.

The sample from a dacitic dyke intruding the Niat metavolcanics is very close in composition to the andesite dykes from Niat Gah in the studied intrusive complex (e.g., A100 and A102). Trace element pattern for this rock is characterised by a slope towards the right and a distinct negative anomaly for Nb (Figure 5.11b).

Thor Gah

Eight samples were analyzed from part of the Thak granitoid sheets exposed in the Thor Gah. These include two gabbro (A130 and A136), one diorite (A141), one tonalite (A143), one granites (A149), one granodiorite (A144), one trondhjemite (A146) and an andesite from a dyke (A139). All major oxides and trace elements are plotted against SiO_2 to understand their behaviour and comagmatic relationship with the rocks of the granitoid sheets (Figure 5.12).

The gabbroic rocks are characterized by major and trace element composition matching with rocks of this composition elsewhere in the complex. The

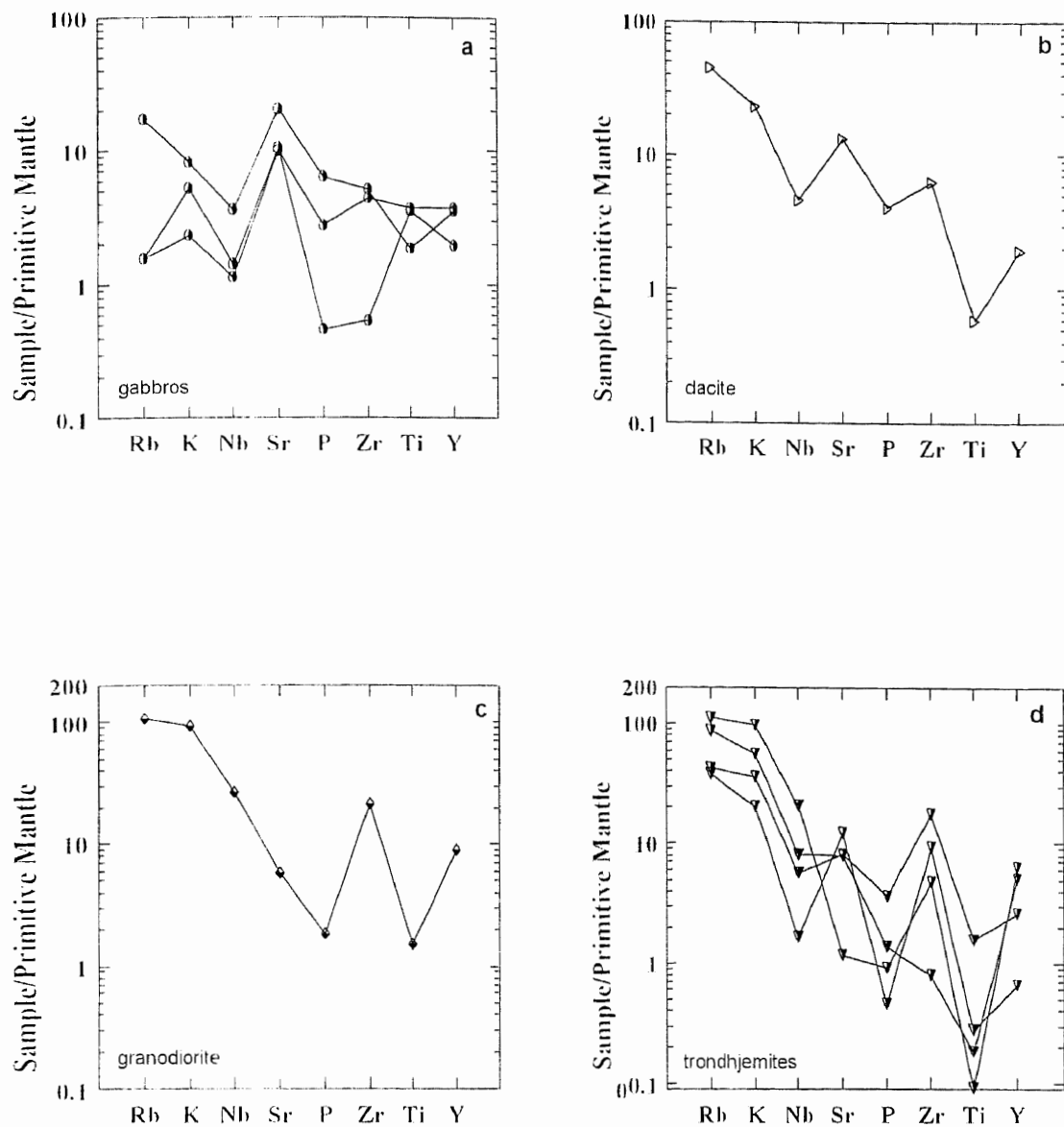


Figure 5.11. Spidergrams showing the trends of intrusive rocks from Buto Gah.

Normalizing values of Primordial Mantle: Rb 0.635, K 250, Nb 0.713, Sr 21.1, P 95, Zr 11.2, Ti 1300 and Y 4.55 after Sun and McDonough, 1989.

Symbols: ○ gabbro; □ diorite; ▵ dacite; △ tonalite; ◇ granodiorite; ▽ trondhjemite

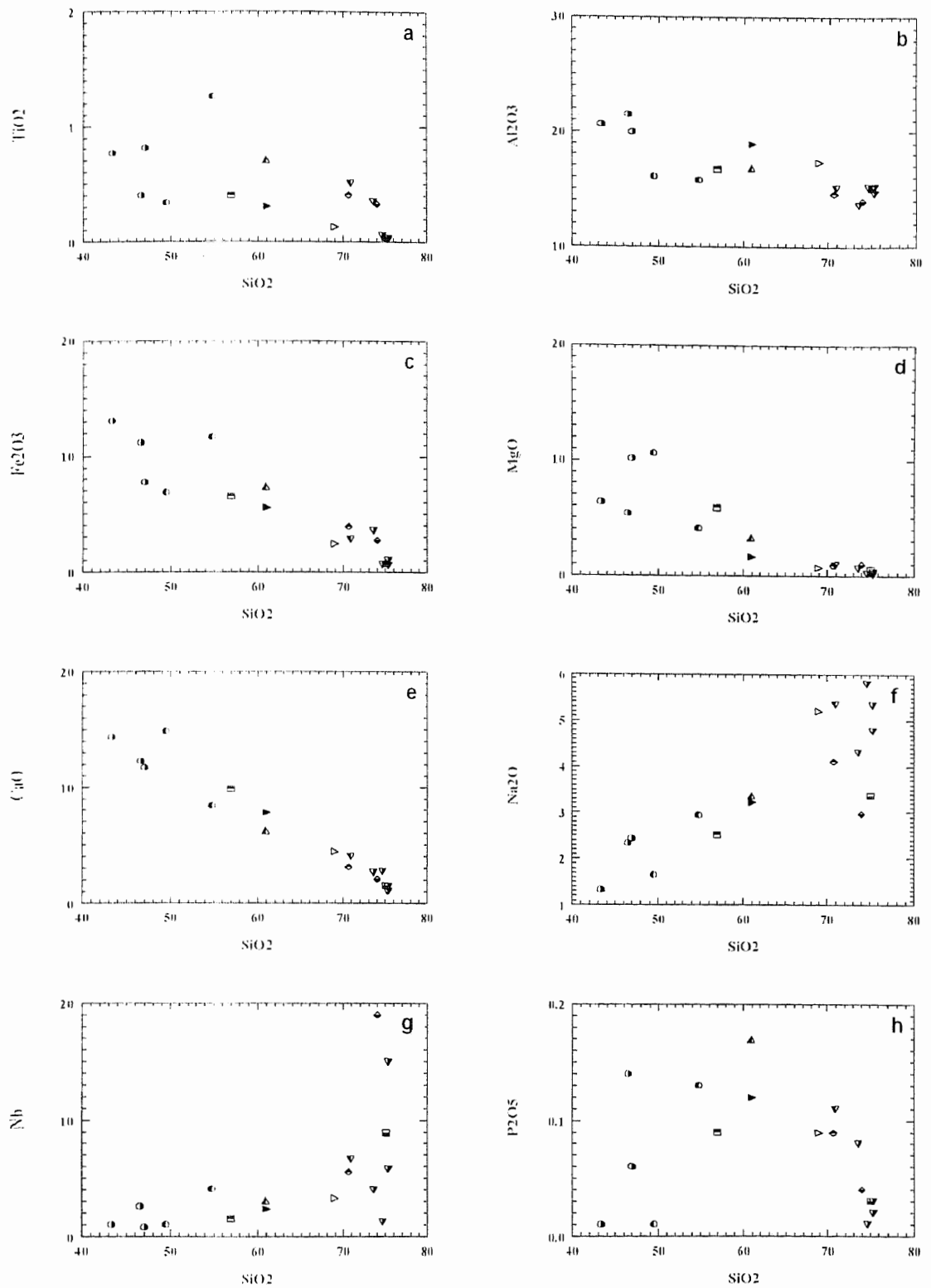
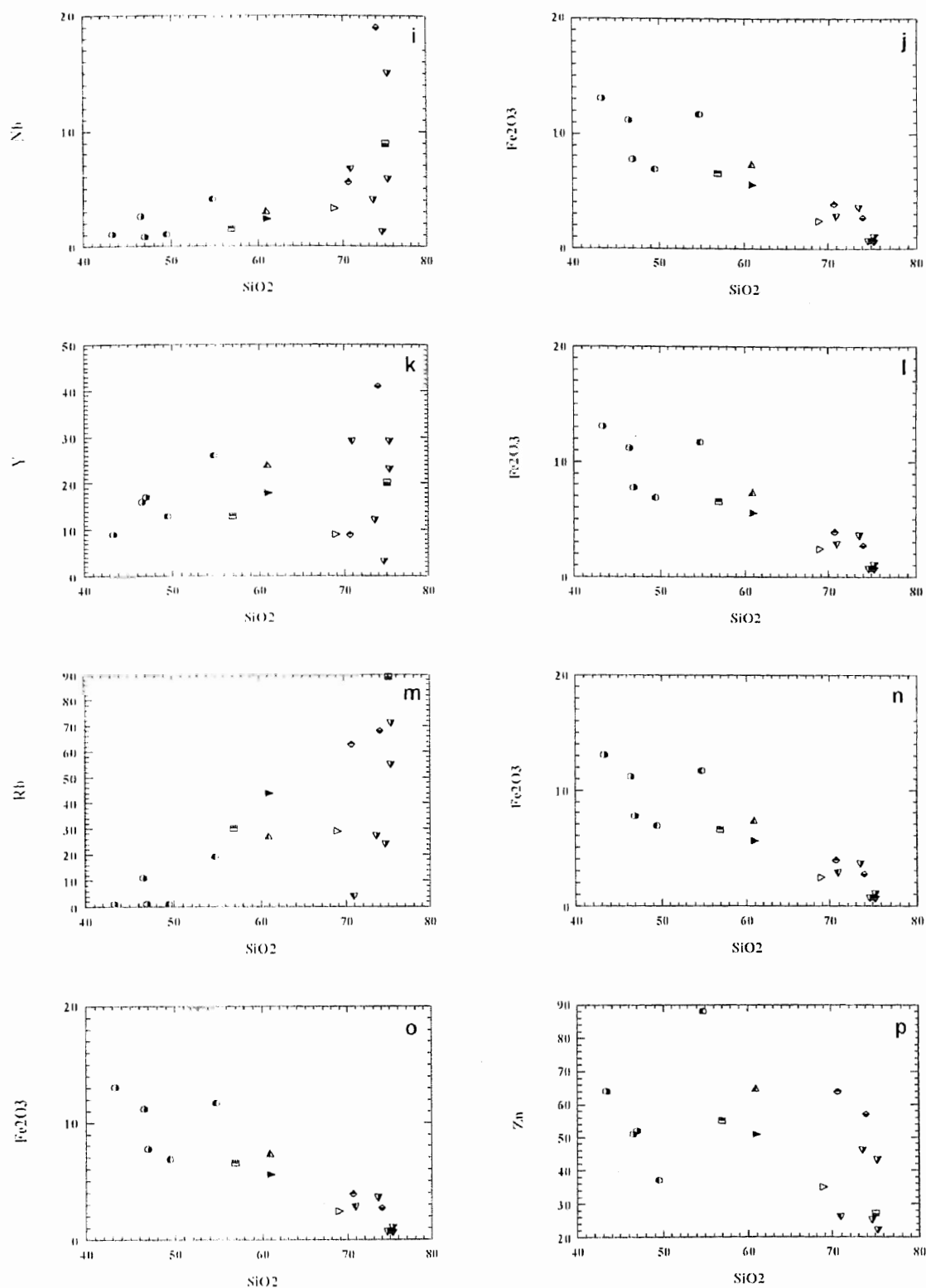


Figure 5.12. Binary plots showing the behaviour of granitoid rocks from Buto and Thor valleys.

Figure 5.12 continued



trace element patterns are characterized by a slight to moderate LILE enrichment relative to HFSE resulting in slopes towards right, and positive Sr and negative Nb anomalies (Figure 5.13). The diorite, tonalite, granodiorite and andesite all have trace element patterns mutually similar and close to those of the gabbro. This suite is characterized by relative enrichment in LILE compared to HFSE and a distinct negative Nb anomaly.

The sample A149 (granite) has a pattern which is inclined towards the right at a much steeper angle than the rest of the suite including the granodiorite sample (A144), as it is more enriched in LILE and more depleted in HFSE. Fractional crystallization of minerals like zircon, sphene and apatite accounting for depletion of HFSE and a truly incompatible behaviour of the Rb and K can explain this relationship.

The trondhjemite sample (A146) has a major-element composition not very different from the granite and granodiorite, except for high Na_2O and low K_2O . The trace element pattern for this sample is, however, very different from the granite and granodiorite, enriched in HFSE and depleted in LILE (Figure 5.13g).

Petrogenesis

The analyzed rocks from the Thak granitoid sheets, based on geochemical characteristics, can be subdivided into two principal groups; HFSE enriched and HFSE depleted.

HFSE Enriched Group

The HFSE enriched rocks are characterized by their occurrence as thin sheets (commonly only a few centimeters thick) intercalated with metavolcanics of the Jal and Niat units. They are pervasively foliated and contain abundant amphibole. They include a gabbro (A97), tonalite (BS26), andesite (BS01) and

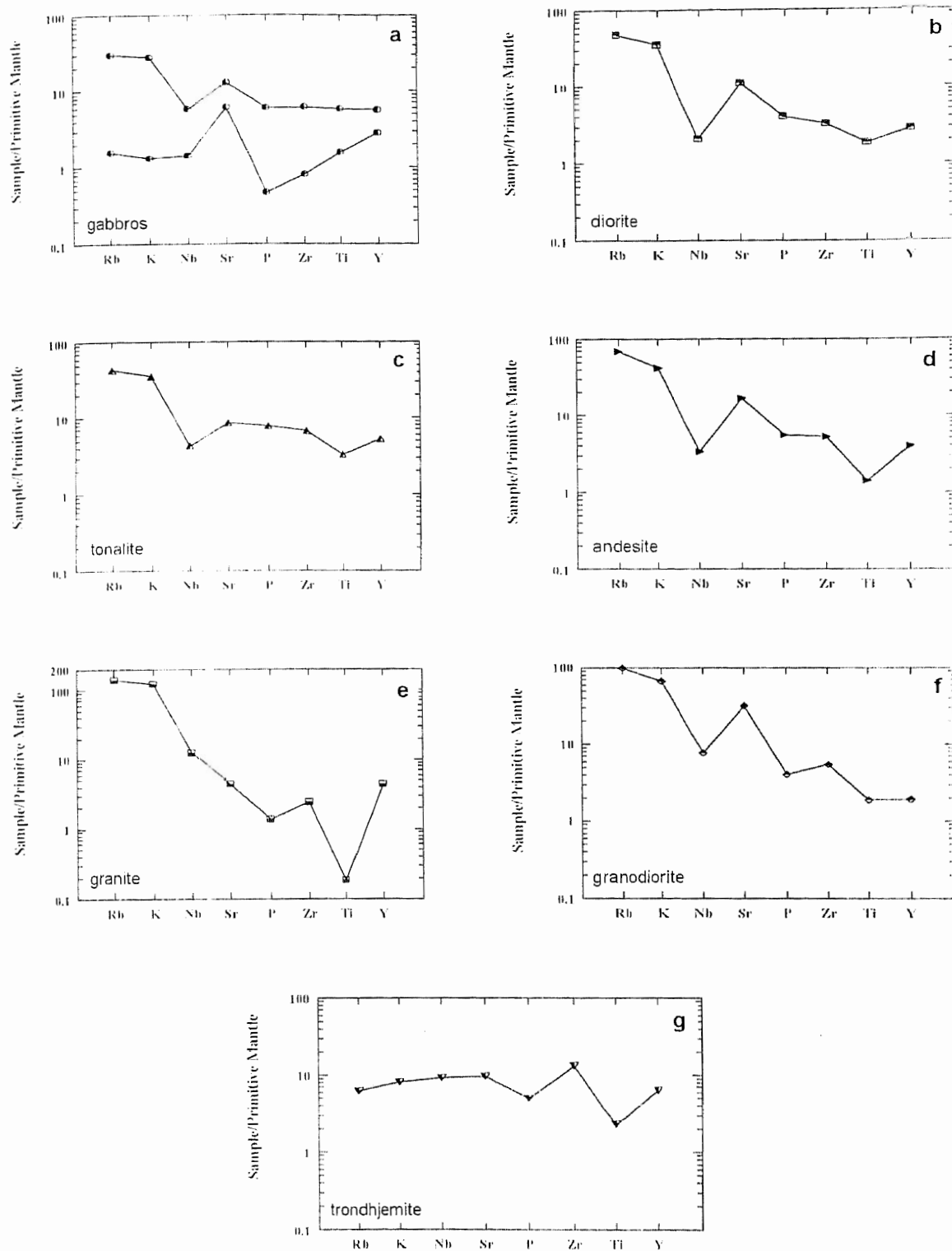


Figure 5.13. Spidergrams showing the patterns of intrusive rocks from Thor Gah.

Normalizing values of Primordial Mantle: Rb 0.635, K 250, Nb 0.713, Sr 21.1, P 95, Zr 11.2, Ti 1300 and Y 4.55 after Sun and McDonough, 1989.

trondhjemites (BS25, A62). In terms of chemical composition these rocks are characterized by lower Al_2O_3 and K_2O , and higher Fe_2O_3 and TiO_2 compared to the rest of the samples in the complex. These rocks are enriched in HFSE, particularly Y, Zr, and P. Nb is variable but displays a positive spike rather than a negative one as is the case in HFSE depleted group (see later). Sr is about 10 times higher, while Rb and K approach the primordial mantle values.

Several of the compositional attributes of this group from the Thak granitoid sheets are comparable with the host metavolcanics of Jal/Niat units (Figure 5.6c compare the trace element patterns), particularly the relative enrichment of the HFSE over LILE. The detailed differences in the trace-element patterns of various rocks are probably related with processes like fractional crystallization and/or partial melting. Considering that the Niat/Jal metavolcanics are MORB type, occurrence of gabbros, tonalites and trondhjemites as their plutonic equivalents or differentiates, is not unusual. There is a partial REE data available for some samples from this group, which when compared to the REE patterns of the Jal/Niat metavolcanic units, show a close similarity in terms of comparable slopes inclined towards the left. This further supports the petrogenetic link between this group of granitoids and the Jal/Niat metavolcanic units.

HFSE Depleted Group

Much of the Thak granitoid sheets belongs to this group. As the name signifies, the distinguishing feature is a slight to high enrichment of LILE (mainly Rb and K) over HFSE (Y, Zr, Yb, P and Nb), resulting in trace element patterns which predominantly slope towards the right. The gabbroic samples show lesser enrichment of LILE over HFSE relative to the dioritic and tonalitic rocks, but negative Nb and positive Sr anomalies are present. This group includes rock types

like gabbro, diorite, tonalite, granodiorite and granite which show coherent behavior and trends. Majority of the rocks of this group have typical subduction-related chemistries, with characteristics such as low TiO_2 and high Al_2O_3 contents (Chappell and White, 1974), high LIL/HFS element ratios (Tarney and Saunders, 1979; Saunders et al., 1980; Pearce et al., 1984), variable inter-alkali ratios and distinct Nb depletion anomalies (Saunders et al., 1980; Saunders et al., 1988), all consistent with magma derivation from a metasomatized mantle wedge above a subduction zone. These magmas are characterized by enrichments in LILE relative to HFSE.

On Harker-type variation diagrams, the samples from this suite exhibit coherent trends for most of the major and trace elements. All these compositional features point to a petrogenetic relation between the rocks of this group at least in terms of a common source. The compositional variations from gabbros, through diorites/tonalites to granodiorites are either due to variations in extent of partial melting or fractional crystallization or both. A depleted mantle, metasomatized by fluid phases released during subduction, was probably a source for this group of rocks.

Whereas the gabbro-diorite-tonalite-granodiorite series shows mutually comparable geochemical characteristics, the trondhjemites have compositional attributes which suggest a different petrogenesis. Figure (5.14) is used to compare a representative tonalite (A96), a granodiorite (A87) and a trondhjemite (A103). The trace element patterns of all the three rocks have lots of similarities as well as differences. The granodiorite has a pattern which matches closely with the tonalite in terms of HFSE, but is distinctly enriched in Rb and K. In essence the granodiorite is even slightly depleted in HFSE (Y, Ti, P, and Sr) relative to the

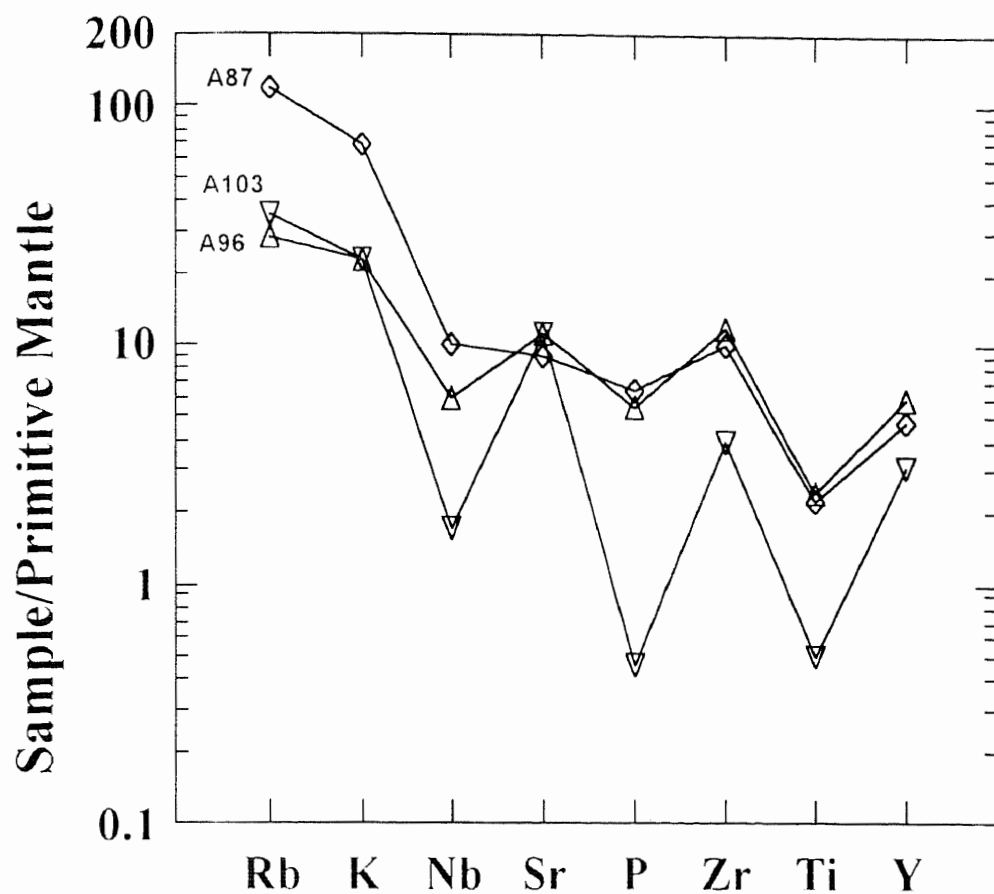


Figure 5.14. Spidergram showing the similar pattern of three distinctive samples; e.g., A96 (tonalite), A87 (granodiorite) and A103 (trondhjemite).

Normalizing values of Primordial Mantle: Rb 0.635, K 250, Nb 0.713, Sr 21.1, P 95, Zr 11.2, Ti 1300 and Y 4.55 after Sun and McDonough, 1989.

diorite/tonalite. It may be noted that the distribution coefficients of trace elements are different in granitic systems compared to basaltic systems. For instance, HFSE, which are incompatible in basaltic systems become compatible in granitic systems due to crystallization of phases like . The only true incompatible trace elements (other than the REEs), in the granitic system, are Rb and K (Pearce et. al., 1984). If it is so, the enrichment of Rb and K in granodiorite relative to the tonalite may be attributed to fractional crystallization from a common magma. The trace element pattern of the trondhjemite, in comparison, is very different from those of the diorite/tonalite and granodiorite. It is depleted in all HFSE, particularly strongly in Ti, P and Nb relative to the tonalite and the granodiorite (Figure 5.14). The concentrations of K, Rb and Sr are comparable with those in the tonalite, but not enriched, negating relationship between the two through the process of fractional crystallization. Thus whereas the tonalites and granodiorites (and granites) are probably comagmatic mutually as well as so with gabbros and diorites, being fractional crystallization products of a common parental melt, the trondhjemites ~~are~~ are product of partial melting from a source which was different from that of the gabbro-diorite-granodiorite-granite series. In the following section the petrogenesis of trondhjemites is addressed in detail.

Trondhjemites

Trondhjemites are found in a variety of geologic environments. The principal occurrences are in the Archean grey gneiss terranes and greenstone belts and at Proterozoic-Paleozoic continental margins. The Mesozoic-Cenozoic trondhjemites occur in two major associations: 1) ophiolites, 2) subduction-related settings at the continental margins and island arcs. In majority of cases, the trondhjemites from the ophiolites are "plagiogranites" and represent a product of fractional

crystallization from a MORB, controlled by crystallization of minerals like olivine, pyroxenes, etc. These trondhjemites are characterized by low Al_2O_3 and K_2O , and high TiO_2 , Fe_2O_3 and Na_2O . When compared with those from subduction-related complexes. The subduction-related trondhjemites are further distinguishable on the basis of their petrogenesis; one type is a product of fractional crystallization from a mantle derived arc-tholeiite magma, while the other is a product of partial melting from the arc basement. The two types are easily distinguishable on the basis of REE, the type-I trondhjemites are enriched in middle and heavy REEs compared to the type-II, which are typically depleted in these elements due to occurrence of amphibole and garnet as the residual phases in the arc basement.

In the presently investigated part of the Kohistan terrane, a variety of trondhjemites are encountered. The trondhjemites characterized by enriched HFSE and an origin in an ocean-floor setting occur in intimate association with Niat-Jal metavolcanics (see section on petrogenesis of the HFSE enriched group). The remainder of the trondhjemites are distinguished from the HFSE enriched trondhjemites of ocean-floor type by their highly spiked patterns with distinct slopes towards the right. These trondhjemites could have formed by two processes; either as differentiates of the gabbro-diorite-tonalite-granodiorite-granite series present in the investigated area, or by partial melting of the Niat-Jal metavolcanic units. Almost all the trondhjemites in this group have incompatible trace element abundances lower than the gabbros, diorites, tonalites, granodiorites and granites negating possibility of the trondhjemites as a fractional crystallization product. Partial melting of a basaltic source material is recently considered to be the most viable mechanism for the generation of high-Al trondhjemites similar to those of the area studied by Drummond and Defant (1990). Basalts converted to amphibolites

and eclogites when involved in subduction-zone setting are partially fused to generate trondhjemites (De Vore, 1983a, b; Windley, 1984; Martin, 1986, 1987). The geochemical modelling and experimental studies (Drummond and Defant, 1990) favour a hot oceanic crust (20-30 Ma old) subducting and melting to produce trondhjemites. The high-Al trondhjemites of the present study are probably a product of partial melting but a direct role of subduction is not observed. Field evidence suggests that the studied trondhjemites 1) occur as thin veins and dykes intimately associated with Jal amphibolites (and rarely with the Niat amphibolites), 2) are syn- to post kinematic. The amphibolite-facies metamorphism and deformation in the Kamila belt is considered related with the Kamila shear zone of 80 Ma (Treloar et al., 1990), suggesting a similar age for the trondhjemites. If it is so, the Jal amphibolites did not melt in a subduction setting rather in an intra-arc shear zone. The Chilas complex of 90-80 Ma might have played an equally important role in the genesis of the trondhjemites as a heat source. In summary, the trondhjemites of the studied area are considered 1) to be unrelated with gabbro-diorite-tonalite-granodiorites-granite series, and 2) to have resulted from partial melting of Jal-Niat amphibolite due to intrusion of the Chilas Complex and crustal shortening accompanying the Jal shear zone. The exact petrogenesis of the trondhjemite suite in the Thak granitoid sheets, however cannot be properly evaluated without data of rare-earth elements.

Chapter 6

SUMMARY AND CONCLUSION

Introduction

This thesis is based on results outcoming from geological mapping of about 600 km² area in SE Kohistan. Previously this area was considered to comprise mainly of the Kamila amphibolites (Tahirkheli and Jan, 1978), with subordinate diorites in the middle reaches of the Thak Gah (Shams, 1975; Ahmed and Chaudhry, 1978) and minor ultramafic bodies in the vicinity of the Babusar Pass (Ahmed and Chaudhry, 1978). The present work and that of Ghazanfar et al. (1991) have resulted in bringing the geological understanding of this area at par with better known sections in southern Kohistan like Indus, Swat and Dir valleys.

The preceding chapters include details of field relationships, petrology, geochemical behaviour and petrogenesis of the three principal units of the SE Kohistan, i.e., the Sapat mafic-ultramafic complex, the Amphibolite belt and the Thak granitoid sheets. In this chapter, an attempt is made at presenting a synthesised account of the geology of SE Kohistan, highlighting differences with better known section through southern Kohistan along the Jijal-Kamila transect in the Indus valley. The results from this work when integrated with that of the Jijal-Kamila transect, provide better constraints on the internal constitution of the lower-middle part of the island-arc crust in Kohistan.

Geology of SE Kohistan: A Synthesis

The presently studied part of SE Kohistan (Figure 1.2) is bounded by the Main Mantle Thrust (MMT) at its southern and eastern side and the Jal shear zone (at the southern contact of the Chilas complex) at its northern side. A large part of the

Kohistan terrane (approximately 2000 square km) between the western edge of the presently mapped area and the Jijal-Kamila transect in the Indus valley remains unmapped. The salient features of the geology of the three principal constituents of the island-arc terrane in the presently mapped part of SE Kohistan are as under.

The Sapat Mafic-ultramafic Complex

Ahmed and Chaudhry (1976) first noted the presence of ultramafic bodies at the Babusar Pass, which they described to be enclosed within a succession of amphibolites. A medium- and coarse-grained texture and presence of relict graded and isomodal layering typical of stratiform ultramafic-mafic complexes suggests that the amphibolites enclosing the ultramafic rocks are derived from layered gabbros. These amphibolites are in physical continuity towards the west with amphibolitized gabbroic rocks overlying a larger ultramafic body in the hanging wall of the MMT, displaying good layering (Jan et al., 1993; Khan et al., 1994; 1995). The physical continuity and a close lithological and compositional similarity between the rocks of these adjacent areas point to the presence of a stratiform-type mafic-ultramafic complex in the previously poorly mapped part of the Kohistan terrane, which, following Jan et al. (1993), is termed Sapat complex.

The ultramafic rocks of the complex are lenticular in shape but have concordant contact relations with the enclosing gabbroic amphibolites. These bodies consist of dunites, peridotites and pyroxenites, which are commonly interlayered. Chromitites occur as small local pods thin streaks interlayered with the rest of the ultramafic rocks and veins cross cutting them. The olivine-rich rocks show varying degrees of alteration to serpentine and magnesite, accompanied by Mg-rich chlorite around chromite with some talc and a carbonate mineral. The secondary minerals occur as fine-grained matrix surrounding the relicts of primary

minerals such as olivine, clinopyroxene and chromite. Serpentinization is particularly intense close to the suture. Amphibole occurs in appreciable amounts in pyroxene-rich ultramafic rocks. In peridotites, both clinopyroxene and amphibole occur as poikilitic grains, suggesting post-cumulus origin. Amphibole and plagioclase form the principal constituents of the amphibolitized gabbros and clinopyroxene has survived amphibolitization in rare cases. The presence of epidote, chlorite and carbonate suggests an epidote-amphibolite facies retrograde metamorphism.

The Sapat complex has several attributes which suggest its affinity with the Kohistan crust rather than being remnant of the oceanic crust of the Neo-tethys: a) it is overlain by amphibolites of distinct island-arc affinity with an arc-tholeiite chemistry (Khan and Thirlwall, 1988), b) chromium spinels from the Sapat complex are characterized by a high Cr No. [$100\text{Cr}/(\text{Cr}+\text{Al}) = >70$] akin to arc-related environments (Jan et al., 1993); chromites formed in oceanic environments contain Cr. No. below 60 (Dick and Bullen, 1984; Jan and Windley, 1990), and c) the trace-element patterns for the Sapat complex rocks are characterized by a relative enrichment in large-ion lithophile elements (LILE) relative to the high-field strength elements (HFSE), a negative anomaly for Nb, and a strong positive spike for Sr (this study). Additionally, TiO_2 is low in the rocks from the complex, distinctly lower than that typical of the mid-ocean ridge basalts but comparable with that of arc-related magmas. Within Kohistan, the Sapat complex imitates tectonic locale of the Jijal complex together with chromite chemistry (Jan et al., 1993), though grade of metamorphism in the epidote-amphibolite facies is distinctly lower than that of the garnet-granulite facies of the Jijal complex (Jan and Howie, 1981). No direct evidence of age is available from the Sapat complex. It may be noted that the Jijal

complex, in equivalent tectonic locale westward in the Indus valley, has yielded Sm-Nd ages of $104 \pm$ Ma on garnet (Coward et al., 1986), $115 \pm$ Ma (Sano et al., 1996), 118 ± 13 Ma (Yammamoto and Nakamura, 1996) 96 ± 3 Ma Sm-Nd mineral isochron (Anczkiewicz and Vance, 1997), and a Rb-Sr mineral isochron age of 101 ± 6 Ma (Anczkiewicz and Vance, 1997).

The Amphibolite Belt

Amphibolites constitutes one of the principal components of the arc crust in Kohistan (Jan, 1979, 1988). They are widespread in SE Kohistan, occurring between the Sapat complex in the south and the Chilas complex in the north. Four compositional varieties of amphibolites have been identified in the studied area, which are named as Babusar, Niat, Jal and Sumal amphibolites (Fig 2.12).

The Babusar amphibolites form a linear east-west oriented belt of about 1.5 km width, overlying the Sapat complex which occurs immediately to the south. The original contact relations between the two are not preserved due to strong shearing. The amphibolites comprise both homogeneous and banded varieties. A fine- to medium-grained general texture distinguishes them from amphibolitized gabbros of the Sapat complex. Modal composition is dominated by amphibole and epidote, with common plagioclase, quartz and chlorite, and rarely garnet. Minor mineral phases include sphene, magnetite, muscovite and biotite. Whole-rock geochemistry suggests a tholeiitic composition with trace element patterns characterized by high Sr and low Nb anomaly, typical of subduction-related complexes (Khan and Thirlwall, 1988). The Babusar amphibolites show low TiO_2 (0.8 mean%) and very low Zr (8.7ppm mean). This group shows Fe-Ti depletion and alumina enrichment with fractionation, suggesting the role of iron-bearing

minerals (possibly spinels) from the onset of crystallization and absence of the control of plagioclase from the fractionation assemblage.

Much of the area in SE Kohistan between the Babusar amphibolite and the Chilas complex is occupied by fine-grained, strongly foliated amphibolites. These amphibolites are divided into two units; Niat and Jal amphibolites. The latter is pervasively intruded by veins and dykes of trondhjemitic/granitic composition, but otherwise is exactly alike to the Niat amphibolite in terms of mineralogical and chemical composition. The Jal-Niat amphibolites are characteristically fine-grained, strongly foliated and homogenous in composition. Locally, however, greenish epidote-rich layers alternate with dark layers, furnishing a banded appearance to the amphibolites. Such rocks, at a few places, are observed to have relict pillow structures, suggesting that at least in some cases the banded amphibolites are derived from pillowed basalts through shearing. Gabbroic amphibolites, common in parts of the Kamila belt exposed in the Indus and Swat valleys, are characteristically absent from the Jal-Niat amphibolites. The rocks contain amphibole, plagioclase and quartz as essential minerals, whereas epidote, chlorite, muscovite and sphene occur in subordinate amounts. Opaque mineral (magnetite), apatite and zircon occur as accessory minerals. Khan et al. (1993) noted ocean-floor affinity for these rocks. A larger set of samples have been analyzed from these units confirming the MORB-type character reflected in high content of HFSE, including TiO_2 and Y, relative to the arc-related basalts. They show depletion of MgO , CaO and Al_2O_3 with advancing fractionation, suggesting early crystallization of olivine and plagioclase, which is a typical feature of MORB tholeiites.

The Sumal amphibolites are restricted to a narrow belt (~ 500 m thick) tectonically sandwiched within the Niat amphibolites. These amphibolites are best exposed in the Buto Gah. These are typically fine-grained, and much lighter in colour than the Niat amphibolites. A volcanogenic protolith is confirmed by the presence of stretched but intact pillow structures. Modal composition is dominated by amphibole, epidote and quartz with plagioclase, chlorite, sphene, muscovite and biotite. Relict clinopyroxene, mantled by amphibole, is noticed in some sections. Whole-rock geochemistry suggests a basaltic andesite composition, with a distinct calc-alkaline nature. Incompatible trace elements have mutual ratios suggestive of a subduction-related origin. They are enriched in Al_2O_3 and K_2O and depleted in TiO_2 and Fe_2O_3 as compared with the tholeiitic rocks (Babusar, Jal and Niat units). These are depleted in HFS elements and enriched in LIL elements and, together with spiked signatures of Sr and K, are suggestive of derivation from subducted lithospheric slab.

The Thak Granitoid Sheets

The Thak intrusive complex comprises gabbros, diorites, tonalites, granodiorites, granites and trondhjemites. Two modes of occurrence are observed in the studied area; 1) large sheet-like lenticular masses, and 2) minor intrusives in the form of veins, sills or dykes. Two bodies (i.e., Shai and Khun) are thick, sheet-like and stretch east-west for a distance of ~ 40 km. They are composite, comprising gabbros, diorite/tonalite, granodiorite and granite. The minor intrusions, forming veins, sills and dykes are also abundantly present, but are characterized by variance in distribution and composition. They are predominantly granitic or trondhjemitic in composition with aplitic as well as pegmatitic textures.

The Thak granitoid sheets consist of a series of three main petrogenetic groups comprising gabbro; gabbro-diorite/tonalite-granodiorite-granite; and trondhjemite. Al_2O_3 and MgO distinguish the three discrete groups. All the granitoid rocks display calc-alkaline trend. The magmatism becomes progressively more acidic with time in the first two groups. The major elements (TiO_2 , Fe_2O_3 , and CaO) display a linear variation trends against SiO_2 and Al_2O_3 , Na_2O , K_2O and P_2O_5 show scatter. Amongst the trace elements, Nb and Zr display a positive trends for the group of tonalite-granodiorite, while gabbro and trondhjemites show no particular trend either mutually or with this group. Y is high in gabbros, intermediate in gabbro-tonalite-granodiorites and is low in trondhjemites. All other trace elements display a considerable scatter when plotted against SiO_2 . Major and trace element variations clearly suggest that trondhjemites are not comagmatic with the rest of the granitoids, and so is the case, probably, with the gabbro.

Like major and trace element variations, patterns of incompatible trace elements classify the granitoid rocks into three groups: I) Foliated, metamorphosed gabbros, showing incompatible trace element concentrations eight to ten times higher than that of the primordial mantle. The patterns are mostly flat or slightly inclined towards left, with HFSE (Zr and Y) slightly enriched relative to LILE (K and Rb) and negative Nb anomaly is missing. The trace element pattern for this group is closely comparable with that of the host Jal-Niat amphibolites. II) Foliated gabbro, diorite/tonalite and granodiorite with trace-element patterns inclined towards right due to relative enrichment in LILE, and showing Nb anomaly. Patterns of granodiorite are strongly inclined towards right, with strong enrichment in K and Rb. The trace element patterns for all these rocks show a close similarity with the subduction-related plutonic rocks from Kohistan (e.g., Chilas Complex and

Kohistan batholith). III) The trondhjemites showing highly spiked patterns with overall inclination towards the right.

On the basis of field observations, petrography and geochemical behavior of the granitoid rocks, the following salient features of the rocks from the Thak granitoid sheets are deduced:

1) Diorites and tonalites form the principal component of the intrusive complex in SE Kohistan in terms of volume proportions, followed by granodiorites and gabbros. Of the minor intrusions, trondhjemites are the most abundant, granites are subordinate, while andesites and dacites are uncommon.

2) Almost all the granitoid intrusive complex is younger than the host metavolcanic amphibolites. Amongst the various constituent phases the order of intrusion appears to be as follow:

i) high Ti-gabbro-tonalite-trondhjemite gneisses intercalated with Niat metavolcanic unit have composition very close to the host metavolcanics and share the same phase of metamorphism and deformation, suggesting an early stage of intrusion.

ii) gabbros, diorites and tonalites.

iii) trondhjemites, granites and andesite/dacite dykes and veins.

3) Tronhjemites have a preferred distribution in SE Kohistan, mainly restricted to the northern parts of the amphibolite belt in the Jal unit. Their restricted distribution close to the Jal shear zone and the lower contact of the Chilas complex suggest a role of these tectonic elements in their genesis.

4) All the granitoid rocks, in SE Kohistan are ductily deformed. The deformation is particularly strong in the most southerly bodies (e.g., Babusar RH), where the rock is transformed into blastomylonite gneisses. Smoky gabbros and

gabbroic diorites to the south of the Khun bridge (Thak Gah) are the least deformed rocks in SE Kohistan. Rather than being post tectonic, these rocks escaped deformation due to their location in the interior of the 5 km thick sheeted body. Even the trondhjemites which cross-cut the fabric in the amphibolites are syntectonic in origin. Presence of foliation in the granitoid rocks of SE Kohistan enables their correlation with stage-I Kohistan batholith of Petterson and Windley (1985).

Discussion

The geological investigations in SE Kohistan have added to the existing understanding of the Kohistan magmatic arc. Amongst other things, this study has implications for many models, for the growth of continental crust acknowledge the important role played by the evolution of island arcs from their intra-oceanic initiation through to their incorporation, through collision and suturing, into continental crust. Despite their parental significance, through growth and lateral accretion, to continental crust, details of the internal structure of island arc crust is, as yet, understood only poorly. The existence of plutonic xenoliths in the volcanic rocks of modern island arcs has been noticed (Laxroix, 1904), with the xenoliths interpreted as indicating the presence of cumulate ultramafic and gabbroic rocks at depth (Arculus and Wills, 1980). However, the presence of large plutonic bodies is still considered atypical of the oceanic island arcs (Moores and Twiss, 1995). This mapping along a transect at the south eastern margin of the Kohistan terrane discuss the implications for : 1) the constitution of the lower arc crust, and 2) mechanisms of thickening of the lower arc crust.

Constitution of the Lower Arc Crust

Mapping of the SE Kohistan terrane has added considerable new and important informations regarding the constitution of the lower arc crust. Identification of the Sapat mafic-ultramafic complex in the hangingwall of the MMT has highlighted the importance of stratiform complexes in the basal part of lower arc crust. The close similarities in terms of silicate mineralogy (Jan et al., 1993) between the Sapat complex and the Jijal complex of the Indus valley suggest a mutually similar origin and tectonic setting in the basal crust of the Kohistan arc terrane. Miller et al. (1991) and Jan et al. (1997) have demonstrated that garnetiferous gabbroic rocks in the Jijal complex have a primarily high-pressure origin, superimposed by granulite-facies metamorphism probably soon after their crystallization (Anczkiewicz and Vance, 1997). Although compositional factors cannot be ignored, the absence of garnet in the Sapat complex probably precludes a high-pressure emplacement and metamorphism for it. Hence, it is considered that the Sapat complex had a shallower depth of emplacement than the Jijal complex. Of the three gabbroic plutons (Pattan, Kiru, Dassu) located upsection from the Jijal complex in the Indus valley (Loucks et al., 1993), either the Pattan or Kiru body could be the western continuation or equivalent of the Sapat complex. The occurrence of the Sapat complex in the hangingwall of the MMT may be explained by a lateral ramping of the MMT upsection away from Jijal. The staircase geometry of the MMT supports this conclusion.

The part of the Kamila amphibolite belt exposed between the Sapat and Chilas complexes in the presently studied transect is significant in several respects. Firstly, gabbroic plutons are rare and metabasalts constitute the principal component of the belt here. The metavolcanic component becomes subordinate

westward in the Indus and Swat valleys but remains an essential constituent of the belt, ranging from screens between the gabbroic plutons in the Indus and Swat valleys (Treloar et al., 1990) to thick successions of banded, frequently pillowed, amphibolites in the Swat and Dir sections (Jan, 1979; Treloar et al., 1997). Secondly, a composite nature of the belt has become evident and supported by trace-element geochemistry. High-Ti metabasalts tectonically intercalated with a belt of calc-alkaline meta-andesite and a belt of island-arc tholeiites suggest that the Kamila amphibolite belt has a complex origin. Khan et al. (1993), identifying MORB-like geochemistry of the high-Ti metabasalts, suggested that the Kamila belt represents, at least partially, a remnant oceanic basement which was subsequently intruded by subduction-related magmas of the Kohistan island arc. Since then, two other possibilities have been proposed. On the basis of trace element data, Treloar et al. (1996) suggested an oceanic-plateau origin for the high-Ti metabasalts of the Kamila belt, while Khan et al. (1997), on the basis of existence of subduction-related tholeiitic and calc-alkaline meta-volcanics in close association with MORB-type metabasalts, argued for a back-arc origin. The data is, as yet, insufficient to ascertain in which of these tectonic settings the Kamila belt evolved. Nevertheless, the existence of pillow structures in both the high-Ti metabasalts and calc-alkaline meta-andesites indicate initial formation in a basin of either oceanic or island-arc origin. This raises a question relating to the mechanisms responsible for transporting the Kamila belt from its initial position at shallow crustal levels to the lower-middle crust which will be addressed later.

The position of the Chilas complex in the magmatic stratigraphy of the Kohistan crust has been debated. Coward et al. (1982, 1986) raised the possibility that the Chilas complex is a folded limb of the Jijal complex, emplaced at the very

base of the arc crust. Jan et al. (1992) demonstrated that, beside other differences, the chromite in the Chilas complex is characterized by low Cr No. than that of the Jijal complex at equivalent mg no. ($100 \text{ Mg}/(\text{Mg}+\text{Fe}^{2+})$). Mapping at the southern margin of the Chilas complex provides unequivocal evidence regarding the stratigraphic position of the Chilas complex. The southern contact of the Chilas complex against the Kamila amphibolite is sheared in the Babusar-Chilas transect. However, presence of xenoliths closely resembling the Kamila amphibolites close to the contact suggests an intrusive nature for the Chilas complex. In the Indus valley section, hydrated gabbro-norites of the Chilas complex are clearly intrusive into a metavolcanic succession, containing calc-silicate horizons, that belong to the Kamila belt. First noted by Khan (1988), these xenoliths on both sides of Chilas complex have been reported in several recent publications including Khan, T. and Shirahase (1996), Takahashi et al. (1996) and Treloar et al. (1996). Treloar et al. (1996), additionally, suggest that the fabric in the xenoliths, which dates from the time of suturing of Kohistan to Asia, predated the intrusion of the Chilas complex, which they consider to have occurred contemporaneously with, or closely following, the closure of the northern suture.

Thickening of the Lower Arc Crust

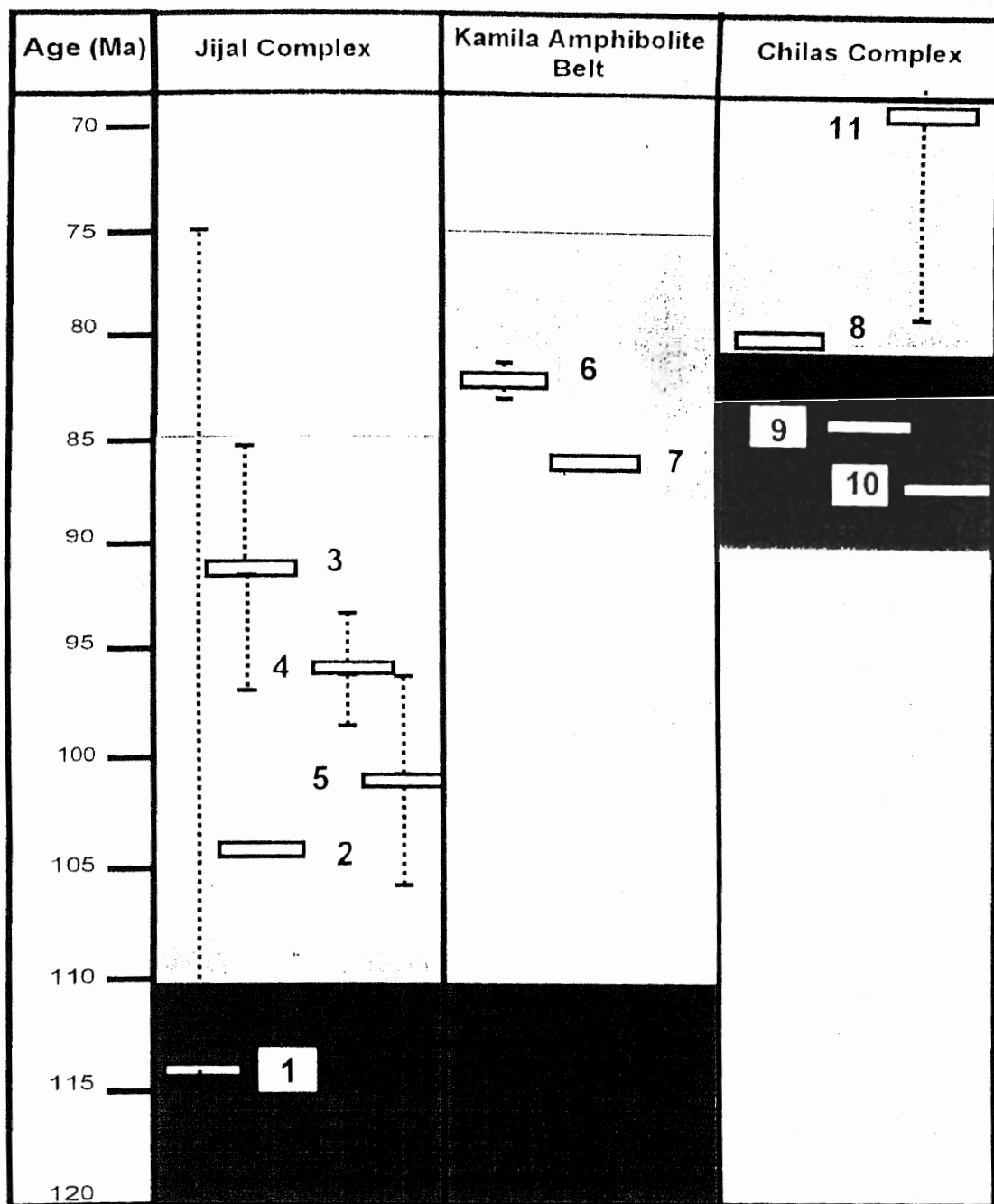
As demonstrated above, the Kamila amphibolite belt is essentially comprised of metabasalts with some relict pillow structures, intruded by gabbros. This infers that the Kamila belt represents a marine volcanic sequence that capped, and was intruded by, the Sapat complex which, in turn, occurred at the top of a stack of plutonic ultramafic-gabbroic complexes including the Jijal complex. This raises two questions. 1) Was this crust thick enough to have crystallized garnet gabbros at its base, such as those of the Jijal complex? 2) How was the

Kamila belt subsequently transported and buried to its position at lower to middle levels in the arc crust?

Loucks et al. (1993) discussed mechanism for thickening of the arc crust based on their studies in the Indus valley section. They considered the Kamila belt to comprise a stack of ultramafic-gabbroic plutons, which included from south to north (i.e., from base, upwards) Jijal, Pattan, Kayal, Dassu and Chilas complexes (also see Miller et al., 1991; Miller and Christensen, 1994). In order to explain the primary crystallization of garnet-clinopyroxene assemblages in the gabbros of the Jijal complex, these authors considered that the arc crust in Kohistan was thickened by the magmatic emplacement of ultramafic-mafic plutons one below the other, with the Jijal complex being the youngest and the most basal in terms of its magmatic emplacement.

Figure 6.1 summarises the existing radiometric age data from southern Kohistan. Despite being limited in number, the mineral as well as the whole-rock radiometric data indicate ages for the Jijal complex distinctly older than those for the Kamila amphibolite belt, which are likely to be metamorphic ages, and for the Chilas complex. These results are contrary to those predicted by the model of Loucks et al. (1993) and suggest that the lower to middle arc crust in Kohistan experienced a more complex history of crustal growth, thickening, and metamorphism than that envisaged by Loucks et al. (1993). On the basis of the existing radiometric age data (Figure 6.1), combined with reasoning based on field relations, a three-stage evolution of the arc crust in Kohistan is inferred in terms of thickening and associated metamorphism ⁱⁿ Figure 6.2.

As indicated earlier, the Jijal and Chilas complexes cannot be considered together as they are fundamentally different in, among other things, their petrology



Probable ages of magmatic emplacement.

Cooling ages.

1. Sm-Nd whole-rock (wr) isochron, 114 ± 39 Ma. Sano et al. (1996)
2. Sm-Nd on garnet, 104 Ma. Thirlwall, M.F. in Coward et al. (1986)
3. Sm-Nd mineral isochron, 91 ± 6.3 Ma. Yamamoto and Nakamura (1996)
4. Sm-Nd mineral isochron, 95.7 ± 2.7 Ma. Anczkiewicz and Vance (1997)
5. Rb-Sr mineral isochron, 101.3 ± 5.7 Ma. Anczkiewicz and Vance (1997)
6. Ar-Ar spectrum, 83 ± 1 Ma. Treloar et al. (1989)
7. Ar-Ar spectrum, 86 Ma. Zeitler (1985)
8. Ar-Ar base of a U-shaped spectrum, 80 Ma. Treloar et al. (1989)
9. U-Pb on zircon, 84 Ma. Zeitler et al. (1980)
10. Rb-Sr (wr) isochron, 87 Ma. Mikooshiba et al. (1996)
11. Sm-Nd mineral isochron, 69.5 ± 9.3 Ma. Yamamoto and Nakamura (1996)

Figure 6.1. A summary of radiometric ages from southern Kohistan. The subdivision into "emplacement" and "cooling" ages is purely interpretative.

and silicate mineralogy (Khan et al., 1989; Jan et al., 1991; Jan and Windley, 1991), age of emplacement and their position of magmatic emplacement with one at the base and the other on the top of the Kamila amphibolite belt. The present author considers that the mechanism for crustal thickening proposed by Loucks et al. (1993) could be appropriate for those plutons, including the Jijal, Sapat, Pattan, Kayal and Dassu bodies, but excluding the younger Chilas complex, that were emplaced at the base of the arc crust below, and into, the Kamila amphibolite belt Figure 6.2a. This phase of magmatic crustal thickening, and associated metamorphism of the deep crust, occurred prior to 90 Ma and was responsible for base of the arc attaining pressures in excess of 10 kbar needed to crystallize primary garnet-clinopyroxene assemblages in gabbros of the Jijal complex. Although volcanic rocks of the Kamila amphibolite belt might have experienced low temperature metamorphism at this stage. The peak metamorphism within the belt is defined on microtextural criteria (Treloar et al., 1990) as occurring synchronously with, or shortly after, deformation associated with crustal thickening linked to Kohistan-Asia suturing. Hornblende Ar-Ar data (Treloar et al., 1989) date cooling after this event at ca. 83 Ma.

The second stage of crustal evolution is related to the transportation and burial of the Kamila belt to mid-crustal levels. Two mechanisms are possible: 1) south-verging thrusting of the northern parts of the arc terrane (including Chilas complex and overlying metasediments/ metavolcanics of the Jaglot-Chalt groups) onto the Kamila amphibolite belt causing its burial and internal thickening, or 2) magmatic emplacement of the Chilas complex into the top of the metavolcanic pile that forms the Kamila amphibolite belt, at its stratigraphic interface with overlying metasedimentary / metavolcanic succession of Jaglot Group. Field evidence

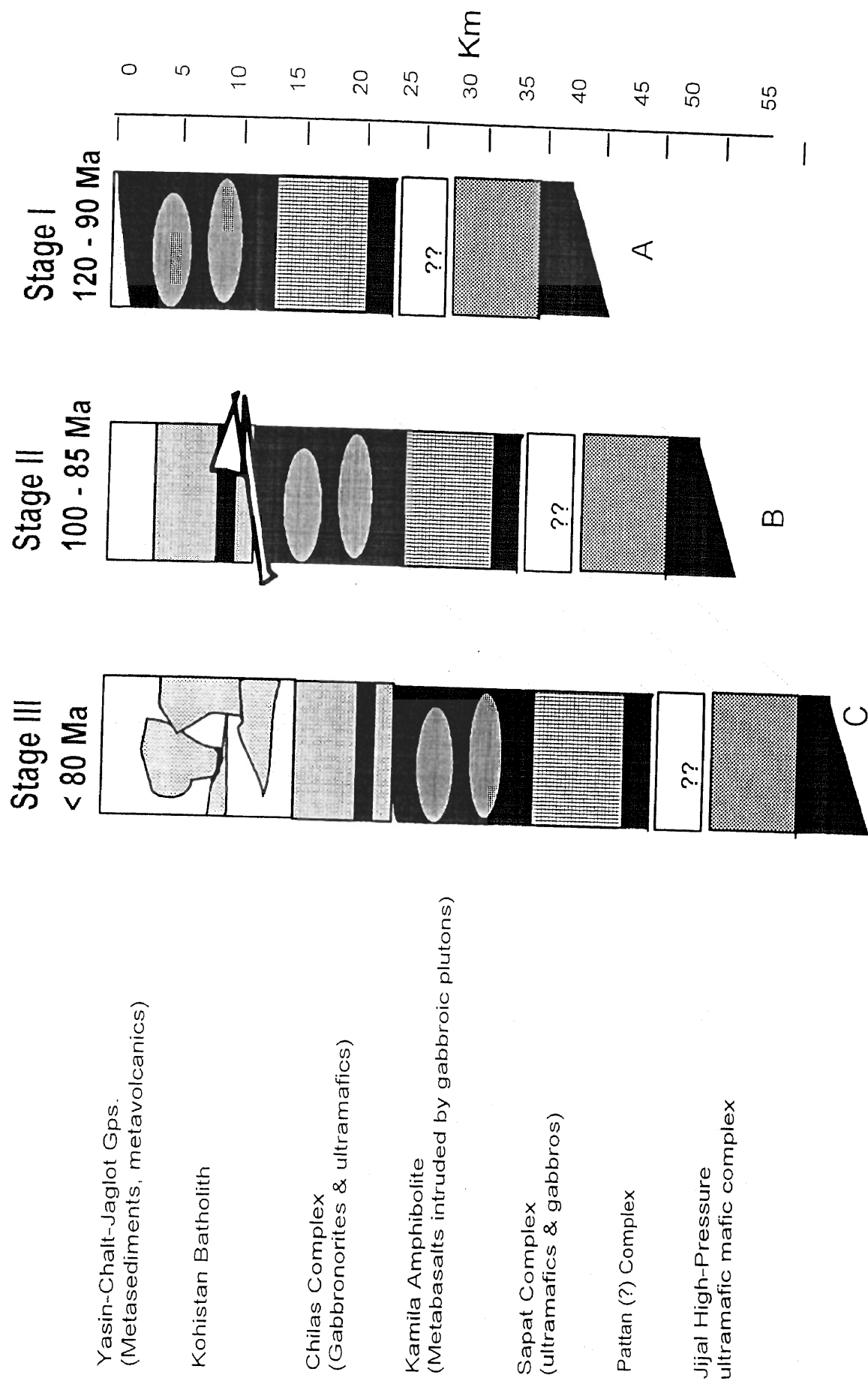


Figure 6.2. Schematic representation of three-stage model of crustal thickening in Kohistan terrane.

suggests a role for both of these processes in thickening of the arc crust in Kohistan and burial of the Kamila belt to mid-crustal levels (Figure 6.2b).

Treloar et al. (1990) have described the presence of a 28 km wide shear zone, the Kamila Shear Zone, within the Kamila belt in the Indus valley section. This is an anastomosing continuation of the shear zone at the southern contact of the Chilas complex exposed in the Babusar valley (Khan and Coward, 1990). The Kamila Shear Zone is a crustal scale shear zone that accommodated south-vergent crustal shortening and was responsible for internal imbrication and stacking of the arc crust. Internal deformation and associated amphibolite-facies metamorphism is of Cretaceous age (80 Ma and older; Treloar et al., 1989). In the upper arc, structures of a similar age are recorded in the Jaglot syncline and thrusts to the north and south of Gilgit, and in the flattening of pillows in the volcanic sequences. All of these structures relate to whole arc thickening associated with suturing to Asia. Field evidence, including the occurrence of xenoliths of deformed Kamila metavolcanic rocks in the lower or southern margins of the Chilas complex, and of deformed meta-sediments (pelitic schists, paragneisses and migmatites) of the Gilgit Formation in the uppermost or northern parts of the complex, suggest post-deformational magmatic emplacement of the complex on top of the Kamila amphibolite and below the Gilgit Formation, probably at the stratigraphic interface between the two. Thus the burial of the Kamila amphibolite belt from an initially shallow crustal position in a basin of oceanic or island-arc origin to middle or lower crustal levels in the arc crust occurred both by crustal shortening accompanying suturing, including stacking along the Kamila shear zone, and by burial beneath the Chilas complex by magmatic emplacement of granodiorite magmas. On the basis of data presented in Treloar et al. (1989), the

author envisages that this stage of crustal thickening took place between 90 and 80 Ma. Treloar et al. (1996) suggested that peak metamorphism within the volcano-sedimentary units of the Kamila amphibolite belt, Jaglot and Chalt Groups could be related to a combination of heat generation through radioactive decay within the thickened arc complex. Hornblende Ar-Ar ages date cooling back through 500°C after this metamorphism at ca. 80-85 Ma (Figure 6.1; Treloar et al. 1989).

Finally, during the continental margin stage of crustal growth, much of the Kohistan batholith was emplaced into the deformed volcano-sedimentary cover units of the upper part of the arc crust (Figure 6.2c). Batholithic emplacement, associated with the construction of volcanic pile during the sub-aerial felsic volcanism recorded within the Dir Group (Sullivan et al., 1993) represents a third stage of crustal thickening. This final stage of, dominantly magmatic, crustal thickening followed collision along the Shyok suture between Kohistan and Asia and lasted until the closure of the Indus suture between the Kohistan and Indian plates.

Conclusion

The Kohistan terrane exposes a superb section through an island arc crust right down to near its contact with upper mantle. Much of the lower arc crust comprises extensive plutons of gabbroic composition, some with minor layered ultramafic soles. These plutons were intruded into the base of a pile of meta-volcanic rocks of the Kamila amphibolite belt which, at lower crustal levels, occur as screens between the plutons. This phase of arc-crustal growth (120-90 Ma), was controlled primarily by magmatic emplacement of mafic-ultramafic plutons into the base of the arc. It caused sufficient magmatic thickening of the arc crust ~35 km to result in the crystallization of high-P (~10-11 kbar) mineral phases in the Jijal

complex. The second stage of crustal thickening has two components and followed on from collision of the Kohistan arc with the Asian plate at between 100 and 85 Ma. During this stage volcanic rocks of the Kamila amphibolite were transported and buried from their former position at upper crustal levels to a mid-crustal position. This burial was accomplished by a combination of whole arc thickening caused by south-vergent crustal shortening which included crustal stacking along the Kamila Shear Zone, and by the emplacement of a large body of ultramafic-gabbroic rocks (the Chilas complex) along the interface between the Kamila belt and the overlying sedimentary-volcanic succession. Finally, the third stage of substantial crustal thickening was by magmatic processes during the late-Cretaceous to early Tertiary Andean-margin stage of its evolution through the addition of voluminous amounts of intermediate to felsic magma some of which was emplaced as granitoid components of the Kohistan batholith and some of which was extruded as part of the Dir Group volcanic series.

REFERENCES

- Ahmed, Z., 1978.** Petrology of the Taghma area, Swat district NWFP, Pakistan. *Geological Bulletin, Punjab University*, **15**, 25-29.
- Ahmed, Z., 1978.** Chromite from Skhakot-Qila area, Malakand Agency, Pakistan. *Mineralogical Magazine*, **42**, 155-157.
- Ahmed, Z., 1982.** Porphyritic-nodular, nodular and orbicular chrome ores from the Sakhakot-Qila complex, Pakistan, and their chemical variation. *Mineralogical Magazine*, **45**, 167-178.
- Ahmed, Z., 1984.** Stratigraphic and textural variations in the chromite composition of the ophiolitic Sakhakot-Qila complex, Pakistan. *Economic Geology*, **79**(6), 1334-1359.
- Ahmed, Z., 1988.** Bulk-rock chemistry and petrography of the Sakhakot-Qila ophiolite, Pakistan. *Acta Mineralogica, Pakistanica*, **4**, 4-29.
- Ahmed, Z. and Chaudhry, M. N., 1976.** Petrology of the Babusar area, Diamir district, Gilgit, Pakistan. *Geological Bulletin, Punjab University*, **12**, 67-78.
- Anczkiewicz, R. and Vance, D. 1997.** Chronology of subduction, collision and regional metamorphism in Kohistan, Pakistan Himalaya. *European Union of Geoscientists, Strasberg*, 345.
- Anderson, J. L. and Cullers, R. L., 1987.** Crust-enriched, mantle-derived tonalites in the early Proterozoic Penokean orogen of Wisconsin. *Journal of Geology*, **95**, 139-154.
- Arculus, R. J. and Powell, R., 1986.** Source component mixing in the regions of arc magma generation. *Journal of Geophysical Research*, **91**, 5913-5926.
- Arculus, R. J. and Wills, K. J. A., 1980.** The Petrology of plutonic blocks and inclusions from the lesser Antilles island arc. *Journal of Petrology*, **21**, 743-799.
- Arif, M. and Jan, M. Q., 1993.** Chemistry of chromite and associated phases from the Shangla ultramafic body in the Indus suture zone of Pakistan. In: Treloar, P. J. & Searle, M. P. (eds.) Himalayan Tectonics. *Journal of the Geological Society of London*, Special Publication, **74**, 101-112.
- Arth, J. G. and Barker, F., 1976.** Rare-earth partitioning between hornblende and dacitic liquid and implications for the genesis of trondhjemitic-tonalitic magmas. *Geology*, **4**, 534-536.
- Arth, J. G., Barker, F., Peterman, Z. E. and Friedman, I., 1978.** Geochemistry of the gabbro-diorite-tonalite-trondhjemite suite of southwest Finland and its implications for the origin of tonalitic and trondhjemitic magmas. *Journal of Petrology*, **19**, 289-316.

- Arth, J. G. and Hanson, G. N., 1972.** Quartz diorites derived by partial melting of eclogite or amphibolite at mantle depth. *Contributions to Mineralogy and Petrology*, **37**, 161-174.
- Arth, J. G. and Hanson, G. N., 1975.** Geochemistry and origin of the early Precambrian crust of northeastern Minnesota. *Geochimica Cosmochimica Acta*, **39**, 325-362.
- Ashraf, M., Loucks, R.R. and Awan, M.A., 1989.** Serpentinization of cumulate ultramafites and development of heazlewoodite-pentlandite-awaruite-magnetite and pentlandite-chalcopyrite-pyrrhotite-pyrite association in Alpurai and Kishora, Swat, Pakistan. *Kashmir Journal of Geology*, **6-7**, 1-17.
- Atherton, M. P. and Petford, N., 1993.** Generation of sodium-rich magmas from newly underplated basaltic crust. *Nature*, **362**, 144-146.
- Baig, M.S., 1989.** New occurrences of blueschist from Shin-Kamer and Marin areas of Allai-Kohistan, NW Himalaya. *Pakistan. Kashmir Journal of Geology*, **6-7**, 103-108.
- Bakr, M.A. and Jackson, R.O., 1964.** Geological map of Pakistan. *Geological Survey of Pakistan*, Quetta.
- Bard, J.P., 1983a.** Metamorphism of an obducted island arc: Example of the Kohistan sequence (Pakistan) in the Himalayan collided range. *Earth and Planetary Science Letters*, **65**, 133-144.
- Bard, J.P., 1983b.** Metamorphic evolution of an obducted island arc: Examples of the Kohistan sequence (Pakistan) in the Himalayan collided range. *Geological Bulletin, Peshawar University*, **16**, 105-184.
- Bard, J.P., Maluski, H., Matte, Ph. and Proust, F., 1980.** The Kohistan sequence; Crust and mantle of an obducted island arc. *Geological Bulletin, Peshawar University*, **13**, 87-93.
- Barker, F., 1979.** Trondhjemite: definition, environment and hypotheses of origin. *Trondhjemites, Dacites, and Related Rocks*, edited by F. Barker, Elsevier, New York. 1-12.
- Barnes, C. G., Petersen, S. W., Kistler, R. W., Murray, R. and Kays, M. A., 1996.** Source and tectonic implications of tonalite-trondhjemite magmatism in the Klamath Mountains. *Contributions to Mineralogy and Petrology*, **123**, 40-60.
- Barth, T. F. W., 1962.** A final proposal for calculating the mesonorm of metamorphic rocks. *Journal of Geology*, **70**, 497-498.
- Battey, M. H., 1956.** The petrogenesis of spilitic rock series from New Zealand. *Geological Magazine*, **93**, 83-110.
- Beard, J. S., 1986.** Characteristic mineralogy of arc-related cumulate gabbros; Implications for the tectonic setting of gabbroic plutons and for andesite genesis. *Geology*, **14**, 848-851.

- Beard, J. S. and Lofgren, G. E., 1991.** Dehydration melting and water-saturated melting of basaltic and andesitic greenstones and amphibolites at 1, 3, and 6.9 kb. *Journal of Petrology*, **32**, 365-401.
- Bird, M.L. and Clark, A.L., 1976.** Microprobe studies of olivine chromitites of the Goodnews Bay ultramafic complex, Alaska, and the occurrence of Platinum. *Journal of Research, Geological Survey of USA*, **4**, 717-725.
- Blaise, J., Bordet, P., Carbonnet, J. P. and Montenat, C., 1978.** Flysch et ophiolites dans le region de Panjau: une suture neocimmerienne en Afghanistan central. *Bulletin of de la Society Geologique de France*, **7**, 795-798.
- Brewer T.S. and Atkin B.P., 1989.** Element mobilities produced by low grade metamorphic events. A case study from the Proterozoic of southern Norway. *Precambrian Research*, **45**, 143-158.
- Bryan, W. B., 1983.** Systematics of model phenocryst assemblages in submarine basalts: petrologic implications. *Contributions to Mineralogy and Petrology*, **83**, 62-74.
- Bugge, J. A. W., 1945.** The geological importance of diffusion in the solid state, *Norske Vidensk.-akad. Oslo Skr., I. Math.-Naturev. Kl*, **13**, 5-59.
- Burbank, D.W. and Johnson, G.D., 1983.** The late Cenozoic chronologic and stratigraphic development of the Kashmir intermontane basin, northwest Himalaya. *Paleogeography of the Paleoclimatology and Paleoecology*, **43**, 205-235.
- Burg, J. P. and Chen, G. M., 1984.** Tectonic and structural zonation of southern Tibet, China. *Nature*, **311**, 219-223.
- Burg, J. P., Guiraud, M., Chen, G. M. and Li, G. C., 1984c.** Himalayan metamorphism and deformations in the North Himalayan Belt (southern Tibet, China). *Earth and Planetary Science Letters*, **69(2)**, 391-400.
- Burg, J. P., Leyreloup, A., Girardeau, J. and Chen, G. M., 1987.** Structure and metamorphism of a tectonically thickened continental crust: the Yalu Tsangpo suture zone Tibet. *Philosophical Transactions of the Royal Society of London*, **321**, 67-86.
- Burns L. E., 1985.** The Border Ranges ultramafic and mafic complex, South-Central Alaska: Cumulate fractionates of island-arc volcanics. *Contributions to the Journal of Earth. Sciences*, **22**, 1020-1038.
- Butler, R. W. H., 1986.** Thrust tectonics, deep structures and crustal subduction in the Alps and Himalayas. *Journal of the Geological Society of London*, **143**, 857-873.
- Butt, K. A., Chaudhry, M. N. and Ashraf, M., 1980.** An interpretation of petrotectonic assemblage west of W. Himalayan syntaxis in Dir district and adjoining areas in northern Pakistan. *Geological Bulletin, Peshawar University*, **13**, 79-86.

Calkins, J. A., Jamiluddin, S., Bhuyan, K. and Hussain, A., 1981. Geology and mineral resources of the Chitral-Paristan area, Hindu Kush Range, northern Pakistan. *U. S. Geological Survey Professional Paper*, **716-G**, 1-33.

Casnedi, R., 1976. The ophiolites of the Indus suture line (Dras and Astor zones - Kashmir). *Ophioliti Bologna*, **1(3)**, 365-371.

Casnedi, R., 1976. Geological Reconnaissance in Yasin Valley (NW Pakistan). Estratto dal fasc. 6. Ser VIII, LIX-Dec, *Accademia Nazionale Dei Lincei, Rome*, 793-799.

Casnedi, R., Desio, A., Forecella, F., Nicoletti, M. and Petrucciani, C. , 1978. Absolute age of some granitoid rocks between Hindu Raj and Gilgit (Karakoram). *Rend. Accad. Naz. Lincei*, **63**, 204-210.

Cawthorn, R. G., Strong, D. F. and Brown, P. A., 1976. A model for the formation and crystallization of corundum-normative calc-alkaline magmas through amphibole fractionation. *Journal of Geology*, **84**, 467-476.

Cerveny, P. F., Johnson, N. M., Tahirkheli, R. A. K. and Bonis, N. R., 1989. Tectonic and geomorphic implications of Siwalik Group heavy minerals, Potwar Plateau, Pakistan. In: Malinconico Jr., L. L. and Lillie, R. J. (ed.) Tectonics of the western Himalayas. *Geological Society of America, Special Paper*, **232**, 129-136.

Chamberlain, C. P., Jan, M. Q. and Zeitler, P. K., 1989a. A petrologic record of the collision between the Kohistan island arc and Indian plate, northwest Himalaya. In: Malinconico, L.L. & Lillie, R.J. (eds.) Tectonics of the Western Himalayas. *Geological Society of America, Special Paper*, **232**, 23-32.

Chamberlain, C. P., Zeitler, P. K. and Erickson, E., 1991. Constraints on the tectonic evolution of the northwestern Himalaya from geochronologic and petrologic studies of Babusar Pass, Pakistan. *Journal of Geology*, **99**, 829-849.

Chamberlain, C. P., Zeitler, P. K. and Jan, M. Q., 1989b. The dynamics of the suture between the Kohistan island arc and Indian plate, northwest Himalaya. *Journal of Metamorphic Geology*, **7**, 135-145.

Chang, C. and 27 others, 1986. Preliminary conclusions of the Royal Society and Academia Sinica 1985 Geotraverse of Tibet. *Nature*, **323**, 501-507.

Chappell, B. W. and White, A. J., 1974. Two contrasting granite types. *Pacific Geology*, **8**, 173-174.

Chaudhry, M. N. and Chaudhry, A. G., 1974. Geology of Khagram area, Dir district. *Geological Bulletin, Punjab University*, **11**, 21-43.

Chaudhry, M. N. and Ghazanfar, M., 1987. Geology, structure and geomorphology of upper Kaghan valley, North-West Himalaya, Pakistan. *Geological Bulletin, Punjab University*, **22**, 13-57.

- Chaudhry, M. N., Ghazanfar, M., Ashraf, M. and Shahid, S. S., 1984.** Geology of Shewa-Dir-Yasin area and its plate tectonic interpretation. *Kashmir Journal of Geology*, **2**, 53-63.
- Chaudhry, M. N., Ghazanfar, M. and Qayyum, M., 1986.** Metamorphism at the Indo-Pak plate margin, Kaghan valley, district Mansehra, Pakistan. *Geological Bulletin, Punjab University*, **21**, 62-85.
- Chaudhry, M. N., Hussain, S. S. and Iqbal, M., 1976.** Geology and petrology of Malakand and a part of Dir (Toposheet 38 N/4). *Geological Bulletin, Punjab University*, **12**, 17-39.
- Chaudhry, M. N., Kausar, A. B. and Lodhi, S. A. K., 1974.** Geology of Timurgara-Lal Qila area, Dir district, NWFP. *Geological Bulletin, Punjab University*, **11**, 53-73.
- Chaudhry, M. N., Mahmood, A. and Chaudhry, A. G., 1974.** The orthoamphibolites and the para amphibolites of the Dir district, NWFP. *Geological Bulletin, Punjab University*, **11**, 89-96.
- Cheney, E. C. and Stewart, R. J., 1975.** Subducted graywacke in the Olympic Mountains, USA - implications for the origin of Archean sodic gneisses. *Nature*, **258**, 60-61.
- Coleman, R.G., 1967.** Low-temperature reaction zones and alpine ultramafic rocks of California, Oregon, and Washington. *U.S. Geological Survey Bulletin*, **49**, 1247.
- Coleman, R.G., 1971.** Petrologic and geophysical nature of serpentinites: *Geological Society of America Bulletin*, **82**, 897-918.
- Coleman, R.G., 1977.** Ophiolites: Ancient Oceanic Lithosphere, New York. *Springer-Verlag*, 229 p.
- Coleman, R. G. and Peterman, Z. E., 1975.** Oceanic plagiogranite. *Journal of Geophysical Research*, **80**, 1099-1108.
- Coward, M.P., 1985.** A section through the Nanga Parbat syntaxis, Indus Valley, Kohistan. *Geological Bulletin, Peshawar University*, **18**, 147-152.
- Coward, M. P. and Butler, R. W. H., 1985.** Thrust tectonics and the deep structure of the Pakistan Himalayas. *Geology*, **13**, 417-420.
- Coward, M. P., Butler, R. W. H., Khan, M. A. and Knipe, R. J., 1987.** The tectonic history of Kohistan and its implications for Himalayan structure. *Journal of the Geological Society of London*, **144**, 377-391.
- Coward, M. P., Butler, R. W. H., Chamberlain, A. F., Graham, R. H., Izatt, C. N., Khan, M. A., Knipe, R. J., Prior, D. J., Treloar, P. J. and Williams, M. P., 1988.** Folding and imbrication of the Indian crust during Himalayan collision. *Philosophical Transactions of the Royal Society of London*, **A326**, 89-116.

- Coward, M. P., Jan, M. Q., Rex, D., Tarney, J., Thirlwall, M. and Windley, B. F., 1982. Geotectonic framework of the Himalaya of N. Pakistan. *Journal of the Geological Society of London*, **139**, 299-303.
- Coward, M. P., Jan, M. Q., Rex, D., Tarney, J., Thirlwall, M. and Windley, B. F., 1982. Structural evolution of a crustal section in the western Himalaya. *Nature*, **295**(5844), 22-24.
- Coward, M. P., Windley, B. F., Broughton, R. D., Luff, I. W., Petterson, M. G., Pudsey, C. J., Rex, D. C. and Khan, M. A., 1986. Collision tectonics in the NW Himalayas. In: Coward, M.P. and Ries, A.C. (eds.) *Collision Tectonics*. Geological Society of London, Special Publication, **19**, 203-219.
- Cox, K. G., Bell, J. D. and Pankhurst, R. J., 1979. The interpretation of igneous rocks. *George, Allen and Unwin*, London.
- Cronin, V. S., 1989. Structural setting of the Skardu intermontane basin, Karakoram Himalaya, Pakistan. In: Malinconico Jr., L. L. and Lillie, R. J. (eds.) *Tectonics of western Himalayas*. Geological Society of America, Special Paper, **232**, 183-201.
- Davies, R. G., 1965. The nature of the Upper Swat Hornblende Group of Martin et al. (1962). *Geological Bulletin, Punjab University*, **2**, 51-52.
- DeBari S. M. and Coleman, R. G., 1989. Examination of the deep levels of an island arc: Evidence from the Tonsina ultramafic-mafic assemblage, Tonsina, Alaska. *Journal of Geophysical Research*, **94**, 4373-4391.
- Debon, F. and Le Fort, P., 1983. A chemical - mineralogical classification of common plutonic rocks and associations. *Earth Sciences*, **73**, 135-149.
- Debon, F., Le Fort, P., Dautel, D., Sonet, J. and Zimmermann, J. L., 1987. Granites of western Karakorum and northern Kohistan (Pakistan): A composite Mid-Cretaceous to upper Cenozoic magmatism. *Lithos*, **20**, 19-40.
- Debon, F., 1995. Incipient India-Eurasia collision and plutonism: the Lower Cenozoic Batura granites (Hunza Karakorum, North Pakistan). *Journal of Geological Society, London*, **152**, 785-795.
- Debon, F. and Khan, N. A., 1996. Alkaline orogenic plutonism in the Karakorum batholith: the Upper Cretaceous Koz Sar complex (Karambar valley, N. Pakistan). *Geodinamica Acta (Paris)*, **9**, 4, 145-160.
- Deer, W. A., Howie, R. A. and Zussman, J., 1982. An Introduction to the Rock-Forming Minerals, 13th edition: Essex, England, Longman.
- Defant, M. J., and Drummond, M. S., 1990. Derivation of some modern arc magmas by melting of young subducted lithosphere. *Nature*, **347**, 662-665.
- Defant, M. J. and Drummond, M. S., 1993. Mount St. Helens: Potential example of partial melting of the subducted lithosphere in a volcanic arc. *Geology*, **21**, 547-550.

De la Roche H., Leterrier J., Grande Claude P. and Marchal M., 1980. A classification of volcanic and plutonic rocks using R1-R2 diagrams and major element analyses - its relationships and current nomenclature. *Chemical Geology*, **29**, 183-210.

Deniel, C., Vidal, Ph., Dietrich, V. and Le Fort, P., 1985. Origin of the leucogranites of the High Himalayas. *Terra Cognita*, **5**, 292p.

Deniel, C., Vidal, P., Fernandez, A., Le Fort, P. and Pecaut, J. J., 1987. Isotopic study of the Manaslu granite (Himalayas, Nepal): inferences on the age and source of Himalayan leucogranites. *Contributions to the Mineralogy and Petrology*, **96**, 78-92.

Desio, A., 1959. Cretaceous beds between Karakorum and Hindukush ranges (Central Asia). *Rivista Italiana di Palaeontologia e Stratigrafia*, **65**, 221-229.

Desio, A., 1963. Review of the geological "formations" of the western Karakorum (Central Asia). *Rivista Italiana di Palaeontologia e Stratigrafia*, **69**, 475-501.

Desio, A., 1964. Geological tentative map of the western Karakorum. Scale 1:500,000. *Instituto Geology, University of Milano*.

Desio, A., 1964. Tectonic relationship between the Karakorum, Pamir and Hindu Kush, Central Asia. *Proc. 22nd International Geological Congress, New Delhi*, **11**, 192-213.

Desio, A., 1978. On the geology of the Deosai Plateau (Kashmir). *Memoirs Atti. Della Accademy Naz. Lincei*, **15**, 1-19.

Desio, A., 1979. Geological evolution of the Karakorum. *In: Farah, A. and DeJong, K.A. (eds.) Geodynamics of Pakistan*. Geological Survey of Pakistan, Quetta, 111-124.

Desio, A. and Zanettin, B., 1970. Geology of the Baltoro Basin. Italian Expeditions to the Karakorum (K2) and Hindu Kush (leader A. Desio). *Sci. Rept., Sec.II, vol.2*, Brill, Leiden, 308p.

De Vore (83a)(83b)

Dick, H. J. B. and Bullen, T., 1984. Chromian spinel as a petrogenetic indicator in abyssal and alpine-type peridotites and spatially associated lavas. *Contributions to the Mineralogy and Petrology*, **86**, 54-76.

Dietrich, V. J., Frank, W., and Honegger, K., 1983. A Jurassic-Cretaceous island arc in the Ladakh-Himalayas. *Journal of Volcanology and Geothermal Research*, **18**, 405-433.

Donnelly, T. W., and Rogers, J. J. W., 1979. Igneous series in Island arcs the northeastern Caribbean compared with world-wide Island arc assemblages. *Bulletin of Volcanology*, **42**.

Drummond, M. S. and Defant, M. J., 1990. A model for trondhjemite-tonalite-dacite genesis and crustal growth via slab melting: Archean to modern comparisons. *Journal of Geophysical Research*, **95**, 503-521.

Dupuy, C., Dostal, J. and Leblanc, M., 1981. Geochemistry of an ophiolitic complex from New Caledonia. *Contributions to the Mineralogy and Petrology*, **76**, 77-83.

Evans, B. W. and Trommsdorf, V., 1970. Regional metamorphism of ultramafic rocks in the central Alps: Paragenesis in the system CaO-MgO-SiO₂-H₂O. *Schweizerische mineralogische und petrographische Mitteilungen*, **50**, 481-492.

Feeley, T. C. and Hacker, M. D., 1995. Intracrustal derivation of Na-rich andesitic and dacitic magmas: an example from Volcan Ollague, Andean Central Volcanic Zone. *Journal of Geology*, **103**, 218-225.

over
dal. } Floyd, P. A. and Winchester J. A., 1975. Magma-type and tectonic setting discrimination using immobile elements. *Earth and Planetary Science Letters*, **27**, 211-218.

Fomin, A. B. and Kozak, S. A., 1971. Distribution of Cr, Co, and Ni in ultramafic rocks of the Middle Bug region. *Geochemical Instructions*, **8 (6)**, 878-884.

Fuchs, G., 1979. On the geology of Western Ladakh. *Geologisches Jahrbuch*, **122**, 513-540.

Gaetani, M., Garzanti, E. and Jadoul, F., 1985. Main structural elements of Zaskar, NW Himalayas (India). *Rendiconti della Societa Geologica Italiana*, **8 (Suppl.)**, 3-8.

Gaetani, M., Garzanti, E., Jadoul, F., Nicora, A., Tintori, A., Pasini, M. and Kanwar, S.A.K., 1990a. The North Karakorum side of the Central Asia geopuzzle. *Geological Society of America Bulletin*, **102**, 54-62.

Gaetani, M., Gosso, G. and Pognante, U., 1990b. A geological transect from Kun Lun to Karakorum (Sinkiang, China). The western termination of the Tibetan Plateau. Preliminary note. *Terra Nova Research*, **2**, 23-30.

Gaetani, M., Le Fort, P., Tanoli, S., Angiolini, L., Nicora, A., Dario Schlunnach, and Khan, A., 1996. Reconnaissance geology in Upper Chitral, Baroghil and Karambar districts (northern Karakorum, Pakistan). *Geol Rundsch*, **85**, 683-704.

Gansser, A., 1964. *Geology of the Himalayas*. Wiley, New York, 289p.

Gansser, A., 1979. Preliminary report on a reconnaissance visit of some sections in Pakistan. In: Farah, A. and DeJong, K.A. (eds.) *Geodynamics of Pakistan*. Geological Survey of Pakistan, Quetta, 1-17.

Gansser, A., 1979. Reconnaissance visit to the ophiolites in Baluchistan and the Himalaya. In: Farah, A. and DeJong, K.A. (eds.) *Geodynamics of Pakistan*. Geological Survey of Pakistan, Quetta, 193-214.

Gansser, A., 1980. The division between Himalaya and Karakoram. *Geological Bulletin, Peshawar University*, **13**, 9-22.

- Gansser, A., 1980.** The significance of the Himalayan suture zone. *Tectonophysics*, **62**, 37-52.
- Gariepy, C., Allegre, C. J. and Xu, R. H., 1985.** The Pb-isotope geochemistry of granitoids from the Himalaya-Tibet collision zone: implications for crustal evolution. *Earth and Planetary Science Letters*, **74**, 220-235.
- Garzanti, E., Baud, A. and Mascle, G., 1987.** Sedimentary record of the northward flight of India and its collision with Eurasia (Ladakh Himalayas, India). *Geodinamica Acta*, **1(4/5)**, 297-312.
- Ghazanfer, M., Chaudhry, M. N. and Hussain, M. S., 1991.** Geology and petrotectonics of southeast Kohistan, northwest Himalaya, Pakistan. *Kashmir Journal of Geology*, **8 & 9**, 67-97.
- Gill, J. B., 1981.** Orogenic Andesites and Plate Tectonics: New York, *Springer-Verlag*, 390p.
- Girardeau, J., Mercier, J. C. C. and Yougong, Z., 1985.** Origin of the Xigaze ophiolite, Yarlung Zangbo Suture Zone, Southern Tibet. *Tectonophysics*, **119**, 407-433.
- Glikson, A. Y., 1972.** Early Precambrian evidence of a primitive ocean crust and island nuclei of sodic granite. *Geological Society of America Bulletin*, **83**, 3323-3344.
- Glikson, A. Y., 1976.** Trace element geochemistry and origin of early Precambrian acid igneous series, Barberton Mountain Land, Transvaal. *Geochemica Cosmochimica Acta*, **40**, 1261-1280.
- Glikson, A. Y. and Lambert, I. B., 1976.** Vertical zonation and petrogenesis of the early Precambrian crust in western Australia. *Tectonophysics*, **30**, 55-89.
- Glikson, A. Y. and Sheraton, J. W., 1972.** Early Precambrian trondhjemitic suites in western Australia and northwestern Scotland, and the geochemical evolution of shields. *Earth and Planetary Science Letters*, **17**, 227-242.
- Goldschmidt, V. M., 1916.** Geologisch-petrographische studien im hochgebirge des sudlichen Norwegens, IV. Übersicht der eruptivgesteine im Kaledonischen Gebirge zwischen Stavanger und Trondhjem. *Vid. Skr. I. Mat.-Nat. Klasse*, **2**, 75-112.
- Goldschmidt, V. M., 1922.** Stammestypen der Eruptivegesteine. Norway. *Vidensk.-Akad. Skr., Math-Nature*, **10**, 6.
- Green, D. H., 1972.** Magmatic activity as the major process in the chemical evolution of the Earth's crust and mantle. *Tectonophysics*, **13**, 47-71.
- Green, T. H. and Hellman, P. L., 1982.** Fe-Mg partitioning between coexisting garnet and phengite at high pressure, and comments on a garnet-phengite barometer. *Lithos*, **15**, 253-266.

- Gupta, V. J. and Kumar, S., 1975.** Geology of Ladakh, Lahaul and Spiti regions of Himalaya with special reference to the stratigraphic position of flysch deposits. *Geological Rundschau*, **64**, 540-563.
- Hamidullah, S., 1994.** Chemistry of hornblendes from the Deosai volcanics, Baltistan, northern Pakistan. *Geological Bulletin, Peshawar University*, **27**, 1-8.
- Hamidullah, S., Jan, M. Q. and Khan, B., 1992.** Petrography of the Deosai volcanics, N. Pakistan. *Geological Bulletin, Peshawar University*, **25**, 17-22.
- Hamidullah, S. and Onstot, T.C., 1991.** $^{40}\text{Ar}/^{39}\text{Ar}$ evidence for Late Cretaceous formation of the Kohistan Island Arc, NW Pakistan. *Kashmir Journal of Geology*, **10**, 105-122.
- Hamidullah, S., Zahid M. and Majid, M., 1991.** Mineralogy and mineral chemistry of the amphibolite belt and Main Mantle Thrust rocks from Gantar area, Allai Kohistan, north Pakistan. *Geological Bulletin, Peshawar University*, **24**, 133-146.
- Hanson, C.R., 1989.** The northern suture in the Shigar valley, Baltistan, northern Pakistan. In: Malinconico, L.L. and Lillie, R.J. (eds.) *Tectonics of the Western Himalayas*. Geological Society of America, Special Paper, **232**, 203-215.
- Hanson, G. N., 1978.** The application of trace elements to the petrogenesis of igneous rocks of Granitic composition. *Earth and Planetary Science Letters*, **38**, 26-43.
- Hanson, G. N. and Goldich, S. S., 1972.** Early Precambrian rocks in the Saganaga Lake-Northern Light Lake area, Minnesota-Ontario--Pt. 2. *Petrogenesis*. Geological Society of America, Memoirs, **135**, 179-192.
- Harris, N. B. W., Hawkesworth, C. J. and Tindle, A. G., 1993.** The growth of continental crust during the Late Proterozoic: geochemical evidence from the Arabian shield. In: H. M. Prichard, T. Alabaster, N. B. W. Harris and C. R. Neary (Editors), *Magmatic Processes and Plate Tectonics*. *Geological Society Special Publication*, **76**, 363-371.
- Hawkesworth, C. J., O'Nions, R. K., Pankhurst, P. J. and Evensen, N. M., 1977.** A geochemical study of island arc and back-arc tholeiites from the Scotia Sea. *Earth and Planetary Science Letters*, **36**, 253-262.
- Hayden, H.H., 1911.** Geology of Northern Afghanistan. *Records of the Geological Survey of India*, **39**, 1-97.
- Hayden, H.H., 1916.** Notes on the geology of the Chitral, Gilgit and Pamirs. *Records of the Geological Survey of India*, **45**, 271-335.
- Herbert, R., 1982.** Petrography and mineralogy of oceanic peridotites and gabbros: Some comparisons with ophiolite complexes. *Ophioliti*, **7** (2/3), 299-324.
- Herren, E., 1987a.** Structures, deformation and metamorphism of the Zaskar area Ladakh, NW Himalayas. *Diss ETH, Zurich*, Nr, **8419**, 148p.

- Herren, E., 1987b.** The Zaskar shear zone: Northeast - southeast extension within the Higher Himalayas Ladakh, India. *Geology*, **15**, 409-419.
- Himmelberg, G. R. and Loney, R. A., 1973.** Petrology of the Vulcan Peak alpine-type peridotite, southwestern Oregon. *Geological Society of America Bulletin*, **84**, 1585-1600.
- Hodges, K. V., Hubbard, M. S. and Silverberg, D. S., 1988.** Metamorphic constraints on the thermal evolution of the central Himalayan Orogen. In: Shackleton, R. M., Dewey, J. F., Windley, B. F. (eds.) *Tectonic evolution of the Himalayas and Tibet*. Philosophical Transactions of the Royal Society of London, Series A: Mathematical and Physical Sciences, **326**, 257-280.
- Honegger, K., Dietrich, V., Frank, W., Gansser, A., Thoni, M. and Trommsdorff, V., 1982.** Magmatism and metamorphism in the Ladakh Himalayas the Indus-Tsang-Po Suture Zone. *Earth and Planetary Science Letters*, **60**, 253-292.
- Hussain, S. S., Khan, T., Dawood, H. and Khan, I., 1984.** A note on Kot-Prang Ghar melange and associated mineral occurrences. *Geological Bulletin, Peshawar University*, **17**, 61-68.
- Irvine, T. N. and Barager, W. R. A., 1971.** A guide to the chemical classification of the common volcanic rocks. *Canadian Journal of Earth Sciences*, **8**, 523-548.
- Ivanac, J. F., Traves, D. M. and King, D., 1956.** The geology of the northwest portion of the Gilgit Agency. *Records of the Geological Survey of Pakistan*, **3**, 1-27.
- Jackson, E. D., 1967.** Ultramafic cumulates in the Stillwater, Great Dyke, and Bushveld intrusions, in Wyllie, P. J., ed., *Ultramafic and related rocks*: New York, Wiley Interscience, 20-38.
- Jan, M. Q., 1970.** Petrography of the upper part of Kohistan and southwestern Gilgit Agency along the Indus and Kandia rivers. *Geological Bulletin, Peshawar University*, **5**, 27-48.
- Jan, M. Q., 1977.** The Mineralogy, Petrology and Geochemistry of Swat Kohistan, NW Pakistan. Unpub. Ph.D. thesis, University of London.
- Jan, M. Q., 1977.** The Kohistan basic complex: A summary based on recent petrological research. *Geological Bulletin, Peshawar University*, **9-10**, 36-42.
- Jan, M. Q., 1979.** Petrography of the Jijal complex, Kohistan. *Geological Bulletin, Peshawar University*, **11**, 31-49.
- Jan, M. Q., 1979.** Petrography of the amphibolites of Swat and Kohistan. *Geological Bulletin, Peshawar University*, **11**, 51-64.
- Jan, M. Q., 1979.** Petrography of quartz diorites of Kalam, Swat. *Geological Bulletin, Peshawar University*, **11**, 89-97.

Herren, E., 1987b. The Zaskar shear zone: Northeast - southeast extension within the Higher Himalayas Ladakh, India. *Geology*, **15**, 409-419.

Himmelberg, G. R. and Loney, R. A., 1973. Petrology of the Vulcan Peak alpine-type peridotite, southwestern Oregon. *Geological Society of America Bulletin*, **84**, 1585-1600.

Hodges, K. V., Hubbard, M. S. and Silverberg, D. S., 1988. Metamorphic constraints on the thermal evolution of the central Himalayan Orogen. In: Shackleton, R. M., Dewey, J. F., Windley, B. F. (eds.) *Tectonic evolution of the Himalayas and Tibet*. Philosophical Transactions of the Royal Society of London, Series A: Mathematical and Physical Sciences, **326**, 257-280.

Honegger, K., Dietrich, V., Frank, W., Gansser, A., Thoni, M. and Trommsdorff, V., 1982. Magmatism and metamorphism in the Ladakh Himalayas the Indus-Tsang-Po Suture Zone. *Earth and Planetary Science Letters*, **60**, 253-292.

Hussain, S. S., Khan, T., Dawood, H. and Khan, I., 1984. A note on Kot-Prang Ghar melange and associated mineral occurrences. *Geological Bulletin, Peshawar University*, **17**, 61-68.

Irvine, T. N. and Barager, W. R. A., 1971. A guide to the chemical classification of the common volcanic rocks. *Canadian Journal of Earth Sciences*, **8**, 523-548.

Ivanac, J. F., Traves, D. M. and King, D., 1956. The geology of the northwest portion of the Gilgit Agency. *Records of the Geological Survey of Pakistan*, **3**, 1-27.

Jackson, E. D., 1967. Ultramafic cumulates in the Stillwater, Great Dyke, and Bushveld intrusions, in Wyllie, P. J., ed., *Ultramafic and related rocks*: New York, Wiley Interscience, 20-38.

Jan, M. Q., 1970. Petrography of the upper part of Kohistan and southwestern Gilgit Agency along the Indus and Kandia rivers. *Geological Bulletin, Peshawar University*, **5**, 27-48.

Jan, M. Q., 1977. The Mineralogy, Petrology and Geochemistry of Swat Kohistan, NW Pakistan. Unpub. Ph.D. thesis, University of London.

Jan, M. Q., 1977. The Kohistan basic complex: A summary based on recent petrological research. *Geological Bulletin, Peshawar University*, **9-10**, 36-42.

Jan, M. Q., 1979. Petrography of the Jijal complex, Kohistan. *Geological Bulletin, Peshawar University*, **11**, 31-49.

Jan, M. Q., 1979. Petrography of the amphibolites of Swat and Kohistan. *Geological Bulletin, Peshawar University*, **11**, 51-64.

Jan, M. Q., 1979. Petrography of quartz diorites of Kalam, Swat. *Geological Bulletin, Peshawar University*, **11**, 89-97.

- Jan, M. Q., 1980.** Petrology of the obducted mafic metamorphites from the southern part of the Kohistan island arc sequence. . *Geological Bulletin, Peshawar University*, **13**, 95-107.
- Jan, M. Q., 1983.** Further data on orth- and clinopyroxenes from the Pyroxene Granulites of Swat Kohistan, Northern Pakistan. *Geological Bulletin, Peshawar University*, **16**, 55-64.
- Jan, M. Q., 1984.** Some K/Ar ages from the Chilas complex in Swat. *Geological Bulletin, Peshawar University*, **17**, 171-173.
- Jan, M. Q., 1985.** High P rocks along the suture zones around Indo-Pakistan plate and phase chemistry of blueschists from eastern Ladakh. *Geological Bulletin, Peshawar University*, **18**, 1-40.
- Jan, M. Q., 1988.** Geochemistry of amphibolites from the southern part of the Kohistan arc, N. Pakistan. *Mineralogical Magazine*, **52**, 147-159.
- Jan, M. Q., 1988.** Relative abundances of minor and trace elements in mafic phases from the southern part of the Kohistan arc. *Geological Bulletin, Peshawar University*, **21**, 15-25.
- Jan, M. Q., 1990.** Petrology and geochemistry of the southern amphibolites of the Kohistan arc, N. Pakistan. *Physical Chemistry of Earth*, **17**, 71-92.
- Jan, M. Q., 1992.** Highly aluminous hornblende-cummingtonite coronas in gabbro-norites of the southern amphibolite belt, Kohistan. *Geological Bulletin, Peshawar University*, **25**, 127-131.
- Jan, M. Q. and Asif, M., 1981.** A speculative tectonic model for the evolution of tectonic Himalaya and Karakoram. *Geological Bulletin, Peshawar University*, **14**, 199-201.
- Jan, M. Q. and Asif, M., 1983.** Geochemistry of tonalites and quartz diorites of the Kohistan-Ladakh (Transhimalayan) granitic belt in Swat, N. Pakistan. In: Sham F.A. (ed.) *Granites of Himalayan, Karakorum and Hindu Kush*. Institute of Geology, Punjab University, Lahore, 355-376.
- Jan, M. Q., Banaras, M., Ghani, A. and Asif, M., 1983.** The Tora Tigger ultramafic complex, southern Dir district. *Geological Bulletin, Peshawar University*, **16**, 11-29.
- Jan, M. Q. and Howie, R. A., 1981.** The mineralogy and geochemistry of the metamorphosed basic and ultrabasic rocks of the Jijal complex, Kohistan, NW Pakistan. *Journal of Petrology*, **22**, 85-126.
- Jan, M. Q. and Howie, R. A., 1981.** Petrology of minor olivine gabbros and ultramafic rocks from Upper Swat, NW Pakistan. *Geological Bulletin, Punjab University*, **16**, 1-10.
- Jan, M. Q. and Jabeen, N., 1990.** A review of mafic-ultramafic plutonic complexes in the Indus suture zone of Pakistan. *Physical Chemistry of Earth*, **17**, 93-113.

- Jan, M. Q. and Karim, A., 1995.** Coronas and high-P veins in metagabbros of the Kohistan island arc, northern Pakistan: evidence for crustal thickening during cooling. *Journal of Metamorphic Geology*, **13**, 357-366.
- Jan, M. Q. and Kempe, D. R. C., 1973.** The petrology of the basic and intermediate rocks of Upper Swat, Pakistan. *Geological Magazine*, **110**, 285-300.
- Jan, M. Q., Kempe, D. R. C and Symes, R. F., 1972.** A green chromian tourmaline from Swat, West Pakistan. *Mineralogical Magazine*, **38**, 756-759.
- Jan, M. Q., Khan, M. A. and Qazi, M. S., 1993.** The Sapat mafic-ultramafic complex, Kohistan arc, North Pakistan. In: Treloar, P. J. and Searle, M. P. (eds.) *Himalayan Tectonics*. Geological Society of London, Special Publication, **74**, 113-121.
- Jan, M. Q. and Mian, I., 1971.** Preliminary geology and petrography of Swat Kohistan. *Geological Bulletin, Peshawar University*, **6**, 1-32.
- Jan, M. Q. and Symes, R. F., 1977.** Piemontite schists from upper Swat, northwest Pakistan. *Mineralogical Magazine*, **41**, 537-540.
- Jan, M. Q. and Tahirkehl, A. Z., 1990.** The Tora Tigga complex, southern Dir, NW Pakistan: an example of mafic-ultramafic rocks in the bottom of an island arc. *Geological Bulletin, Peshawar University*, **23**, 231-251.
- Jan, M. Q., Weaver, B. L. and Windley, B. F., 1997.** General petrology of garnet granulites of the Jijal complex, Kohistan, N. Pakistan. *12th Himalayan-Karakoram-Tibet International Workshop*. (Abstract).
- Jan, M. Q. and Windley, B. F., 1990.** Chromian spinel-silicate chemistry in ultramafic rocks of the Jijal complex, northwest Pakistan. *Journal of Petrology*, **31**, 667-715.
- Jensen, L. S., 1976.** A new cation plot for classifying subalkalic volcanic rocks. Ontario Division Mines. Misc. Pap., 66.
- Johnson, N. M., Stix, J., Tauxe, L., Cerveney, P. F. and Tahirkheli, R. A. K., 1985.** Paleomagnetic chronology, fluvial processes, and tectonic implications of Siwalik deposits near Chinji village, Pakistan. *Journal of Geology*, **93**, 27-40.
- Kakar, S. K., Badshah, M. S. and Khan, J., 1971.** The geology of Jandul valley, western Dir. *Geological Bulletin, Peshawar University*, **6**, 54-73.
- Kay, S. M., Kay, R. W., Brueckner, H. K. and J. L. R., 1983.** Tholeiitic Aleutian arc plutonism: the Finger Bay Pluton, Adak, Alaska. *Contributions in Mineralogy and Petrology*, **82**, 116.
- Kazmer, C., 1986.** The Main Mantle Thrust Zone at Jewan Pass area, Swat, Pakistan. MSc Thesis, University of Cincinnati.

Kazmi, A. H., Lawrence, R. D., Dawood, H., Snee, L.W. and Hussain, S. S., 1984. Geology of the Indus suture zone in the Mingora-Shangla area of Swat, northern Pakistan. *Geological Bulletin, Peshawar University*, **17**, 127-144.

Keleman, P. B., Johnson, K. T. M., Kinzler, R. J. and Irving, A. J., 1990. High-field-strength element depletions in arc basalts due to mantle-magma interaction. *Nature*, **345**, 521-524.

Khalil, M. A. and Afridi, A. G., 1973. The Geology and petrography of Deshai-Diwangar area, Ushu Gol valley, Swat Kohistan, NWFP, Pakistan. Unpublished M.Sc. thesis, University of Peshawar.

Khalil, M. A. and Afridi, A. G., 1979. The Geology and petrography of Deshai-Diwangar area, Ushu Gol valley, Swat Kohistan. *Geological Bulletin, Peshawar University*, **11**, 99-111.

Khan, A. G. and Tahirkheli, T. K., 1983. Geology of a section along MMT, Jijal, Kohistan, Northern Pakistan. Unpublished M.Sc. thesis, University of Peshawar, 63p.

Khan, J., 1979. Geology of the Baraul valley, Dir. *Geological Bulletin, Peshawar University*, **11**, 153-162.

Khan, M. A., 1988. Petrology and Structure of the Chilas Ultramafic-Mafic Complex, N. Pakistan. Ph.D. thesis, University of London.

Khan, M. A. and Coward, M. P., 1990. Entrapment of an island arc in collision tectonics: A review of the structural history of the Kohistan arc complex, N. W. Himalayas. *Physical Chemistry of Earth*, **17**, 1-18.

Khan, M. A., Habib, M. and Jan, M. Q., 1985. Ultramafic and mafic rocks of Thurlly Gah and their relationship to the Chilas complex, northern Pakistan. *Geological Bulletin, Peshawar University*, **18**, 83-102.

Khan, M. A., Jan, M. Q., Windley, B. F., Tarney, J. and Thirlwall, M. F., 1989. The Chilas mafic-ultramafic igneous complex; the root of the Kohistan island arc in the Himalaya of northern Pakistan. In: Malinconico, L.M., Jr. and Lillie, R.J. (eds.) *Tectonics of the Western Himalayas*. Geological Society of America, Special Paper, **232**, 75-94.

Khan, M. A. and Jan, M. Q., 1992. Some fundamental field and petrographic aspects of the Chilas mafic-ultramafic complex, Kohistan arc, northern Pakistan. *Acta Mineralogica Pakistan*, **6**, 126-147.

Khan, M. A., Jan, M. Q. and Weaver, B. L., 1993. Evolution of the lower arc crust in Kohistan, N. Pakistan: temporal arc magmatism through early, mature and intra-arc rift stages. In: Treloar, P.J. and Searle, M.P. (eds.) *Himalayan Tectonics*. Geological Society of London, Special Publication, **74**, 123-138.

Khan, M. A., Stern, R. J., Gribble, R. F. and Windley, B. F., 1997. Geochemical and isotopic constraints on subduction polarity, magma source, and palaeogeography of Kohistan intra-oceanic arc, northern Pakistan Himalaya. *Journal of Geological Society of London* (in press).

Khan, M. A. and Thirlwall, M. F., 1988. Babusar amphibolites: arc tholeiites from the southern Kohistan arc, N. Pakistan. *Geological Bulletin, Peshawar University*, **21**, 147-158.

Khan, T., 1994. Evolution of the "upper and middle crust in Kohistan island arc", northern Pakistan. Ph.D. thesis, University of Peshawar.

Khan, T., Khan, M. A. and Jan, M. Q., 1993. Kohistan, a collage of island arc and back-arc basin assemblages in the Himalaya of Pakistan. *Geological Society of America, Abstracts Program*, A-122.

Khan, T., Khan, M. A. and Jan, M. Q., 1994. Geology of a part of the Kohistan terrane between Gilgit and Chilas, northern areas, Pakistan. *Geological Bulletin, Peshawar University*, **27**, 99-112.

Khan, T. and Shirahase, T., 1996. Evolution of the Kohistan terrane with reference to the Jaglot group and the Chilas complex, Gilgit-Chilas, northern Pakistan. *Proceedings of Geoscience Colloquium, Geoscience Laboratory, Geological Survey of Pakistan*, **15**, 15-36.

Klootwijk, C.T. and Conaghan, P.T., 1978. The extent of greater India: Preliminary paleomagnetic data from the Hindukush, Chitral (Pakistan). *Earth and Planetary Science Letters*, **42**, 167-182.

Klootwijk, C., Sharma, M. L., Gergan, J., Tirkey, B., Shah, S. K. and Agarwal, V., 1979. The Extent of Greater India, II. Palaeomagnetic data from the Ladakh Intrusives at Kargil, Northwestern Himalayas. *Earth and Planetary Science Letters*, **44**, 47-64.

Klootwijk, C. T., Gee, J. S., Peirce, J. W., Smith, G. W. and McFadden, P. L., 1992. An early India-Eurasia contact; Palaeomagnetic constraints from the Ninetyeast Ridge, ODP Leg 121. *Geology*, **20**, 395-398.

Kuno, H., 1968. Differentiation of basalt magmas. *In: Basalts; the Poldervaart treatise on rocks of basaltic composition*, **2**, 623-688.

La Fortune, J. R., Snee, L.W. and Baig, M. S., 1992. Geology and geochemistry of Indian plate rocks south of the Indus suture zone, Besham area, northwest Himalaya, Pakistan. *Kashmir Journal of Geology*, **10**, 27-52.

Lawrence, R. D., 1984. Suture tectonics of Pakistan. *1st Pakistan Geological Congress, Lahore*, 49, (abst.).

Lawrence, R. D. and Ghauri, A. A. K., 1983. Observations on the structure of the Main Mantle Thrust at Jijal, Kohistan, Pakistan. *Geological Bulletin, Peshawar University*, **16**, 1-10.

- Lawrence, R. D. and Ghauri, A. A. K., 1983. Evidence of active faulting in Chilas dsitric, Northern Pakistan. *Geological Bulletin, Peshawar University*, **16**, 185-186.
- Lawrence, R. D., Kazmer, C. and Tahirkheli, R. A. K., 1983. The Main Mantle Thrust: a complex zone. *Geological Society of America Abstracts, with Program*, **15**, 624.
- Lawrence, R. D., Madin, I. and Ghauri, A. A. K., 1987. Neotectonics of the west end of the Himalayan Thrust system. *Geological Congress, University of Peshawar*, abstracts.
- Laxroix, A., 1904. La Montagne Pe. Il ses eruptions. *Paris, Masson et Cie*.
- Le Bas, M. J., Le Maitre, R. W., Streckeisen, A. and Zanettin, B., 1986. A chemical classification of volcanic rocks based on total alkali-silica diagram. *Journal of Petrology*, **27**, 745-750.
- Le Fort, P., 1975. Himalayas: The collided range, present knowledge of the continental arc. *American Journal of Science*, **275-A**, 1-44.
- Le Fort, P., Debon, F. and Sonet, J., 1980. The "Lesser Himalayan" corderite granite belt typology and age of the pluton of Mansehra (Pakistan). *Geological Bulletin, Peshawar University*, **13**, 51-61.
- Le Fort, P., 1981. Manaslu Leucogranite: a collisional signature of the Himalayas, a model for its genesis and emplacement. *Journal of Geophysical Research*, **86**, 10545-10568.
- Le Fort, P., Cuney, M., Deniel, C., France-Lanord, C., Sheppard, S. M. F., Upreti, B. N. and Vidal, P., 1987. Crystal generation of the Himalayan leucogranites. *Tectonophysics*, **134**, 39-57.
- Le Fort, P., Debon, F. and Sonet, J., 1983. The Lower Palaeozoic "Lesser Himalayan Granitic Belt": Emphasis on the Simchar Pluton of Central Nepal. In: Shams, F.A. (ed.) *Granites of Himalayas, Karakorum and Hindu Kush*. Institute of Geology, Punjab University, Lahore, 217-255.
- Le Fort, P., Lemennicier, Y., Lombardo, B., Pecher, A., Pertusati, P., Pognante, H. and Rolfo, F., 1995. Preliminary geological map and description of the Himalayan-Karakorum junction in Chogo Lungma to Turmik area (Baltistan, northern Pakistan). *Journal of Nepal Geological Society*, **11**, 17-38.
- Le Fort, P., Michard, A., Sonet, J. and Zimmermann, J. L., 1983. Petrography, geochemistry and geochronology of some samples from Karakorum axial batholith (northern Pakistan). In Shams, F.A. (eds.) *Granites of Himalayas, Karakorum and Hindu Kush*. Institute of Geology, Punjab University, Lahore, 377-387.
- Le Maitre, R. W., Bateman, P., Dudek, A., Keller, J., Lameyre, Le Bas, M. J., Sabine, P. A., Schmid, R., Sorensen, H., Streckeisen, A., Woolley, A. R. and Zanettin, B., 1989. A classification of igneous rocks and glossary of terms. Blackwell, Oxford.

Lin, J. and Watts, D. R., 1988. Palaeomagnetic constraints on Himalayan Tibetan tectonic evolution. *Philosophical Transactions of the Royal Society of London, Series A*, **326**, 177-188.

Loney, R. A., Himmelberg, G. R. and Coleman, R. G., 1971. Structure and petrology of the Alpine-type peridotite at Burro Mountain, California, U.S.A. *Journal of Petrology*, **12**, 245-309.

Loucks, R. R., Miller, D. J., Ashraf, M., Awan, M. A. and Khan, M. S., 1990. The Jijal Complex: layered mafic-ultramafic arc cumulates from the crust-mantle boundary, Pakistani Himalayas. *EOS*, **71**, 664.

Loucks, R. R., Ashraf, M., Awan, M. A., Khan, M. S. and Miller, D. J., 1992. Subdivisions of the Kamila Amphibolite Belt in southern Kohistan Island Arc complex, Pakistan. *Kashmir Journal of Geology*, **10**, 147-152.

Ludden, J. N. and Thompson, G., 1979. An evaluation of the behavior of the rare earth elements during the weathering of sea-floor basalt. *Earth and Planetary Science Letters*, **43**, 85-92.

Lyddekar, R., 1882. Geology of northwest Kashmir and Kaghan. *Records of Geological Survey of India*, **15**, 14-24.

Lyddekar, R., 1883. Geology of Baltistan and adjoining areas. *Memoirs of Geological Survey of India*, **22**.

Macdonald, K. C., Fox, P. J., Perram, L. L., Eisen, M. F., Hayman, R. M., Miller, S. P., Carbotte, S. M., Cormier, M. H. and Shor, A. N., 1988. A new view of the mid-ocean ridge from the behaviour of ridge-axis discontinuities. *Nature*, **335**, 217-225.

MacKenzie, W. S. and Guilford, C., 1980. Atlas of rock-forming minerals in thin section. Longman, London.

MacKenzie, W. S., Donaldson, C. H. and Guilford, C., 1982. Atlas of igneous rocks and their textures. Longman, London.

Madin, I. P., Lawrence, R. D., and Rehman, S., 1989. The north-western Nanga Parbat-Haramosh Massif; evidence for crustal uplift at the northwestern corner of the Indian Craton. In: Malinconico, L. L. and Lillee, R. J. (eds.) *Tectonics of the Western Himalayas*. Geological Society of America, Special Paper, **232**, 169-182.

Malinconico, L. L. Jr., 1982. Structure of the Himalayan suture zone of Pakistan interpreted from gravity and magnetic data. Unpublished Ph.D., thesis, Dartmouth College, Hanover.

Malinconico, L. L. Jr., 1986. The structure of the Kohistan arc terrain in northern Pakistan as inferred from gravity data. *Tectonophysics*, **124**, 297-307.

Malinconico, L. L. Jr., 1989. Crustal shortening in the west Himalaya. *Geological Bulletin, Peshawar University*, **22**, 55-64.

Martin, N. R., Siddiqui, S. F. A. and King, B. H., 1962. A geological reconnaissance of the region between the lower Swat and Indus rivers of Pakistan. *Geological Bulletin, Punjab University*, **2**, 1-13.

Martin, H., 1987. Petrogenesis of Archean Trondhjemites, Tonalites, and Granodiorites from Eastern Finland: Major and Trace Element Geochemistry. *Journal of Petrology*, **23, Part 5**, 921-953.

McMahon, H., 1900. Notes on the geology of Gilgit. *Quarterly Journal of Geological Society of London*, **56**, 337-369.

Meschede, M., 1986. A method of discriminating between different types of mid ocean ridge basalts and continental tholeiites with the Nb-Zr-Y diagram. *Chemical Geology*, **56 (3-4)**, 207-218.

Mikoshiba, M., Takahashi, Y., Takahashi, Y., Kausar, A. B., Khan, T., Kubo, K. and Shirahase, T., 1996. Rb-Sr isotope study of the Chilas igneous complex, Kohistan, northern Pakistan. *11th Himalaya-Karakoram-Tibet International Workshop*, (Abstract).

Miller, D. J., Loucks, R. R. and Ashraf, M., 1991. Platinum-group element mineralization in the Jijal layered ultramafic-mafic complex, Pakistani Himalaya. *Economic Geology*, **86**, 1093-1102.

Miller, D. J. and Christensen, N. I., 1994. Seismic signature and geochemistry of an island arc: A multidisciplinary study of the Kohistan accreted terrane, northern Pakistan. *Journal of Geophysical Resources*, **99, B6**, 11623-11642.

Misch, P., 1949. Metasomatic granitization of batholithic dimensions, Part I: syntectonic granitization in Nanga Parbat area, North West Himalaya. *American Journal of Science*, **247**, 209-245.

Miyashiro, A., 1974. Volcanic rock series in island arcs and active continental margins. *American Journal of Science*, **274, No. 4**, 321-355.

Molnar, P. and Tapponier, P., 1977. The collision between India and Eurasia. *Science*, **236**, 30-41.

Montenat, C., Sornay, J., Vachard, D., Bordet, P., Carbonnel, J. P. and Desmet, A., 1979. Un jalon de la Mesogee eocretacee dans la region de Kandahar. *C. R. Acad Sci Paris Ser.*, **289**, 651-655.

Moores, E. M. and Twiss, R. J., 1995. *Tectonics*. W. H. Freeman and company, New York.

Mullan, H. S. and Bussell, M. A., 1977. The basic rock series in batholithic associations. *Geological Magazine*, **114**, 265-280.

Nicora, A., Garzanti, E. and Fois, E., 1987. Evolution of the Tethys Himalayas continental shelf during Maastrichtian to Paleocene (Zaskar, India). *Rivista Italiana di Palaeontologia e Stratigrafia*, **92**, 439-496.

O'Donnell (65)
O'Donnell, T. H. and Presnall, D. C., 1980. Chemical variation of the glass and mineral phases in basalts dredged from 250 - 300 N along the Mid-Atlantic Ridge. *American Journal of Science*, **280A**, 845-868.

Ogawara (65)
Ogaswara, M., Watanabe, Y., Khan, F., Khan, T., Khan, M. S. Z. and Khan, K. S. A., 1994. Late Cretaceous igneous activity and tectonism of the Karakoram block in the Khunjerab valley, northern Pakistan. In: Ahmed, R. and Sheikh, A. M. (eds.) *Geology in South Asia-1*. Hydrocarbon Development Institute of Pakistan, Islamabad, 203-207.

Patriat, P. and Achache, J., 1984. India-Eurasia collision chronology and its implications for crustal shortening and driving mechanisms of plates. *Nature*, **311**, 615-621.

Pearce, J. A., 1976. Statistical analysis of major element patterns in basalts. *Journal of Petrology*, **17**, 15-43.

Pearce, J. A., 1982. Trace elements characteristics of lavas from destructive plate boundaries. In: Thrope, R. S. (ed.), *Andesites: orogenic andesites and related rocks*. John Wiley & Sons, Chichester, 525-548.

Pearce, J. A., 1983. Role of the sub-continental lithosphere in magma genesis at active continental margins. In: Hawkesworth, C. J. and Norry, M. J. (eds.) *Continental Basalts and Mantle Xenoliths*. Shiva Publishing, Nantwich, 230-249.

✓
Pearce, J. A. and Cann, J. R., 1973. Tectonic setting of basic volcanic rocks determined using trace element analyses. *Earth and Planetary Science Letters*, **19**, 290-300.

✓
Pearce, J. A., Harris, N. B. W. and Tindle, A. G., 1984. Trace element discrimination diagrams for the tectonic interpretation of Granitic rocks. *Journal of Petrology*, **25**, 956-983.

Pearce, J. A. and Norry, M. J., 1979. Petrogenetic implications of Ti, Zr, Y and Nb variations in volcanic rocks. *Contributions to Mineralogy and Petrology*, **69**, 33-47.

Perfit, M. R., Gust, D. A., Bence, A. E., Arculus, R. J. and Taylor, S. R., 1980. Chemical characteristics of island arc basalts: implication for mantle sources. *Chemical Geology*, **30**, 227-257.

Petterson, M. G., 1984. The structure, petrology and geochemistry of the Kohistan batholith, Gilgit, Kashmir, N. Pakistan. Ph.D. thesis, Leicester University.

Petterson, M. G., Crawford, M. B. and Windley, B. F., 1993. Petrogenetic implications of neodymium isotope data from the Kohistan batholith, North Pakistan. *Journal of Geological Society of London*, **150**, 125-129.

Petterson, M. G. and Windley, B. F., 1985. Rb-Sr dating of the Kohistan arc batholith in the Trans Himalaya of N. Pakistan and tectonic implications. *Earth and Planetary Science Letters*, **74**, 54-75.

Petterson, M. G. and Windley, B. F., 1986. Petrology and geochemical evolution of the Kohistan arc-batholith, Gilgit, N. Pakistan. *Geological Bulletin, Peshawar University*, **19**, 121-149.

Petterson, M. G. and Windley, B. F., 1991. Changing source regions of magmas and crustal growth in the Trans-Himalayas: Evidence from the Chalt volcanics and Kohistan batholith, Kohistan, N. Pakistan. *Earth and Planetary Science Letters*, **102**, 326-346.

Petterson, M. G. and Windley, B. F., 1992. Field relations, geochemistry and petrogenesis of the Cretaceous basaltic Jutal dykes, Kohistan, northern Pakistan. *Journal of Geological Society of London*, **149**, 107-114.

Petterson, M. G., Windley, B. F. and Luff, I. W., 1990a. The Chalt volcanics, Kohistan, N. Pakistan: High-Mg tholeiitic and low-Mg calc-alkaline volcanism in a Cretaceous island arc. *Physics and Chemistry of the Earth*, **17**, 19-30.

Petterson, M. G., Windley, B. F. and Sullivan, M., 1990b. A petrological, chronological, structural and geochemical review of Kohistan batholith and its relationship to regional tectonics. *Physics and Chemistry of the Earth*, **17**, 47-70.

Pognante, U., Benna, P. and Le Fort, P., 1983. High pressure metamorphism in the High Himalayan Crystallines of the Stak Valley, northeastern Nanga Parbat-Haramosh syntaxis, Pakistan Himalaya. In: Treloar, P. J. and Searle, M. P. (eds.) *Himalayan Tectonics*. Geological Society of London, Special Publication, **74**, 161-172.

Pogue, K. R., DiPietro, J. A., Khan, S. R., Hughes, S. S., Dilles, J. H. and Lawrence, R. D., 1992. Late Paleozoic rifting in northern Pakistan. *Tectonics*, **11**, 871-883.

Powell, C. McA., 1979. A speculative tectonic history of Pakistan and surroundings: Some constraints from the Indian Ocean. In: Farah, A. and DeJong, K. A. (eds.) *Geodynamics of Pakistan*. Geological Survey of Pakistan, Quetta, 5-24.

Powell, C. McA. and Vernon, R. H., 1979. Growth and rotation history of garnet porphyroblasts with inclusion spirals in a Karakorum schist. *Tectonophysics*, **54**, 25-43.

Pudsey, C. J., Coward, M. P., Luff, I. W., Shackleton, R. M., Windley, B. F. and Jan, M. Q., 1985. Collision zone between the Kohistan arc and the Asian plate in NW Pakistan. *Transactions of the Royal Society of Edinburgh: Earth Sciences*, **76**, 463-479.

Pudsey, C. J. and Maguire, P. K. H., 1986. Magnetic profiles across the northern suture, Kohistan, NW Pakistan. *Geological Bulletin, Peshawar University*, **19**, 47-60.

Rafiq, M., 1984. Extension of Sakhakot-Qila ultramafic complex in Utman Khel, Mohmand Agency, NWFP, Pakistan. *Geological Bulletin, Peshawar University*, **17**, 53-59.

Rai, H., 1983. Geology of the Nubra valley and its significance in the evolution of the Ladakh-Himalaya. In: Thakur, V. C., and Sharma, K. K. (eds.) *Geology of the Indus Suture Zone of Ladakh*, W.I.H.G., Dehra Dun, 79-97.

Rai, H. and Pande, I. C., 1978. Geology of the Kargil Igneous Complex., Ladakh, Jammu and Kashmir, India. *Recent Research in Geology*, **5**, 219-228.

Ramberg, H., 1944. The thermodynamics of the earth's crust. *I, Norsk geol. Tidsskr*, **24**, 98-111.

Rapp, R. P., Watson, E. B. and Miller, C. F., 1991. Partial melting of amphibolite/eclogite and the origin of Archean trondhjemites and tonalites. *Precambrian Research*, **51**, 1-25.

Regan, P. F., 1985. The early basic intrusions. In: Pitcher, W. S., Atherton, M. P., Cobbing, E. J. and Beckinsale, R. D. (eds.) *Magmatism at a plate edge - the Peruvian Andes*. Blackie, London, 72-89.

Reuber, I., 1987. Tectonogenesis of the Dras Volcanic Arc, Ladakh - Himalayas. *Terra Cognita*, **7**, 111-112

Reuber, I., 1989. The Dras arc: two successive volcanic events on eroded oceanic crust. *Tectonophysics*, **161**, 93-106.

Reuber, I., Montigny, R., Thuizat, R. and Heitz, A., 1989. K-Ar ages of ophiolites and arc volcanics of the Indus suture zone: clues on the early evolution of the Neo-Tethys. *Eclogae Geologicae Helveticae*, **82**, 699-715.

Rex, A. J., Searle, M. P., Tirrul, R., Crawford, M. B., Prior, D. J., Rex, D. C. and Barnicoat, A. C., 1988. The geochemical and tectonic evolution of the central Karakorum, North Pakistan. *Philosophical Transactions of the Royal Society of London*, **A.326**, 229-255.

Reynolds, P. H. and Brookfield, M. E., 1983. The age and nature of Mesozoic-Tertiary magmatism across the Indus suture zone in Kashmir and Ladakh (N.W. India and Pakistan). *Geology Rundschau*, **72**, 981-1004.

Roeder, P. L. and Emslie, R. F., 1970. Olivine - liquid equilibrium. *Contributions to Mineralogy and Petrology*, **29**, 275-289.

Rogers, J. J. W., Hodges, K. V. and Ghuma, M. A., 1980. Trace elements in Ben Ghnema batholith and nature of the Precambrian crust in central North Africa: *Summary*. Geological Society of America Bulletin Part 1, **91**, 445-447.

Rollinson, H. R., 1993. Using geochemical data: evaluation, presentation, interpretation. *Longman Science and Technical*, England.

Rossmann, D. L. and Abbas, S. G., 1970. Geology and economic potential for chromite in the ultramafic rock complex near Dargai, Peshawar division, Pakistan. *Geological Survey of Pakistan and USGS Representatives*. (unpub.), 68p.

Rushmer, T., 1991. Partial melting of two amphibolites: contrasting experimental results under fluid-absent conditions. *Contributions to Mineralogy and Petrology*, **107**, 41-59.

Sano, S., Nakajima, T. and Khan, S. R., 1996. Geology and isotope geochemistry of the Jijal complex, Kohistan, northern Pakistan. *Proceedings of Geoscience Colloquium, Geoscience Laboratory, Geological Survey of Pakistan*, **15**, 127-136.

Saunders, A. D. and Tarney, J., 1979. The geochemistry of basalts from a back-arc spreading Centre in the East Scotia Sea. *Geochemic and Cosmochimic Acta*, **43**, 555-572.

Saunders, A. D., Tarney, J., Marsh, N. G., Wood, D. A. and Panayiotou, A., 1980. Ophiolites as ocean crust or marginal basin crust ; a geochemical approach. *In: Ophiolites; Proceedings, International ophiolite symposium*, 193-204.

Saunders, A. D., Norry, M. J. and Tarney, J., 1988. Origin of MORB and chemically depleted Mantle Reservoirs: trace Element Constraints. *Journal of Petrology Special Lithosphere Issue*, **29**, 415-445.

Saunders, A. D. and Tarney, J., 1991. Back-arc basins. *In: Floyd, P. A. (eds.) Oceanic basalts*. Blackie and Nostrand Reihold, 219-263.

Scharer, U., Hamet, J. and Allegre, C. J., 1984. The Trans-Himalaya (Gangdese) plutonic belt in the Ladakh region: a U-Pb and Rb-Sr study. *Earth and Planetary Science Letters*, **67**, 327-339.

Searle, M.P., 1989. Thermal model for the Baltoro-Muztagh, Karakoram. *Geological Bulletin, Peshawar University*, **22**, 1-9.

Searle, M.P., 1991. Geology and Tectonics of the Karakoram Mountains. *John Wiley & Sons*, New York, 358p.

Searle, M. P. and others, 1987. The closing of Tethys and the tectonics of the Himalayas. *Geological Society of America Bulletin*, **98**, 378-401.

Searle, M. P., Cooper, D. J. W. and Rex, A. J., 1988. Collision tectonics of the Ladakh-Zaskar Himalayas. *Philosophical Transactions of the Royal Society of London*, **326**, 117-150.

Searle, M. P., Rex, A. J., Tirrul, R., Windley, B. F., Onge, M. St. and Hoffman, P., 1986. A geological profile across the Baltoro-Karakoram Range, NM. Pakistan. *Geological Bulletin, Peshawar University*, **19**, 1-12.

Searle, M. P., Rex, A. J., Tirrul, R., Rex, D. C. and Barnicoat, A., 1989. Metamorphic, magmatic and tectonic evolution of the Central Karakoram in the Biafo-Baltoro-Hushe regions of N. Pakistan. *In: Malinconico, L. L. and Lillee, R. J. (eds.) Tectonics of Western Himalayas*. Geological Society of America, Special Paper, **232**, 47-73.

Searle, M. P. and Treloar, P. J., 1993. Himalayan tectonics - an introduction. *Geological Society of London, Special Publication*, **74**, 1-7.

Sengor, A. M. C., 1986. The dual nature of the Alpine-Himalaya system: progress, problems and prospects. *Tectonophysics*, **127**, 177-195.

Shackleton, R. M., 1981. Structure of Southern Tibet, Report on a traverse from Lhasa to Katmandu organised by Academia Sinica. *Journal of Structural Geology*, **3(1)**, 97-105.

Shah, M. T., 1985. Petrochemistry of the Shergarh Sar complex, Allai Kohistan. M. Phil. thesis, University of Peshawar.

Shah, M. T. and Jan, M. Q., 1993. Mineralogical constraints of the Shergarh Sar amphibolites, Allai Kohistan, northern Pakistan. *Geological Bulletin, Peshawar University*, **26**, 59-73.

Shah, M. T. and Majid, M., 1992. Petrology and chemistry of the ultramafic rocks from the Allai Kohistan section of the Indus suture zone in Hazara, N. Pakistan. *Acta Mineralogica Pakistanica*, **6**, 73-84.

Shah, M. T., Majid, M., Hamidullah, S. and Shervais, J. W., 1992. Petrochemistry of amphibolites from the Shergarh Sar area, Allai Kohistan, N. Pakistan. *Kashmir Journal of Geology*, **10**, 123-139.

Shams, F. A., 1972. Glaucophane-bearing rocks from near Topsin, Swat-First record from Pakistan. *Pak. Journal of Science*, **24**, 343-345.

Shams, F. A., 1975. The petrology of the Thak Valley Igneous Complex, Gilgit Agency, North Pakistan. *Rend. Accad. Naz. Lincie, Ser. VIII, Rome*, 453-464.

Shams, F. A., 1980. Origin of the Shangla blueschists, Swat Himalaya, Pakistan. *Geological Bulletin, Peshawar University (Special Issue)*, **13**, 67-70.

Shams, F. A., 1983. Granites of N.W. Himalayas in Pakistan. In: Shams, F.A. (ed.) *Granites of Himalayas, Karakoram and Hindukush*. Institute of Geology, Punjab University, 75-121.

Shams, F. A. (ed.), 1983. Granites of Himalayas, Karakorum and Hindukush. *Institute of Geology, Punjab University, Lahore, Pakistan*, 427p.

Sharma, K. K., 1983. Granitoid Belts of the Himalayas. In: Shams, F. A. (ed.) *Granites of the Himalayas, Karakoram and Hindu Kush*. Institute of Geology, Punjab University, Lahore, 11-38.

Sharma, K. K., 1991. Petrology, geochemistry and geochronology of the Ladakh Batholith and its role in the evolution of Ladakh magmatic arc. *Geology and geodynamic evolution of the Himalayan collision zone, Part 1. Physics and chemistry of the earth*, **17**, 173-194.

Sharma, K. K. and Gupta, K. R., 1978. Some observations on the geology of the Indus and Shyok valleys between Leh and Panamik, district Ladakh, Jammu and Kashmir, India. *Recent Research in Geology*, **6**, 133-143.

Sharma, K. K., Sinha, A. K., Bagdasarian, G. P. and Gukasian, R. C., 1978. Potassium-argon dating of Dras Volcanics, Shyok Volcanics and the Ladakh Batholith, Northwest Himalayas. *Himalayan Geology*, **8**, 288-295.

Singer, B. S., Myers, J. M. and Frost, C. D., 1992. Mid-Pleistocene lavas from the Senguum volcanic centre, central Aleutian arc: closed-system fractional crystallization of a basalt to rhyodacite eruptive suite. *Contributions to Mineralogy and Petrology*, **110**, 87-112.

Smith, H. A., Chamberlain, C. P. and Zeitler, P. K., 1992. Documentation of Neogene regional metamorphism in the Himalayas of Pakistan using U-Pb in monazite. *Earth and Planetary Science Letters*, **113**, 93-105.

Smith, H. A., Chamberlain, C. P. and Zeitler, P. K., 1994. Timing and duration of Himalaya metamorphism within the Indian plate, northwest Himalaya, Pakistan. *Journal of Geology*, **102**, 493-503.

Spencer, D. A., 1988. Deformation of the Main Mantle Thrust zone at Babusar Pass, Karakorum, Himalaya, Pakistan. M.Sc. thesis, Imperial College, University of London.

Spencer, D. A. and Spencer-Cervato, C., 1992. Exhumation and cooling history of eclogite and amphibolite facies rocks in the Upper Kaghan Nappe, NW Himalaya, Pakistan. In: Searle, M.P. and Treloar P. J. (eds.) *7th Himalaya-Karakoram-Tibet Workshop, Abstracts*. Oxford Department of Earth Science, p. 85.

Srimal, N., 1986. India-Asia collision: implication from the geology of the eastern Karakoram. *Geology*, **14**, 523-527.

Srimal, N., Basu, A. R. and Kyser, T. K., 1987. Tectonic inferences from oxygen isotopes in volcano-plutonic complexes of the India-Asia collision zone, N.W. India. *Tectonics*, **6**, 261-274.

Srimal, N., Bhandari, A. K. and Chakravarti, S. K., 1982. Island-arc volcanism in the Ladakh Himalaya. *Indian Journal of Earth Sciences*, **9**, 44-58.

Streckeisen, A., 1976. To each plutonic rock its proper name. *Earth Science Reviews*, **12**, 1-33.

Sullivan, M., 1992. The geology of the roof zone of the Kohistan batholith, northwestern Pakistan. Unpublished Ph. D thesis, University of Leicester (UK).

Sullivan, M. A., Windley, B. F., Saunders, A. D., Haynes, J. R. and Rex, D. C., 1993. A palaeogeographic reconstruction of the Dir Group: Evidence for magmatic arc migration within Kohistan, N. Pakistan. In: Treloar, P. J. and Searle, M. P. (eds.) *Himalayan Tectonics*. Geological Society of London, Special Publication, **74**, 139-160.

Tahirkheli, R. A. K., 1979. Geology of Kohistan and adjoining Eurasian and Indo-Pakistan continents, Pakistan. *Geological Bulletin, Peshawar University*, **11**, 1-30.

Tahirkheli, R. A. K., 1979. Geotectonic evolution of Kohistan. *Geological Bulletin, Peshawar University*, **11**, 113-130.

Tahirkheli, R. A. K., 1982. Geology of the Himalaya, Karakoram and Hindukush in Pakistan. *Geological Bulletin, Peshawar University*, **15 (Spec. Issue)**, 1-51.

Tahirkheli, R. A. K., 1983. Geological evolution of Kohistan island arc on the southern flank of the Karakoram-Hindukush in Pakistan. *Bollitino Geofisica Teorica Applicata*, **25**, 351-364.

Tahirkheli, R. A. K. and Jan, M. Q. (eds.), 1979. Geology of Kohistan, Karakoram Himalaya, northern Pakistan. *Geological Bulletin, Peshawar University*, **11 (Special Issue)**, 187p.

Tahirkheli, R. A. K. and Jan, M. Q., 1979. A preliminary geological map of Kohistan and the adjoining areas, N. Pakistan. *Geological Bulletin, Peshawar University*, **11 (Special Issue)**, (in pocket).

Takahashi, Y., Takahashi, Y., Kausar, A. B. and Mikoshiba, M., 1996. Geology and geochemistry of the eastern part of the Chilas complex, northern Pakistan: Implications for the tectonic development of the Kohistan island arc. *Proceedings of Geoscience Colloquium, Geoscience Laboratory, Geological Survey of Pakistan*, **15**, 183-206.

Talent, J. A., Conaghan, P. J., Mawson, R., Molloy, P. D. and Pickett, J. W., 1982. Intricacy of tectonics in Chitral (Hindu Kush): faunal evidence and some regional implications. *Himalayan Geology*, Section IIa. Geological Survey of India Miscellaneous Publications, **41**, 77-101.

Tapponnier, P., Mattaur, M., Proust, F. and Cassaigneau, C., 1981. Mesozoic ophiolites, sutures and large scale tectonic movements in Afghanistan. *Earth and Planetary Science Letters*, **52**, 355-371.

Tarney, J., Saunders, A. D., Weaver, S. D., Donnellan, N. C. B. and Hendry, G. L., 1979. Minor element geochemistry of basalts from Leg 49. In: Luyendyk, B. P., Cann, J. R. et al. (eds). *Initial Reports of the Deep Sea Drilling Project*, **49**, 660-685.

Tarney, J., Wood, D. A., Saunders, A. D., Cann, J. R. and Varet, J., 1980. Heterogeneity in the North Atlantic: evidence from Deep Sea Drilling. *Philosophical Transactions of the Royal Society of London*, **A297**, 179-202.

Taylor, S. R. and McLennan, S. M., 1985. The continental crust: Its composition and Evolution. Blackwell.

Terrell, D. J., Pal, S., Lopez, M. and Perez, R. J., 1979. Rare-earth elements in basalt samples, Gulf of California. *Chemical Geology*, **26**, 267-275.

Thakur, V. C., 1981. Regional framework and geodynamic evolution of the Indus Tsang-Po Suture Zone in the Ladakh Himalayas. *Transactions of the Royal Society of Edinburgh, Earth Sciences*, **72**, 89-97.

Thompson, G., Bryan, W. B. and Melson, W. G., 1980. Geological and geophysical investigation of the Mid-Cayman Rise spreading center: geochemical variation and petrogenesis of basalt glasses. *Journal of Geology*, **88**, 41-55.

Treloar, P. J., 1989. Imbrication and unroofing of the Himalayan thrust stack of the north Indian plate, north Pakistan. *Geological Bulletin of the University of Peshawar*, **22**, 25-44.

Treloar, P. J., Bignold, A., Jan, M. Q. and Khan, M. A., 1997. A re-evaluation of the stratigraphic set-up of the Kohistan arc terrane, N. Pakistan (*in preparation*).

Treloar, P. J., Brodie, K. H., Coward, M. P., Jan, M. Q., Knipe, R. J., Rex, D. C. and Williams, M. P., 1990. The evolution of the Kamila shear zone, Kohistan, Pakistan. In: Salisbury, M.H. and Fountain, D. M. (eds.) *Exposed Cross-sections of the Continental Crust*. Kluwer Academic Publishers, Amsterdam, 175-214.

Treloar, P. J., Broughton, R. D., Williams, M. P., Coward, M. P. and Windley, B. F., 1989a. Deformation, metamorphism and imbrication of the Indian Plate south of the Main Mantle Thrust, North Pakistan. *Journal of Metamorphic Petrology*, **7**, 111-125.

Treloar, P. J., Coward, M. P., Williams, M. P. and Khan, M. A., 1989b. Basement cover imbrication south of the Main Mantle Thrust, north Pakistan. In: Malinconico, L. L. and Lillie, R. J. (eds.) *Tectonics of the Western Himalayas*. Geological Society of America, Special Paper, **232**, 137-152.

Treloar, P. J. and Izatt, C. N., 1993. Tectonics of the Himalayan collision between the Indian Plate and the Afghan Block: a synthesis. In: Treloar, P. J. and Searle, M. P. (eds.) *Himalayan Tectonics*. Geological Society Special Publication, **74**, 69-87.

Treloar, P. J., Petterson, M. G., Jan, M. Q. and Sullivan, M. A., 1996. A re-evaluation of the stratigraphy and evolution of the Kohistan arc sequence, Pakistan Himalaya: implications for magmatic and tectonic arc-building processes. *Journal of Geological Society of London*, **153**, 681-693.

Treloar, P. J., and Rex, D. C., 1990. Cooling and uplift histories of the crystalline thrust stack of the Indian Plate internal zones west of Nanga Parbat, Pakistan Himalayas. *Tectonophysics*, **180**, 323-349.

Treloar, P. J., Rex, D. C., Guise, P. G., Coward, M. P., Searle, M. P., Windley, B. F., Petterson, M. G., Jan, M. Q. and Luff, I. W., 1989c. K-Ar and Ar-Ar geochronology of the Himalayan collision in NW Pakistan: constraints on the timing of suturing, deformation, metamorphism and uplift. *Tectonics*, **4**, 881-909.

Treloar, P. J., Rex, D. C., Guise, P. G., Coward, M. P., Searle, M. P., Windley, B. F., Petterson, M. G., Jan, M. Q. and Luff, I. W., 1989d. K/Ar and Ar/Ar geochronology of the Himalayan collision in NW Pakistan: constraints on the timing of suturing, deformation, metamorphism and uplift. *Tectonics*, **4**, 881-909.

Treloar, P. J., Coward, M. P. and Harris, N. B. W., 1992a. Himalayan Tibetan analogies for the evolution of the Zimbabwe Craton and Limpopo Belt. *Precambrian Research*, **55** (1-4), 571-587.

Treloar, P. J., Coward, M. P., Chambers, A. F., Izatt, C. N. and Jackson, K. C., 1992b. Thrust geometries, interferences and rotations in the Northwest Himalayas. In: McClay, K. R. (ed.), *Thrust tectonics*, 325-342.

Turekian, N. K. K., and Kulp, J. R., 1956. The geochemistry of strontium. *Geochemic and Cosmochimic Acta*, **9**, 245-247.

Vidal, Ph., Cocherie, A., and Le Fort, P., 1982. Geochemical investigations of the origin of the Manaslu leucogranite Himalayas, Nepal. *Geochemic and Cosmochimic Acta*, **46**, 2279-2292.

Vince, K. J. and Treloar, P. J., 1996. Miocene, north-vergent extensional displacements along the Main Mantle Thrust, NW Himalaya, Pakistan. *Journal of the Geological Society, London*, **153**, 677-680.

Virdi, N. S., 1992. Cretaceous Marginal basins of the Indus-Kohistan Collision Zone: Development and evolution. In: Sinha, A. K.(ed.) *Himalayas orogen and Global Tectonics*. Publication No. 197of International Lithosphere programme, Dehra Dun, India, 157-168.

Wadia, D. N., 1932. Notes on the geology of Nanga Parbat, Mt. Diamir, and adjoining parts of Chilas, Gilgit district, Kashmir. *Geological Survey of India Records*, **66**, 212-234.

Wadia, D. N., 1961. *Geology of India*. Macmillan, Lond., 536p.

Weaver, B. L. and Tarney, J., 1981. Chemical changes during dyke metamorphism in high-grade basement terrains. *Nature*, **289**, 47-49.

Weaver, B. L., Tarney, J. and Windley, B., 1981. Geochemistry and petrogenesis of the Fiskenaesset anorthosite complex southern West Greenland: nature of the parent magma. *Geochemic and Cosmochimic Acta*, **45**, 711-725.

Weeden, D. S., 1970. The ultrabasic / basic igneous rocks of the Huntly region. Scotland. *Journal of Geology*, **6**, 26-40.

Wilson (86)

Wilson, M., 1989. *Igneous petrogenesis, a global tectonic approach*. Unwin Hyman, London.

Winchester, J. A. and Floyd, P. A., 1976. Geochemical magma type discrimination application to altered and metamorphosed basic igneous rocks. *Earth and Planetary Science Letters*, **28**, 459-469.

Winchester, J. A. and Floyd, P. A., 1977. Geochemical discrimination of different magma series and their differentiation products using immobile elements. *Chemical Geology*, **20**, 325-343.

Windley, B. F., 1983. Metamorphism and tectonics of the Himalaya. *Journal of Geological Society of London*, **140**, 849-865.

Windley, B. F., 1988. Tectonic framework of the Himalay, Karakoram and Tibet, and problems of their evolution. *Philosophical Transactions of the Royal Society of London*, **A326**, 3-16.

Windley, B. F., Coward, M. P. and Jan, M. Q., 1986. The geology and tectonic evolution of the Karakoram-Kohistan range of Himalayas of N. Pakistan. *Geological Society of China*, 60th Anniversary. Symposium on Mesozoic and Cenozoic Geology, Peking, 455-467.

Winther, K. T. and Newton, R. C., 1991. Experimental melting of hydrous low-K tholeiite: evidence on the origin of Archean cratons. *Bulltin of Geological Society of Denmark*, **39**, 213-228.

Wolde, B., and Team, G. G., 1996. Tonalite-trondhjemite-granite genesis by partial melting of newly underplated basaltic crust: an example from the Neoproterozoic Birbir magmatic arc, western Ethiopia. *Precambrian Research*, **76**, 3-14.

Wolf, M. B. and Wyllie, P. J., 1994. Dehydration-melting of amphibolite at 10 kbar: the effects of temperature and time. *Contributions to Mineralogy and Petrology*, **115**, 369-383.

Wood, D. A., Joron, J. L., and Teruil, M., 1979. A re-appraisal of the use of the trace elements to classify and discriminate between magma series erupted in different tectonic settings. *Earth and Planetary Science Letters*, **45**, 326-336.

Wyllie, P. J., 1982. Subduction products according to experimental prediction. *Geological Society of America Bulletin*, **93**, 468-476.

Wyllie, P. J., 1984. Constraints imposed by experimental petrology on possible and impossible magma sources and products. *Philosophical Transactions of the Royal Society of London*, **A310**, 439-456.

Wyllie, P. J., 1984. Sources of granitoid magmas at convergent plate boundaries. *Physics of the Earth and Planetary Interiors*, **35**, 12-18.

Wyllie, P. J. and Wolf, M. B., 1993. Amphibolite dehydration-melting: sorting out the solidus. In: Prichard, H. M., Alabaster, T., Harris, N. B. W. and Neary, C. R. (eds). Magmatic Processes and plate tectonics. *Geological Society of London Special Publication*, **76**, 405-416.

Xu, R. H., Scharer, U. and Allegre, C. J. 1985. Magmatism and metamorphism in the Lhasa block (Tibet): a geochronological study. *Journal of Geology*, **93**, 41-57.

Yamamoto, H., 1993. Contrasting metamorphic P-T-time paths of the Kohistan granulites and tectonics of the western Himalayas. *Journal of Geological Society of London*, **150**, 843-856.

Yamamoto, H. and Nakamura, E., 1996. Sm-Nd dating of garnet granulites from the Kohistan complex, northern Pakistan. *Journal of Geological Society of London*, **153**, 965-969.

Zeitler, P.K., 1985. Cooling history of the NW Himalaya, Pakistan. *Tectonics*, **4**, 127-151.

Zeitler, P. K., Tahirkheli, R. A. K., Naesser, C., Johnson, N. and Lyons, J., 1980. Preliminary fission-track ages from Swat valley, northern Pakistan. *Geological Bulletin, Peshawar University*, **13**, ~~63-65~~

Appendices

Appendix 1. Location, unit and description of rock samples.

Highlighted sample numbers were selected for petrography and the sample numbers with stars were used for geochemical analyses.

Sample Nos.	Location	Unit	Field description
A-1	Gittidas	Indian Plate	Granite, fine to medium-grained, locally banded and bands are rich in micas. Granite veins cut the gneisses.
A-2	Gittidas	Indian Plate	Gneiss consisting of garnet.
A-3	Saleh Di Baik	Indian Plate	Garnet Mica Schist
A-4	Saleh Di Baik	Indian Plate	Garnet Mica Schist
A-5	Saleh Di Baik	Indian Plate	Garnet Mica Schist
A-6	Saleh Di Baik	Indian Plate	Marble, dusty brown in weather colour.
A-7	South of Buto Gali	Babusar Complex	Porphyritic gabbros with large crystals of plagioclase.
A-8	South of Buto Gali	Babusar Complex	Pyroxenite
A-9	South of Buto Gali	Babusar Complex	Diorite
A-10	South of Buto Gali	Babusar Complex	Banded gabbros
A-11	South of Buto Gali	Babusar Complex	Diorite
A-12	South of Buto Gali	Babusar Complex	Amphibolite, fine-grained and presents as mafic band in diorite.
A-13*	South of Buto Gali	Babusar Complex	Gabbros, coarse-grained.
A-14	South of Buto Gali	Babusar Complex	Amphibolite, fine-grained and occurs as dykes which are cutting the gabbros.
A-15	South of Buto Gali	Babusar Complex	Pyroxene bearing anorthosite, coarse-grained.
A-16*	South of Buto Gali	Babusar Complex	Leuco gabbro, coarse-grained.
A-17	Just below Buto Peak	Babusar Complex	Gabbro, fine-grained.
A-18	Just below Buto Peak	Babusar Complex	Gabbro, fine-grained.
A-19	Just below Buto Pass	Babusar Complex	Diorite, medium-grained.
A-20	Just below Buto Gali	Babusar Complex	Quartz, presents as veins and layers in gabbros.
A-21	At Buto Gali	Babusar Unit	Amphibolite, fine- to medium-grained and very mafic.
A-22*	At Buto Gali	Babusar Unit	Amphibolite from mafic band of unit.
A-23	At Buto Gali	Babusar Unit	Amphibolite from banded variety.
A-24	At Buto Gali	Babusar Unit	Mafic part of the banded amphibolite.
A-25	At Buto Gali	Babusar Unit	Felsic part of the banded amphibolite.
A-26	South of Buto Gali	Babusar Complex	Ultramafic, pyroxene bearing dunite.
A-27	South of Buto Gali	Babusar Complex	Ultramafic, serpentinized dunite.
A-28	South of Buto Gali	Babusar Complex	Ultramafic, Pyroxenite.
A-29	South of Buto Gali	Babusar Complex	Ultramafic, dunite cut by veins and dykes of pyroxenite.
A-30	South of Buto Gali	Babusar Complex	Ultramafic, hornblendite with dusty brown weather colour.
A-31	Kalawan	Babusar Complex	Ultramafic, serpentinite with grey green colour.
A-32	Kalawan	Babusar Complex	Gabbro, very fine-grained, oriented and mylonitized from shearing at MMT.
A-33	Kalawan	Babusar Complex	Gabbro, mylonitized, very fine-grained and oriented.

Appendix 1 continued

A-34	East of Kalawan	Babusar Complex	Gabbro, layered. Layering is fine to coarse-grained.
A-35*	East of Kalawan	Babusar Complex	Gabbro, layered and fine-grained.
A-36	East of Kalawan	Babusar Complex	Gabbro, layered and coarse-grained.
A-37	North east of Kalawan	Babusar Complex	Gabbro, mafic and shows dark colour.
A-38*	North east of Kalawan	Babusar Complex	Gabbro, felsic and shows light colour.
A-39	South of Tatabai	Babusar Complex	Ultramafic, pyroxene bearing dunite and looks blackish in colour.
A-40	South of Tatabai	Babusar Complex	Ultramafic, serpentinized dunite and shows light grey colour.
A-41	South of Tatabai	Babusar Complex	Ultramafic, serpentinized dunite and shows dark grey shades.
A-42	South of Tatabai	Babusar Complex	Ultramafic, pyroxene bearing serpentinite.
A-43	South of Tatabai	Babusar Complex	Gabbro, layered and cut by layers of anorthosite and hornblende pyroxenite.
A-44	South of Tatabai	Babusar Complex	Gabbro, homogeneous and dark grey in colour.
A-45	South of Tatabai	Babusar Complex	Gabbro, homogeneous and dark grey in colour.
A-46	Tatabai	Babusar Complex	Ultramafic, pyroxene bearing dunite of light colour.
A-47	Tatabai	Babusar Complex	Ultramafic, pyroxene bearing dunite of dark colour.
A-48	Tatabai	Babusar Complex	Ultramafic, peridotite of grey colour.
A-49	Tatabai	Babusar Complex	Ultramafic.
A-50	Tatabai	Babusar Complex	Ultramafic.
A-51	Tatabai	Babusar Complex	Ultramafic.
A-52	Tatabai	Babusar Complex	Ultramafic.
A-53	Tatabai	Babusar Complex	Ultramafic, dunite interlayered with pyroxenite from the middle part of the main body.
A-54	Tatabai	Babusar Complex	Ultramafic, pyroxene bearing dunite.
A-55	Tatabai	Babusar Complex	Ultramafic, dunite with segregated chromite veins.
A-56	South of Utla Babusar	Babusar Unit	Amphibolite, banded showing green and white bands.
A-57	South of Utla Babusar	Babusar Unit	Amphibolite, from mafic part of the rock and looks fine- to medium-grained.
A-58	South of Utla Babusar	Babusar Unit	Amphibolite, looks less mafic.
A-59	Near Utla Babusar	Minor Body	Granite, fine-grained, foliated and shows minor biotite along foliation.
A-60	Near the Utla Babusar	Shai Unit	Granitic gneiss, foliated.
A-61	North of Utla Babusar	Shai Unit	Granitic gneiss, foliated.
A-62*	North of Utla Babusar	Minor bodies Trondhjemite	Granite, foliated and intruded in Niat Unit.
A-63	North of Utla Babusar	Shai Body	Original basaltic material changed into amphibolite.

Appendix 1 continued

A-64	North of Utla Babusar	Shai Body	Plagioclase bearing amphibolite.
A-65*	North of Utla Babusar	Shai Body	Granite, coarse-grained, deformed and chlorite presents along foliation.
A-66	North of Utla Babusar	Shai Body	Diorite, weakly deformed, hornblende with minor biotite and chlorite.
A-67	North of Utla Babusar	Khun Body	Amphibolite, fine-grained.
A-68	Near Jal	Khun Body	Andesite, band in amphibolite.
A-69*	South of Jal	Jal Unit	Amphibolite, dark grey micaceous.
A-70	South of Jal	Minor Body	Pegmatite, coarse-grained and weakly deformed.
A-71*	South of Jal	Minor Body	Pegmatite, deformed and white in colour.
A-72*	Near Jal	Jal Unit	Amphibolite, medium-grained, grey in colour intruded by granite.
A-73	At Halala	Indian Plate	Granite gneiss.
A-74*	North of Halala	Jal Unit	Amphibolite, medium-grained and sheared.
A-75	North of Halala	Minor Body	Granite, very fine-grained, strongly foliated mylonitized, biotite presents along the foliation and cut by quartz veins.
A-76	Further north from Halala	Jal Unit	Amphibolite, fine-grained, mylonitized and may be derived from gabbro norites.
A-77	Near the cotact with Chilas Complex	Jal Unit	Amphibolite, fine-grained, strongly foliated mylonitized and garnet is present.
A-78*	Close to Chilas Complex	Jal Unit	Amphibolite, fine-grained, strongly deformed, mylonitized and may be derived from gabbro norites.
A-79	At contact	Jal Unit	Amphibolite, fine-grained and orientd.
A-80*	South of Lomar	Niat Unit	Amphibolite, fine-grained with lot of chlorite, highly sheared and intruded by granites. Two phases of shearing are seen.
A-81	South of Lomar	Shai Body	Diorite, fine-grained and mylonitised.
A-82	South of Lomar	Shai Body	Diorite, very fine-grained, highly sheared and mylonitized.
A-83*	South of Lomar	Niat Unit	Amphibolite, fine-grained and shows dark grey colour.
A-84	South of Lomar	Niat Unit	Amphibolite, fine-grained, foliated and shows locally shearing.
A-85	At Lomar	Khun Body	Diorite, medium-grained.
A-86*	At Lomar	Khun Body	Amphibolite, fine- to medium-grained.
A-87*	North of Lomar	Khun Body	Diorite, medium-grained.
A-88*	North of Lomar	Khun Body	Granodiorite, mylonitized and biotite presents along the foliation planes.
A-89	North of Lomar	Khun Body	Granodiorite, mylonitized and strongly sheared.
A-90	North of Lomar	Khun Body	Diorite, strongly lineated.
A-91*	North of Lomar	Khun Body	Granodiorite, mylonitized and biotite presents along the foliation planes.
A-92*	At Nigaran	Niat Unit	Amphibolite, fine-grained and dark grey.
A-93*	At Nigaran	Niat Unit	Amphibolite, fine-grained and dark grey.
A-94	At Nigaran	Niat Unit	Amphibolite, fine-grained and dark grey.
A-95	At Nigaran	Khun Body	Diorite, coarse-grained.
A-96*	At Nigaran	Khun Body	Diorite, strongly foliated with hornblende.
A-97*	At Nigaran	Khun Body	Diorite, strongly foliated with lot of hornblende.

Appendix 1 continued

A-98*	At Gurmāl	Jal Unit	Amphibolite, banded and dark grey with quartz and andesite veins.
A-99*	At Gurmāl	Minor Body	Granite pegmatite, weakly foliated, biotite presents in the foliation planes.
A-100*	At Gurmāl	Minor Body	Andesite dyke in banded amphibolites.
A-101*	North of Gurmāl	Jal Unit	Amphibolite, medium-grained.
A-102*	South of Jal	Minor Body	Andesite, fine-grained.
A-103*	South of Jal	Minor Body	Granite, fine- to medium-grained, weakly foliated and occurs as thin sill.
A-104*	Near Jal	Minor Body	Granite, fine-grained, very felsic, foliated, biotite and chlorite in the foliation planes.
A-105*	Near Jal	Jal Unit	Amphibolite, fine- to medium-grained.
A-106*	At Jal	Minor Body	Diorite, medium to coarse-grained.
A-107	At Gutomāl	Khun Body	Granite, coarse-grained intruded Niat volcanics.
A-108*	At Gutomāl	Minor Body	Granodiorite, coarse-grained.
A-109*	North of Gutomāl	Niat Unit	Amphibolite, fine- to medium-grained and shows dark grey colour.
A-110*	North of Gutomāl	Khun Body	Diorite, medium- to coarse-grained and occurs as sheet in Niat amphibolites.
A-111	North of Gutomāl	Niat Unit	Amphibolite, fine-grained, sheared and shows dark grey colour.
A-112*	North of Gutomāl	Niat Unit	Amphibolite, fine-grained, strongly sheared and looks like mylonite.
A-113*	Near Butogāl	Khun Body	Granite, garnetiferous and intruded the Niat amphibolites.
A-114*	Near Butogāl	Sumāl Unit	Amphibolite, very fine-grained and mylonitized.
A-115*	North of Butogāl	Sumāl Unit	Amphibolite, very fine-grained, dark grey and mylonitized.
A-116*	South of Sumāl	Sumāl Unit	Amphibolite, fine-grained, green and occurs as thin and thick bands.
A-117*	At Sumāl	Sumāl Unit	Amphibolite, medium-grained and grey.
A-118	North of Sumāl	Sumāl Unit	Pillow lava shows dark shades along crust with light green core.
A-119*	At Sumāl	Sumāl Unit	Amphibolite, fine-grained.
A-120	Dalupār Gah	Sumāl Unit	Amphibolite, fine-grained and dark.
A-121*	Daupār Gah	Sumāl Unit	Andesite, fine-grained.
A-122*	At Birodhat	Sumāl Unit	Amphibolite, fine-grained.
A-123*	At Birodhat	Minor Body	Granite pegmatite, weakly foliated with abundant muscovite and chlorite.
A-124*	North of Birodhat	Khun Body	Granodiorite, fine-grained, foliated with biotite and chlorite, and minor muscovite.
A-125*	North of Birodhat	Sumāl Unit	Amphibolite, fine-grained.
A-126*	South of Chakkar	Khun Body	Diorite, medium-grained and foliated.
A-127*	At Chakkar	Minor Body	Granite pegmatite, weakly deformed and intruded in diorites.
A-128*	At Chakkar	Khun Body	Diorite, medium-grained and foliated.
A-129*	North of Chakkar	Minor Body	Granite pegmatite, coarse-grained and weakly deformed and altered.
A-130*	At Makheli	Khun Body	Diorite, medium-grained, mafic and foliated.
A-131	At Makheli	Khun Body	Diorite, medium-grained and foliated.
A-132*	Near Makheli	Niat Unit	Amphibolite, fine-grained and strongly foliated.
A-133*	North of Makheli	Niat Unit	Amphibolite, fine-grained with dark grey colour and strongly foliated.
A-134	North of Makheli	Niat Unit	Andesite and shows light grey colour.

Appendix 1 continued

A-135*	North of Makheli	Niat Unit	Amphibolite, fine-grained and strongly foliated.
A-136*	North of Makheli	Khun Body	Diorite, medium-grained, more mafic and strongly foliated.
A-137	North of Makheli	Niat Unit	Amphibolite, fine-grained and strongly foliated.
A-138	South of Gabbar	Khun Body	Granodiorite, medium- to coarse-grained and weakly foliated.
A-139*	South of Gabbar	Khun Body	Granite, intruded the diorites and strongly foliated.
A-140	South of Gabbar	Khun Body	Diorite, fine-grained and strongly foliated.
A-141*	South of Gabbar	Khun Body	Diorite, fine-grained and strongly foliated.
A-142	South of Gabbar	Khun Body	Diorite, fine-grained and strongly foliated.
A-143*	South of Gabbar	Khun Body	Xenolith in diorites, fine-grained and shows dark grey colour.
A-144*	South of Gabbar	Khun Body	Granitic dyke in diorites, strongly foliated, mylonitized with abundant biotite.
A-145	South of Gabbar	Khun Body	Diorite, medium-grained with greenish white colour.
A-146*	South of Gabbar	Minor Body	Granite, coarse-grained sheet in the banded amphibolite.
A-147*	Just south of Gabbar	Jal Unit	Amphibolite, banded and dark grey.
A-148*	Just south of Gabbar	Jal Unit	Amphibolite.
A-149*	Just south of Gabbar	Minor Body	Granite, strongly foliated and cut by quartz veins.
A-150	At Gabbar	Jal Unit	Amphibolite, fine-grained with green colour.
A-151*	At Gabbar	Jal Unit	Amphibolite, banded with grey colour.
A-152	At Gabbar	Minor Body	Granite, foliated.
A-153	At Thak	Minor Body	Granite, fine-grained and strongly sheared
A-154*	At Thak	Jal Unit	Amphibolite, fine-grained, strongly sheared and mylonitized.
A-155*	At Thak	Minor Body	Granite, fine-grained and mylonitized.
A-156*	South of Thak	Jal Unit	Amphibolite, fine-grained and mylonitized with grey colour.
A-157*	South of Thak	Jal Unit	Amphibolite, fine-grained and mylonitized with grey colour.
A-158	South of Thak	Jal Unit	Amphibolite, fine-grained and strongly sheared with grey colour.
A-159	South of Thak	Khun Body	Diorite, medium-grained, slightly rich in biotite.
A-160*	South of Thak	Khun Body	Diorite, medium-grained with grey colour.
A-161*	South of Thak	Minor Body	Diorite, medium-grained with grey colour.
A-162*	North of Domain	Khun Body	Diorite, consisting of big crystals of black amphibole.
A-163*	North of Domain	Khun Body	Diorite, fine- to medium-grained with light colour.
A-164*	North of Domain	Khun Body	Smoky diorite, fine- to medium-grained with grey colour.
A-165*	At Domain	Khun Body	Diorite, dark green colour and rich in amphibole.
A-166*	At Domain	Khun Body	Diorite of light colour.
A-167*	At Loshi	Khun Body	Diorite of light green colour.
A-168	Ktai Nala	Shai Body	Diorite, coarse-grained with xenoliths.
A-169	Ktai Nala	Shai Body	Diorite, very coarse-grained.
A-170	Ktai Nala	Shai Body	Diorite, foliated.
A-171	Ktai Nala	Shai Body	Diorite, coarse-grained.
A-172	Ktai Nala	Shai Body	Diorite, medium-grained.

Appendix 1 continued

A-173	South of Buto gali	Babusar Complex	Gabbros, coarse-grained with quartz veins.
A-174	At Buto gali	Babusar Unit	Amphibolite, banded.
A-175	At Buto gali	Babusar Unit	Amphibolite, banded.
A-176	At Buto gali	Babusar Unit	Amphibolite, banded, medium-grained.
A-177	North of gali	Shai Body	Diorite, coarse-grained with grey colour.
A-178	North of gali	Shai Body	Diorite, coarse-grained and foliated.
A-179	North of gali	Shai Body	Diorite, foliated with quartz veins.
A-180	North of gali	Shai Body	Diorite, very coarse-grained.
A-181	North of gali	Shai Body	Diorite, coarse-grained with green colour.
A-182	North of gali	Shai Body	Granodiorite, coarse-grained and foliated.
A-183	North of gali	Shai Body	Granodiorite, very coarse-grained, white.
A-184	North of gali	Shai Body	Diorite, medium-grained with layering.
A-185	North of gali	Minor Body	Tonalite, coarse-grained with light colour.
A-186	North of gali	Niat Unit	Volcanics, fine-grained with green colour.
A-187	North of gali	Niat Unit	Volcanics, fine-grained with green colour.
A-188	North of gali	Niat Unit	Volcanics, fine-grained with green colour.
A-189	North of gali	Niat Unit	Volcanics, fine-grained with green colour.
A-190	5km from Buto gali	Shai Body	Diorite, medium-grained with greenish colour at the contact with Niat Unit.
A-191	5km from Buto gali	Shai Body	Diorite, medium-grained with greenish colour.
A-192	6km	Niat Unit	Volcanics, fine-grained.
A-193	7km from Buto gali	Shai Body	Granodiorite, coarse-grained with mica, biotite, quartz and plagioclase.
A-194	7km from Buto gali	Shai Body	Granodiorite, coarse-grained with mica, biotite, quartz and plagioclase.
A-195	8km from Buto gali	Shai Body	Diorite, fine-grained with different sets of quartz veins cut the rock.
A-196	8km from Buto gali	Shai Body	Diorite, fine-grained with different sets of quartz veins cut the rock.
A-197	South of Gutomal	Minor Body	Granodiorite, medium-grained with plagioclase, quartz and mica.
A-198	South of Gutomal	Minor Body	Granodiorite, medium-grained with plagioclase, quartz and mica.
A-199	Just south of Gutomal	Shai Body	Granodiorite, medium-grained with plagioclase, quartz and mica.
A-200	At Gutomal	Niat Unit	Amphibolite, medium-grained and banded
A-201	At Gutomal	Niat Unit	Amphibolite, fine-grained.
A-202	South of Sumal	Sumal Unit	Amphibolite, fine-grained with grey colour.
A-203	South of Sumal	Sumal Unit	Amphibolite, fine-grained with grey colour.
A-204	At Sumal	Khun Body	Granodiorite, coarse-grained and green.
A-205	At Sumal	Sumal Unit	Amphibolite, fine-grained with grey colour.
A-206	At Sumal	Khun Body	Diorite, rich in quartz and hornblende.
A-207	South of Rehmal	Niat Unit	Volcanics, fine-grained, foliated and sheared.
A-208	South of Rehmal	Minor Body	Diorite, medium-grained.
A-209	South of Rehmal	Minor Body	Trondhjemite, medium-grained with elongated hornblende crystals.
A-210	South of Rehmal	Khun Body	Diorite, medium-grained with more elongated crystals of hornblende.
A-211	North of Tushkal	Minor Body	Trondhjemite, medium-grained with more elongated crystals of hornblende and rounded crystals of mica.
A-212	North of Tushkal	Minor Body	Diorite, medium-grained.
A-213	North of Tushkal	Niat Unit	Volcanics, fine-grained.

Appendix 1 continued

A-214	North of Tushkal	Shai Body	Diorite, medium-grained and strongly foliated.
A-215	At Tushkal	Minor Body	Granite, medium-grained.
A-216	At Tushkal	Niat Unit	Amphibolite, medium-grained.
A-217	South of Tushkal	Niat Unit	Amphibolite, medium-grained with dark grey colour.
A-218	South of Tushkal	Niat Unit	Amphibolite, medium-grained with dark grey colour.
A-219	South of Tushkal	Niat Unit	Amphibolite, coarse-grained with dark grey colour.
A-220	South of Tushkal	Niat Unit	Amphibolite, medium-grained with dark grey colour.
A-221	North of Keo Gali	Shai Body	Diorite, fine-grained, strongly sheared and foliated.
A-222	North of Gali	Niat Unit	Amphibolite, fine-grained and mylonitized
A-223	North of Gali	Niat Unit	Amphibolite, fine-grained and mylonitized
A-224	North of Gali	Babuser Unit	Amphibolite, fine-grained and banded.
A-225	Just below the Gali	Babuser Unit	Amphibolite, very fine-grained and mylonitized.
A-226	At Keo Gali	Minor Body	Granite, intruded in mylonitized Babuser amphibolite.
A-227	At Keo Gali	Babuser Unit	Amphibolite, very fine-grained and mylonitized.
A-228	South of Keo Gali	Babuser Unit	Amphibolite, fine-grained and mylonitized.
A-229	South of Gali	Babuser Unit	Quartz, occur as veins in amphibolites.
A-230	South of Gali	Babuser Unit	Amphibolite, medium-grained.
A-231	South of Gali	Shai Body	Diorite, fine-grained and mylonitized.
A-232	South of Gali	Shai Body	Diorite, medium-grained and mylonitized.
A-233	South of Gali	Babuser Unit	Volcanics, intruded by diorite.
A-234	South of Gali	Shai Body	Diorite, intruded in the country rocks.
A-235	South of Gali	Shai Body	Diorite, medium-grained.
A-236	South of Gali	Minor Body	Diorite, coarse-grained with dark colour.
A-237	East of Gali	Babuser Unit	Volcanics, fine-grained at the contact with Shai dioritic body.
A-238	East of Gali	Babuser Unit	Amphibolite, fine-grained and grey colour.
A-239	East of Gali	Babuser Unit	Amphibolite, fine-grained and grey colour.
A-240	At Batsi Sangar	Babuser Unit	Amphibolite, fine-grained with dark grey colour.
A-241	At Batsi Sangar	Babuser Unit	Amphibolite, fine- to medium-grained and banded.
A-242	At Batsi Sangar	Babuser Complex	Gabbros, medium-grained and strongly sheared.
A-243	Northwest of Batsi Sangar	Babuser Unit	Amphibolite, homogeneous with dark grey colour.
A-244	Northwest of Batsi Sangar	Babuser Unit	Amphibolite, dark grey colour.
A-245	Northwest of Batsi Sangar	Babuser Complex	Gabbros, light colour at the contact with Babuser amphibolites.
A-246	West of Batsi Sangar	Shai Body	Diorite, coarse-grained.
A-247	West of Batsi Sangar	Shai Body	Diorite, coarse-grained and foliated.
A-248	North of Tuno	Babuser Unit	Amphibolite, medium-grained and banded.
A-249	North of Tuno	Babuser Unit	Amphibolite, medium-grained and banded.
A-250	Shikaro gah	Babuser Unit	Amphibolite, medium-grained, banded.
A-251	Shikaro gah	Babuser Unit	Amphibolite, medium-grained, banded.
A-252	Shikaro gah	Babuser Complex	Gabbros, medium-grained, layered and cut by different quartz veins.
A-253	Shikaro gah	Babuser Complex	Gabbros, medium-grained, layered and cut by different quartz veins.
A-254	Shikaro gah	Minor Body	Granite, coarse-grained with light colour.

Appendix 1 continued

A-255	North of Chochargah	Minor Body	Granite, medium- to coarse-grained with white colour.
A-256	North of Chochargah	Minor Body	Granite, medium- to coarse-grained with white colour.
A-257	Chochargah	Babusar Complex	Gabbros, medium-grained, layered and cut by different quartz veins.
A-258	Chochargah	Babusar Complex	Gabbros, medium-grained, layered and cut by different quartz veins.
A-259	Chochargah	Babusar Complex	Gabbros, medium-grained and layered.
A-260	Chochargah	Babusar Complex	Gabbros, fine-grained, layered and cut by very thin quartz veins.
A-261	West of Chochargah	Babusar Complex	Gabbros, medium-grained, layered and sheared.
A-262	West of Chochargah	Babusar Complex	Gabbros, medium-grained, layered and sheared.
A-263	South of Kot Gali	Babusar Complex	Gabbros, medium-grained and layered.
A-264	At Kot Gali	Babusar Complex	Gabbros, medium-grained and layered.
A-265	At Karape	Babusar Complex	Gabbros, medium-grained and layered with white bands of anorthosite containing large crystals of amphibole.
A-266	North of Karape	Babusar complex	Gabbros, foliated and banded, fine-grained mafic bands are dominant than the coarse-grained felsic bands.
A-267	North of Karape	Babusar complex	Gabbros, medium-grained and foliated.
A-268	North of Karape	Babusar complex	Gabbros, medium-grained and foliated.
A-269	North of Karape	Babusar complex	Gabbros, medium-grained and foliated cut by coarse-grained diorite.
A-270	6km south of Ghurman	Babusar complex	Gabbros, more felsic and sheared than A-269.
A-271	6km south of Ghurman	Babusar complex	Gabbros, more felsic and strongly sheared than A-270.
A-272	2km south of Ghurman	Babusar Unit	Amphibolite, medium-grained and strongly foliated and sheared.
A-273	1km south of Ghurman	Minor Body	Tonalite, coarse-grained and intruded the amphibolites.
A-274	1km south of Ghurman	Minor Body	Anorthosite band in the the amphibolite containing hornblende crystals.
A-275	At Ghurman Gali	Babusar Unit	Amphibolite, medium-grained and foliated.
A-276	At Gali	Babusar Unit	Amphibolite, strongly sheared.
A-277	At Gali	Babusar Unit	Amphibolite, fine-grained and mylonitized
A-278	At Gali	Babusar Unit	Amphibolite, with mafic and felsic bands.
A-279	At Gali	Babusar Unit	Amphibolite, fine-grained and mylonitized
A-280	North of Gali	Shai Body	Diorite, medium-grained and foliated.
A-281	South of Kuba	Shai Body	Diorite, coarse-grained, strongly foliated with xenoliths of country rocks.
A-282	South of Kuba	Shai Body	Diorite, medium-grained, strongly foliated with xenoliths of country rocks.
A-283	At Kuba	Niat Unit	Volcanics, fine-grained.
A-284	North of Kuba	Shai Body	Diorite, medium-grained.
A-285	North of Kuba	Shai Body	Diorite, medium-grained.
A-286	North of Kuba	Shai Body	Diorite, medium-grained with xenoliths of volcanics.
A-287	North of Kuba	Niat Unit	Volcanics, fine-grained and strongly foliated.
A-288	South of Zure	Shai Body	Diorite, strongly foliated with more quartz.
A-289	South of Zure	Shai Body	Diorite, coarse-grained, more felsic and foliated.

Appendix 1 continued

A-290	Just south of Zure	Shai Body	Diorite, medium-grained, sheared and foliated
A-291	Just south of Zure	Minor Body	Tonalite, coarse-grained with light colour.
A-292	At Zure	Niat Unit	Volcanics, fine-grained with quartz veins.
A-293	At Zure	Niat Unit	Volcanics, medium-grained.
A-294	North of Zure	Shai Body	Diorite, medium-grained and foliated.
A-295	North of Zure	Shai Body	Diorite, medium-grained and strongly foliated.
A-296	South of Sarin	Khun Body	Diorite, medium-grained and strongly foliated.
A-297	At Sarin	Niat Unit	Volcanics, fine-grained and sheared.
A-298	At Sarin	Niat Unit	Volcanics, fine-grained and sheared.
A-299	At Sarin	Niat Unit	Volcanics, fine-grained and foliated.
A-300	At Sarin	Niat Unit	Volcanics, fine-grained and mylonitized.
A-301	North of Sarin	Niat Unit	Volcanics, very fine-grained and highly mylonitized.
A-302	South of Ganotak	Jal Unit	Amphibolite, medium-grained and banded.
A-303	South of Ganotak	Khun Body	Diorite, medium-grained.
A-304	At Ganotak	Jal Unit	Amphibolite, fine-grained.
A-305	South of Mulimum	Jal Unit	Amphibolite, fine-grained.
A-306	South of Mulimum	Jal Unit	Amphibolite, medium-grained.
A-307	At Mulimum	Khun Body	Diorite, medium-grained.
A-308	North of Mulimum	Jal Unit	Amphibolite, fine-grained.
A-309	North of Mulimum	Jal Unit	Amphibolite, medium-grained with banding.
A-310	South of Khai	Jal Unit	Amphibolite, medium-grained, contact with Chilas Complex.
A-311	South of Khai	Chilas Complex	Gabbro norite, medium-grained.
A-312	South of Khai	Chilas Complex	Diorite / gabbro norite.
A-313	South of Gabbar	Jal Unit	Amphibolite, medium-grained and sheared.
A-314	Further south of Gabbar	Khun Body	Diorite, medium-grained with light grey colour.
A-315	North of Sasing Baik	Niat Unit	Amphibolite, fine-grained, foliated and sheared.
A-316	At Sasing Baik	Niat Unit	Amphibolite, fine-grained, foliated and sheared.
A-317	At Makheli		Diorite, consisting more mafic minerals.
A-318	At Singodal	Niat Unit	Amphibolite, medium-grained, foliated.
A-319	At Singodal	Niat Unit	Amphibolite, fine-grained and foliated.
A-320	South of Jachal Baik	Shai Body	Diorite, medium-grained with long crystals of hornblende.
A-321	South of Jachal Baik	Niat Unit	Volcanics, fine-grained and foliated.
A-322	At Jachal Baik	Shai Body	Diorite, medium-grained with parallel veins of fine-grained mafic material.
A-323	At Jachal Baik	Shai Body	Diorite, medium-grained with the xenoliths of volcanics.
BS-1	East of Babusar RH	Shai Body	Diorite, strongly foliated and mylonitized.
BS-2	East of Babusar RH	Shai Body	Diorite, medium-grained and foliated.
BS-3	East of Babusar RH	Babusar Unit	Amphibolite, interbanded with gneisses.

Appendix 1 continued

BS-4	East of Babusar RH	Minor Body	Granite, coarse-grained with bands of fine-grained mylonitized diorite.
BS-5	West of Babusar RH	Minor Body	Mylonitized zone interbanded with granitic gneisses.
BS-6	At Babusar	Babusar Unit	Amphibolite, garnet bearing from feldspathic band.
BS-7*	At Babusar	Babusar Unit	Amphibolite, medium-grained mafic band interbanded with feldspathic amphibolite band.
BS-8*	At Babusar	Babusar Unit	Amphibolite, foliated but unbanded containing porphyroclasts of feldspathic minerals.
BS-9*	At Babusar	Babusar Unit	Amphibolite, medium-grained from massive part of unit.
BS-10*	Southwest of Babusar	Babusar Unit	Amphibolite, fine-grained with green colour and interbanded with medium- to coarse-grained amphibolites.
BS-11*	Southwest of Babusar	Babusar Unit	Amphibolite, mylonitized from 4 m thick strongly sheared zone.
BS-12	Southwest of Babusar	Babusar Complex	Ultramafic, mylonitized and occurs along shear zone.
BS-13*	Southwest of Babusar	Babusar Complex	Ultramafic, medium-grained and massive.
BS-14*	Southwest of Babusar	Babusar Complex	Ultramafic, containing large crystals in fine matrix of pyroxene or serpentine.
BS-15*	Southwest of Babusar	Babusar Complex	Ultramafic, fine-grained with black colour and very hard.
BS-16*	Southwest of Babusar	Babusar Complex	Ultramafic, black shining megacrysts, along one surface lenticular grains are present.
BS-17*	Southwest of Babusar	Babusar Complex	Ultramafic, from the northern margin of the body.
BS-18*	At Babusar	Babusar Unit	Amphibolite, fine-grained, massive, strongly sheared and mylonitized.
BS-19*	North of Babusar RH	Babusar Unit	Amphibolite, fine-grained and massive. This sample comes from 200 m thick relic of massive amphibolites surrounded by two shear zones.
BS-20	One km north of RH	Minor Body	Granite, medium-grained intruded in amphibolites.
BS-21	South of RH	Niat Unit	Amphibolite, medium-grained.
BS-22	South of Tarla Babusar	Niat Unit	Amphibolite, medium-grained and foliated.
BS-23	Just south of Tarla Babusar	Niat Unit	Amphibolite, fine-grained and strongly foliated.
BS-24	Near Chikidas	Niat Unit	Amphibolite, fine-grained, massive and foliated.
BS-25*	Near Chikidas	Shai Body	Diorite, medium-grained and strongly foliated.
BS-26*	At Chikidas	Shai Body	Diorite, fine-grained, strongly sheared and mylonitized.
BS-27	At Chikidas	Shai Body	From boudinaged quartzose band interbanded with amphibolites.
BS-28*	North of Shai	Minor Body	Granite, medium- to coarse-grained, whitish rock and foliated.
BS-29*	North of Shai	Shai Body	Diorite, medium-grained and foliated.
BS-30	Near Shai	Niat Unit	Amphibolite, fine-grained, foliated with green colour.

Appendix 2. Appendix showing the Topographic sheets used during the mapping of area.

Topographic sheets used during this research study are Government of Pakistan 1:50,000 scale, 1st and 2nd editions. These cover the entire mapping area. One sheet NI 43 (2nd edition) of 1:250,000 scale is also used. First edition of this sheet is prepared in 1953 and revised (second edition) in 1962 by Army Map Services (LU), Corps of Engineers, U.S. Army, Washington DC.

Map numbers	Main locations	Main valley	Edition	Surveyed	Notes
43E/12	Kot Gali	Jalkot Nala	1st	1976	Restricted
43E/15	Gabbar, Makheli, Chakkar and Sumal	Thor Valley and Buto Valley	1st	1974	Restricted
43E/16	Tuno, Batsi Sangar, Gittidas and Besal	Shikaro Valley and Chochar Gah	2nd	1976	Restricted
43I/3	Jal	Thak and Niat Valley	1st	1974	Restricted
43I/4	Babusar	Thak Valley	1st		Restricted
43I/7	Halala	Bunar Valley	1st	1980	Restricted
43I/8	Manuguch	Niat Valley	1st	1980	Restricted